

University of Warwick institutional repository: <http://go.warwick.ac.uk/wrap>

A Thesis Submitted for the Degree of PhD at the University of Warwick

<http://go.warwick.ac.uk/wrap/3794>

This thesis is made available online and is protected by original copyright.

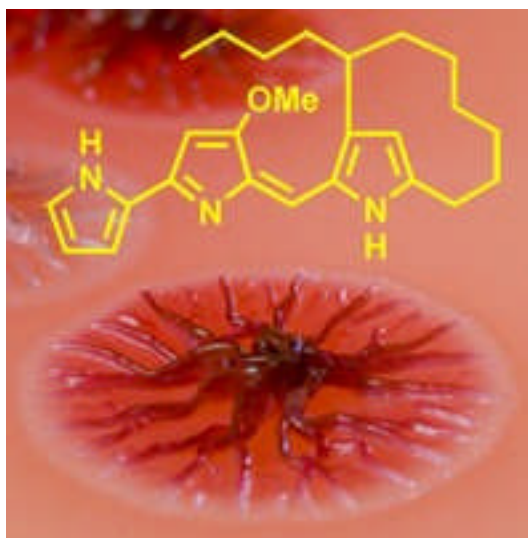
Please scroll down to view the document itself.

Please refer to the repository record for this item for information to help you to cite it. Our policy information is available from the repository home page.

Elucidation of the Prodiginine Biosynthetic Pathway in *Streptomyces coelicolor* A3(2)

Paulina K. Sydor

Thesis submitted in partial fulfilment of the requirements for the degree of Doctor of Philosophy in Chemistry.



University of Warwick
Department of Chemistry
February 2010

Contents

Contents	i
List of Figures	v
List of Tables	xii
Acknowledgements	xiii
Declaration	xiv
Abstract	xv
Abbreviations	xvii
1. Introduction	1
1.1 <i>Streptomyces coelicolor</i> A3(2).....	2
1.2 Secondary Metabolites of <i>Streptomyces coelicolor</i> A3(2) – Overview of their Biosynthesis and Biological Activities	4
1.2.1 Prodiginines.....	6
1.2.2 Actinorhodins.....	10
1.2.3 Calcium-Dependent Antibiotics (CDAs)	10
1.2.4 Coelichelin	11
1.2.5 Grey Spore Pigment.....	12
1.2.6 Methylenomycins	13
1.2.7 γ -Butyrolactones (GBLs).....	13
1.2.8 Methylenomycin Furans (MMFs)	14
1.2.9 Germicidins.....	14
1.2.10 Geosmin and 2-Methyl-isoborneol.....	15
1.2.11 Albaflavenone	15
1.2.12 Post Translational Phosphopantetheinylation of Carrier Proteins (CPs) During Secondary Metabolite Biosynthesis.....	16
1.3 Biosynthesis of Prodiginines in <i>Streptomyces</i> Species.....	18
1.3.1 Early studies of prodiginine biosynthesis and identification of the <i>red</i> gene cluster in <i>S. coelicolor</i> A3(2)	18
1.3.2 The <i>red</i> Cluster Encodes Enzymes that Are Similar to those Involved in the Biosynthesis of Other Metabolites.....	22
1.3.2.1 Fatty Acid Synthases (FASs).....	22
1.3.2.2 Polyketide Synthases (PKSs).....	24
1.3.2.3 Nonribosomal Peptide Synthetases (NRPSs).....	26
1.3.3 2-Undecylpyrrole Biosynthesis	29
1.3.4 4-methoxy-2,2'-bipyrrole-5-carboxaldehyde (MBC) Biosynthesis.....	32
1.3.5 Condensation of 2-Undecylpyrrole and MBC to Form Undecylprodiginine	34
1.3.6 Oxidative Cyclisation of Undecylprodiginine to Form Streptorubin B	36
1.3.6.1 Rieske Non-Haem Iron-Dependent Oxygenases.....	37
1.3.6.2 Proposed Oxidative Cyclisation Reaction of Undecylprodiginine Catalysed by RedG.....	39
1.4 Aims of the Project.....	43
2. Materials and Methods	45

2.1	Materials	46
2.1.1	Chemicals and Equipment.....	46
2.1.2	Buffers and General Solutions	47
2.1.3	Antibiotics.....	47
2.1.4	Microbial Strains	48
2.1.5	Plasmids	49
2.1.6	Cosmids	49
2.1.7	Primers	50
2.1.8	Culture Media.....	53
2.1.8.1	Liquid Media.....	53
2.1.8.2	Solid Media.....	54
2.2	Growth, Storage and Manipulation of <i>E. coli</i>	55
2.2.1	Growth Conditions	55
2.2.2	Storage of Strains	55
2.2.3	Preparation of Electrocompetent <i>E. coli</i> cells	55
2.2.4	Transformation of Electrocompetent <i>E. coli</i>	56
2.3	Growth, Storage and Manipulation of <i>Streptomyces</i>	56
2.3.1	Surface Grown Cultures for Spore Stock Generation.....	56
2.3.2	Liquid Grown Cultures for Genomic DNA Isolation	57
2.3.3	Transfer of DNA from <i>E. coli</i> to <i>S. coelicolor</i> and <i>S. venezuelae</i> by conjugation.....	57
2.4	Isolation and Manipulation of DNA	58
2.4.1	Genomic DNA Isolation from <i>S. coelicolor</i>	58
2.4.2	Plasmid or Cosmid Isolation from <i>E. coli</i>	59
2.4.3	Digestion of DNA with Restriction Enzymes	59
2.4.4	Ligation of DNA into plasmid vectors.....	60
2.4.5	Agarose Gel Electrophoresis	60
2.5	PCR Methods	60
2.5.1	Standard PCR Method	61
2.5.2	PCR Amplification of the Gene Replacement Cassette.....	62
2.6	PCR Targeting Gene Replacement in <i>S. coelicolor</i>	62
2.6.1	Primer Design.....	62
2.6.2	Purification of PCR Template (Resistance Cassette).....	62
2.6.3	PCR Amplification of the Gene Replacement Cassette	63
2.6.4	Introduction of Cosmids into <i>E. coli</i> BW25113/pIJ790 by Electroporation	63
2.6.5	PCR-targeting of Cosmids	63
2.6.6	Transfer of the Mutant Cosmids into <i>Streptomyces</i>	65
2.6.7	Construction of “scar” mutants	66
2.7	Southern Blot.....	68
2.7.1	Probe Labelling	68
2.7.2	Genomic DNA Digestion.....	69
2.7.3	Capillary Transfer and DNA Fixing	69
2.7.4	Hybridization.....	70
2.7.5	Detection	71
2.8	Construction of a <i>S. longispororuber</i> Fosmid Library.....	71
2.8.1	Shearing and End-repairing of DNA	71
2.8.2	Ligation of DNA into pCC1FOS, Packaging and Transfection of <i>E. coli</i>	72
2.8.3	Screening the Fosmid Library for Clones containing <i>redG/redH</i> Orthologues	72
2.9	Growth and extraction of <i>Streptomyces</i> species for analyses of metabolite production	73
2.9.1	Prodiginines.....	73

2.9.2	Actinorhodins	74
2.9.3	Coelichelin	75
2.9.4	Methylenomycin Production Bioassay	75
2.9.5	CDA Production Bioassay	76
2.10	Chemistry Techniques	76
2.10.1	Conversion of desmethylundecylprodiginine to undecylprodiginine	76
2.10.2	Purification of prodiginines from <i>S. coelicolor</i> extract.....	76
2.10.2.1	Circular Dichroism (CD) spectroscopy	78
2.10.3	Purification of Desmethylundecylprodiginine	78
2.10.4	LC-MS	79
2.10.5	High Resolution Mass Spectrometry	80
3.	Mutagenesis of Genes in the <i>S. coelicolor</i> red Cluster	81
3.1	PCR-targeting Strategy	82
3.2	Gene Replacements Generated within the <i>red</i> Cluster	87
3.3	Genetic Complementation of the Mutants	93
3.4	Conclusions	96
4.	Investigation of Genes Involved in Biosynthesis and Condensation of 2-Undecylpyrrole and 4-Methoxy-2,2'-bipyrrole-5-carboxaldehyde.....	97
4.1	Analysis of Prodiginine Production.....	98
4.2	Elucidation of the Biosynthetic Pathway to 2-Undecylpyrrole	102
4.2.1	Investigation of <i>Streptomyces coelicolor</i> W37 Mutant (M511/ <i>redLA::apr</i>).....	103
4.2.2	Investigation of <i>Streptomyces coelicolor</i> W36 Mutant (M511/ <i>redK::oriT-apr</i>).....	108
4.2.3	Investigation of <i>Streptomyces coelicolor</i> W35 Mutant (M511/ <i>redJ::oriT-apr</i>) ..	114
4.3	Role of RedT in Prodiginine Biosynthesis.....	117
4.4	Condensation of 2-Undecylpyrrole and MBC to Yield Undecylprodiginine.....	120
4.4.1	Genetic Complementation of the <i>redH</i> Mutant.....	121
4.4.2	Heterologous Expression of <i>redH</i> in <i>S. venezuelae</i> and Feeding of Synthetic MBC and 2-Undecylpyrrole.....	122
4.5	Conclusions	124
5.	Investigation of Oxidative Cyclisation Reactions in Prodiginine Biosynthesis	127
5.1	Oxidative Cyclisation Reaction of Undecylprodiginine to Give Streptorubin B in <i>Streptomyces coelicolor</i>	128
5.1.1	Analysis of a <i>Streptomyces coelicolor</i> M511/ <i>redI::oriT-apr</i> (W34) Mutant Indicates the Likely Substrate of RedG	129
5.1.2	Genetic Complementation of the <i>redG</i> Mutant	133
5.1.3	Expression of <i>redG</i> and <i>redHG</i> in <i>Streptomyces venezuelae</i> to Establish if RedG is the Only Enzyme from the <i>red</i> Cluster Required for Streptorubin B Biosynthesis	135
5.1.4	Introduction of Additional Copies of <i>redG</i> and <i>redH</i> into <i>S. coelicolor</i> M511...	139
5.2	Cloning, Sequencing and Functional Analysis of <i>Streptomyces longispororuber redG</i> Orthologue: <i>mcpG</i>	144
5.2.1	Construction of a <i>Streptomyces longispororuber</i> Fosmid Library	145
5.2.2	Fosmid 3G3 Analysis – Sequence Determination of <i>redG</i> and <i>redH</i> Orthologues (<i>mcpG</i> and <i>mcpH</i>) of <i>Streptomyces longispororuber</i>	148
5.2.3	Heterologous Expression of <i>Streptomyces longispororuber mcpG</i> in the <i>Streptomyces coelicolor/redG::scar</i> Mutant.....	151
5.3	The Role of <i>redG</i> Orthologues in Other Microorganisms	157

5.3.1	Expression of Four <i>redG</i> Orthologues from <i>Streptomyces griseoviridis</i> in <i>Streptomyces coelicolor</i> W31.....	159
5.4	Conclusions	161
6.	Genetic Engineering of <i>Streptomyces coelicolor</i> to Create Prodiginine Analogues	164
6.1	Undecylprodiginine and Streptorubin B Halogenated Analogues.....	165
6.2	Construction of a <i>Streptomyces coelicolor</i> Mutant Abolished in Production of Both 2-undecylpyrrole and MBC	171
6.3	Conclusions	173
7.	Investigation of the Roles of Phosphopantetheinyl Transferases in <i>Streptomyces coelicolor</i> Metabolite Biosynthesis	174
7.1	Phosphopantetheinyl Transferases.....	175
7.2	Construction of PPTase Mutants	177
7.3	Investigation of the Role of PPTases in Secondary Metabolite Biosynthesis in <i>Streptomyces coelicolor</i> A3(2).....	182
7.3.1	Prodiginine Production	182
7.3.2	Actinorhodin Production.....	187
7.3.3	Methylenomycin Production.....	191
7.3.4	Calcium-Dependent Antibiotic (CDA) Production	193
7.3.5	Coelichelin Production	195
7.3.6	Grey Spore Pigment Production and Colony Morphology	198
7.4	Conclusions	201
8.	Summary, Conclusions and Future Work.....	204
8.1	Investigation of the Prodiginine Biosynthetic Pathway in <i>Streptomyces coelicolor</i> M511.....	205
8.2	Investigation of an Oxidative Carbocyclisation Reaction in Streptorubin B Biosynthesis	208
8.3	Cloning, sequencing and analysis of <i>redG</i> and <i>redH</i> orthologues from <i>Streptomyces longispororuber</i>	209
8.4	Novel Approaches for Generating Prodiginine Analogues.....	211
8.5	Investigation of the Roles of Enzymes Catalysing Post-translational Phosphopantetheinylation of ACP and PCP Proteins/Domains	212
References	214

List of Figures

Figure 1.1 The Streptomycete life cycle (www.chem.leidenuniv.nl).....	3
Figure 1.2 Structures of several secondary metabolites produced by <i>S. coelicolor</i> A3(2).	5
Figure 1.3 Colonies of <i>Streptomyces coelicolor</i> , left: secreting blue Actinorhodin antibiotics, right: with red pigmented mycelia due to production of Prodiginines. In both cases the colonies are covered with grey aerial mycelium and spores (John Innes Centre).....	6
Figure 1.4 <i>Serratia marcescens</i> colonies growing on an agar plate (photo by Brudersohn).	7
Figure 1.5 Structures of some prodiginines produced by a variety of bacteria.	8
Figure 1.6 Structures of obatoclax and PNU-156804, synthetic prodiginine analogues.	9
Figure 1.7 Reaction catalyse by PPTases. The <i>apo</i> form is termed inactive form, without the arm and the <i>holo</i> form is called active form, with phosphopantetheinyl arm attached.	16
Figure 1.8 Proposed biosynthetic origin of undecylprodiginine and its cyclic derivative streptorubin B in <i>S. coelicolor</i>	19
Figure 1.9 Organisation of the <i>red</i> cluster in <i>S. coelicolor</i> with proposed functions of encoded proteins. Arrows indicate four transcription units within the cluster.	21
Figure 1.10 The fatty acid biosynthetic pathway of <i>E. coli</i> from the two carbon precursor, acetyl-CoA. In <i>Streptomyces</i> species primarily isobutyryl-, 2-methylbutyryl-, isovaleryl-CoA are used instead of acetyl-CoA.	23
Figure 1.11 Elongation of fatty acid chain by KASII.....	23
Figure 1.12 Domain organisation of the DEBS modular PKS and proposed biosynthetic intermediates in the assembly of 6-dEB. Domains are as follows: AT – acyltransferase, ACP – Acyl Carrier Protein, KS – ketosynthase, KR – ketoreductase, DH – dehydratase, ER – enoylreductase, TH – thioesterase.	26
Figure 1.13 Basic steps during nonribosomal biosynthesis of peptides, domains: A – adenylation, T (PCP) – thiolation, C – condensation, TE – thioesterase.....	28
Figure 1.14 Reaction catalysed by 8-amino-7-oxononanoate synthase (AONS).	29
Figure 1.15 Proposed 2-undecylpyrrole (21) biosynthesis.	31
Figure 1.16 MBC (20) intermediate, common in prodigiosin and undecylprodiginine biosynthesis.	32
Figure 1.17 Proposed MBC (20) biosynthesis.	34
Figure 1.18 Reaction catalysed by PPDK.	35
Figure 1.19 Proposed mechanism for condensation reaction catalysed by RedH.	36
Figure 1.20 Oxidative cyclisation reactions in the biosynthesis of clinically-used natural products. Highlighted in blue – hydrogen atoms removed in the reactions. Highlighted in red – new bonds formed.	37
Figure 1.21 A – reaction catalysed by naphthalene dioxygenase (NDO), B – Representation of the NDO active site.	38
Figure 1.22 Amino-acid sequence alignment of NDO α subunit from <i>Pseudomonas putida</i> , RedG from <i>S. coelicolor</i> and RedG orthologue from <i>S. longispororuber</i> . Conserved residues that ligate the [2Fe-2S] cluster and Fe(II) atom – highlighted in yellow. An Asp residue in NDO (mutated to Glu in RedG and RedG orthologue) proposed to mediate electron transfer between the [2Fe-2S] cluster and the Fe(II) atom is highlighted in green.	39
Figure 1.23 Proposed catalytic mechanism for RedG.	41
Figure 1.24 Predicted intermediates during <i>S. coelicolor</i> and <i>S. longispororuber</i> prodiginine biosynthetic pathway.....	42

Figure 2.1 Homologous recombination of the disruption cassette with cosmid DNA to create a gene deletion in the cosmid, followed by conjugation from <i>E. coli</i> into <i>S. coelicolor</i> and double homologous recombination to give a mutant in which the gene of interest is replaced by the disruption cassette. Yellow gene – apramycin resistance, orange region – origin of transfer (<i>oriT</i>), green regions = FRT sites.....	64
Figure 2.2 Flip recombinase-mediated step to give an 81 bp “scar” in place of the disruption cassette in the cosmid. Conjugal transfer of the cosmid to <i>S. coelicolor</i> can give a “scar” mutant. Yellow gene – apramycin resistance, orange region – origin of transfer (<i>oriT</i>), green regions = flip recombinase target (FRT) sites.....	67
Figure 3.1 Feature map of pIJ773.....	83
Figure 3.2 Design of PCR primers for making a gene replacement or in-frame deletion using PCR-targeting (Gust et al., 2002).....	83
Figure 3.3 Homologous recombination of the disruption cassette with cosmid DNA to create a gene deletion in the cosmid, followed by conjugation from <i>E. coli</i> into <i>S. coelicolor</i> and double homologous recombination to give a mutant in which the gene of interest is replaced by the disruption cassette. Yellow gene – apramycin resistance, orange region – origin of transfer (<i>oriT</i>), green regions = FRT sites.....	84
Figure 3.4 Flip recombinase-mediated step to give an 81 bp “scar” in place of the disruption cassette in the cosmid. Conjugal transfer of the cosmid to <i>S. coelicolor</i> can give a “scar” mutant. Yellow gene – apramycin resistance, orange region – origin of transfer (<i>oriT</i>), green regions = flip recombinase target (FRT) sites.....	86
Figure 3.5 PCR analyses of mutagenised Sc3F7 cosmids and genomic DNA extracted from <i>S. coelicolor</i> M511 and M595 mutants, A: a – Sc3F7 cosmid, b – wild type, M511 DNA, c – Sc3F7/ <i>redI::oriT-apr</i> , d – M511/ <i>redI::oriT-apr</i> , with <i>redI</i> test primers; B: a – Sc3F7 cosmid, b – wild type, M511 DNA, c – Sc3F7/ <i>redJ::oriT-apr</i> , d – M511/ <i>redJ::oriT-apr</i> , with <i>redJ</i> test primers; C: a – wild type, M511 DNA, b – M511/ <i>redJ::scar</i> , with <i>redJ</i> test primers; D: a – Sc3F7 cosmid, b – wild type, M511 DNA, c – Sc3F7/ <i>redK::oriT-apr</i> , d – M511/ <i>redK::oriT-apr</i> , with <i>redK</i> test primers; E: a – Sc3F7 cosmid, b – wild type, M511 DNA, c – Sc3F7/ <i>redLA::oriT-apr</i> , d – M511/ <i>redLA::oriT-apr</i> , with <i>redLA</i> test primers; F: a,b – Sc3F7 cosmid, c – wild type, M511 DNA, d – M511/ <i>redT::oriT-apr</i> , with <i>redT</i> test primers; G: a – Sc3F7 cosmid, b – wild type, M511 DNA, c – Sc3F7/ <i>redV::oriT-apr</i> , d – M511/ <i>oriT-redV::apr</i> , with <i>redV</i> test primers; H: a – wild type, M511 DNA (expected size in wild type DNA 7502 bp), b – Sc3F7/ <i>redL::oriT-apr</i> , d – M595/ <i>redL::oriT-apr</i> , with <i>redL</i> test primers; M – 1 kb ladder.....	89
Figure 3.6 Agarose gel electrophoresis analysis of restriction enzymes digest of genetically-engineered cosmids used to disrupt the <i>S. coelicolor</i> genes within <i>red</i> cluster. A – <i>Bam</i> HI, B – digestion with <i>Sac</i> I. Top gels show high molecular weight bands, bottom gels show low molecular weight bands. Numbers indicated by arrows show the digestion pattern of Sc3F7 cosmid. Number written on the gel shows additional and/or changed bands characteristic for modified Sc3F 7 cosmids. B – 752 bp band indicate the presence of the cassette.....	90
Figure 3.7 Southern blot hybridisation using labelled Sc3F7 cosmid as a probe confirming the nature of <i>S. coelicolor</i> mutants with genes deleted from the <i>red</i> cluster. Bands highlighted in red are all present in <i>S. coelicolor</i> M511. Bands highlighted in white are characteristic for each mutant. The 8347 bp band in the Sc3F7 are derived from the SuperCos backbone. M511/ <i>redV::oriT-apr</i> – green 1718bp and ~6500 bp bands should not be present in the mutant.....	92
Figure 3.8 Feature and restriction site map of pOSV556.....	93
Figure 4.1 Typical HPLC chromatogram monitoring absorbance at 533 nm of acidified organic extracts of <i>S. coelicolor</i> M511, showing resolution of undecylprodiginine (2) and streptorubin B (3).	98
Figure 4.2 Extracted ion chromatograms (EICs) for <i>m/z</i> = 392-394 in positive ion mode from LC-MS analyses of acidified organic extracts of <i>S. coelicolor</i> M511. Both samples were eluted through a C-18 column with water and an organic solvent (A – MeCN or B – MeOH).....	99

Figure 4.3 LC-MS/MS spectra for: A – undecylprodiginine (2) ($m/z = 394$) and B – streptorubin B (3) ($m/z = 392$) in positive ion mode. The proposed origins of the observed fragment ions are shown above the spectra.	100
Figure 4.4 EICs and MS/MS spectra from LC-MS analyses of synthetic A – MBC (20) ($m/z = 191$); B – 2-UP (21) ($m/z = 222$).	101
Figure 4.5 Entire proposed pathways to 2-UP including alternative mechanisms for transfer of the dodecanoyl chain from RedQ to the first ACP domain of RedL: (a) direct transacylation; (b) hydrolysis and reactivation by the RedLA domain.	103
Figure 4.6 EIC ($m/z = 392$ -394) from LC-MS analysis of acidified organic extracts of the <i>S. coelicolor</i> W38 (blue line) and W38 mutant fed with synthetic 2-UP (red line).	104
Figure 4.7 EIC ($m/z = 392$ -394) from LC-MS analysis of acidified organic extracts of <i>S. coelicolor</i> W37 (blue line), W37 fed with dodecanoic acid (black line), and W37 fed with synthetic 2-UP (red line)	105
Figure 4.8 EIC ($m/z = 191$) and MS/MS spectra from LC-MS/MS analyses of acidified organic extracts of <i>S. coelicolor</i> W37.	106
Figure 4.9 EIC ($m/z = 392$ -394) from LC-MS analyses of acidified organic extracts of <i>S. coelicolor</i> W37 (blue line), W37 + pOSV556 <i>redLA</i> (black line) and <i>S. coelicolor</i> M511 (red line).	107
Figure 4.10 EIC ($m/z = 392$ -394) from LC-MS analysis of acidified organic extracts of <i>S. coelicolor</i> M511 (red) and the W36 mutant (blue).	109
Figure 4.11 EIC ($m/z = 392$ -394) from LC-MS analyses of acidified organic extracts of the W36 mutant (blue) and the W36 mutant fed with synthetic 2-UP (3) (red).	109
Figure 4.12 A – EIC ($m/z = 410$) from LC-MS analyses of acidified organic extracts from the W36 mutant (dark green) and <i>S. coelicolor</i> M511 (pink); B – MS/MS spectrum of compound with $m/z = 410$ accumulated in the W36 mutant. C, D – UV chromatogram monitoring absorbance at 533 nm from LC-MS analysis of acidified organic extract of the C – W36 mutant, D – M511.	110
Figure 4.13 A – proposed structure and fragment ions observed in MS/MS analysis for the hydroxylated analogue of undecylprodiginine (14) with $m/z = 410$; B – structure and proposed fragment ions observed in MS/MS analysis of undecylprodiginine (2).	111
Figure 4.14 Top: EIC ($m/z = 238$) from LC-MS analyses of acidified organic extracts of the W36 mutant (light blue) and M511 (dark blue). Bottom: mass spectrum for the peak with retention time ~6 minutes in the chromatogram for the W36 mutant.	112
Figure 4.15 Reaction proposed to be catalysed by RedK.	112
Figure 4.16 EIC ($m/z = 392$ -394) from LC-MS analysis of acidified organic extracts of the W36 and W38 mutants grown in co-culture.	113
Figure 4.17 Proposed roles for RedJ in prodiginine biosynthesis: A – RedJ could catalyse hydrolytic release of dodecanoic acid from RedQ; B – RedJ could produce active <i>holo</i> forms of carrier proteins and carrier protein domains involved in prodiginine biosynthesis that results from posttranslational modification with acetyl-CoA instead of coenzyme A.	114
Figure 4.18 LC-MS analysis of undecylprodiginine (2) and streptorubin B (3) production by the W35 mutant.	115
Figure 4.19 A – Time-course of antibiotic production by <i>S. coelicolor</i> M511 wild type (red line) and the W35 (M511/ <i>redJ::oriT-apr</i>) mutant (brown line) grown on R5 medium B – HPLC analyses monitoring absorbance at 533 nm of acidified organic extracts of M511 (red line) and the W35 mutant (brown line) from the same amount of WCW after 4.5 days of growth. Errors bars indicate standard error calculated from three samples.	116
Figure 4.20 A, C – Time-course of prodiginine production by the M511 strain (red line) and W28 (M511/ <i>redT::oriT-apr</i>) mutant (brown line) grown on R5 medium; B, D – HPLC analysis monitoring absorbance at 533 nm of acidified organic extract of M511 (red line) and W28 mutant (brown line), extracted after five days of growth from the same amount of WCW; D – zoomed UV chromatogram from extract of the W28 mutant. Errors bars indicate standard error calculated from three samples.	118

Figure 4.21 EIC ($m/z = 392-394$) from LC-MS analyses of acidified organic extracts of the <i>S. coelicolor</i> W28 mutant (violet line), the W28 mutant fed with 2-UP (21) (blue line) and the W28 mutant fed with synthetic MBC (20) (red line).....	119
Figure 4.22 EIC ($m/z = 222$) from LC-MS analyses of acidified organic extracts of the <i>S. coelicolor</i> W28 mutant.....	119
Figure 4.23 Proposed role of RedH in undecylprodiginine biosynthesis.	120
Figure 4.24 EIC ($m/z = 392-394$) from LC-MS analyses of organic extracts of the M511/ <i>redH::oriT-apr</i> (blue line) and M511/ <i>redH::oriT-apr</i> + pOSV556 <i>redH</i> (red line)mutants.	122
Figure 4.25 Top: EIC ($m/z = 394$) from LC-MS analyses of acidified organic extracts of <i>S. venezuelae</i> + 2-UP + MBC (bottom, blue trace) and <i>S. venezuelae</i> + pOSV556 <i>redH</i> + 2-UP + MBC (top, red trace). Bottom: mass spectrum of peak with retention time of ~5.75 minutes of the upper (red) chromatogram.	123
Figure 5.1 Possible pathways for the formation of streptorubin B (3) from 2-UP and MBC catalysed by RedG and RedH.	129
Figure 5.2 EICs ($m/z = 392-394$) from LC-MS analyses of acidified organic extracts of <i>S. coelicolor</i> M511 (red line) and a M511/ <i>redI::oriT-apr</i> mutant (black line).	130
Figure 5.3 A – Proposed role for RedI in MBC biosynthesis; B – proposed structure of the undecylprodiginine derivative accumulated in the M511/ <i>redI::oriT-apr</i> mutant.	130
Figure 5.4 A – EICs ($m/z = 380$) from LC-MS analysis of organic extracts of the W34 mutant (top) and the M511 wild type (bottom). B,C – MS/MS spectra for $m/z = 380$ ions from organic extracts of the W34 mutant, B – peak with retention time ~6 min, C – peak with retention time ~9 min.....	131
Figure 5.5 A – Reaction scheme for conversion of desmethylundecylprodiginine to undecylprodiginine. B – EIC ($m/z = 394$) from LC-MS/MS analysis of the methylation reaction. C – MS/MS spectra for peak with retention time of ~5 min.....	133
Figure 5.6 EIC ($m/z = 392-394$) from LC-MS analyses of acidified organic extracts of the W31 mutant (black line) and the W31/pOSV556 <i>redG</i> strain (red line).....	134
Figure 5.7 EIC ($m/z = 392-394$) from LC-MS analyses of acidified organic extracts from <i>S. venezuelae</i> /pOSV556 <i>redHG</i> + 2-UP + MBC (red line) and from <i>S. venezuelae</i> + 2-UP + MBC (black line).	136
Figure 5.8 EIC ($m/z = 392-394$) from LC-MS/MS analyses of acidified organic extracts of A – <i>S. venezuelae</i> + W31 extract (black line), B – <i>S. venezuelae</i> /pOSV556 <i>redG</i> + W31 extract (blue line), C – <i>S. venezuelae</i> /pOSV556 <i>redHG</i> + W31 extracts (red line); D – MS/MS spectra for the peak with a retention time of ~10.5 min in the extract of <i>S. venezuelae</i> /pOSV556 <i>redG</i> fed with W31 extract.....	137
Figure 5.9 EIC ($m/z = 392-394$) from LC-MS analyses of acidified organic extracts of A – <i>S. venezuelae</i> + synthetic undecylprodiginine (2) (black line), B – <i>S. venezuelae</i> /pOSV556 <i>redG</i> + synthetic 2 (blue line, C – <i>S. venezuelae</i> /pOSV556 <i>redHG</i> + synthetic 2 (red line); D – MS/MS spectra for the peak with retention time of ~10 minutes in the extract from <i>S. venezuelae</i> /pOSV556 <i>redG</i> fed with synthetic 2.	138
Figure 5.10 HPLC analysis monitoring absorbance at 533 nm of acidified organic extracts of <i>S. coelicolor</i> A – W31, B – W31/pOSV556 <i>redG</i> , C – W31/pOSV556 <i>redHG</i> , D – M511, E – M511/pOSV556 <i>redG</i> , F – M511/pOSV556 <i>redHG</i> ; 2 = undecylprodiginine, 3 = streptorubin B.	140
Figure 5.11 HPLC analyses monitoring absorbance at 533 nm of acidified organic extracts of <i>S. coelicolor</i> W38 (black line) and W38/pOSV556 <i>redHG</i> (red line) fed with synthetic 2-UP.....	141
Figure 5.12 Feature map of pIJ86.	142
Figure 5.13 Analyses of acidified organic extracts from W31/pIJ86 <i>redG</i> (black line) and W31/pIJ86 <i>redHG</i> (red line); A – HPLC analyses monitoring absorbance at 533 nm, B – EICs ($m/z = 392-394$) from LC-MS analyses.....	143
Figure 5.14 Prodiginines produced by <i>S. coelicolor</i> and <i>S. longispororuber</i>	144
Figure 5.15 Map of the pCC1 FOS vector.	145

Figure 5.16 A – <i>S. longispororuber</i> genomic DNA after shearing, B – <i>S. longispororuber</i> genomic DNA after ~40 kb band DNA was excused, C – <i>S. longispororuber</i> ~40 kb genomic DNA fraction; D – agarose gel electrophoresis analysis of 6 fosmid clones digested with <i>Bam</i> HI. For A-C, M = 40 kb molecular size marker; for D – M = 10 – 0.25 kb and 20 – 0.1 kb molecular size markers.....	146
Figure 5.17 Steps involved in creating a genomic fosmid library(EpicentreBiotechnologies, 2007).	147
Figure 5.18 Screening of <i>S. longispororuber</i> fosmid library for clones containing the <i>redG</i> orthologue. 500 colonies grown in 96 well plates were screened in two stages: A – first, screening with twelve clones in each PCR reaction, B – second screening of twelve clones from two positive PCR reactions checked separately; M – DNA marker; C – control PCR reaction with genomic DNA as a template.....	148
Figure 5.19 Comparison of genetic organisation of the <i>S. coelicolor red</i> cluster with the fragment of the <i>S. longispororuber mcp</i> cluster cloned in the 3G3 fosmid.	149
Figure 5.20 A – sequence alignment of the <i>McpH</i> and <i>RedH</i> ; B – sequence alignment of the <i>McpG</i> and <i>RedG</i> ; conserved residues within <i>RedG</i> and <i>McpG</i> that ligate the [2Fe-2S] cluster and Fe(II) atom in NDO are highlighted in blue, an Asp residue of NDO (mutated to Glu in <i>RedG</i> and <i>McpG</i>) proposed to mediate electron transfer between the [2Fe-2S] cluster and the Fe(II) atom is highlighted in red. Black letters, no background – non-similar amino acids, black letters, green background – block of similar amino acids, red letter, yellow background – identical amino acids.....	150
Figure 5.21 A, B, D, E: EICs ($m/z = 392-394$) from LC-MS analyses of acidified organic extracts of: A – <i>S. coelicolor</i> W31 (top black line), B – W31/pOSV556 <i>mcpG</i> (blue line), D – <i>S. longispororuber</i> (black line), E – <i>S. coelicolor</i> M511 (red line); C – HPLC analysis monitoring absorbance at 533 nm of acidified organic extracts of W31/pOSV556 <i>mcpG</i> , F – MS/MS spectra of the cyclic undecylprodiginine derivative produced by W31/pOSV556 <i>mcpG</i>	153
Figure 5.22 Proposed fragment ions of streptorubin A (metacycloprodigiosin) and streptorubin B observed in positive ion ESI-MS/MS spectra.	154
Figure 5.23 ¹ H NMR spectra (CDCl ₃ , 700 MHz) of streptorubin A (top) and streptorubin B (bottom). The characteristic signals at 0.2 ppm and -1.53 ppm for streptorubin A and B, respectively are highlighted by a box.....	155
Figure 5.24 ¹ H NMR spectrum of the cyclic undecylprodiginine derivative produced by <i>S. coelicolor</i> W31/pOSV556 <i>mcpG</i> . The characteristic signal at 0.2 ppm is highlighted by a box; a – methane protons, b - hydrocarbon protons α to the pyrrole ring.....	155
Figure 5.25 A – CD spectra of streptorubin A (blue line) and streptorubin B (red line); B – CD spectrum of compound with $m/z = 392$ produced by <i>S. coelicolor</i> W31/pOSV556 <i>mcpG</i>	156
Figure 5.26 Proposed roles for RphG1, RphG2, RphG3 and RphG4 in 18 and 19 biosynthesis.	158
Figure 5.27 Sequence alignment of the <i>RedG</i> , <i>RphG</i> , <i>RphG2</i> , <i>RphG3</i> and <i>RphG4</i> . Conserved residues within <i>RedG</i> , <i>RphG</i> , <i>RphG2</i> , <i>RphG3</i> and <i>RphG4</i> that ligate the [2Fe-2S] cluster (missing in the <i>RphG3</i>) and Fe(II) atom in NDO are highlighted in blue, an Asp residue of NDO (mutated to Glu in <i>RedG</i> , <i>RphG</i> , <i>RphG2</i> and <i>RphG4</i>) proposed to mediate electron transfer between the [2Fe-2S] cluster and the Fe(II) atom is highlighted in red. Black letters, no background – non-similar amino acids; black letters, green background – block of similar amino acids; red letters, yellow background – identical amino acids; dark blue letters, torques background – conservative amino acids; dark green letters, no background – weakly similar amino acids.....	159
Figure 5.28 HPLC analyses monitoring absorbance at 533 nm of acidified organic extracts of A – W31/pOSV556 <i>rphG1</i> (blue line), B – W31/pOSV556 <i>rphG2</i> (black line), C – W31/pOSV556 <i>rphG3</i> (green line), D – W31/pOSV556 <i>rphG4</i> (red line).....	160
Figure 6.1 Hypothetical pyrrole-2-carboxyl thioester-5-halogenation reactions in the biosynthesis of hormaomycin (31) (<i>S. griseoflavus</i>) and in the formation of the new clorobiocin (32) derivatives novclorobiocin 124 (33) and novclorobiocin 125 (34) (<i>S. roseochromogenes</i>). HrmK, CloN4 – prolyl-AMP ligases; HrmL, CloN5, CloN1 – acyl carrier proteins; HrmM, CloN3 – flavin-dependent dehydrogenases; CloN2, CloN7 – acyltransferases; HrmQ – halogenase.....	166

Figure 6.2 A – EICs ($m/z = 426-428$) from LC-MS analyses of acidified organic extracts of M511 (black line) and M511/pOSV556hrmQ (blue line), B – LC-MS analysis monitoring absorbance at 533 nm of acidified organic extracts of M511/pOSV556hrmQ, C – MS spectrum of the $m/z = 426$ and $m/z = 428$ ions, D – zoom of MS spectra of $m/z = 426$ and $m/z = 428$ ions showing a characteristic isotopic ratio for chlorinated compounds.....	168
Figure 6.3 LC-MS/MS spectra for 1 A – chlorinated undecylprodiginine (35) ($m/z = 428$) and 2 A – chlorinated streptorubin B (36) in positive ion mode. The proposed origins of the observed fragment ions are shown above the spectra. 1 B, 2 B – zoomed fragment ions with characteristic isotope ratio for chlorinated molecules indicating that the chlorine atom was incorporated into the A pyrrole ring.....	169
Figure 6.4 Hypothetical pyrrole halogenation reactions in the biosynthesis of <i>S. coelicolor</i> prodiginines (black scheme); future experiment to investigate when chlorination is taking place is shown in blue. RedM – prolyl-PCP synthase, RedO – peptidyl carrier protein (PCP), RedW – prolyl-PCP-oxidase/ desaturase.	170
Figure 6.5 EICs ($m/z = 392-394$) from LC-MS analyses of acidified organic extracts from <i>S. coelicolor</i> 119 (M511redN::scar+redL::oriT-apr) (black line), W119 fed with synthetic 2-UP (blue line), W119 fed with synthetic MBC (green line) and W119 fed with synthetic 2-UP + MBC (red line).	172
Figure 7.1 Agarose gel electrophoresis analysis of restriction enzyme digests of genetically-engineered cosmids used to disrupt the <i>S. coelicolor</i> PPTase genes. A – digestion with <i>Bam</i> HI; B – digestion with <i>Pst</i> I. Top gels show high molecular weight bands, bottom gels show low molecular weight bands. Numbers indicated by arrows show the digestion pattern of Sc5A7 cosmid. Numbers written on the gel shows additional bands characteristic for genetically-engineered Sc5A7 cosmid. Digestion pattern of Sc3F7/redU::oriT-apr is written on the gels.	180
Figure 7.2 A – PCR analyses of genomic DNA extracted from M145, M145/acpS::oriT-apr+pOSV556acpS and M511/acpS::oriT-apr+pOSV556acpS, B – PCR analyses of genomic DNA extracted from <i>S. coelicolor</i> M145 and <i>S. coelicolor</i> PPTase mutants. A, B – PCR reactions were carried out with test primers priming ~100 bp outside the disrupted regions. Size differences between PCR products are caused by size differences between wild type DNA and <i>oriT-apr</i> or “scar” sequence introduced in its place. C – Southern blot analysis of <i>redU::oriT-apr</i> mutant in the M145/sco6673::scar background. Bands in red are the same as in M511 (for <i>redU</i> mutant band 4662 bp is missing), white bands are characteristic for the <i>redU</i> mutant (3494 bp and 1759 bp). M – molecular size markers.....	181
Figure 7.3 Prodiginine biosynthetic pathway with ACP and PCP domains (highlighted in red). Intermediates or analogues of intermediates fed to double mutant are in blue.	182
Figure 7.4 EICs ($m/z = 392-394$) from LC-MS analyses of acidified organic extracts of: A – <i>S. coelicolor</i> M145 (wild type), B – <i>redU</i> mutant, C – <i>redU</i> mutant complemented with <i>redU</i> , D – <i>sco6673</i> mutant, E – <i>sco6673</i> mutant complemented with <i>sco6673</i>	184
Figure 7.5 EICs ($m/z 392-394$) from LC-MS analyses of acidified organic extracts of <i>S. coelicolor</i> : A – <i>redU</i> mutant, B – <i>redU</i> mutant fed with pyrrole-2-carboxyl NAC thioester (37), C – <i>sco6673 redU</i> mutant, D – <i>sco6673 redU</i> mutant fed with 37, E – <i>sco6673 redU</i> mutant fed with 37 and 2-UP (21), F - <i>sco6673 redU</i> mutant fed with MBC (21) and 2-UP (20).	186
Figure 7.6 Structure of actinorhodin, one of the blue pigmented antibiotics produced by <i>S. coelicolor</i> A3(2).	187
Figure 7.7 Production of actinorhodins by PPTase mutants grown in SMM medium determined in μg of pigment extracted per mg of DCW (dry cell weight) by UV-Vis spectroscopy.	188
Figure 7.8 Structures of some shunt metabolites from the actinorhodin pathway produced by the M145 parent strain and the PPTase mutants. Structures of SEK4a, SEK4b, SEK34, SEK34b, EM18 were previously known (McDaniel et al., 1994). The structure of LJS1 is novel (Song and Challis, unpublished results).	189
Figure 7.9 PPTase mutants plated onto R5 agar medium (top view of the plate). Pictures were taken two (2d) and four (4d) days after incubation.	190

Figure 7.10 Structures of methylenomycins produced by <i>S. coelicolor</i> A3(2).	191
Figure 7.11 Analysis of methylenomycin production by bioassay in A – <i>S. coelicolor</i> M145, B – M145/C73_787/ <i>mmyR::oriT-apr</i> , C – M145/ <i>sco6673::scar+redU::oriT-apr+C73_787/mmyR::oriT-apr</i> . M145 was used as a methylenomycin sensitive indicator strain.....	193
Figure 7.12 Structures of CDAs produced by in <i>S. coelicolor</i>	194
Figure 7.13 Analysis of PPTase mutants for CDA production using a bioassay. <i>Bacillus mycoides</i> was used as an indicator strain. A – + Ca(NO ₃) ₂ (top plates), B – - Ca(NO ₃) ₂ (bottom plates).	195
Figure 7.14 Structure of coelichelin produced by <i>S. coelicolor</i> A3(2).....	196
Figure 7.15 LC-MS analyses of culture supernatants of <i>S. coelicolor</i> M145 and PPTase mutants; 1: EIC at <i>m/z</i> = 619. 2: UV chromatogram at 435 nm; A – M145 wild type, B – <i>redU</i> mutant, C – <i>sco6673</i> mutant, D – <i>sco6673 redU</i> mutant, E – <i>redU</i> mutant + <i>redU</i> , F - <i>sco6673</i> mutant + <i>sco6673</i> . 3: mass spectrum for the peak with retention time ~2.2 minutes.	197
Figure 7.16 Phenotypes of PPTase mutants plated onto SFM medium, after 2 days (2d) and 4 days (4d) of growth.	199
Figure 7.17 Growth of single colonies of PPTase mutants on SFM agar medium.....	200
Figure 8.1 Proposed biosynthetic pathway to undecylprodiginine and streptorubin B. The functions of genes highlighted in red were investigated in this work.	207
Figure 8.2 Prodiginines produced by <i>S. coelicolor</i> and <i>S. longispororuber</i>	210

List of Tables

Table 2.1 Chemicals stock solution.....	47
Table 2.2 Antibiotics stock solution.....	48
Table 2.3 The microbial strain used.....	48
Table 2.4 List of plasmids.....	49
Table 2.5 List of cosmids.....	49
Table 2.6 List of primers used for PCR-targeting; underlined sequence is homologous to the cassette.....	50
Table 2.7 List of test primers used to confirm inserted mutation.....	51
Table 2.8 List of the others primers used.....	52
Table 2.9 PCR reaction conditions.....	61
Table 2.10 HPLC conditions used for purification of metacycloprodigiosin on Agilent Zorbax C18 column (150 x 21.2 mm, 5µm).....	77
Table 2.11 HPLC conditions used to purify metacycloprodigiosin on an Agilent Zorbax Phenyl column (250 x 21.2 mm, 7µm).....	78
Table 2.12 HPLC conditions used in desmethylundecylprodiginine purification.....	79
Table 2.13 Gradient elution profile used in LC-MS analyses of prodiginine production.....	80
Table 2.14 Gradient elution profile used in LC-MS analyses of actinorhodin and coelichelin production.....	80
Table 3.1 Mutants with genes from the <i>red</i> cluster deleted analysed in this study.....	87
Table 3.2 Created constructs in pOSV556 plasmid analysed in Chapters 4, 5 and 6.....	95
Table 5.1 Comparison of the proteins encoded by the four CDSs identified in the <i>mcp</i> cluster of <i>S. longispororuber</i> with their orthologues encoded by the <i>S. coelicolor red</i> cluster.....	151
Table 7.1 Secondary metabolite production by PPTase mutants. Number of pluses indicates the level of production compared to the M145 parent strain. Grey spore pigment was estimated by looking at growth of single colonies.....	202

Acknowledgements

I wish to express my thanks to Professor Greg Challis for giving me the opportunity to work on this exciting project and for introducing me to the world of natural product discovery. His enthusiasm, encouragement, support and sense of humour were and are still invaluable to me.

A special thank you goes to Christophe for his positive thinking and for all our discussions. To Malek for keeping my sugar level very high and for friendship. To Nadia for lab advices and for all the gossips we had. To Sarah and Stuart for constant help especially with my chemistry problems. To Daniel for keeping me smiling and for all the “nasty pranks”. To Lijiang for his help and optimism. Last but not least a huge thank goes to the rest of the Challis Group (past and present), a bunch of great and positive people, to Amaël, Mansoor, Nicolas, Prakash, Joanna, Lauren, Laura, Anna and to our technician Anne. Huge thanks go as well to all the friends I have met during my time at Warwick.

Najbardziej chciałabym podziękować moim rodzicom, Bogusi i Januszowi, Tomkowi Anicie i Hani, rodzinie i przyjaciółom. Dziękuję za Wasze wsparcie, dobre rady, pomoc i że zawsze mogę na Was liczyć.

Dziękuję Piotrowi za motywację, pomoc, wspieranie mnie i niekończące się pokłady dobrego humoru.

Kasi i Mirkowi dziękuję za ich przyjaźń.

This study was financially supported by the Warwick Postgraduate Research Fellowship.

Declaration

Experimental work contained in this thesis is original research carried out by the author, unless otherwise stated, in the Department of Chemistry at the University of Warwick, between September 2006 and December 2009. No material contained herein has been submitted for any other degree, or at any other institution.

Results from other authors are referenced in the usual manner throughout the text.

Date: _____

Paulina K. Sydor

Abstract

The prodiginine antibiotics are produced by eubacteria, in particular members of the actinomycete family. Interest in this group of compounds has been stimulated by their antitumour, immunosuppressant and antimalarial activities at non-toxic levels. *Streptomyces coelicolor* A3(2) produces two prodiginines: undecylprodiginine and its carbocyclic derivative streptorubin B, which are both derived from the two intermediates 4-methoxy-2,2'-bipyrrrole-5-carboxaldehyde (MBC) and 2-undecylpyrrole (2-UP). The *red* gene cluster of *S. coelicolor* contains 23 genes responsible for prodiginine biosynthesis.

PCR-targeting was used to generate rapid in-frame deletions or replacements of several genes in the *S. coelicolor red* cluster. Using this method *redI*, *redJ*, *redK*, the A domain encoding region of *redL*, *redT* and *redV* were disrupted. Prodiginine production by these mutants was analysed by LC-MS allowing roles for the genes investigated to be hypothesised. A major focus was investigating the function of RedH (proposed to catalyse the condensation of 2-UP and MBC) and RedG (proposed to be responsible for the oxidative carbocyclisation of undecylprodiginine to form streptorubin B) by genetic complementation of existing mutants and heterologous expression of the genes in *S. venezuelae* coupled with feeding of synthetic MBC and 2-UP. The results of these experiments clearly defined the roles of RedH in the condensation of MBC and 2-UP and RedG in the oxidative carbocyclisation of undecylprodiginine.

Streptomyces longispororuber is known to produce undecylprodiginine (like *S. coelicolor*) and a carbocyclic undecylprodiginine derivative called metacycloprodiginosin

(streptorubin A), which contains a 12-membered carbocycle instead of the 10-membered carbocycle of streptorubin B. A *S. longispororuber* fosmid library was constructed, from which a clone containing a previously identified *redG* orthologue was isolated and partially sequenced. Expression of the *S. longispororuber redG* orthologue in the *S. coelicolor redG* mutant resulted in production of metacycloprodigiosin instead of streptorubin B showing that RedG and its *S. longispororuber* orthologue catalyse carbocyclisation reactions during prodiginine biosynthesis.

Another aim of the work was to investigate *redU*, a gene from the *red* cluster that encodes a phosphopantetheinyl transferase (PPTase). PPTases are responsible for post-translational modification of acyl carrier proteins (ACPs) and peptidyl carrier proteins (PCPs). A pre-existing *redU* mutant and two newly constructed mutants lacking PPTases encoded elsewhere in the *S. coelicolor* genome were analysed to investigate the role of PPTases in *S. coelicolor* metabolite biosynthesis. Production of prodiginines, actinorhodins, methylenomycins, calcium dependent antibiotics, coelichelin and grey spore pigment was investigated as ACPs and PCPs are involved in biosynthesis of these compounds. Different specific PPTases were found to be required to modify the ACP/PCP domains/proteins in the biosynthesis of these metabolites.

Abbreviations

A	Adenylation (domain)
aa	amino acid
ACP	Acyl Carrier Protein
ADP	Adenosine diphosphate
amp	Ampicillin
AONS	8-amino-7-oxo-nonanoate synthase
apra	Apramycin
AT	Acyl Transferase (domain)
ATP	Adenosine triphosphate
BC	Before Christ
BLAST	Basic Local Alignment Search Tool
bp	Base pairs
C	Condensation (domain)
CD	Circular Dichroism
CDA	Calcium-dependent antibiotic
CoA	Coenzyme A
DH	Dehydratase (domain)
DMSO	Dimethylsulfoxide
DNA	Deoxyribonucleic acid
E	Epimerisation (domain)
EDTA	Ethylenediaminetetraacetic acid

EIC	Extracted ion chromatogram
ER	Enoyl Reductase (domain)
ESI-MS	Electrospray ionization – Mass spectrometry
EtOAc	ethyl acetate
EtOH	Ethanol
FAD	Flavin Adenine Dinucleotide
FAS	Fatty Acid Synthase
FMN	Flavin mononucleotide
FRT	FLP recognition targets
GC	Guanine-Cytosine
HBC	4-hydroxy-2,2'-bipyrrole-5-carbaldehyde
HBM	4-hydroxy-2,2'-bipyrrole-5-methanol
HPLC	High-performance liquid chromatography
hyg	Hygromycin
kan	Kanamycin
kb	kilo base pairs
KASII	β -ketoacyl-ACP synthase II
KASIII	β -ketoacyl-ACP synthase III
KR	Ketoreductase (domain)
KS	Ketosynthase (domain)
LB	Luria-Bertani (Medium)
LC	(High Pressure) Liquid Chromatography
LC-MS	Liquid Chromatography – Mass Spectrometry

M	Methylation (domain)
MAP	2-methyl-3-n-amylypyrrole
MBC	4-methoxy-2,2'-bipyrrole-5-carboxaldehyde (BP)
Me	Methyl
min.	minute
MS	Mass Spectroscopy
NADH	Nicotinamide adenine dinucleotide
NADPH	Nicotinamide adenine dinucleotide phosphate
NDO	Naphthalene dioxygenase
NMR	Nuclear Magnetic Resonance
NRPS	Nonribosomal peptide synthetase
nt	Nucleotide
OAS	α -oxoamine synthase
OD	Optical Density
ORF	Open Reading Frame
<i>oriT</i>	Origin of Transfer
PCR	Polymerase Chain Reaction
PCP	Peptidyl Carrier Protein
PEPS	Phosphoenol Pyruvate Synthase
PKS	Polyketide synthase
PLP	Pyridoxal phosphate
PPDK	Phosphate Pyruvate Dikinase
PPTase	Phosphopantethienyl transferase

R	resistente
RBS	Ribosome binding site
rpm	revolutions per minute
s	sensitive
SAM	S-adenosylmethionine
CDS	CoDing Sequence
SFM	Soya Flour Mannitol medium
Sfp	Surfactin phosphopantetheinyl transferase
SMM	Supplemented Minimal Medium
T	Thiolation (domain)
<i>Taq</i>	<i>Thermus aquaticus</i> (polymerase)
TBE	Tris-boric acid EDTA buffer
TE	Thioesterase (domain)
tet	tetracycline
TMS	trimethylsilyl
TOF	Time-of-flight
Tris	Tris(hydroxymethyl)aminomethane
2-UP	2-Undecylpyrrole
UV	ultra-violet

1. Introduction

1.1 *Streptomyces coelicolor* A3(2)

Streptomyces are GC-rich, Gram-positive actinobacteria that reside in soil and water and have a complex life cycle (Kieser et al., 2000). Actinobacteria are important in the decomposition of organic matter in soil, contributing in part to the earthy odour of soil, which results from production of a volatile metabolite, geosmin (Gust et al., 2003). They also produce a wide variety of secondary metabolites that include over two-thirds of the clinically useful antibiotics produced by microorganisms, of which around 80% are made by *Streptomyces* ssp. Many of these compounds have important applications in human medicine as antibacterial, antitumor, immunosuppressant and antifungal agents (Kieser et al., 2000). Apart from their beneficial role in the pharmaceutical industry, actinomycetes are also pathogenic to plants, animals and humans, causing illnesses like tuberculosis, which results from infection by *Mycobacterium tuberculosis* (Madigan and Martinko, 2005).

The complex life cycle of *Streptomyces* begins with a spore, which germinates to produce one or two germ tubes. These tubes grow by extension and by forming branches leading to multinucleoid hyphae, known as the substrate mycelium. After two or three days aerial hyphae develop and grow into the air from the surface of the colony. Extended hyphae form a spiral and undergo septation into separate pre-spore compartments, and metamorphose into chains of grey-pigmented spores, which are ready to be released as single spores to start the new life cycle. Production of pigments, antibiotics and other secondary metabolites is often associated with the beginning of differentiation (Figure 1.1) (Kieser et al., 2000).

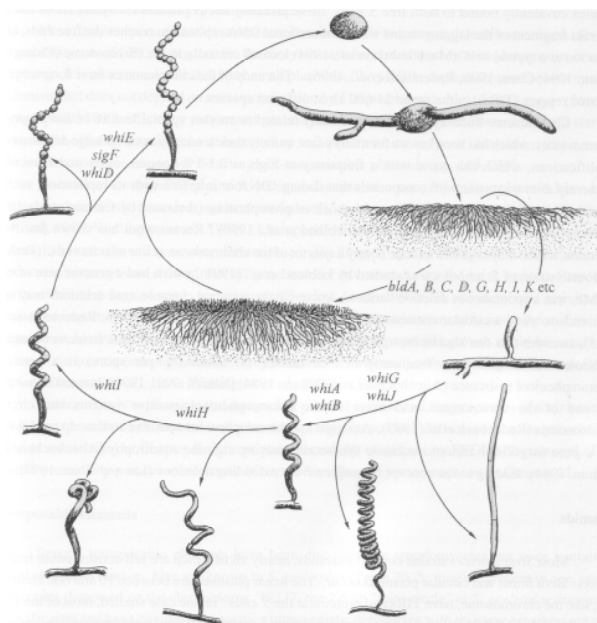


Figure 1.1 The Streptomyces life cycle (www.chem.leidenuniv.nl).

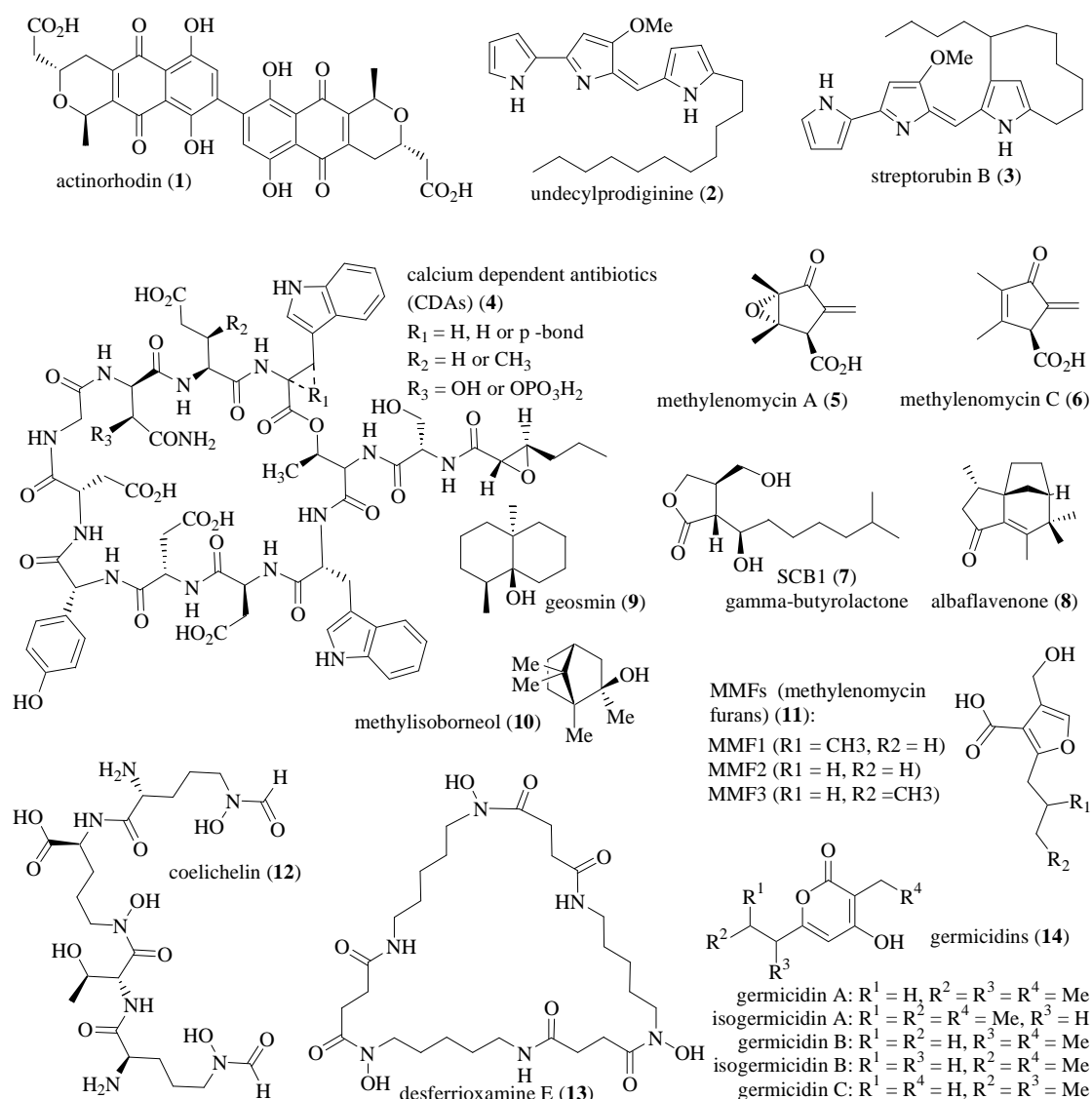
The complete genome of the model organism *Streptomyces coelicolor* A3(2) was published in 2002 (Bentley et al., 2002) and at the time this genome was thought to contain the largest number of genes of any bacteria (since other bacteria have been found to have the largest number of genes). The linear chromosome is 8.7 Mb long with a GC-content of 72% and is predicted to contain around 7,800 protein encoding genes (Bentley et al., 2002). *S. coelicolor* also contains a 360 kb linear plasmid called SCP1 (Bentley et al., 2004) and a 30 kb circular plasmid called SCP2, giving it over 9 Mb of DNA in total (Haug et al., 2003). Over 20 gene clusters that direct the production of known or predicted secondary metabolites were identified by analysis of the genome sequence (Bentley et al., 2002) and prior genetic experiments.

In order to create a *S. coelicolor* strain which is easier to work with, prototrophic derivatives of the A3(2) strains were constructed. In this study, the prototrophs *S.*

coelicolor M145, which lacks the two plasmids SCP1 and SCP2, and *S. coelicolor* M511, which also lacks plasmids SCP1 and SCP2 and the actinorhodin pathway-specific activator gene (*actII-ORF4*) (Floriano and Bibb, 1996) were used.

1.2 Secondary Metabolites of *Streptomyces coelicolor* A3(2) – Overview of their Biosynthesis and Biological Activities

Some of the natural product biosynthesis genes identified within the *S. coelicolor* A3(2) genome were already known prior to the genome sequence and direct the production of secondary metabolites such as the antibiotics (actinorhodins (**1**), prodiginines (**2** and **3**), calcium dependent antibiotics (CDAs) (**4**) and methylenomycins (**5** and **6**)), a grey spore pigment and γ -butyrolactones (GBLs) (**7**) (Figure 1.2, Figure 1.3). In addition, many cryptic gene clusters, the metabolic products of which were not known were identified by genome sequence analysis. These gene clusters encode a variety of characteristic enzymes commonly involved in secondary metabolite biosynthesis, such as type I modular and iterative polyketide synthases (PKSs), type II PKSs, type III PKSs, nonribosomal peptide synthases (NRPSs), NRPS-independent siderophore (NIS) synthetases and terpene synthases (Bentley et al., 2002). The products of several of these cryptic gene clusters, including albaflavenone (**8**), geosmin (**9**), methyl-isoborneol (**10**), methylenomycin furans (MMFs) (**11**), coelichelin (**12**), desferioxamines (**13**), germicidins (**14**) and have since been discovered by a variety of approaches (Figure 1.2) (Gust et al., 2003; Lautru et al., 2005; Song et al., 2006; Corre et al., 2008; Zhao et al., 2008).

Figure 1.2 Structures of several secondary metabolites produced by *S. coelicolor* A3(2).

The production of secondary metabolites in *Streptomyces* species is regulated in different ways, including by pathway-specific transcriptional regulators, by pleiotropic mechanisms and by coordination of antibiotic production and morphological development (Bibb, 2005).

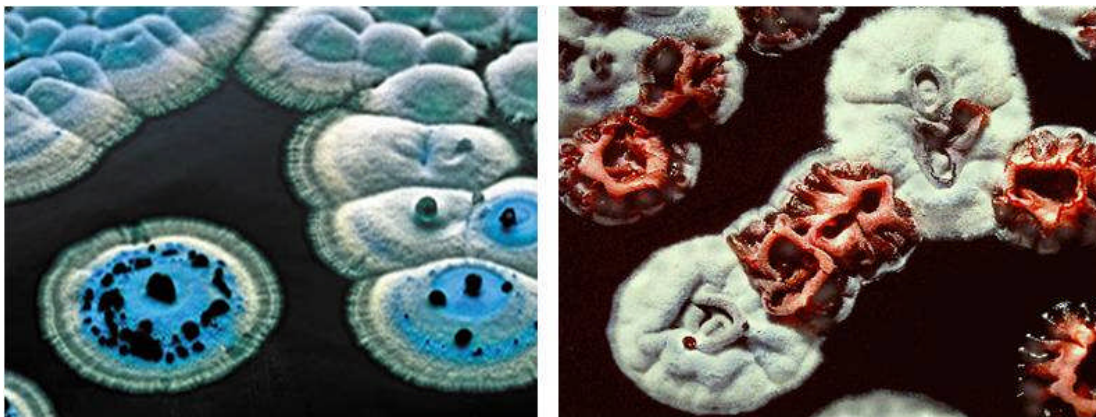


Figure 1.3 Colonies of *Streptomyces coelicolor*, left: secreting blue Actinorhodin antibiotics, right: with red pigmented mycelia due to production of Prodiginines. In both cases the colonies are covered with grey aerial mycelium and spores (John Innes Centre).

1.2.1 Prodiginines

Prodiginines are a group of red-coloured tripyrrole antibiotics produced by actinomycetes and other eubacteria. These red compounds have been linked to many historical events (Bennett and Bentley, 2000; Furstner, 2003). The first time they were reported was in the biography of Alexander the Great. During the siege of Tyre in the 332-331 BC Macedonian soldiers noticed “blood” dropping from a piece of bread. It was interpreted as a good omen, because blood would be shed within the city of Tyre, and was believed to predict victory (Furstner, 2003). Since then, this phenomenon has been observed many times, especially in bread and has been interpreted in many ways (Bennett and Bentley, 2000). Now it is known that these “miracles” are caused by living organisms, mainly *Serratia marcescens* (Figure 1.4), from which the first prodiginine, prodigiosin, was isolated (Gaughran, 1969; Bennett and Bentley, 2000).

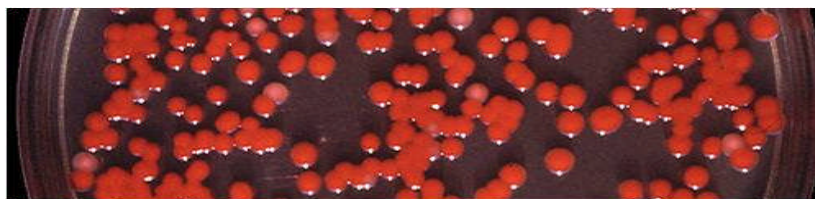


Figure 1.4 *Serratia marcescens* colonies growing on an agar plate (photo by Brudersohn).

The structural core of the prodiginines is a tripyrrole rings system, in which the rings are designated A, B and C (see prodigiosin (**15**) structure, Figure 1.5). The conjugated tripyrrole system is responsible for their characteristic intense red colour. The first member of the prodiginine family to be discovered was prodigiosin (**15**), which was first isolated in 1902, but the structure was not elucidated until 1960 by total synthesis (Bentley et al., 2002). The prodiginine family also includes undecylprodiginine (**2**) produced by *Streptomyces coelicolor* and *Streptomyces longispororuber* (Wasserman et al., 1969; Gerber, 1975), and its carbocyclic derivatives (with unusual *ansa*-bridged rings incorporating on the pyrrole C ring) streptorubin B (**3**) (produced by *S. coelicolor*) (Mo et al., 2008) and metacycloprodigiosin (**16**) (produced by *S. longispororuber*) (Wasserman et al., 1969), the biosynthesis of which (Cerdeño et al., 2001; Stanley et al., 2006; Haynes et al., 2008; Mo et al., 2008) is discussed below. In other prodiginines such as methylcyclodecylprodiginine (**17**) an alkyl chain is attached to the A and C rings to form part of a macrocycle. Prodigiosin R1 (**18**), recently isolated from *Streptomyces griseoviridis*, is another member of the prodiginine family, together with roseophilin (**19**), which contains a methoxyfuran rather than a methoxypyrrole B-ring and a chloro substituent on the A ring, and is produced by the same microorganism (Figure 1.5).

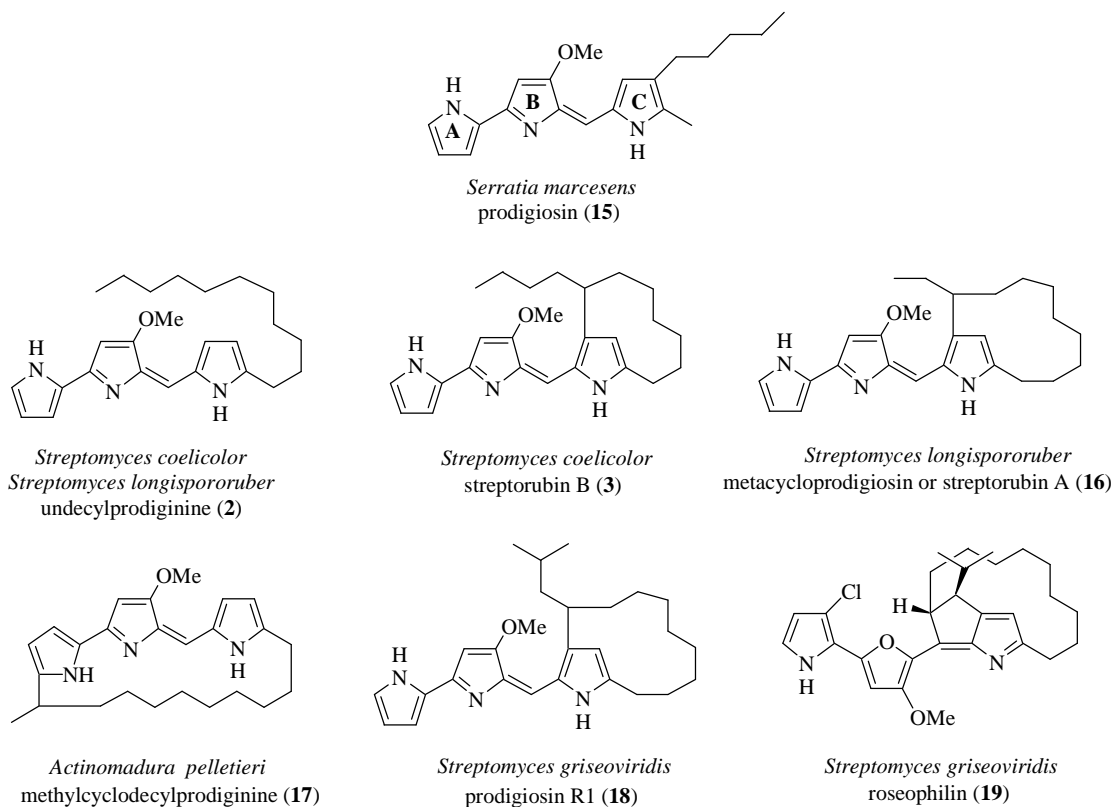


Figure 1.5 Structures of some prodiginines produced by a variety of bacteria.

There has been much recent interest in prodiginines, arising from the broad range of biological activities displayed by these antibiotics with potent immunosuppressant, antimalarial and anti-cancer properties (Williamson et al., 2007).

Several analogues of undecylprodiginine have been prepared by chemical synthesis and they show promising immunosuppressant activity at non-toxic doses (Magae et al., 1996; Lee et al., 2000). Undecylprodiginine can inhibit the proliferation of human T-cells and suppress T-cell-dependent antibody responses without damaging the lymphoid organs (Azuma et al., 2000). One undecylprodiginine analogue PNU-156804 (Figure 1.6) was shown to be equally effective but less toxic than the natural product (Mortellaro et al., 1999).

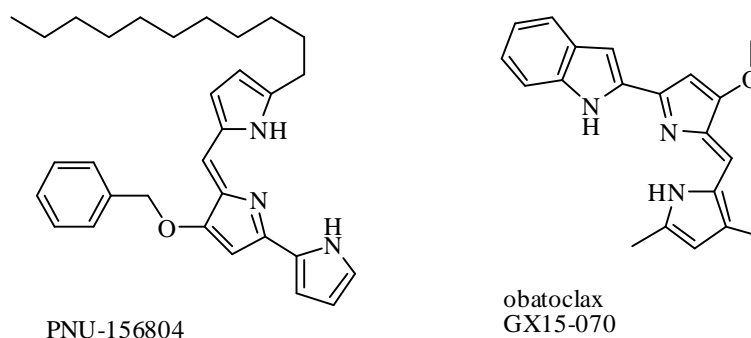


Figure 1.6 Structures of obatoclax and PNU-156804, synthetic prodiginine analogues.

Recently, the potential of prodiginines as pro-apoptotic anticancer agents became more interesting. It was shown that prodiginines have anticancer activity against many cell lines, including lung, colon, kidney and breast with little cytotoxicity against non-cancerous cells. Prodigiosin (from *Serratia marcescens*) is now in preclinical trials for the treatment of pancreatic cancer (Zhang et al., 2005). Moreover, a synthetic analogue of streptorubin B and metacycloprodigosin, obatoclax (GX15-070) (Figure 1.6), is currently in phase I and II oncology trials for leukaemia, lymphoma, lung cancer and other solid tumours (Trudel et al., 2007). Obatoclax can interact with anti-apoptotic members of the BCL-2 family of proteins, which have been shown to be overexpressed in numerous cancer cell lines, blocking the function of pro-apoptotic proteins. Apoptosis in cells treated with obatoclax is stimulated and the normal cell death process is restored (Danial and Korsmeyer, 2004; Nguyen et al., 2007).

Prodiginines also have anti-malarial activity. Interestingly, the carbocyclic undecylprodiginine derivatives are more potent than undecylprodiginine itself, particularly metacycloprodigosin which shows potent *in vitro* activity against *Plasmodium falciparum*, the causal agent of malaria (Gerber, 1975; Isaka et al., 2002).

The biosynthesis of prodiginines in *S. coelicolor* was a major focus in this thesis and is discussed in details in section 1.3.

1.2.2 Actinorhodins

Actinorhodin (**1**) (Figure 1.2) is a blue-pigmented antibiotic produced by *Streptomyces coelicolor* A3(2) (Wright and Hopwood, 1976). It belongs to a class of aromatic polyketides, the benzoizochromanequinones (BIQs), some of which possess anticancer, antibacterial, anticoccidial or platelet aggregation inhibitory properties (Brockmann et al., 1950). **1** has a characteristic pH-dependent colour. It is blue at high pH and red in acid. This results from its unique dimeric structure with two naphthazarine rings connected by a C-C bond (Hopwood, 1997).

The actinorhodin biosynthetic gene cluster, which contains twenty two genes, was the first antibiotic biosynthetic gene cluster to be cloned in its entirety. The type II PKS encoded by the cluster has been the model system for genetic and biochemical studies of bacterial aromatic type II PKSs. During actinorhodin biosynthesis, the PKS is responsible for producing a linear octaketide, which is then modified by a series of tailoring enzymes, such as ketoreductases (KRs), aromatases (AROs), cyclases (CYCs), oxygenases and others, to form the mature antibiotic (Fernandez-Moreno et al., 1992).

1.2.3 Calcium-Dependent Antibiotics (CDAs)

Calcium-dependent antibiotics (CDAs) (**4**) (Figure 1.2), produced by *S. coelicolor*, belong to a family of anionic lipo-undecapeptides that also includes daptomycin (produced by *Streptomyces roseosporus*) and friulimicins (produced by *Actinoplanes friuliensis*) (Debono et al., 1988; Vertesy et al., 2000). CDAs were identified as meta-

bolic products of *S. coelicolor* in 1978 (Lakey et al., 1983). They are composed of eleven amino acid residues linked to a six-carbon fatty acid chain and they require calcium ions for their antibacterial activity (Kempter et al., 1997).

The 82 kb CDA biosynthetic gene cluster consists of forty genes, with twenty genes proposed to be involved in the biosynthesis of CDA, three in the regulation of biosynthesis, four in self-resistance and thirteen with no identified function (Hojati et al., 2002). CDAs are biosynthesised by three NRPSs, a fatty acid synthase and enzymes involved in precursor biosynthesis and tailoring of the peptide (Hojati et al., 2002).

CDAs are effective against a wide range of Gram-positive bacteria and have been reported to induce the formation of cation specific channels within bacterial membranes (Lakey et al., 1983), resulting in membrane depolarisation leading to cell death. Daptomycin, which works by a similar mechanism (active against methicillin-resistant *Staphylococcus aureus* and vancomycin-resistant *Enterococci*), has recently been approved for clinical treatment of skin and soft tissue infections (Jung et al., 2004).

1.2.4 Coelichelin

Siderophores are small organic molecules produced by many microorganisms to sequester ferric iron from the environment. Iron is required for essential processes in cells such as respiration and DNA synthesis (Wandersman and Delepelaire, 2004). It was reported by Imbert *et al.* that under iron-deficient conditions *S. coelicolor* produces the hydroxamate siderophores desferrioxamines G and E (Imbert et al., 1995). A more recent report from the Challis group showed desferrioxamines B and E (**13**) (Figure 1.2) are produced (Barona-Gomez et al., 2006). The hydroxamate siderophore coelichelin was predicted to be produced from a bioinformatics analysis of the *S. coelicolor* genome

sequence (Challis and Ravel, 2000) and was subsequently isolated and structurally characterised (Lautru et al., 2005). Coelichelin (**12**) (Figure 1.2) is biosynthesised by enzymes encoded by the *cch* gene cluster (Challis and Ravel, 2000). This cluster encodes an NRPS (CchH) containing three modules that was predicted to catalyse the condensation of three amino-acid residues: *N*-formyl-*N*-hydroxyornithine, threonine and *N*-hydroxyornithine, in this order to form a tripeptide (Challis and Ravel, 2000). However, structural analyses of isolated coelichelin showed that it is a tetra-peptide rather than a tri-peptide, leading to the hypothesis that the first B module is used iteratively to incorporate to molecules of *N*-formyl-*N*-hydroxyornithine into coelichelin (Lautru et al., 2005).

It was shown by Barona-Gómez et al. (2006) that at least one of desferrioxamine B, desferrioxamine E and coelichelin is required for growth of *S. coelicolor* on a xeno-siderophore-free colloidal silica medium.

1.2.5 Grey Spore Pigment

The colour of the spores in *S. coelicolor* arises from the production of grey pigmented compounds during sporulation (Davis and Chater, 1990). The *whiE* gene cluster, which direct biosynthesis of the grey spore pigment, contains eight genes including a minimal type II PKS (Davis and Chater, 1990). Normally the *whiE* genes are transcribed just before sporulation in the aerial mycelium (Yu and Hopwood, 1995). The polyketide nature of the pigments was proposed based on analyses of mutants of the *whiE* cluster. However the spore pigments have never been isolated, perhaps because they are covalently attached to macromolecular components of the spore (Kelemen et al., 1998).

1.2.6 Methylenomycins

Methylenomycins A and B were first isolated in 1974 from *S. violaceoruber* (Haneishi et al., 1974). Methylenomycin B was subsequently demonstrated to result from the spontaneous degradation of methylenomycin A in acidic conditions (Corre and Challis, 2005). Two methylenomycins were also shown to be produced by *S. coelicolor* A3(2): methylenomycin A (**5**) and its desepoxy-4,5-dehydro derivative, methylenomycin C (**6**) (Figure 1.2) (Wright and Hopwood, 1976; Hornemann and D.A., 1978). All twenty one genes responsible for the self-resistance to, regulation of production of and biosynthesis of these compounds in *S. coelicolor* A3(2) are clustered (*mmy* gene cluster) and are located on the large linear plasmid SCP1, which is not essential for *S. coelicolor* growth (Kirby and Hopwood, 1977; Bentley et al., 2004). Labelling experiments demonstrated that methylenomycins derive from two acetate units and one pentulose unit (a very unique combination of biosynthetic precursors), which are condensed to form the common 4,5-dimethyl-3-oxo-2-methylene cyclopentane carboxylic acid core of **5** and **6** (Corre and Challis, 2005).

Methylenomycin A exhibits a wide spectrum of activity against Gram-positive bacteria and some Gram-negative strains, especially *Proteus* species. A mechanism of resistance to methylenomycins was discovered as early as 1975; however the mode of action of these antibiotics remains unclear (Haneishi et al., 1974).

1.2.7 γ -Butyrolactones (GBLs)

γ -Butyrolactones are low molecular-weight molecules produced by actinomycetes. They induce secondary metabolism, morphological development and other

ecological responses (Takano, 2006). *S. coelicolor* A3(2) produces at least seven GBLs. SCB1 (7) (Figure 1.2) is the most studied one and is proposed to directly control the expression of a pathway-specific regulatory gene in the cryptic type I PKS gene cluster *cpk* (Takano et al., 2000; Takano et al., 2005). GBLs are derived from intermediates of fatty acid biosynthesis and require the FAS ACP for their biosynthesis.

1.2.8 Methylenomycin Furans (MMFs)

Within the *mmy* gene cluster responsible for the biosynthesis of the methylenomycins there is an operon of three genes, *mmfLHP*. These genes direct the biosynthesis of MMFs (11) (Figure 1.2) signalling molecules which induce the methylenomycins production in *S. coelicolor* A3(2). The biological function of MMFs is analogous to GBLs. They are derived from the same primary metabolic precursors and a key step in their biosynthesis is directed by homologous enzymes (Corre et al., 2008).

1.2.9 Germicidins

Germicidins (14) (Figure 1.2) can inhibit germination of streptomycete spores. Five of them were recently discovered in the *S. coelicolor* as the products of the type III PKS. Germicidins catalyse elongation of specific β -ketoacyl-ACP thioester intermediates in fatty acid biosynthesis with ethyl- or methylmalonyl-CoA and subsequently cyclisation of the resulting triketide (Song et al., 2006). Like AHFCAs and GBLs, germicidins require the FAS ACP for their biosynthesis as they are derived from intermediates in fatty acid biosynthesis.

1.2.10 Geosmin and 2-Methyl-isoborneol

Geosmin (**9**) and 2-methyl-isoborneol (**10**) (Figure 1.2) are responsible for the characteristic odour of moist soil as well as musty or muddy off-taste of drinking water and food products. They are produced by a number of microorganisms, mainly by streptomycetes but as well as by cyanobacteria, myxobacteria and fungi. Geosmin and 2-methyl-isoborneol have an exceptionally low threshold for human detection of the order of 10-100 ppt. making its detection and elimination important in the management of water and food quality (Jiang et al., 2006; Jiang et al., 2007; Wang and Cane, 2008).

The formation of **9** and **10** is catalysed by a single terpene synthases. Therefore, they do not require ACPs for their biosynthesis (Jiang et al., 2006; Jiang et al., 2007; Wang and Cane, 2008).

1.2.11 Albaflavenone

The biosynthesis of the recently discovered antibiotic albaflavenone (**8**) (Figure 1.2) is directed by a two-gene cluster. The *sco5222* gene encodes for a sesquiterpene cyclase that catalyses the cyclisation of farnesyl diphosphate (universal sesquiterpene synthase substrate) to the novel tricyclic hydrocarbon, epi-isozizaene. The product of *sco5223* gene then catalyses the two step allylic oxidation of epi-isozizaene to form albaflavenone. This antibiotic does not require ACPs for biosynthesis (Zhao et al., 2008).

1.2.12 Post Translational Phosphopantetheinylation of Carrier Proteins (CPs) During Secondary Metabolite Biosynthesis

All fatty acid synthases involved in primary metabolism, as well as polyketide synthases (PKSs) and nonribosomal peptide synthases (NRPSs) involved in secondary metabolism, require post-translational modification of their constituent carrier protein (CP) domain(s) in order to become active (Figure 1.7) (Lambalot et al., 1996).

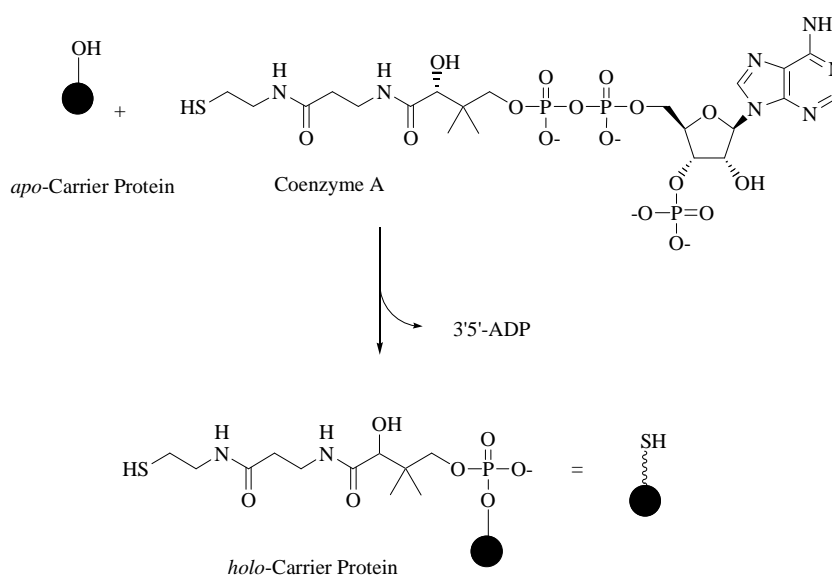


Figure 1.7 Reaction catalysed by PPTases. The *apo* form is termed inactive form, without the arm and the *holo* form is called active form, with phosphopantetheinyl arm attached.

During the activation reaction, the phosphopantetheinyl transferase catalyses the attack of a conserved serine residue in the carrier protein on the diphosphate group of coenzyme A. 3',5'-adenosine diphosphate (ADP) is released and the *holo*-carrier protein with a phosphopantetheine thiol group is generated (Figure 1.7) allowing biosynthetic intermediates to be bound to the carrier proteins by a thioester bond and modified by the other synthase activities prior to acyl or peptide chain extension (Walsh et al., 1997).

PPTases can be classified in two categories: AcpS-type and Sfp-type (Lambalot et al., 1996; Reuter et al., 1999). The AcpS-type is responsible for primary metabolism, catalysing phosphopantetheinylation of ACPs required for fatty acid biosynthesis and representatives are present in almost every microorganism (Mofid et al., 2002). The Sfp-type plays a role in secondary metabolism and demonstrates extraordinarily broad substrate specificity (Mofid et al., 1999).

Three genes encoding putative PPTase enzymes were identified within the *S. coelicolor* chromosome: one AcpS-type SCO4744 (AcpS) and two Sfp-type, SCO5883 (RedU) and SCO6673 (Cox et al., 2002). SCO4744 is expected to play a role in fatty acid biosynthesis and is hypothesised to be essential for *S. coelicolor* growth. It was proposed by Cox et al. (2002) to possess unusually broad substrate specificity, catalysing phosphopantetheinylation of a large variety of *S. coelicolor* ACPs. The *redU* gene is located within the *red* gene cluster and is the only *S. coelicolor* PPTase gene that is clustered with genes that direct biosynthesis of a metabolite. RedU was shown to be involved for prodiginine biosynthesis, it is only required to activate the ACP RedO (Stanley et al., 2006). SCO6673 shows high similarity to SePptII from *Saccharopolyspora erythraea*, which was shown to be a PPTase involved in erythromycin biosynthesis (Weissman et al., 2004). Thus, SCO6673 was proposed to be a PPTase and was recently shown to be required for CDA biosynthesis (Lu et al., 2008).

Because in the *S. coelicolor* genome there are just three PPTase-encoding genes, but there are many compounds produced, that require active CPs for their biosynthesis, it is expected that these enzymes are multifunctional and can activate a wide range of CPs (Cox et al., 2002).

1.3 Biosynthesis of Prodiginines in *Streptomyces* Species

1.3.1 Early studies of prodiginine biosynthesis and identification of the *red* gene cluster in *S. coelicolor* A3(2)

Early studies of prodiginine biosynthesis were carried out on undecylprodiginine and metacycloprodigiosin in *S. longispororuber* (Wasserman et al., 1969). The precursors of undecylprodiginine and metacycloprodigiosin were investigated by incorporation experiments using ^{13}C -labelled precursors (Wasserman et al., 1973; Wasserman et al., 1974; Gerber et al., 1978). The results of these experiments led to the hypothesis that in *S. coelicolor* undecylprodiginine (**2**) is made by the condensation of the two putative intermediates 4-methoxy-2,2'-bipyrrole-5-carboxaldehyde (MBC) (**20**) and 2-undecylpyrrole (2-UP) (**21**) (Cerdeño et al., 2001). In *S. longispororuber* 2-UP-derived portion of undecylprodiginine is generated from seven units of acetate and a unit of glycine (with loss of the carboxyl group) and MBC-derived portion of undecylprodiginine is generated from one unit each of acetate, L-proline and L-serine (again with loss of the carboxyl group). Butyl-*meta*-cycloheptylprodiginine (streptorubin B) (**3**) is proposed to be formed from undecylprodiginine by an oxidative cyclisation (Wasserman et al., 1969; Cerdeño et al., 2001).

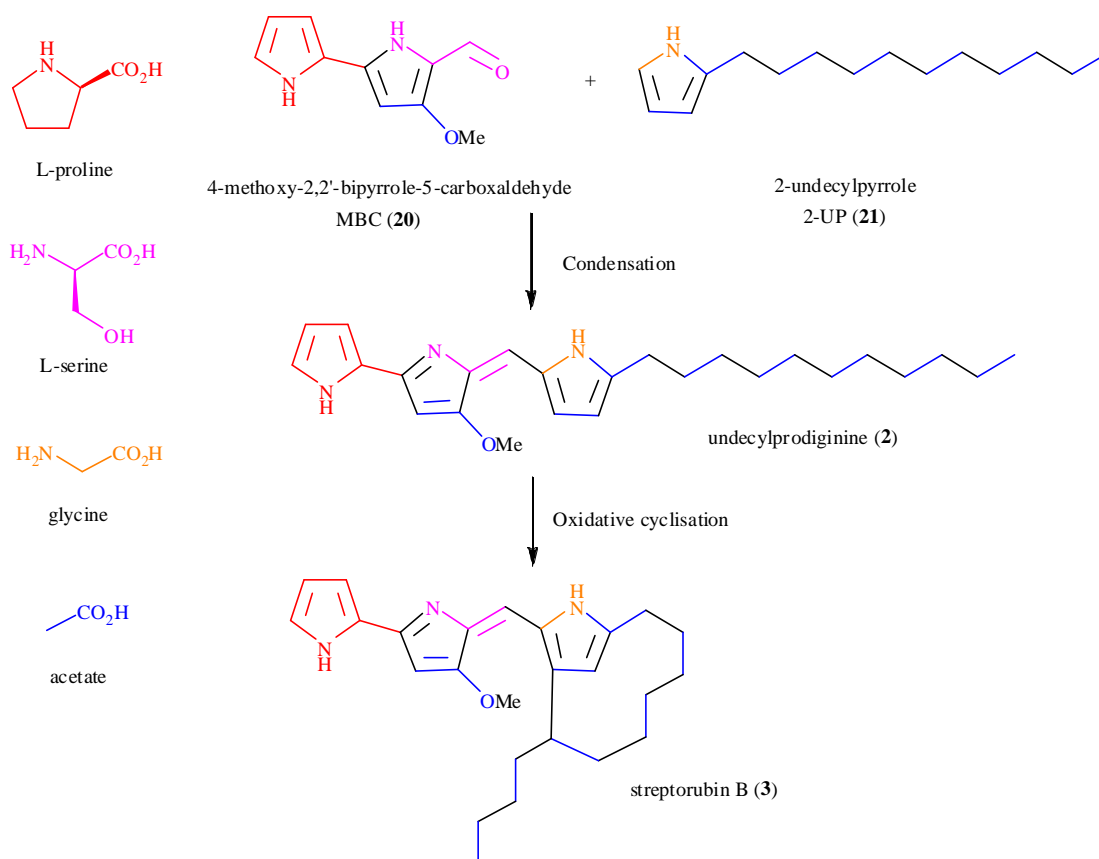


Figure 1.8 Proposed biosynthetic origin of undecylprodiginine and its cyclic derivative streptorubin B in *S. coelicolor*.

The prodiginine biosynthetic gene cluster (the *red* cluster) was identified in the 1970s by Rudd and Hopwood (Rudd and Hopwood, 1980) and cloned and expressed in a heterologous host (in 1990) by Malpartida and Hopwood (Malpartida et al., 1990). The sequence of the *red* cluster became available in 2001 when the *Streptomyces coelicolor* A3(2) genome sequence was published (Bentley et al., 2002). This allowed bioinformatics analysis of the protein sequences encoded by genes within the cluster (Cerdeño et al., 2001). The predicted biosynthetic proteins belong to different families, including FASs,

type I PKSs, NRPSs, α -oxoamine synthases (OASs), phosphate pyruvate dikinase/phosphoenol pyruvate synthase (PPDK/PEPS) and Rieske oxygenases.

The *red* cluster contains twenty three genes, which are arranged in four transcription units (Figure 1.9). The complete cluster is contained within two overlapping cosmid clones (Sc2E9 and Sc3F7) from the *S. coelicolor* ordered genomic cosmid library (Redenbach et al., 1996; Cerdeño et al., 2001). Putative functions of the products of most of the genes were suggested on the basis of sequence comparisons and this led to a proposed biosynthetic pathway (Cerdeño et al., 2001), which has subsequently been revised in the light of experimental evidence, mainly from gene deletion experiments (Stanley et al., 2006; Haynes et al., 2008; Mo et al., 2008).

Two genes from the cluster (*redD* and *redZ*) encode pathway specific regulators (Narva and Feitelson, 1990; White and Bibb, 1997; Guthrie et al., 1998). At the outset of this work six genes were known to be required for the biosynthesis of MBC (**8**) (Stanley et al., 2006), and four genes were known to be involved in the biosynthesis of 2-UP (**9**) (Mo et al., 2005; Mo et al., 2008). The *redH* gene was hypothesised to be responsible for the condensation of MBC and 2-UP to give undecylprodiginine (Stanley, 2007) and the *redG* gene was proposed to be required for the oxidative cyclisation of undecylprodiginine to form streptorubin B (Cerdeño et al., 2001). Three genes (*redE*, *redF* and *redY*) appear not to be required for prodiginine biosynthesis (Cerdeño et al., 2001; Barry, 2007; Stanley, 2007). Two genes (*redT* and *redS*) are of unknown function, but the latter appears to encode a truncated, non functional protein (Cerdeño et al., 2001). The roles of the *redJ*, *redV*, *redI* and *redK* genes of *S. coelicolor* in prodiginine biosynthesis had not been experimentally investigated.

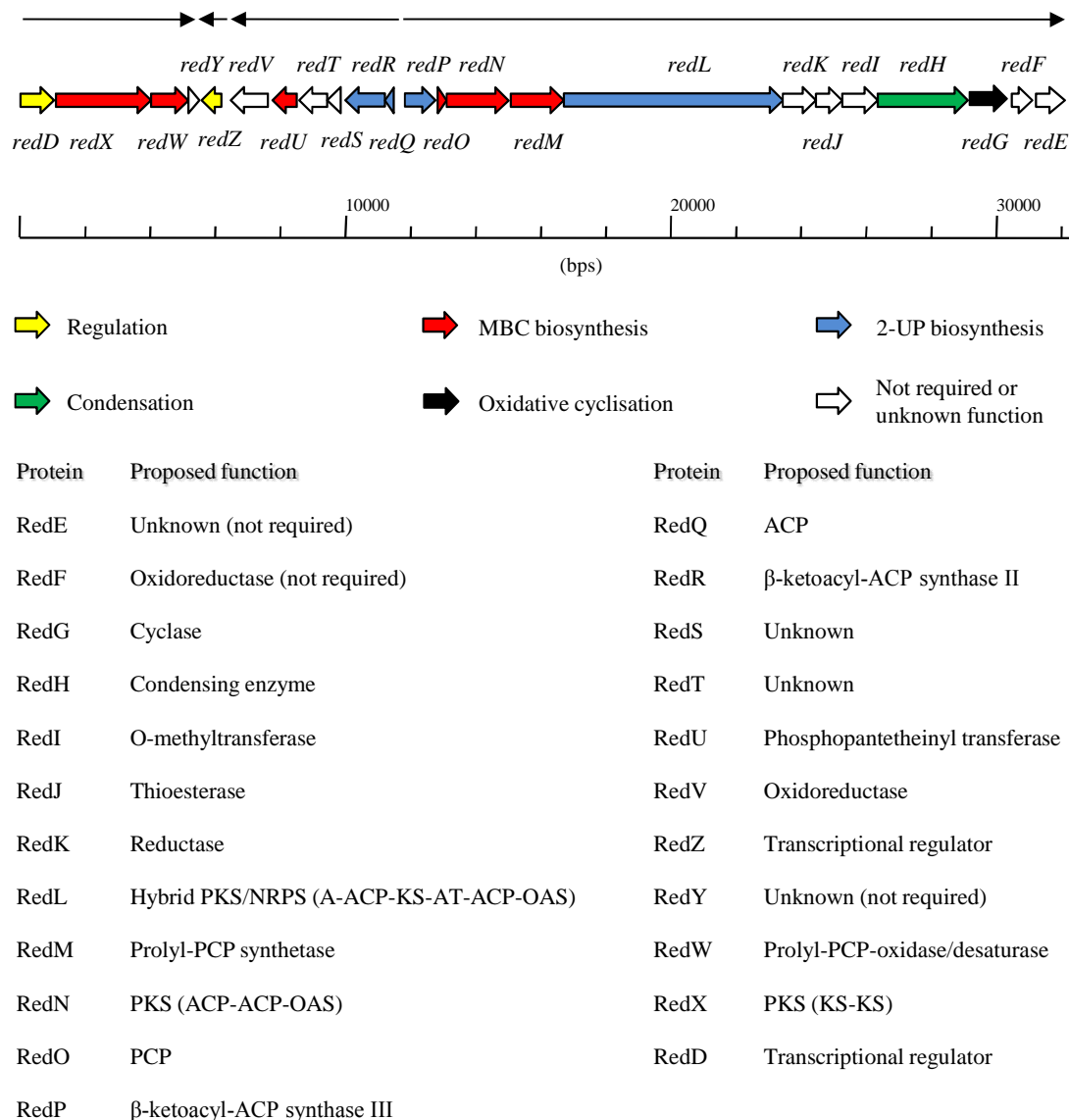


Figure 1.9 Organisation of the *red* cluster in *S. coelicolor* with proposed functions of encoded proteins. Arrows indicate four transcription units within the cluster.

1.3.2 The *red* Cluster Encodes Enzymes that Are Similar to those Involved in the Biosynthesis of Other Metabolites.

1.3.2.1 Fatty Acid Synthases (FASs)

In bacteria fatty acids are derived from an acyl-CoA starter unit by addition of several two-carbon units. During fatty acid biosynthesis, acetyl-CoA is converted to malonyl-CoA, by condensation of bicarbonate with acetyl-CoA in a reaction catalysed by acetyl-CoA carboxylase (ATP-dependent reaction with biotin as a cofactor). Malonyl-CoA is then loaded onto an acyl carrier protein (ACP) in a reaction catalysed by malonyl-CoA:ACP transacylase (MCAT). The acyl-CoA starter unit (acetyl-CoA in *E. coli* and primarily isobutyryl-, 2-methylbutyryl-, or isovaleryl-CoA in *Streptomyces*) is then loaded onto β -ketoacyl-ACP synthase III (KASIII) and condensed with the malonyl-ACP to yield β -ketobutyryl-ACP. The β -keto group is reduced to the corresponding alcohol by β -ketoacyl-ACP reductase in a NADPH-dependent reaction and this is followed by dehydration catalysed by β -hydroxyacyl-ACP dehydratase. Final reduction by enoyl-ACP reductase gives butyryl-ACP (Figure 1.10) (McMurry and Begley, 2005).

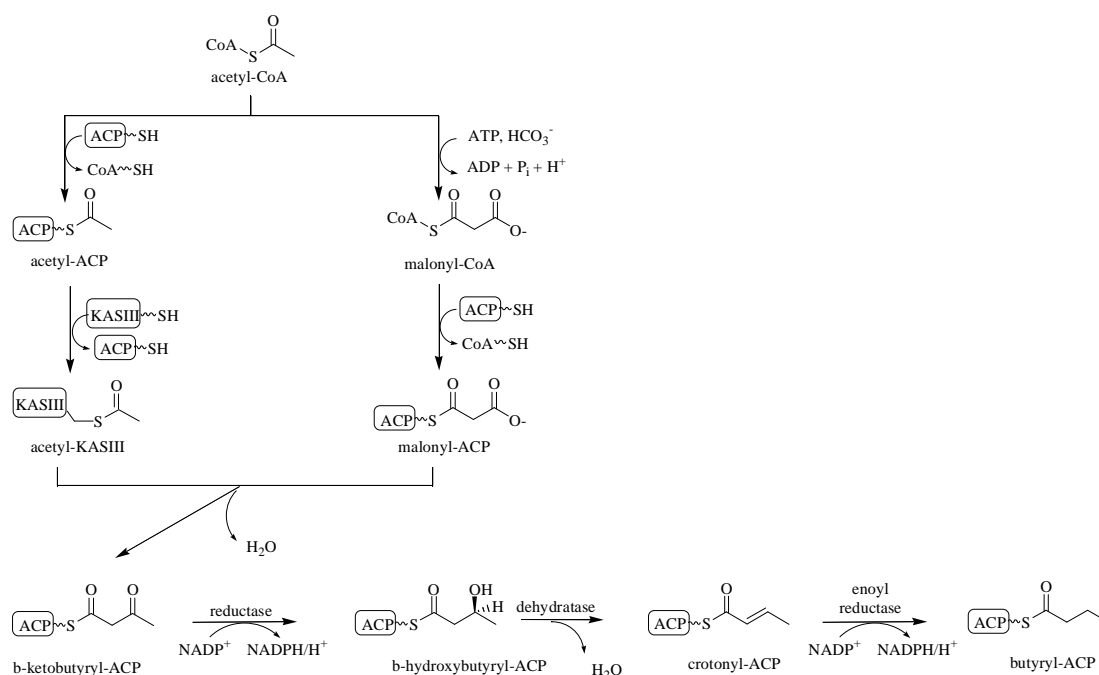


Figure 1.10 The fatty acid biosynthetic pathway of *E. coli* from the two carbon precursor, acetyl-CoA. In *Streptomyces* species primarily isobutyryl-, 2-methylbutyryl-, isovaleryl-CoA are used instead of acetyl-CoA.

The butyryl-ACP intermediate is condensed with another malonyl-ACP in a reaction performed by β -ketoacyl-ACP synthase II (KASII), to yield a β -keto-hexanoyl-ACP intermediate that undergoes reduction and dehydration as before. Further repetitions of this catalytic cycle add two more carbons to the chain each time until the chain reaches the required length, which is sensed by KASII (Figure 1.11) (McMurry and Begley, 2005).

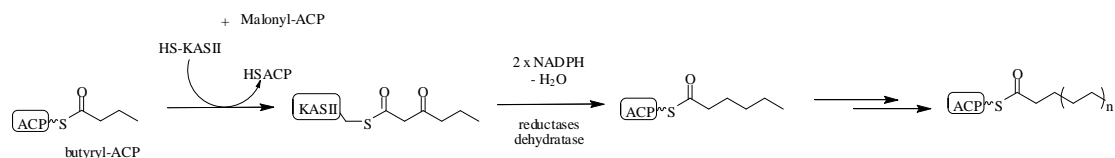


Figure 1.11 Elongation of fatty acid chain by KASII.

In early studies on the prodiginine biosynthetic pathway, it was proposed that 2-undecylpyrrole (**21**) was biosynthesised by condensation of one unit of a β -ketomyristoyl thioester, generated from seven units of acetate and one unit of glycine (Wasserman et al., 1973; Gerber et al., 1978). Following this suggestion, three genes from the *red* cluster, *redP*, *redR* and *redQ*, encoding homologues of FabH (KASIII), FabF (KASII) and ACP, respectively (components of the fatty acid synthase (FAS) in streptomycetes) were proposed to initiate **21** biosynthesis by generating a dodecoyl chain attached to the RedQ-ACP (Rock and Cronan, 1996; Cerdeño et al., 2001). Mo et al. showed that when *redP*, *redR* and *redQ* are deleted, prodiginine production was reduced but not abolished, suggesting that the elongation steps of dodecanoyl-RedQ biosynthesis could be catalysed by FabH and FabF (from primary metabolism) but that the efficiency and selectivity is reduced. This led to branched chain prodiginine analogues derived from isovaleryl, isobutyryl and 2-methylbutyryl starter units (Mo et al., 2005; Mo et al., 2008).

1.3.2.2 Polyketide Synthases (PKSs)

Like fatty acids, polyketides are derived from the Claisen condensation of extender units (malonyl-, methylmalonyl- or ethylmalonyl-CoA) with an acyl-CoA starter unit. Once the carbon chain is assembled it is released from the enzyme and further transformations can be carried out to give the final product (McMurry and Begley, 2005). Structural differences between naturally occurring polyketides result largely from differences in the polyketide synthases such as use of different starter units, different numbers and types of extender unit and different biosynthetic reactions during

chain assembly e.g. reduction and cyclisation (Figure 1.12) (Cortes et al., 1995; McMurry and Begley, 2005).

The different architectural organisation of PKS proteins has led them to be classified into three types. Type I PKSs contain multiple catalytic domains in a single protein where as in type II PKSs each catalytic activity resides in an independent protein. Type III PKSs use acyl-CoA substrates directly without the involvement of an acyl carrier protein. There are many hybrid of typeI/typeII PKS systems as well as hybrid type I PKS/nonribosomal peptide synthetases known (Saxena et al., 2003; Foerstner et al., 2008).

The model example of a type I polyketide synthase involves the biosynthesis of the antibiotic erythromycin in *Saccharopolyspora erythrea* (McGuire et al., 1952; Weber et al., 1990). 6-deoxyerythronolide B (6-dEB), the polyketide core of erythromycin, is biosynthesised by three modular type I PKSs, designated DEBS I, II and III, which collectively consist of a loading module, to incorporate the first acyl group into the six polyketide chain extension modules to add six further acyl groups to the polyketide chain, and a termination domain to release the polyketide product. The loading module consists of acyl transfer (AT) and acyl carrier protein (ACP) domains and each extension module has a minimum of three domains: an AT, an ACP and a ketosynthase (KS). The acyl-CoA starter unit (propionyl-CoA for erythromycin biosynthesis) is loaded onto the AT domain of the loading module and is then transferred to the adjacent ACP domain. During chain extension, the module I AT domain loads an extender unit (methylmalonate for erythromycin biosynthesis), transfers it to the ACP domain within the same module, and the KS domain catalyses a Claisen condensation reaction between

this acyl-ACP and the acyl-ACP in the upstream loading module to extend the chain. Some extension modules contain additional domains like a ketoreductase (KR), a dehydratase (DH) and an enoyl reductase (ER). At the C-terminal end of DEBSIII, a thioesterase (TE) domain releases the product from the multienzyme by catalysing a cyclisation to give the macrocyclic lactone 6-dEB (Figure 1.12) (Staunton and Wilkinson, 1997; McMurry and Begley, 2005).

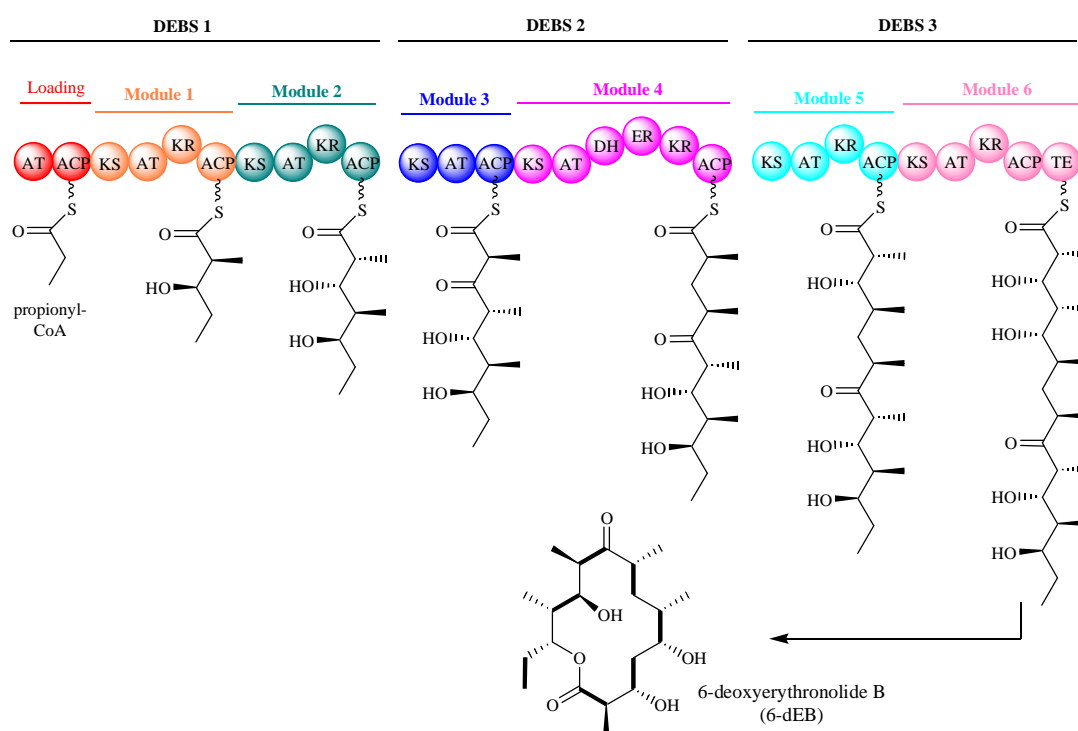


Figure 1.12 Domain organisation of the DEBS modular PKS and proposed biosynthetic intermediates in the assembly of 6-dEB. Domains are as follows: AT – acyltransferase, ACP – Acyl Carrier Protein, KS – ketosynthase, KR – ketoreductase, DH – dehydratase, ER – enoylreductase, TH – thioesterase.

1.3.2.3 Nonribosomal Peptide Synthetases (NRPSs)

Nonribosomal peptide synthetases are multifunctional proteins that direct the biosynthesis of nonribosomal peptide secondary metabolites, produced mainly by bacteria and fungi (Challis et al., 2000). NRPSs catalyse the condensation of proteino-

genic and non-proteinogenic amino acids as well as D-amino acids to form peptides. In many cases NRPSs work in conjunction with polyketide synthases to give hybrid products (Ansari et al., 2004).

Usually each NRPS chain elongation module consists of three domains: adenylation (A) domain, thiolation (T) domain (PCP domain) and condensation (C) domain. A loading module (containing just A and T domains) and a chain terminating TE domain, completes the common NRPS architecture, although there are exceptions. Specialised domains within elongation modules, such as epimerisation (E), methylation (M) and reduction (R) domains can carry out modifications to the growing peptide chain and add to the diversity of possible peptide products (Finking and Marahiel, 2004). During nonribosomal peptide biosynthesis, the A domains select each amino acid that is incorporated and after activation as an amino acyl adenylate, transfers it to the adjacent T domain. The amino acid loaded onto the T domain is condensed with an amino acid loaded onto the T domain of the following module by the C domain. The last module usually contains a TE domain, which hydrolyses the thioester, or catalyses cyclisation, to release the finished polypeptide from the NRPS (Figure 1.13) (Donadio et al., 2007).

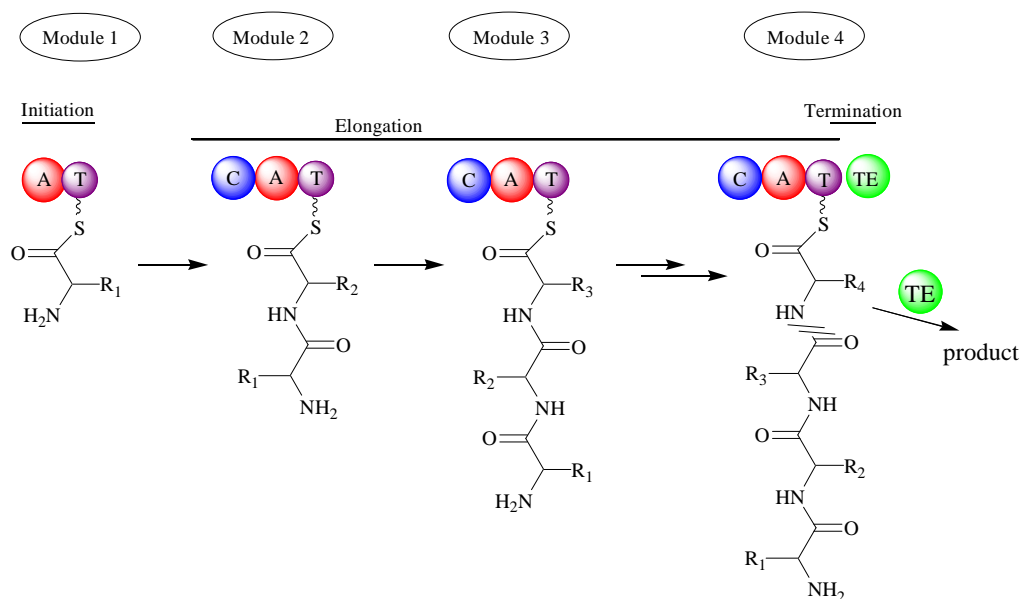


Figure 1.13 Basic steps during nonribosomal biosynthesis of peptides, domains: A – adenylation, T (PCP) – thiolation, C – condensation, TE – thioesterase.

Among the genes responsible for prodiginine biosynthesis, there are two that encode PKS-like enzymes involved in MBC biosynthesis: RedX and RedN. One PKS-NRPS hybrid (RedL) is involved in 2-UP biosynthesis. RedX contains two ketosynthase domains which are similar (~30%) to the KS domain of type I modular PKSs and also to each other (29%). The C-terminal RedX KS domain contains a cysteine residue in the conserved active site and the N-terminal domain has aspartate in this position. RedN is predicted to consist of three domains: two ACP domains with conserved serine residues, in the N-terminal region of RedN and a C-terminal α -oxoamine synthase (OAS) domain (Cerdeño et al., 2001; Stanley et al., 2006).

RedL is a PKS-NRPS hybrid and consists of six domains. The N-terminal A domain is homologous to NRPS adenylation domains. Adjacent to the A domain is an ACP domain followed by a KS, AT and another ACP domain, all of which are homolo-

gous to the type I PKS domains. The C-terminal α -oxoamine synthase (OAS) domain is similar to the C-terminal OAS domain of RedN (34% identity) (Cerdeño et al., 2001; Mo et al., 2008).

α -Oxoamine synthases are pyridoxal phosphate (PLP)-dependent enzymes, which are mainly involved in the biosynthesis of amino acids, amino-acids derived metabolites and other amine-containing metabolites. PLP-dependent enzymes act on amino acids and can catalyse a variety of reactions, including transfer of the amino group, decarboxylation, racemisation, elimination or replacement of groups at the α -, β - or γ -carbon (Percudani and Peracchi, 2003).

The archetype example of an OAS is 8-amino-7-oxononanoate synthase (AONS) involved in biotin biosynthesis, also known as vitamin H or B₇. AONS catalyses the condensation of alanine with pimeloyl-CoA, followed by decarboxylation of the α -amino- β -o acid (Figure 1.14) (Eliot and Kirsch, 2004).

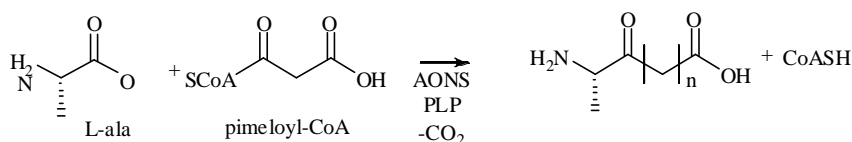


Figure 1.14 Reaction catalysed by 8-amino-7-oxononanoate synthase (AONS).

1.3.3 2-Undecylpyrrole Biosynthesis

The original proposition by Cerdeño *et al.* that RedP, RedQ, and RedR, together with enzymes from fatty acids biosynthesis, are involved in the assembly of a dodecanoyl thioester attached to the RedQ ACP still is supported by the available

experimental evidence (Cerdeño et al., 2001; Mo et al., 2005; Mo et al., 2008). Dodecanoyl-RedQ was proposed to be transformed to 2-UP by the complex of PKS-like proteins RedX and RedN (Cerdeño et al., 2001). More recent work has shown that RedL is involved in the assembly of 2-UP (probably from dodecanoic acid) and that RedN and RedX are required for MBC biosynthesis (Stanley et al., 2006; Mo et al., 2008).

Formation of dodecanoyl-ACP starts from RedP, which generates an acetoacyl thioester by decarboxylative condensation of an acetyl-CoA starter unit with a malonyl-ACP extender unit (attached to RedQ). Presumably, appropriate primary metabolic FAS enzymes would then convert the resulting acetoacetyl thioester to butyryl-ACP by ketoreduction, dehydration and enoylreduction. RedR could then carry out four subsequent chain extension steps with malonyl units, using the appropriate FAS enzymes to catalyse the reduction to the alkyl chain after each round of chain extension, resulting in dodecanoyl-RedQ (Cerdeño et al., 2001; Mo et al., 2005; Mo et al., 2008).

In the next step, the dodecanoyl group must be transferred from RedQ to the first ACP domain of RedL. There are two possible ways for this transfer to occur: via direct trans-acylation from RedQ, or via hydrolysis of dodecanoyl-RedQ to give dodecanoic acid (**22**), which is subsequently loaded onto the first RedL ACP domain after activation as an adenylate, catalysed by the A domain in RedL. If the transfer took place via the second mechanism, a specific hydrolase would be required to cleave the thioester bond in dodecanoyl-RedQ, which could be encoded by *redJ* gene (Figure 1.15) (Cerdeño et al., 2001; Mo et al., 2008).

The dodecanoyl thioester on the first ACP domain of RedL would be condensed with a malonyl thioester attached to the second ACP domain of RedL in reaction catalysed by the ketosynthase (KS) domain of RedL and β -ketomyristoyl-ACP would be generated. The pyridoxal 5'-phosphate (PLP)-dependent OAS domain of RedL could then catalyse decarboxylative condensation of β -ketomyristoyl-ACP with glycine. Spontaneous cyclisation and elimination of water would lead to 4-keto-2-undecylpyrroline (**23**). RedK is proposed to catalyse reduction of the keto group of this intermediate in an NAD(P)H dependent reaction to yield 2-undecylpyrrole (**21**) (Figure 1.15) (Cerdeño et al., 2001; Williamson et al., 2005; Mo et al., 2008).

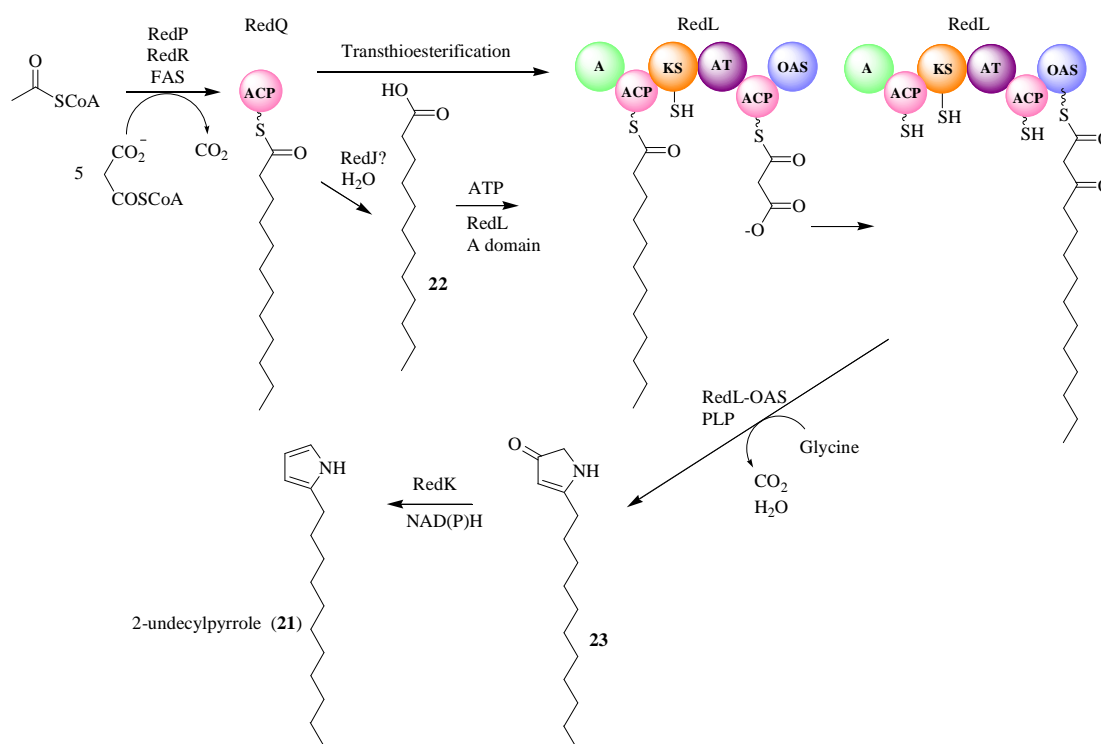


Figure 1.15 Proposed 2-undecylpyrrole (**21**) biosynthesis.

1.3.4 4-methoxy-2,2'-bipyrrole-5-carboxaldehyde (MBC) Biosynthesis

4-methoxy-2,2'-bipyrrole-5-carboxaldehyde (MBC) has been shown to be an intermediate in the prodiginine biosynthetic pathway in *Streptomyces* species as well as in prodigiosin biosynthesis in *Serratia* species (Williamson et al., 2005). Prodigiosin is known to be generated by condensation of MBC (**20**) and 2-methyl-3-amyl pyrrole (MAP) (**24**) (Williamson et al., 2005) (Figure 1.16). Because the monopyrrole precursor is different in these two pathways, but the **20** moiety is common to both, it can be proposed, that genes from prodiginine *red* cluster that show high similarity to genes from the prodigiosin biosynthetic gene cluster (*pig* cluster), could encode homologous gene products involved in analogous biosynthetic steps.

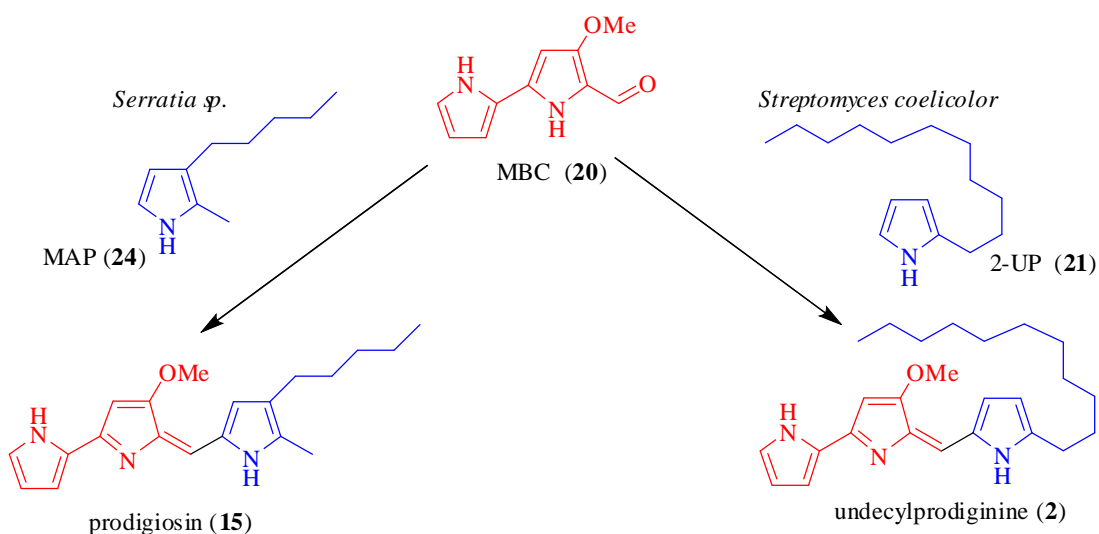


Figure 1.16 MBC (**20**) intermediate, common in prodigiosin and undecylprodiginine biosynthesis.

A mechanism for MBC biosynthesis in *S. coelicolor* was proposed by Cerdeño et al. (2001) and Thomas et al. (2002) and a similar mechanism was later proposed for biosynthesis of MBC in *Serratia* sp. by Harris et al. (Harris et al., 2004). Later, a revised

mechanism for MBC biosynthesis in *Serratia sp.* was proposed by Williamson et al. (2005) and in *S. coelicolor* by Stanley et al. (2006).

The carboxyl group of L-proline is adenylated by RedM to form an amino-acyl adenylate, which is then loaded onto the phosphopantetheine arm of the peptidyl carrier protein (PCP) RedO. L-prolyl-RedO is then dehydrogenated by the oxidase RedW in an FAD-dependent reaction and pyrrole-2-carboxyl-RedO is generated (Thomas et al., 2002). The pyrrole-2-carboxyl group attached to RedO is then transferred to the C-terminal ketosynthase (KS) domain of RedX. Pyrrole-2-carboxyl-RedX is condensed with a malonyl group attached to one of the two acyl carrier protein (ACP) domains in RedN to give the corresponding β -ketoacyl-ACP-thioester. Decarboxylative condensation of L-serine with the RedN ACP-thioester is then catalysed by the C-terminal α -oxoamine synthase (OAS) domain of RedN, resulting in its release from the ACP. The resulting amino diketone is proposed to undergo spontaneous cyclisation and dehydration to give 4-hydroxy-2,2'-bipyrrole-5-methanol (HBM) (**25**). In the final steps of the MBC pathway, SAM-dependent methylation of the pyrrole hydroxyl group catalysed by RedI and oxidation of the remaining hydroxyl group by a currently undefined enzyme (possibly RedV) would give 4-methoxy-2,2'-bipyrrole-5-carboxaldehyde (MBC) (**20**) (Figure 1.17).

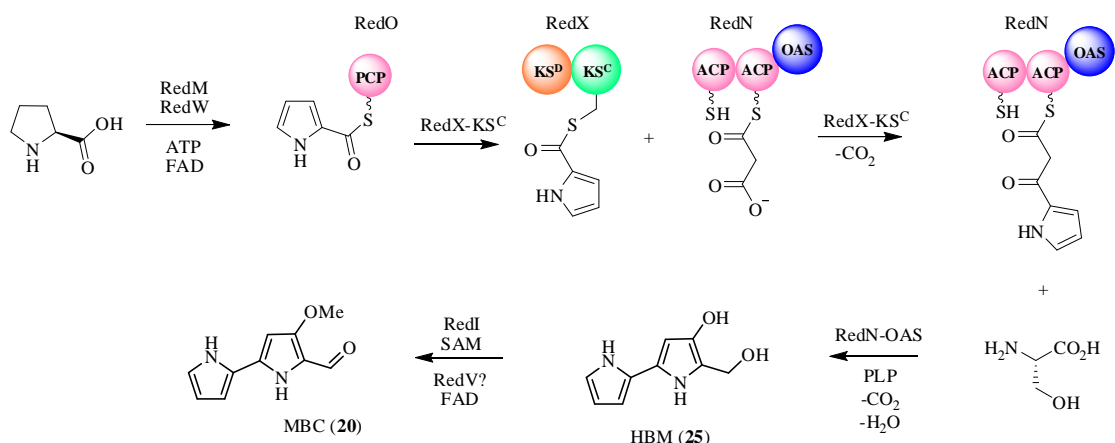


Figure 1.17 Proposed MBC (20) biosynthesis.

1.3.5 Condensation of 2-Undecylpyrrole and MBC to Form Undecylprodiginine

The condensation of chemically-synthesised MBC and 2-UP can happen spontaneously in the presence of a Bronsted acid catalyst (Wasserman et al., 1969). Originally Cerdeño *et al.* did not assign any gene within the *red* cluster to carry out this reaction and they proposed that this step could be spontaneous *in vivo* and thus did not require an enzyme (Cerdeño et al., 2001). However analysis of an *S. coelicolor/redH::oriT-apr* mutant showed that RedH is required for undecylprodiginine biosynthesis but not the biosynthesis of MBC and 2-UP suggesting a role in condensation of MBC and 2-UP (Haynes et al., 2008). This result was consistent with results obtained for the RedH homologue PigC in *Serratia marcescens* which was shown to be required for the condensation of MBC and MAP to give prodigiosin (Williamson et al., 2005).

A phosphotransferase with three functional domains is predicted to be encoded by the *S. coelicolor redH* gene. The central domain does not show any sequence similarity to other proteins with known function but it is proposed to bind MBC. The C- and N-

terminal domains are homologous to the phosphotransfer domain of pyruvate phosphate dikinase (PPDK) and the ATP-binding domain of phosphoenolpyruvate synthetase (PEPS), respectively (Cerdeño et al., 2001).

Pyruvate phosphate dikinase (PPDK) and phosphoenolpyruvate synthase (PEPS) catalyse very similar reactions. Both consist of three domains: one to bind ATP, another to bind pyruvate and a third one with a conserved histidine residue. PPDK catalyses the reversible reaction of AMP, phosphoenolpyruvate (PEP) and pyrophosphate (PP_i) to generate ATP, pyruvate (Pyr) and inorganic phosphate (P_i). The transfer of the phosphoryl group from PEP and PP_i to AMP is mediated by a catalytic histidine residue (His). This histidine residue can rotate between pyruvate-binding domain and the ATP-binding domain after its phosphorylation by PEP (Figure 1.18) (Herzberg et al., 1996). Enzymes functionally and structurally similar to PPDK (like PEP synthase) show the same mechanism of phosphoryl group transfer (Herzberg et al., 1996).

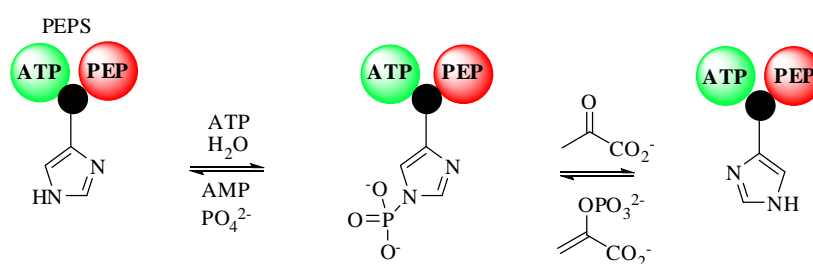


Figure 1.18 Reaction catalysed by PPDK.

A catalytic mechanism for RedH can be proposed based on the known mechanism of PPDK and PEPS. The phosphotransfer domain could phosphorylate the aldehyde oxygen of MBC in an ATP-dependent reaction. The aldehyde carbon would then be activated towards nucleophilic attack by C-5 of 2-UP. This could be followed by

elimination of the aldehyde oxygen (as phosphate) from this intermediate to yield undecylprodiginine (Figure 1.19).

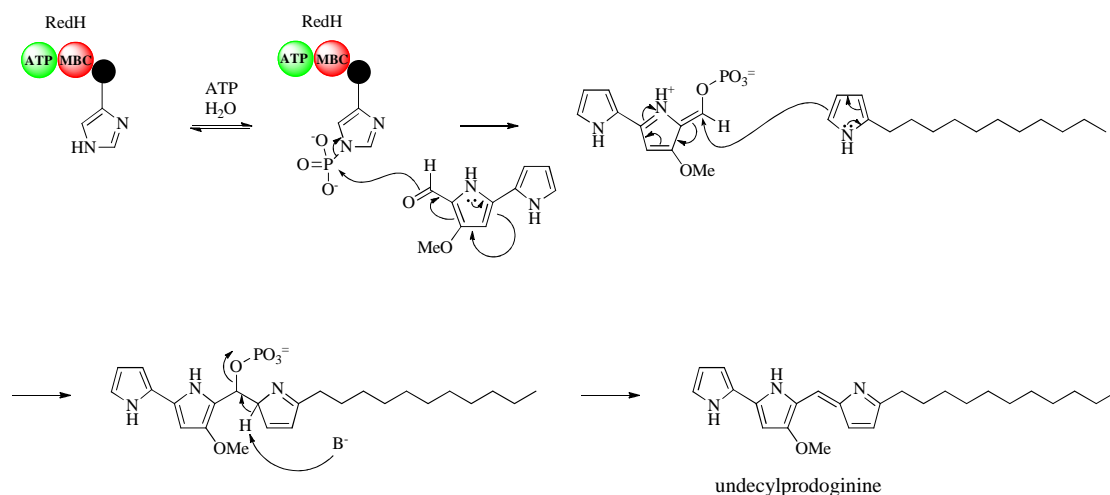


Figure 1.19 Proposed mechanism for condensation reaction catalysed by RedH.

1.3.6 Oxidative Cyclisation of Undecylprodiginine to Form Streptorubin B

The last step in *S. coelicolor* prodiginine biosynthesis is proposed to be the oxidative cyclisation reaction of undecylprodiginine to form streptorubin B and the Rieske non-haem iron-dependent oxygenase-like enzyme RedG is hypothesised to catalyse this reaction (Cerdeño et al., 2001). In the biosynthetic pathway of many natural products e.g. penicillins, fosfomycin and clavulanic acid, oxidative cyclisation reactions are key steps (Figure 1.20) (Konomi et al., 1979; Elson et al., 1987; Hammerschmidt, 1991; Seto et al., 1991; Zerbe et al., 2004). They are usually catalysed by enzymes with a non-haem iron cofactor and use molecular oxygen as a co-substrate (Seto et al., 1991; Roach et al., 1995; Zhang et al., 2000; Liu et al., 2001; Higgins et al., 2005). The

reaction catalysed by RedG would be the first example of an oxidative cyclisation to form a carbon-carbon bond and also a novel type of reaction catalysed by Rieske-oxygenase-like enzymes.

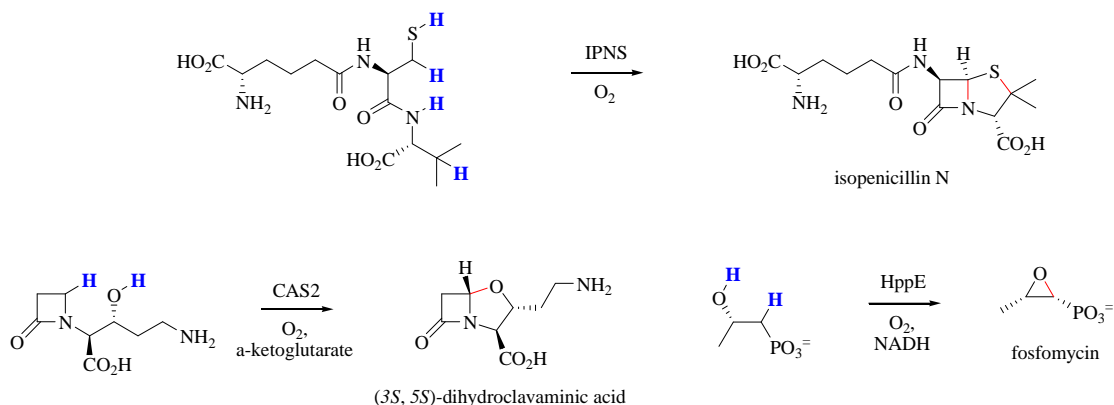


Figure 1.20 Oxidative cyclisation reactions in the biosynthesis of clinically-used natural products. Highlighted in blue – hydrogen atoms removed in the reactions. Highlighted in red – new bonds formed.

1.3.6.1 Rieske Non-Haem Iron-Dependent Oxygenases

Rieske non-haem iron oxygenases commonly catalyse the first step in bacterial degradation of many aromatic compounds in aerobic environments (Gibson et al., 1968; Axcell and Geary, 1975). They are usually regio- and stereoselective, with the ability to produce optically pure compounds (Urlacher and Schmid, 2006).

The most well-studied Rieske non-haem iron-dependent oxygenase is naphthalene dioxygenase (NDO), which catalyses the first step in the degradation of naphthalene through the addition of two-*cis*-hydroxyl groups to one of the benzene rings (Figure 1.21 A) (Eaton and Chapman, 1992). NDO was first Rieske dioxygenase to be structurally-elucidated by X-ray crystallography (Kauppi et al., 1998) and the enzyme consists of a

three component system containing a 36 kDa reductase, a 14 kDa ferredoxin and the 210 kDa dioxygenase .

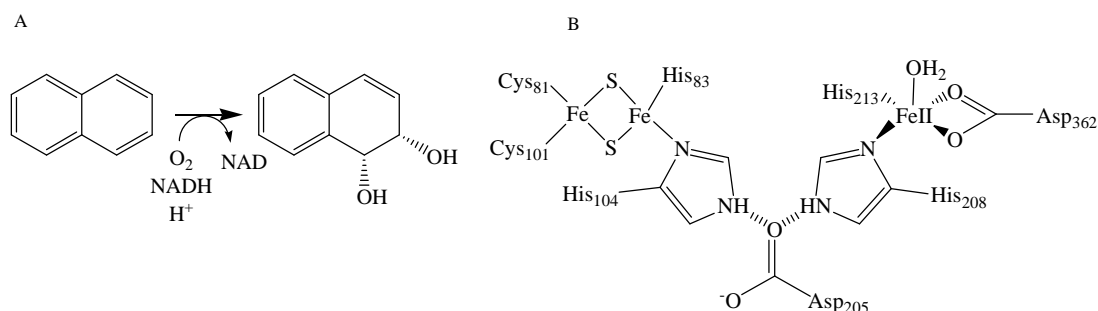


Figure 1.21 A – reaction catalysed by naphthalene dioxygenase (NDO), B – Representation of the NDO active site.

The dioxygenase is a $\alpha_3\beta_3$ hexamer, where in each α -subunit a Rieske domain and a catalytic (non-haem iron-binding) domain can be identified. The Rieske domain, in the N-terminal part of the α -subunit, contains a Rieske center (2Fe-2S) coordinated by Cys-81, Cys-101, His-83 and His-104. The C-terminal part of the α -subunit contains His-208, His-213, Asp-362 and a water molecule, which coordinate the atom of mononuclear ferrous iron in the catalytic centre. In all Rieske non-haem iron oxygenases these seven ligand-binding residues (four to bind 2Fe-2S and three to bind iron) are highly conserved. The 2-His-1-carboxylate triad is characteristic for a large number of non-haem iron-containing enzymes (Figure 1.21 B) (Jiang et al., 1996). In NDO and related enzymes it was shown that the substrate specificity is controlled by α -subunit and the role of the β -subunit is probably structural (Kauppi et al., 1998).

During the reaction catalysed by these enzymes the reductase and the ferredoxin transfer electrons from NAD(P)H to the oxygenase component. The electrons are transferred to the Rieske centre and are proposed to be shuttled via hydrogen bonds

between the conserved Asp-205 residue and His-104/His-208 to the non-haem iron centre, where oxygen is bound and catalysis takes place (Ensley and Gibson, 1983).

1.3.6.2 Proposed Oxidative Cyclisation Reaction of Undecylprodiginine Catalysed by RedG

As previously mentioned, RedG which is a Rieske non-haem iron-dependent oxygenase-like enzymes was proposed to catalyse oxidative cyclisation of undecylprodiginine to form streptorubin B (Cerdeño et al., 2001). The N-terminal domain of RedG contains a sequence motif that matches the consensus sequence of the Fe₂S₂ binding motif in the N-terminal domain of NDO (Kauppi et al., 1998). The C-terminal domain of RedG contains two histidine residues which match the consensus sequence of the two ferrous iron binding His residues in the C-terminal domain of NDO (Kauppi et al., 1998). The conserved aspartate residue in the 2-His-1-carboxylate triad has not been identified and could be substituted by glutamate or histidine. The aspartate residue proposed to mediate electron transfer is glutamate in RedG but this is unlikely to be of functional significance (Figure 1.22).

RedG	ARC PHK GANLGDGRMKGNT-IE C PY H GF-X ₈₅ -L- E FY H VTYV H RD
RedG orthologue	ARC PHK GANLADGRLVGNS-V A CPY H GF-X ₈₃ -L- E FY H VTFV H RD
NDO	NV C RR H RGKTLVSVEAGNAKGFV C SY H GW-X ₉₆ -V G DAY H VGW T H A S
	* *:* .* * .***: : : *** :.* .

Figure 1.22 Amino-acid sequence alignment of NDO α subunit from *Pseudomonas putida*, RedG from *S. coelicolor* and RedG orthologue from *S. longispororuber*. Conserved residues that ligate the [2Fe-2S] cluster and Fe(II) atom – highlighted in yellow. An Asp residue in NDO (mutated to Glu in RedG and RedG orthologue) proposed to mediate electron transfer between the [2Fe-2S] cluster and the Fe(II) atom is highlighted in green.

Rieske oxygenases are multicomponent enzymes so a reductase and a ferredoxin would be expected to be required for RedG activity. They do not, however, appear to be encoded by genes within the *red* cluster (Cerdeño et al., 2001). However in the *S. coelicolor* genome there are six ferredoxins and three reductases encoded outside of the cluster (Lei et al., 2004) which could mediate electron transfer from NAD(P)H to RedG.

To investigate the role of RedG, a *S. coelicolor redG* deletion mutant (W31) was created by a former Challis group PhD student Olanipekun M. Odulate (Odulate, 2005). LC-MS analyses showed that production of streptorubin B, but not undecylprodiginine is abolished in the mutant, giving the first experimental evidence that RedG plays a role in formation of the carbocycle in streptorubin B.

Feeding *S. coelicolor* mutants lacking the genes coding enzymes required for 2-UP (7) biosynthesis with synthetic 2-UP, restores the production of undecylprodiginine and streptorubin B, indicating that oxidative cyclisation must occur after assembly of 7 (Mo et al., 2008). However, it is not clear whether carbocycle formation in streptorubin B biosynthesis occurs prior to, or after condensation with MBC.

Although there is no experimental evidence for the catalytic mechanism of RedG, a mechanism can be proposed based on the mechanisms of other Rieske-oxygenases (Bugg, 2003). Thus it is proposed that the substrate (either 2-UP or undecylprodiginine) is bound to the enzyme when the Rieske centre and the non-haem iron centre are in their reduced states. The non-haem ferrous centre of the enzyme reacts with O₂ to form a ferric-superoxy complex, which is reduced to the peroxy complex by the Rieske centre. Protonation gives the ferric-hydrogen peroxide complex. O-O bond cleavage is coupled to hydrogen atom abstraction from the substrate to form a radical,

which adds to C-4 on the pyrrole. The reactive Fe-O species abstracts a second H from C-4 of the resulting new radical to form the product. The mononuclear iron is reduced to Fe^{2+} by the Rieske centre, to initiate another round of catalysis, after H_2O is lost (Figure 1.23).

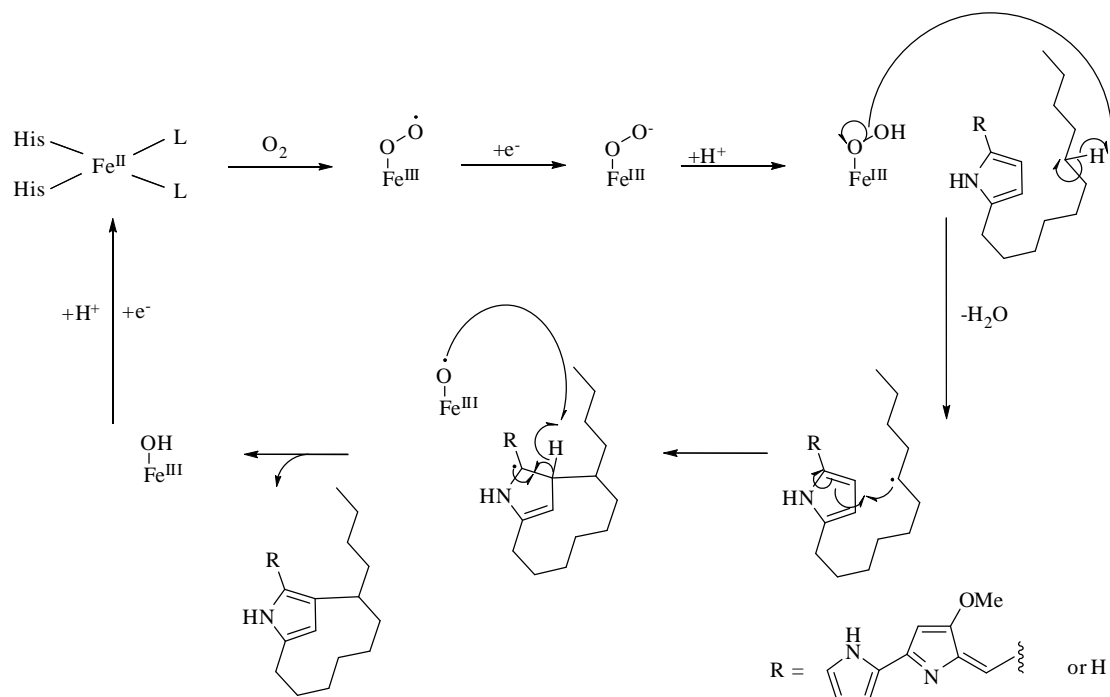


Figure 1.23 Proposed catalytic mechanism for RedG.

S. longispororuber produces undecylprodiginine (**2**) (like *S. coelicolor*) but a different carbocyclic derivative – metacycloprodiginosin (**16**) (Figure 1.24) (Wasserman et al., 1969). A partial gene encoding a RedG orthologue, with the consensus sequences for the Rieske centre and the non-haem iron catalytic centre, was identified in the *S. longispororuber* genome by Sarah Barry, a visiting PhD student in the Challis group (Barry, 2007). This suggested that the formation of the carbocycles in streptorubin B and metacycloprodiginosin could occur via similar mechanism

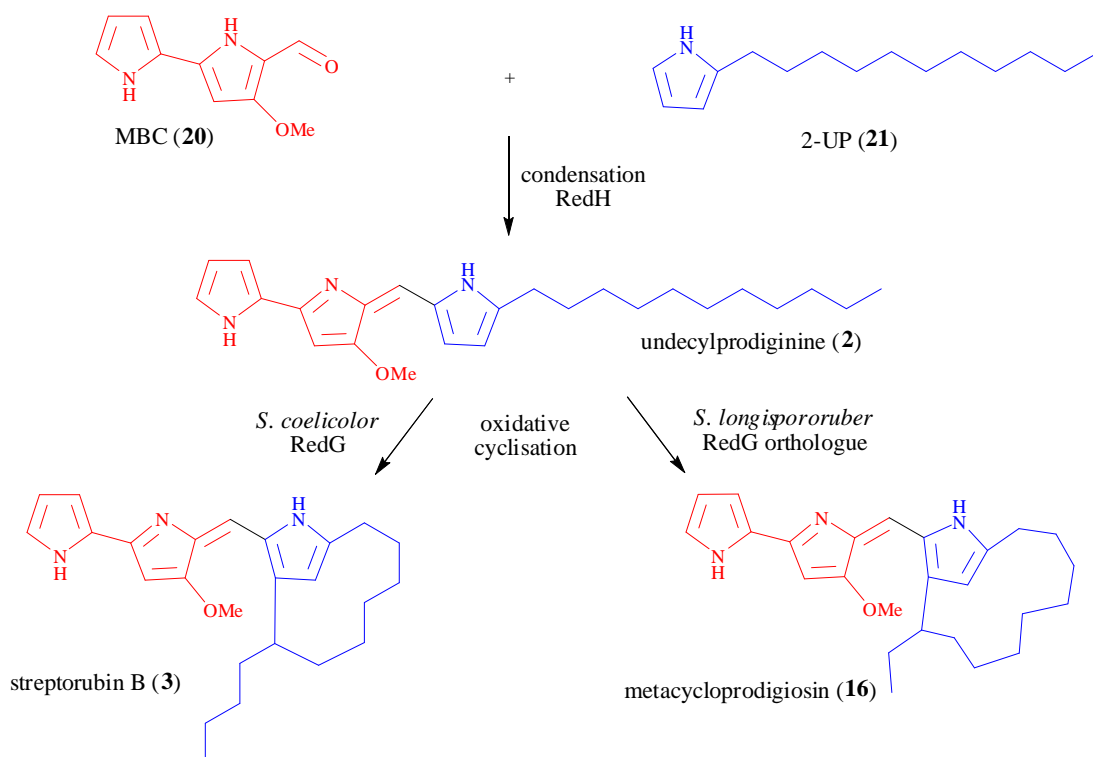


Figure 1.24 Predicted intermediates during *S. coelicolor* and *S. longispororuber* prodiginine biosynthetic pathway.

1.4 Aims of the Project

Interest in prodiginine antibiotics stems from their potent biological activities, in particular they have high therapeutic potential for the treatment of malaria and cancer. Although a prodiginine biosynthetic pathway in *S. coelicolor* A3(2) had already been suggested on the basis of bioinformatic and experimental studies the biosynthetic roles of some genes within the *red* cluster was still not clear. A better understanding of the prodiginine biosynthetic pathway is an important prerequisite for production of new prodiginine analogues with potentially superior bioactivity, by biosynthetic engineering. For example, understanding the oxidative carbocyclisation reactions involved in the formation of streptorubin B and metacycloprodigosin could facilitate the chemoenzymatic synthesis of carbocyclic prodiginine analogues, which are not easily accessible by conventional synthetic methods.

One aim of this project was to complete the elucidation of the prodiginine biosynthetic pathway in *Streptomyces coelicolor* A3(2), replacing genes of interest within the *red* cluster and analysing the mutants to determine whether the gene knockouts affected production of undecylprodiginine (**2**) and streptorubin B (**3**), or resulted in accumulation of the known intermediates MBC (**20**) and 2-UP (**21**) (Figure 1.24). It was also planned to feed the mutants with synthetic **20** and **21** to determine if prodiginine production could be restored.

The second aim was to further investigate the role of RedH and RedG from *S. coelicolor* and the RedH and RedG orthologues from *S. longispororuber*, in the biosyn-

thesis of streptorubin B and metacycloprodigiosin, respectively, via heterologous expression and gene swapping experiments.

The final aim was to elucidate the role of RedU (encoded within the *red* cluster) and two other PPTases (encoded elsewhere in the *S. coelicolor* genome) in the biosynthesis of prodiginines and other metabolites by constructing and analysing mutants lacking each of the three PPTases genes to determine whether the production metabolites is affected.

2. Materials and Methods

2.1 Materials

2.1.1 Chemicals and Equipment

Restriction enzymes and enzymes used to modify DNA were provided by MBI Fermentas (Lithuania), New England Biolabs (USA) and Roche (Germany). High Fidelity Polymerase (Roche) or *Taq* Polymerase (Fermentas) were used to carry PCR reactions. Oligonucleotides were ordered in Sigma Genosys (USA) and synthetic genes in EpochBiolabs (USA).

Kits to extract DNA from gel and to isolate plasmid DNA from *E. coli* were obtained from Qiagen (USA), to isolate *S. coelicolor* genomic DNA on small scale from MP Biomedicals (USA) and to construct fosmid library from EpicentreBiotechnologies (USA).

LB broth was provided by Fisher BioReagents. Most of nutrients to prepare different media were obtained from Difco and Becton, Oxoid, Dickinson and Co.

All other chemicals were bought from Difco (USA), Sigma-Aldrich (USA), Fermentas (Lithuania), Fisher Scientific (UK), Biolab (New Zealand), Duchefa (Netherlands), Melford (UK), Acros Organics (Belgium), Invitrogen (USA).

PCRs were performed in an Eppendorf Mastercycler Personal. A BioRad Gene Pulser II was used for electroporation in conjunction with the BioRad Pulse Controller Plus. A BioRad Power PAC300 was used for agarose gel electrophoresis. A Bio-Rad CHEF MAPPER was used for Pulse Field Gel Electrophoresis. To measure DNA concentrations a nano-drop ND-1000 spectrophotometer was used. Optical density of microbial cultures was measured using a Beckman coulter DU7400 Spectrophotometer or a Thermo BioMate3 Spectrophotometer. Bassaire laminar flow hood was used to

handling *Streptomyces*. During Southern blot hybridisation UV Stratalinker 2400, Stratagene to fix DNA and TechHybridiser HB-1D to carry hybridisation were used. To analyse secondary metabolites an Agilent 1100 HPLC instrument, LC-MS (LC – Agilent 1100, MS – Bruker Esquire HCT Plus ESI-MS-MS) and a Bruker MicroTOF mass spectrometer were used. NMR data was acquired from Bruker Advance spectrometer, 400 MHz instrument. CD spectroscopy was carried out on a Jasco J-815 CD Spectrometer.

2.1.2 Buffers and General Solutions

Stock solutions were prepared using the methods of Sambrook and Russell (2001) (Table 2.1). If it is not stated otherwise, all other stock solutions used in this work were prepared in H₂O and autoclaved or sterilised by filtration through a 0.2 µm filter if necessary.

Table 2.1 Chemicals stock solution.

Chemical	Stock solution	Solvent
Tris-HCl (pH 8)	0.5M	water, pH adjusted with HCl
RNAse	50 mg/mL heat treated (100 °C, 15 min)	water
TE buffer	100 mM Tris-HCl pH 8 10 mM EDTA pH 8	water
TBE (1L 5x stock solution)	53 g Tris base 27.5 g boric acid 10 mM EDTA pH 8	water
Loading buffer for agarose gels	50% glycerol 0.1% bromophenol blue 0.1% xylene cyanol	water

2.1.3 Antibiotics

Antibiotic stock solutions were dissolved in the appropriate solvent and sterilised by filtration through a 0.2 µm filter (Table 2.2) (Sambrook and Russell, 2001).

Table 2.2 Antibiotics stock solution.

Antibiotic	Stock sol. (mg/mL)	Solvent	<i>E. coli</i> ($\mu\text{g/mL}$)	<i>S. coelicolor</i> ($\mu\text{g/mL}$) overlay	<i>S. coelicolor</i> (mg/plate) overlay
ampicillin	100	water	100	-	-
apramycin	50	water	50	25	1.25
chloramphenicol	25	EtOH	25	-	-
hygromycin	50	water	50	25	1.25
kanamycin	50	water	50	100	5.0
nalidixic acid	25	0.3M NaOH	25	20	0.5
tetracycline	5	EtOH	10	10	0.05

2.1.4 Microbial Strains

The microbial strains used in this work are listed in Table 2.3.

Table 2.3 The microbial strain used.

Name	Genotype	Source
<i>E. coli</i> strains		
DH5 α	F- ,f80dlacZDM15, recA1, endA1, gyrA96, thi-1, hsdR17, (r_k^- , mk $^+$), supE44, relA1, deoR, (lacZYA-argF) U169	general cloning host (Woodcock et al., 1989), lab stock
MC1061	araD139 Δ (ara-leu)7696 galE15 galK16 Δ (lac)X74 rpsL (Str r) hsdR2 (r_k^- mk $^+$) mcrA mcrB1	general cloning host, lab stock
BW25113/pIJ790	Plasmid: pIJ790 [oriR101], [repA1001(ts)], araBp-gam-be-exo. Genome: (Δ (araD-aarB)567, Δ lacZ4787(::rrnB-4), lacI p -40000(lacIQ), λ -, rpoS369(Am), rph-1, Δ (rhaD-rhaB)568, hsdR514;	Plant Bioscience Limited (Datsenko and Wanner, 2000)
ET12567/pUZ8002	dam, dcm, hsdM, hsdS, hsdR, cat, tet; plasmid pUZ8002: tra, KanR, RP4 23; Genome: dam, dcm, hsdS, CmR, TetR	JIC, Norwich
DH5 α /BT340	DH5 α /pCP20	JIC, Norwich (Cherepanov and Wackernagel, 1995)
EPI300 $^{\text{TM}}$ -T1 $^{\text{R}}$	F- mcrA D(mrr-hsdRMS-mcrBC) f80dlacZDM15 DlacX74 recA1 endA1 araD139 D(ara, leu)7697 galU galK l- rpsL nupG trfA tonA dhfr	Epicentre Biotechnologies
<i>Streptomyces coelicolor</i> strains		
M145	<i>S. coelicolor</i> A(3)2, SCP1 $^-$, SCP2 $^-$	JIC Norwich
M511	<i>S. coelicolor</i> A(3)2, SCP1 $^-$, SCP2 $^-$ act $^-$ (Δ actII-orf4)	JIC Norwich
W31	M511 Δ redG::scar	Lab stock
W33	M511redH::apr	Lab Stock
W38	M511redL::apr	Lab stock
M595	M511redN::scar	JIC Norwich

W40	M145 <i>redU::apr</i>	Lab stock
-	M145 <i>acpS::apr</i> , single crossing over	Lab stock
-	M511 <i>acpS::apr</i> , single crossing over	Lab stock
Other <i>Streptomyces</i> strains		
<i>S. longispororuber</i>	M-3 DSM40667	DSMZ, Germany
<i>S. venezuelae</i>	ATCC10712	JIC, Norwich

2.1.5 Plasmids

The plasmids used in this work are listed in Table 2.4.

Table 2.4 List of plasmids.

Name	Insert/Use	Source
pBSK <i>rphG</i>	plasmid with cloned <i>rphG</i> gene	Epoch Biolabs Inc.
pBSK <i>rphG2</i>	plasmid with cloned <i>rphG2</i> gene	
pBSK <i>rphG3</i>	plasmid with cloned <i>rphG3</i> gene	
pBSK <i>rphG4</i>	plasmid with cloned <i>rphG4</i> gene	
pIJ773	plasmid to amplify an <i>oriT-apr^R</i> cassette (pBluescript KS(+), (<i>aac3(IV)</i>), <i>oriT</i> (RK2), FRT sites)	Plant Bioscience Limited
pIJ787	plasmid to amplify a <i>tetr^R</i> cassette (pBluescript KS(+), <i>tetr^R</i> , <i>oriT</i> (RK2), FRT sites),	Plant Bioscience Limited
pIJ86	multicopy plasmid to carry out gene complementations in <i>S. coelicolor</i> , not integrated within chromosome,	Bibb Group, JIC Norwich
pOSV556	<i>E. coli-Streptomyces</i> shuttle <i>amp^R</i> , <i>hyg^R</i> vector with <i>ermE*</i> promoter, <i>oriT</i> and <i>attP</i> site to integrate with <i>Streptomyces</i> chromosome,	Pernodet Group, University of Paris-Sud, France
pLW42	<i>E. coli-Streptomyces</i> shuttle <i>apr^R</i> vector pUWL201 with <i>ermE*</i> promoter(Doumith et al., 2000) and <i>Streptomyces griseoflavus hrmQ</i> gene,	Heide Group, University of Tübingen, Germany

2.1.6 Cosmids

The cosmids used in this study are listed in Table 2.5.

Table 2.5 List of cosmids.

Name	Insert	Source
Sc3F7	containing a large part of the <i>red</i> cluster (<i>sco5881-5912</i> CDSs)	Plant Bioscience Limited (Redenbach et al., 1996)
Sc5A7	containing <i>sco6651-6684</i> (to amplify <i>sco6673</i> , putative PPTase)	
Sc6G4	containing <i>sco4723-4768</i> CDSs (to amplify <i>sco4744</i> , <i>acpS</i> gene)	
Sc1G7	containing <i>sco6274-6287</i> (to amplify <i>sco6287</i> , <i>scoT</i>)	

pCC1FOS™	vector to produce fosmid libraries; linearised at the unique <i>Eco</i> 72I site and dephosphorylated	Epicentre Biotechnologies, USA
<i>C73_787/mmyR::oriT-apr</i>	Cosmid with <i>mmy</i> cluster, overexpressing methylenomycin	JIC, Norwich

2.1.7 Primers

Oligonucleotide primers used for PCR targeting mutagenesis are listed in Table 2.6.

Table 2.6 List of primers used for PCR-targeting; underlined sequence is homologous to the cassette.

TARGETING PRIMERS					
Targeted Strain	Cosmid/ Cassette	Targeted gene	Primer Name	Genotype	Primer sequences (5'-3')
<i>S. coelicolor</i> M511	3F7/ 773	<i>redI</i>	redItarget_fw redItarget_rv	M511 <i>redI::oriT-apr</i>	GGAAGCAACATGGACATTCTGAGCCTGGC CAAGAGCGTCAT <u>TCCGGGGATCCGTCGACC</u> ACGTGCGTGTCCATGGCGGGTGTGTCTCC TCGGCGGTCATGTAGGCTGGAGCTGCTTC
<i>S. coelicolor</i> M511	3F7/ 773	<i>redJ</i>	redJtarget_fw redJtarget_rv	M511 <i>redJ::oriT-apr</i>	GCGCCATGTCGCCCGCTGACCTGTCTCTC CCAGCGTTCCAT <u>TCCGGGGATCCGTCGACC</u> CCAGGCTCAGAATGTCCATGTTGCTTCCC TAGTTGCCTTGTAGGCTGGAGCTGCTTC
<i>S. coelicolor</i> M511	3F7/ 773	<i>redK</i>	redKtarget_fw redKtarget_rv	M511 <i>redK::oriT-apr</i>	GACCTCGAACACTCCCTCGACCTCCTGGT GTGATCCATGAT <u>TCCGGGGATCCGTCGACC</u> AGGTGAGCGGGCGACATGGGCGCTCCC TCGGCGGAGTCTGTAGGCTGGAGCTGCTTC
<i>S. coelicolor</i> M511	3F7/ 773	<i>redLA</i>	redLAtarget_fw redLAtarget_rv	M511 <i>redLA::oriT-apr</i>	TTCCTCACCACACCGACGCTACGTCCTG CGCTGGACCA <u>TCCGGGGATCCGTCGACC</u> TTCGCCGTCGGCGTGGGGACGGCGAACG CGGCGCCGTATGTAGGCTGGAGCTGCTTC
<i>S. coelicolor</i> M511	3F7/ 773	<i>redT</i>	redTtarget_fw redTtarget_rv	M511 <i>redT::oriT-apr</i>	GCGCTCGACGCCCTGGAGGACGAGGTGCT ACGGGCGCTGAT <u>TCCGGGGATCCGTCGACC</u> GAAACGGTCCGCTTGGCGACGCCGCTGGA TGAGTTCCATGTAGGCTGGAGCTGCTTC
<i>S. coelicolor</i> M511	3F7/ 773	<i>redV</i>	redVtarget_fw redVtarget_rv	M511 <i>redV::oriT-apr</i>	ATGGCCGGGCGGTGTCCAGTTGCGCCAG GCGCTGGAGAT <u>TCCGGGGATCCGTCGACC</u> CACACCGACCCGGCTCACGAAGAAGGTGC GGCCGGCAGTGTAGGCTGGAGCTGCTTC
<i>S. coelicolor</i> M145	5A7/ 773	<i>sco6673</i>	6673target_fw 6673target_rv	M145 <i>6673::oriT-apr</i>	GGCGTCCGCGCACCGTCGCACAGGAGG TGACCCGTTGAT <u>TCCGGGGATCCGTCGACC</u> TGGTGCCTCCACCTGACCGGGGGCGG GCGCAGTTCATGTAGGCTGGAGCTGCTTC
<i>S. coelicolor</i> M511	3F7/ <i>redJ</i> <i>::scar</i> 773	<i>neo</i>	neotarget_fw neotarget_rv	M511 <i>redJ::scar</i>	ATGATTGAACAAGATGGATTGCACGCAGG TTCTCCGGCA <u>TCCGGGGATCCGTCGACC</u> TCAGAAGAACTCGTCAAGAAGGGATAGA AGGCGATGCGTGTAGGCTGGAGCTGCTTC
<i>S. coelicolor</i> M511/ <i>redJ</i> <i>::scar</i>	1G7/ 773	<i>scoT</i>	scoTtarget_fw scoTtarget_rv	unsuccessful	GGGCCGCACTCGTCAAGCGTAAGGGGAA AAGGCGATGAT <u>TCCGGGGATCCGTCGACC</u> GAGAAGAGACCAGCGGTCCTTCATTG

					TGGGCCAGGATGTAGGCTGGAGCTGCTTC
<i>S. coelicolor</i> M145/6673 ::oriT-apr	5A7/ 6673 ::scar/ 787	Uncod- ing region	tetratarget_fw tetratarget_rv	M145 6673::scar	ACCAAGCGACGCCAACCTGCCATCAC GAGATTTCTCGTCTGGAAGGCAGTACAC GCCGCTGCTGGTTTCTGGATGCCGACG GATTTGCCGTCAGTACGGGCCATAGAG
<i>S. coelicolor</i> M145/6673 ::scar	3F7/ 773	redU	redUtarget_fw redUtarget_rv	M145 6673::scar+ redU:oriT::apr	CGGCCGGGACCGGTGCACGGGGCGGAACG GGGGTCGGTGATTCGGGGGATCCGTCGACC CCGGAAGATCTGCAACACCCGGATGGCGG GCGCGGTTTCATGTAGGCTGGAGCTGCTTC

The oligonucleotide primers used to analyse mutants by PCR are listed in Table 2.7.

Table 2.7 List of test primers used to confirm inserted mutation.

TEST PRIMERS				
Gene deletions	Expected wild type size (bp)	Expected size with cassette instead of gene (bp)	Expected size with scar sequence instead of gene (bp)	Primer sequences 5'-3'
<i>acpS</i>	714	1719	-	CGAGCACGATCTGGTCTGACG CGAGCAGTTGTCTCGTTCATCG
<i>redI</i>	1729	2044	-	GCACAGGAAGGCAACTAGG CGTCGGTGTGGATCATCTC
<i>redJ</i>	1297	1891	602	TGCTGGCAAGCAGATGGTG CTTGGCCAGGCTCAGAATGTCC
<i>redK</i>	1643	1976	-	CGGCTCCGCTTCTTCATCAAC AGTCTGCGGTGCAAGTAGG
<i>redL</i>	7502	1985	-	GCAAGGACCGCATGGTGAAG AGAGTCCGGCGCAGTTGTAG
<i>redLA</i>	2344	1918	-	GCAAGGACCGCATGGTGAAG GACAGGAGTTCACCGACGTC
<i>redT</i>	2009	2654	-	CAGTCCGAAGCCGTAGTACTTG ACCGGACGAAACCTGATCCTC
<i>redV</i>	1482	1830	-	GATGCCGGGCACCTTCTTTTG CATCCGGTGTTCAGATCTTC
<i>redU</i>	1143	1656	-	AGTTGTGGGAGGAGGGACTCAG GGACCGTTTCTGTGCACAACAAC
<i>sco6673</i>	1221	1917	627	TACCCGGAGTTCGCCATGTG TGACCGCTGACGTCGTTGTG
<i>scoT</i>	1270	1852	-	CTCTGGTTCGAACACCTCGG CGCACTGCCTCACACTCCTG
<i>neo</i>	1211	1865	-	GGAAGCGGAACACGTAGAAAGC CGATTCGGAAGCCCAACCTTTC
uncoding sequence (where <i>oriT-tet</i> cassette was introduced)	570	2186	-	CAGCGCATCGCCTTCTATCG GCATTCCACCACCTGTCCCA

The oligonucleotide primers used for cloning and sequencing are listed in Table 2.8.

Table 2.8 List of the others primers used

pOSV556 CLONING PRIMERS			
Gene	Primer name	Sequence	Restriction sites Size (bp)/Template
<i>redLA</i>	redLApOSV_fw redLApOSV_rv	GGGAAGCTTAGGAGGCGGTAGATGGCCCGGAACCG TTTCTCGAGTCACACGACGCTCGCGGCCACCA	<i>HindIII, XhoI</i> 1836/3F7
<i>redH</i>	redHcom_fw redHcom_rv	AAAGGGAAGCTTCGAGGAGACACACCCGCC CCCTTCTCGAGGCGGTCGTGGTCCGGTG	<i>HindIII, XhoI</i> 2880/3F7
<i>redG</i>	redGcom_fw redGcom_rv	AAAGGGAAGCTTCAGACGGGAGACGACCCCG CCCTTCTGCAGCAGGTCACCCGCTCGTC	<i>HindIII, PstI</i> 1383/3F7
<i>redHG</i>	redHcom_fw redHGcom_rv	AAAGGGAAGCTTCGAGGAGACACACCCGCC GGGAAAGCGCCGCGGCCACGGCGACGGTGTG	<i>HindIII, NotI</i> 4224/3F7
<i>mcpG</i>	mcpGclon_fw mcpGclon_rv	AAAGGGAAGCTTGGGAAGCAGGAAGTCCAG CCCTTCTCGAGTTACGGTCCCGTTGGG	<i>HindIII, PstI</i> 1189/3G3
<i>rphG</i>	rphGclon_fw rphGclon_rv	AAAGGGAAGCTTAGGAGGGTCCCGATGATCCCAATCAGT CCCTTCTCGAGTTACGGTCCCGTTGGG	<i>HindIII, XhoI</i> 1182/pBSKRpHrphG
<i>rphG2</i>	rphG2clon_fw rphG2clon_rv	AAAGGGAAGCTTAGGAGGGTCCCGATGATCCCAATCAGT CCCTTCTCGAGTCAGCGCCGGCGGCCG	<i>HindIII, XhoI</i> 1365/pBSKRpHrphG2
<i>rphG3</i>	rphG3clon_fw rphG3clon_rv	AAAGGGAAGCTTAGGAGGGTCCCGATGATGTTCCCA CCCTTCTCGAGTCAGCGCCGGCGGCCG	<i>HindIII, XhoI</i> 1017/pBSKRpHrphG3
<i>rphG4</i>	rphG4clon_fw rphG4clon_rv	AAAGGGAAGCTTAGGAGGGTCCCGATGATGTTCCCA CCCTTCTCGAGTTACGGTCCCGTTGGG	<i>HindIII, XhoI</i> 1137/pBSKRpHrphG4
<i>hrmQ</i>	hrmQclon_fw hrmQclon_rv	AAAGGGAAGCTTAGGAGGGTCCCGATGAGCGACTTCGACT CTCGAGTGGCGAGCTCAGAAGAGCGG	<i>HindIII, PstI</i> 1373/pLW42
<i>acpS</i>	aspSclon_fw acpSclon_rv	TTTCCCAAGCTTGTGGCTAGGGTTCCGGC AAAGGGCTCGAGCACGGCATCTCCGTGAG	<i>HindIII, XhoI</i> 943/6G4
<i>sco6673</i>	6673clon_fw 6673clon_rv	AAAGGGAAGCTTGCACCAGGAGGTGACCCG CCCTTCTCGAGGGCTGGACATGCTCTCG	<i>HindIII, XhoI</i> 1090/5A7
<i>redU</i>	redUclon_fw redUclon_rv	AAAGGGAAGCTTAGGAGGGGTCGGTGCAGGGAG CCCTTCTCGAGGTGCGCACGCCGGAACGCC	<i>HindIII, XhoI</i> 918/3F7
pOSV556 TEST	pOSVtest_rv	GCACCGCATGCTGTTGTGG	used with <i>sco6673</i> and <i>redU</i> rv pOSV556 cloning primers, in control PCRs to confirm if pOSV556 <i>sco6673</i> and pOSV556 <i>redU</i> were introduced in to the <i>sco6673</i> and <i>redU</i> mutants, respectively
pIJ86 CLONING PRIMERS			
<i>redG</i>	redGmulti_fw redGmulti_rv	CCCAAAGGATCCAGACGGGAGACGACCCG TTTGGGAAGCTTGCCACGGCGACGGTGTG	<i>BamHI, HindIII</i> 1325/3F7
<i>redGH</i>	redGHmulti_fw redGmulti_rv	CCCAAAGGATCCCGAGGAGACACCCGCC TTTGGGAAGCTTGCCACGGCGACGGTGTG	<i>BamHI, HindIII</i> 4222/ 3F7
FOSMID LIBRARY SEQUENCING PRIMERS			
Library Screening Primers	SlongLIB_fw SlongLIB_rv	GGCAGGTTCCGCGCTTGTGTC ACACCGCGACATGGTCATGG	Primers used to amplify a fragment of <i>mcpGH</i> genes. Used to find fosmid containing <i>mcpGH</i>
Library Control Primers	pCC1 TM /pEpiFOS TM _fw pCC1 TM /pEpiFOS TM _rv	GGATGTGCTGCAAGGCGATTAAAGTTGG CTCGTATGTTGTGGAAATTGTGAGC	pCC1FOS Sequencing Primers

Primers used to sequence genes from <i>mcp</i> cluster	SlongSEQ1_fw	CCATGACCATGTCGCGGTGT	primers used to sequence the fragment of fosmid SI3G3 containing the <i>mcpUIHG</i> genes
	SlongSEQ2_rv	GACAAGCGCGGAACCTGCC	
	SlongSEQ3_fw	CGGTCCACTACACCCGCTATA	
	SlongSEQ4_rv	GACACGATGGAGCTGTGGGA	
	SlongSEQ5_fw	GAGGTTTCGTGAGTTCTGCG	
	SlongSEQ6_fw	GCCTCGATGATCTCCTTGAC	
	SlongSEQ7_fw	CGGGCGTCGTCGGAGGTCTC	
	SlongSEQ8_fw	CGGGTGGTCTCGCGCAGCTC	
	SlongSEQ9_fw	CCAGGTCCACCTCTCGCTG	
	SlongSEQ10_fw	CCGCTCTCGCGCAGGAACAG	
	SlongSEQ11_rv	TCGTCGGTCCGAGAATCGG	

2.1.8 Culture Media

Unless stated otherwise, the media for culturing *Streptomyces* and *E. coli* were prepared by published procedures as described in the manual by Kieser et al. (2000) and all media were autoclaved directly after preparation.

2.1.8.1 Liquid Media

Recipes for liquid media used are as follows:

<u>2 X YT</u>		<u>TSB (Tryptone Soya Broth)</u>	
Difco Bacto Tryptone	16 g	Oxoid Tryptone Soya Broth powder	30g
Difco Bacto Yeast Extract	10 g	H ₂ O	to 1L
NaCl	5 g	<u>LB Broth</u>	
H ₂ O	to 1L	Luria-Bertani powder	25 g/L
		H ₂ O	to 1L
<u>SMM (Supplement Minimal Medium)</u>		<u>Trace Element Solution</u>	
MgSO ₄ .7H ₂ O (0.2M)	25 mL	ZnSO ₄ .7H ₂ O	0.1 g/L
TES Buffer (0.25M, pH 7.2)	100 mL	FeSO ₄ .7H ₂ O	0.1 g/L
NaH ₂ PO ₄ + K ₂ HPO ₄ (50 mM each)	10 mL	MnCl ₂ .4H ₂ O	0.1 g/L
Trace Element Solution	1 mL	CaCl ₂ .6H ₂ O	0.1 g/L
Casaminoacids (20%)	10 mL	NaCl	0.1 g/L
H ₂ O	804 mL	H ₂ O	to 1 L
Glucose (20%)	50 mL		
All solutions were autoclaved or filtered separately and added to sterile H ₂ O		Sterilised by filtration	

IDM (Iron deficient medium)

Salt concentration		Trace nutrient concentration	
K ₂ SO ₄	2 g	Thiamine	2 mg/L
K ₂ HPO ₄	3 g	ZnSO ₄ .7H ₂ O	2 mg/L
NaCl	1 g	CuSO ₄ (0.5 mg/mL)	10 µL
NH ₄ Cl	5 g	MnSO ₄ .H ₂ O (3.5mg/mL)	10 µL
H ₂ O	to 1 L	MgSO ₄ .H ₂ O	80 mg/L

Salts were dissolved in distilled water in plastic flasks and Chelex-100 resin (Sigma-Aldrich, 50g/L) was added and stirred overnight. The resin was filtered with Watman filter paper (no.1), trace nutrients were added and the medium was autoclaved. Before cultures were started 10mL/L of sterile CaCl₂ (10g/L), glucose (250 g/L) and yeast extract (0.5%) were added to the medium.

2.1.8.2 Solid Media

Recipes for solid media used are as follows:

<u>ONA (Oxoid nutrient agar)</u>		<u>DNA (Difco nutrient agar)</u>	
Oxoid Nutrient Agar	5.6 g	Difco Nutrient Agar	4.6 g
H ₂ O	to 1L	H ₂ O	to 1L
<u>SNA (Soft nutrient agar)</u>		<u>LB Agar</u>	
Difco Nutrient Broth Powder	8.0 g	Luria-Bertani powder	25 g/L
Difco Bacto Agar	5 g	Difco Bacto Agar	15 g/L
H ₂ O	to 1L	H ₂ O	to 1L
<u>SFM (Mannitol soya flour medium)</u>		<u>Ala MM</u>	
Soya flour	20g	Alanine	30 mM
Mannitol	20g	K ₂ HPO ₄	1 mM
Difco Bacto Agar	20g	MgSO ₄ .7H ₂ O	5 mM
H ₂ O	to 1L	Agar	15 g
		H ₂ O	to 1 L

The pH of the medium was adjusted to 5. The medium was autoclaved and before use 10 g/L of sterile glycerol was added.

<u>R5 medium</u>			
Before autoclaving ingredients		After autoclaving ingredients/1L	
Sucrose	103 g	KH ₂ PO ₄ (0.5%)	10 mL
K ₂ SO ₄	0.25 g	CaCl ₂ ·2H ₂ O (5M)	4 mL
MgCl ₂ ·6H ₂ O	10.12 g	L-proline (20%)	15 mL
Glucose	10 g	NaOH (1N)	7 mL
Difco Casaminoacids	1 g	Trace Element Solution	2 mL
Difco Yeast Extract	5 g		
TES Buffer	5.73 g		
Agar	22 g		
H ₂ O	to 1L		

All “Before autoclaving ingredients” were mixed and medium was autoclaved. At the time of use the medium was melted and “After autoclaving ingredients” were added.

2.2 Growth, Storage and Manipulation of *E. coli*

The procedures described by Sambrook and Russell (2001) were used for culturing *E. coli*.

2.2.1 Growth Conditions

E. coli was grown overnight on LB agar or in LB broth (180 rpm, 37 °C). Plasmid-containing cells were selected for using the appropriate antibiotic and the concentration listed in Table 2.2.

2.2.2 Storage of Strains

For long term storage, overnight LB cultures of *E. coli* were mixed with 70% glycerol to a final concentration of 20% and stored at -78 °C.

2.2.3 Preparation of Electrocompetent *E. coli* cells

E. coli was inoculated into 10 mL of LB and the culture was grown overnight with shaking at 37 °C. 100 µL of this preculture was used to inoculate 10 mL of LB the

culture was grown at 37 °C for 3-4 h shaking at 200 rpm until an OD₆₀₀ of ~0.6 was reached. The cells were recovered by centrifugation at 3000 rpm for 7 min at 4 °C. After decanting the medium, the pellet was resuspended by gentle mixing in 10 mL of ice-cold 10% glycerol. The cells were centrifuged as before and resuspended in 5 mL of ice-cold 10% glycerol, centrifuged and resuspended in the remaining ~100 µL of 10% glycerol after decanting the supernatant.

2.2.4 Transformation of Electrocompetent *E. coli*

100 µL of electrocompetent cell suspension were mixed with ~100 ng DNA per transformation. Electroporation was carried out in a 0.2 cm ice-cold electroporation cuvette using a BioRad GenePulser II set to: 200 Ω, 25 µF and 2.5 or 1.8 kV. The expected time constant is 4.5 – 4.9 ms. After electroporation, 1 mL ice-cold LB was added immediately to the shocked cells and incubated for 1 h shaking at 37 °C. Transformants were selected by spreading onto LB agar containing the appropriate antibiotic.

2.3 Growth, Storage and Manipulation of *Streptomyces*

The procedures used were adapted from those described by Kiesser et al. (2000).

2.3.1 Surface Grown Cultures for Spore Stock Generation

Spore suspensions of *S. coelicolor*, *S. longispororuber* and *S. venezuelae* were prepared from confluent lawns growing on SFM agar medium. 3 mL of sterile water was added to the plates and the spores were suspended in the water by carefully scraping the surface of the mycelia with a sterile loop. The suspension was filtered through sterile non-absorbent cotton wool. The filtered suspension was centrifuged (10 min, 3000 rpm) to pellet the spores and the supernatant was poured off. The pellet was resuspended in

the drop of water remaining in the tube and approximately the same volume of sterile 50% glycerol was added. Spores were stored at -20 °C.

2.3.2 Liquid Grown Cultures for Genomic DNA Isolation

Streptomyces cultures for genomic DNA isolation were grown in TSB medium for 48 h at 30 °C and 180 rpm.

2.3.3 Transfer of DNA from *E. coli* to *S. coelicolor* and *S. venezuelae* by conjugation

Electrocompetent cells of *E. coli* ET12567/pUZ8002 were prepared in LB containing chloramphenicol and kanamycin (section 2.2.3) and the plasmid or cosmid of interest was introduced into the strain by electroporation (section 2.2.4). Transformants were selected for by plating on LB with appropriate antibiotics. A 5 mL overnight culture in LB liquid medium was grown from one of the resulting colonies. 100 µL of the overnight culture was inoculated into 10 mL of LB liquid medium containing appropriate antibiotics and the cultures was grown for approximately 5 hours at 37 °C to an OD₆₀₀ of 0.4 – 0.6. The cells were collected by centrifugation and washed twice with LB liquid medium to remove antibiotics. 20 µL of *Streptomyces* spores were added to 0.5 mL 2xYT liquid medium and the mixture was heat-shocked at 50 °C for 10 min, then allowed to cool. 0.5 mL of the *E. coli* cells were mixed with the 0.5 mL *Streptomyces* spore suspension and centrifuged briefly. A dilution series of the resulting *E. coli* – *Streptomyces* mixture was made in sterile water from 10⁻¹ down to 10⁻⁴ and spread on SFM agar plates containing 10 mM MgCl₂ (*S. coelicolor*) or on R2 agar plates with maltose in place of glucose (*S. venezuelae*). The plates were incubated for 16-20 hr at 30

°C. *E. coli* was then selectively killed by overlaying the plates with H₂O containing nalidixic acid. Antibiotics in appropriate concentrations for *Streptomyces* strains (Table 2.2) were also added to select for exconjugants which contain the plasmid or cosmid integrated into chromosome.

2.4 Isolation and Manipulation of DNA

2.4.1 Genomic DNA Isolation from *S. coelicolor*

Streptomyces genomic DNA was isolated from a 2 day 50 mL culture in TSB liquid medium according to a modification of the method of Kieser *et al.* (Kieser *et al.*, 2000)

The cell pellet was washed with 30 mL of dH₂O, centrifuged (10 min, 2000 rpm) and washed again with 50 mL of 10 mM EDTA pH 8. After centrifugation (10 min, 2000 rpm) the mycelia were resuspended in 12.5 mL of SET buffer (75 mM NaCl, 25 mM EDTA pH 8, 20 mM Tris-HCl pH 7.5) containing 250 µL of lysosyme (50 mg/mL). The cell suspension was incubated for 3 h at 37 °C and 350 µL of proteinase K solution (20 mg/mL) and 1.5 mL of 10% SDS were added. The mixture was incubated for a further 2 h at 55 °C. 5 mL of 5M NaCl was added. The mixture was mixed gently to get a homogenous solution and was cooled to 37 °C. After adding 12.5 mL of chloroform the solution was mixed by inversion for 30 min at room temperature and was centrifuged (15 min, 4000 rpm). The supernatant was transferred to a fresh tube and the DNA was precipitated by adding 0.6 volumes of isopropanol. The precipitated DNA was wound on a plastic loop and washed with 70% EtOH. The DNA was then resuspended in TE buffer and was stored at 4 °C.

2.4.2 Plasmid or Cosmid Isolation from *E. coli*

The method used to isolate plasmids or cosmids from *E. coli* was thus described by Sambrook and Russell (2001).

An overnight liquid culture (5 mL of LB liquid medium containing appropriate antibiotic(s)) was centrifuged and the pellet was resuspended in 100 μ L of cold Solution I (25 mM Tris-HCl pH 8, 10 mM EDTA pH 8, 50 mM Glucose). To lyse the cells, 200 μ L of Solution II (0.2 N NaOH, 1% SDS) was added and the mixture was gently mixed (lysis was carried out for a maximum of 5 min). To precipitate proteins, 150 μ L of cold Solution III (5 M Potassium acetate 60 mL, Glacial acetic acid 11.5 mL, H₂O 28.5 mL) was added and the solution was mixed by inverting the tube by hand 10 times. The tube was centrifuged (10 min, 14000 rpm, 4 °C) and the supernatant was transferred to a clean tube. 200 μ L of phenol-chloroform-isoamyl alcohol (25:24:1) was added and the tube was vortexed for 30 s. After centrifugation (5 min, 14000 rpm) the water layer was transferred to a clean tube and plasmid DNA was precipitated with 500 μ L of ice-cold isopropanol. Precipitation was carried out on ice for 10 min and the sample was centrifuged (10 min, 14000 rpm, 4 °C). The DNA was washed with 70% EtOH, centrifuged and left to dry. DNA was resuspended in H₂O or TE buffer.

2.4.3 Digestion of DNA with Restriction Enzymes

Digestions with restriction enzymes were carried out according to the manufacturer's instructions. Restriction enzymes solutions were always 10% of the total reaction volume as was the appropriate buffer (all buffers were 10x concentrated). The rest of the reaction mixture consisted of the DNA solution to be digested and, if needed, water to make up the volume. Digestions to purify DNA from agarose gels were carried out in a

total volume of 20 – 30 μL . Digestions to check the outcome of cloning reactions were carried out in a total volume of 10 μL .

2.4.4 Ligation of DNA into plasmid vectors

DNA for ligation into plasmid vectors was typically purified using a Qiaquick purification column (Qiagen) eluting with H_2O . In general, the molar ratio of vector:insert of 1:3 was used and was quantified by separating 1 μL of the vector and the insert on an agarose gel along with DNA molecular size markers of known concentration. Ligation reactions were carried out in 20 μL final volume for 1 h using a Rapid Ligation Kit (Roche).

2.4.5 Agarose Gel Electrophoresis

Agarose gels were prepared and electrophoresed in 1 x TBE buffer. Depending on the size of the DNA fragments, 0.8%, 1.0% or 1.5% agarose gels with added ethidium bromide were used. Electrophoresis was carried out for 1 h at 100 V. A 1 kb DNA ladder (Fermentas) was used as a molecular size standard.

2.5 PCR Methods

The PCRs were carried out in 20 – 50 μL total volume using High Fidelity Polymerase (Roche) (if the reaction product was used for cloning or PCR-targeting purposes) or *Taq* Polymerase (Fermentas) (if the reaction was for analysis of constructs/mutants). Reaction conditions are summarised in Table 2.9.

Table 2.9 PCR reaction conditions

Solution	Volume	Concentration
Primers (100 pmoles/ μ L)	1 μ L each	100 pmoles each
Template DNA	1 μ L	~50 ng
Buffer (10x)	5 μ L	1 x final concentration
dNTPs (5 mM)	2 μ L	100 μ M each
DMSO	2.5 μ L	5%
DNA polymerase (2.5 U/ μ L)	0.5 μ L	1.25 Units
Distilled water	37 μ L	
Total volume	50 μ L	

2.5.1 Standard PCR Method

PCR conditions for analysis of constructs/mutants and to generate inserts for cloning were as follows:

- | | | |
|----------------------|-------------------|-------------|
| 1) Denaturation: | 94 °C, 2 min | |
| 2) Denaturation: | 94 °C, 45 s | } 35 cycles |
| 3) Primer annealing: | 55 – 67 °C, 45 s | |
| 4) Extension: | 72 °C, 90 – 240 s | |
| 5) Final extension: | 72 °C, 15 min | |

A primer annealing temperature between 55 – 67 °C empirically was chosen to generate the highest quantity product and the extension time was altered according to the product length (1 extra min per 1 extra kb was assumed).

2.5.2 PCR Amplification of the Gene Replacement Cassette

To amplify the cassette purified from digested pIJ773, a PCR reaction with the appropriate primers was performed under the following conditions:

1) Denaturation:	94 °C, 2 min		
2) Denaturation:	94 °C, 45 s	}	10 cycles
3) Primer annealing:	50 °C, 45 s		
4) Extension:	72 °C, 90 s		
5) Denaturation:	94 °C, 45 s	}	25 cycles
6) Primer annealing:	55 °C, 45 s		
7) Extension:	72 °C, 90 s		
8) Final extension:	72 °C, 5 min		

2.6 PCR Targeting Gene Replacement in *S. coelicolor*

PCR-targeting was used to generate rapid in-frame deletions or replacements of genes in *S. coelicolor* (Gust et al., 2002).

2.6.1 Primer Design

Two long PCR primers (targeting primers) were designed for each deletion following the procedure described in section 3.1. The targeting primers are listed in Table 2.6.

2.6.2 Purification of PCR Template (Resistance Cassette)

About 2 µg of plasmid pIJ773 (containing the *oriT*-apramycin resistance gene cassette) was digested with *EcoRI* and *HindIII* restriction enzymes in a total volume of 30 µL. The digestion was left for 3 h at 37 °C and then separated on an agarose gel

(1%). The smaller (1382 bp) of the two DNA bands (containing the cassette) was cut from gel. The DNA was purified from the agarose using a Qiagen gel extraction kit, following the manufacturer's instructions and stored at -20 °C.

2.6.3 PCR Amplification of the Gene Replacement Cassette

The purified cassette from pIJ773 was amplified by PCR with targeting primers (Table 2.6) using the reaction mixture shown in Table 2.9. PCR reactions were carried out using Expand High Fidelity polymerase (Roche) under the conditions described in section 2.5.2. 2 µL of the PCR product were analysed by gel electrophoresis for the presence of the pI773-derived disruption cassette with a size of 1476 bp. The rest of the PCR product was purified using the Qiagen PCR purification kit. The cassette was eluted with 35 µL of H₂O.

2.6.4 Introduction of Cosmids into *E. coli* BW25113/pIJ790 by Electroporation

E. coli BW25113, containing pIJ790 (with the *cat* gene that encodes chloramphenicol resistance) was grown overnight to prepare electrocompetent cells. 50 µL of the cell suspension was mixed with ~100 ng (2 µL) of engineered cosmid DNA. Electroporation was carried out as described above and after 1 h incubation at 30 °C, the cells were spread on LB agar medium containing ampicillin, kanamycin and chloramphenicol and incubated at 30 °C overnight.

2.6.5 PCR-targeting of Cosmids

One transformant from section 2.6.4 was transferred into 5 mL of LB liquid medium containing ampicillin, kanamycin and chloramphenicol and the resulting culture was incubated at 30 °C, 180 rpm overnight.

10 mL of LB liquid medium containing 20 mM MgSO₄, ampicillin, kanamycin and chloramphenicol was inoculated with 100 µL of the overnight culture. 100 µL of a 1 M L-arabinose stock solution (final concentration 10 mM) was added to induce expression of the *red* genes. Competent cells were prepared as described in section 2.2.3 and 50 µL of the cell suspension was mixed with ~100 ng (2 µL) of the PCR product. Electroporation was carried out as described in section 2.2.4 and the cells were incubated at 37 °C and 180 rpm, 1 h (the higher temperature promotes loss of the pIJ790 plasmid as it degenerates at temperature above 30 °C). The cells were spread on LB agar containing ampicillin, kanamycin and apramycin and incubated at 37 °C overnight (Figure 2.1).

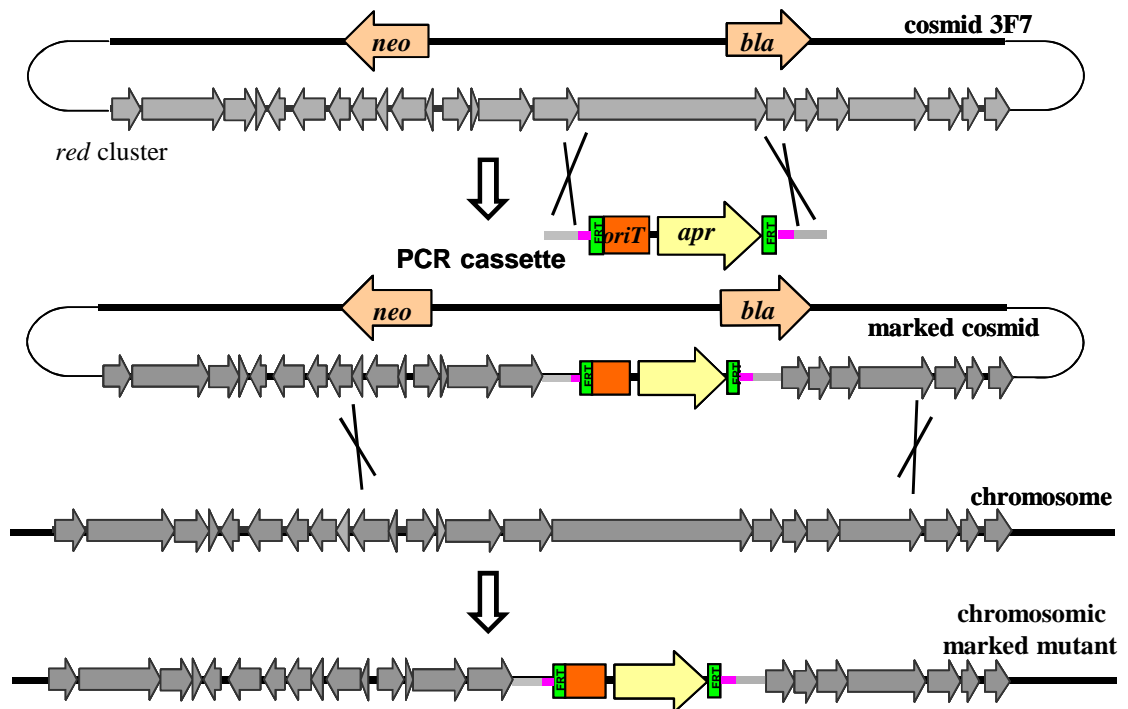


Figure 2.1 Homologous recombination of the disruption cassette with cosmid DNA to create a gene deletion in the cosmid, followed by conjugation from *E. coli* into *S. coelicolor* and double homologous recombination to give a mutant in which the gene of interest is replaced by the disruption cassette. Yellow gene – apramycin resistance, orange region – origin of transfer (*oriT*), green regions = FRT sites.

Colonies were observed the next day and two large colonies were used for preparation and isolation of cosmid DNA. Overnight cultures of each colony in 5 mL of LB liquid medium containing ampicillin and apramycin were prepared and cosmids were isolated from cultures that grew were using the procedure described in section 2.4.2.

To confirm that the desired gene replacement had occurred, restriction analysis carried out. About 20 µg of cosmid DNA was digested with *SacI*, *BamHI* or *XhoI* restriction enzymes in a total volume of 30 µL. The digestions were left for 3 h at 37 °C and then separated on an agarose gel (1%). The expected digestion pattern was confirmed by *in silico* prediction (using Clone Manager or NEBcutter programs). If the digestion result was good, integration of the disruption cassette in the desired place was confirmed by PCR with appropriate test primers (Table 2.7) and the targeted cosmid was introduced into *E. coli* ET12567/pUZ8002 by electroporation (section 2.2.3 and 2.2.4).

2.6.6 Transfer of the Mutant Cosmids into *Streptomyces*

The procedure for conjugal transfer of the engineered cosmid from *E. coli* ET12567/pUZ8002 into *S. coelicolor* is described in section 2.3.3. After the conjugation, the plates were overlaid with H₂O containing nalidixic acid to kill *E. coli*. Apramycin was also added to select for double crossover exconjugants, which are *apra*^R and *kan*^S. Apramycin resistant colonies were then screened for kanamycin sensitivity to select colonies that had undergone the double recombination event to flip out the backbone DNA of the cosmid. This was done by picking single apramycin resistant colonies (~50) and streaking them on both difco nutrient agar/kanamycin and difco nutrient agar/apramycin plates. Genomic DNA from apramycin resistant and kanamycin sensitive colonies was isolated and the desired replacement of the gene on the chromo-

some was confirmed by PCR (section 2.5) with test primers (section 2.1.7) and by Southern blot hybridisation (section 2.7) (Figure 2.1).

2.6.7 Construction of “scar” mutants

To obtain cosmids with an in-frame “scar” sequence in place of the apramycin cassette, *E. coli* DH5 α /BT340 competent cells were prepared and the appropriately engineered cosmid was introduced into them by electroporation. Cells were spread on LB agar containing apramycin and chloramphenicol and were incubated for 2 days at 30 °C. One single colony was streaked out on a new agar plate with no antibiotics to get single colonies and was incubated overnight at 42 °C (to induce FLP recombinase expression, followed by loss of the BT340 plasmid). 20 – 30 single colonies were picked and used to make two LB agar replica plates: one containing apramycin and the other containing kanamycin. The replica-plates were grown overnight at 37 °C. Apramycin^S (without the cassette) and kanamycin^R (from SuperCos of the cosmid) colonies, indicating loss of the cassette, were further verified by PCR analyses with test primers and by restriction digestion (Figure 2.2).

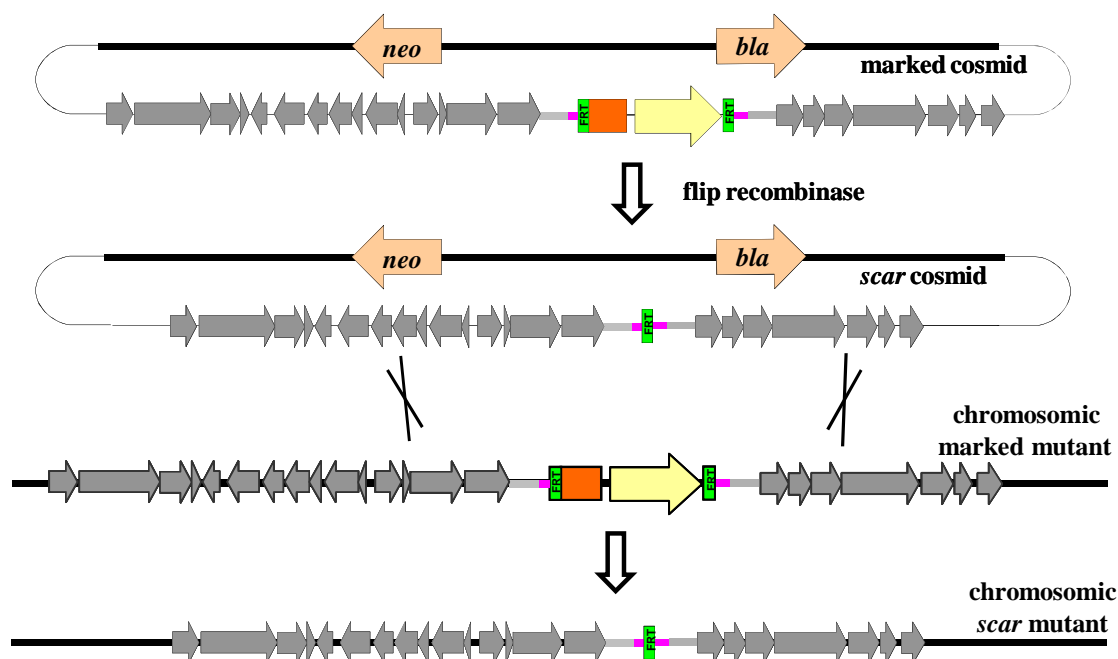


Figure 2.2 Flip recombinase-mediated step to give an 81 bp “scar” in place of the disruption cassette in the cosmid. Conjugal transfer of the cosmid to *S. coelicolor* can give a “scar” mutant. Yellow gene – apramycin resistance, orange region – origin of transfer (*oriT*), green regions = flip recombinase target (FRT) sites.

The cosmid with “scar” sequence in place of targeted gene lacks *oriT* (required for transfer cosmids from *E. coli* to *Streptomyces*). The *oriT*-cassette (*oriT-apr* or *oriT-tet*) was then one more time introduced to the cosmid inside the backbone sequence (*oriT-apr* inside the *neo* gene, *oriT-tet* inside the non-coding sequence) using *E. coli* BW25113/pIJ790, followed the procedures described in sections 2.6.4 and 2.6.5. After electroporation to introduce the *oriT*-cassette to engineered cosmid, the cells were spread on LB agar containing appropriate antibiotics (ampicillin and apramycin for “scar” cosmid + *oriT-apr* cassette) and ampicillin, kanamycin, tetracycline for “scar” cosmid + *oriT-tet* cassette) and the procedure from section 2.6.5 was continued. Once correct cosmid was identified and confirmed, was introduced into *E. coli* ET12567/pUZ8002 by electroporation (section 2.2.3 and 2.2.4) and transferred into

Streptomyces M511 (section 2.6.6). After the conjugation, the plates were overlaid with H₂O containing nalidixic acid to kill *E. coli*. Apramycin (for “scar” cosmid with *oriT-apr* cassette) or kanamycin and tetracycline (for “scar” cosmid with *oriT-tet* cassette) were also added to select for single crossover exconjugants. The antibiotic/s resistant colony was then picked and several rounds of growth of the single crossover mutant on SFM agar plates with no antibiotics were carried out. Spores were collected and spread to have single colonies. Single colonies were then screened for apramycin (for “scar” cosmid with *oriT-apr* cassette) or kanamycin/tetracycline (for “scar” cosmid with *oriT-tet* cassette) sensitivity to select colonies that had undergone the double recombination event to flip out the backbone DNA of the cosmid. This was done by picking single colonies (~50) and streaking them on broth difco nutrient agar/no antibiotics and difco nutrient agar/appropriate antibiotics plates. Genomic DNA from colonies sensitive to appropriate antibiotics was isolated and the desired replacement of the gene on the chromosome with “scar” sequence was confirmed by PCR (section 2.5) with test primers (section 2.1.7) and by Southern blot hybridisation (section 2.7) (Figure 2.2).

2.7 Southern Blot

Southern blot hybridizations were carried out using a DIG High Prime DNA Labelling and Detection Starter Kit (Roche).

2.7.1 Probe Labelling

1 µg of cosmid DNA (5 µL) was diluted to 20 µL with miliQ dH₂O and denatured at 100 °C for 10 min. The sample was cooled on ice, mixed with 4 µL of DIG High Prime solution and incubated overnight at 37 °C. On the next day the reaction was

stopped by adding 2 μL of 0.2 M EDTA and heating for 10 min at 65 °C. The sample was then diluted by adding 980 μL H_2O to give a DNA concentration of ~ 1 ng/mL.

2.7.2 Genomic DNA Digestion

10 μg of genomic DNA from each strain to be analysed was digested with *Bam*HI in a total volume of 50 μL , overnight. The samples were loaded onto a 0.7% agarose gel which was run overnight. The agarose gel was removed from the tank and left under a UV lamp for 5 min (to help denaturation). After UV treatment, the gel was rinsed with dH_2O and washed twice with denaturation buffer (2 x 15 min shaking at room temperature). After washing with dH_2O , the gel was washed twice, with neutralization buffer (2 x 15 min shaking at room temperature).

2.7.3 Capillary Transfer and DNA Fixing

20xSSC was poured into a plastic tray and a glass plate was placed across it. One sheet of Whatman 3MM paper was soaked in 20xSSC and placed on the glass plate so the ends of the paper touched the buffer in the tray. Another soaked square piece of paper was placed as a pad on the paper. The treated and neutralised agarose gel was placed on the paper pad with the well side down. A piece of positively charged nylon membrane (Amersham) was cut to the size of the gel and placed on the top of the gel followed by 3 pieces of Whatman 3MM paper the same size as the gel, stacks of paper towels, a glass plate, and finally a weight (2L flask filled with water). The tray was covered with cling film to prevent evaporation. The transfer was carried out overnight by capillary action. After the transfer, the membrane was removed and the DNA was fixed to it first by briefly washing the membrane with 2xSSC, and then by crosslinking (autocrosslinking option on a UV Stratalinker 2400, Stratagene).

2.7.4 Hybridization

The membrane with DNA crosslinked to it was placed in a hybridization tube (DNA facing inwards) with 20 mL of prehybridization solution (DIG Easy Hyb prepared by adding of 64 mL sterile dH₂O to DIG Easy Hyb granules and leaving for 5 min at 37 °C) and incubated for 2 h, rotating in a hybridisation oven at 67 °C. Hybridization solution was then prepared by adding 400 µL of the DIG labelled DNA probe (section 2.7.1) (boiled for 5 min at 95 °C and rapidly cooled down) to 7 mL of preheated DIG Easy Hyb. The prehybridization solution was poured off after 2 h of incubation and replaced by hybridization solution, and hybridization was carried out overnight, rotating in a hybridisation oven at 67 °C. On the next day, the hybridization solution was removed and the membrane was washed at 67 °C with preheated buffers: twice with 50 mL 0.5xSSC + 0.1% SDS (2 x 15 min with rotation), then three times with 50 mL 0.1xSSC + 0.1% SDS (3 x 20 min with rotation). The membrane was equilibrated by washing with 20 mL of washing buffer for 1 min at room temperature and blocked by incubation with 30 mL of blocking solution by rotating in a hybridisation oven at room temperature. After 1 h of incubation the solution was poured off and the membrane was incubated with 30 mL of blocking solution mixed with 3 µL of antiDIG antibody conjugate by rotating in a hybridisation oven at room temperature. After 30 min of incubation the solution was poured off and the membrane was washed twice with 50 mL of washing buffer (2 x 15 min, rotation in a hybridisation oven at room temperature) and equilibrated for 2.5 min with 30 mL of detection buffer.

2.7.5 Detection

The membrane was placed between 2 sheets of transparent plastic and sealed along 3 edges to create a pocket. 2 mL of chemiluminescence substrate CSPD was added to the membrane. Care was taken to exclude air bubbles and the membrane placed in the dark. After 5 min, the membrane was transferred to a new plastic pocket, sealed and incubated at 37 °C for 15 min. Then the membrane was exposed to film in darkness overnight. The film was developed following standard procedures.

2.8 Construction of a *S. longispororuber* Fosmid Library

A *Streptomyces longispororuber* genomic library was constructed using the commercially available CopyControl™ Fosmid Library Production Kit (Epicentre Biotechnologies, USA).

2.8.1 Shearing and End-repairing of DNA

Total genomic DNA from *Streptomyces longispororuber* was isolated according to the method described in section 2.4.1. The isolated DNA was sheared by pipetting 50 – 100 times through a 1 mL pipette tip to yield approximately 40 kb fragments and 1 µL of the sheared DNA was analysed by PFGE (Pulse Field Gel Electrophoresis) with the Fosmid Control DNA as a 40 kb marker. After further shearing, the DNA was diluted to 0.35 µg/µL and repaired using the End-Repair Enzyme according to the manufacturer's instructions to generate blunt-ended, 5'-phosphorylated DNA. After the reaction, the whole sample was run on a 1% low melting point (LMP) agarose gel using a PFGE apparatus with Fosmid Control DNA as a size standard. A band of ~40 kb was cut from gel and the DNA was recovered from the gel using GELase enzyme preparation.

2.8.2 Ligation of DNA into pCC1FOS, Packaging and Transfection of *E. coli*

The DNA concentration was measured using UV-Vis spectroscopy to be 66.2 ng/ μ L. A solution of the DNA (0.25 μ g, 0.009 pmoles) was used to carry out the ligation reaction with 0.09 pmoles of pCC1FOS vector (0.5 μ g) for 2 h at room temperature. After incubation and enzyme inactivation at 70 °C, the ligation reaction was added to the MaxPlax Lambda Packaging Extract and dilution buffer was added to a final volume of 1 mL. 100 μ L aliquots of the reaction were mixed with 1000 μ L of supplied *E. coli* EPI300-T1^R host cells (fresh day culture with OD₆₀₀ ~0.8 – 1.0, inoculated from overnight culture). After incubation for 20 min at 37 °C, a few aliquots of the infected *E. coli* host cells were stored as a glycerol stock at -80 °C and the rest of the infected EPI300-T1^R cells were spread in different dilutions on LB agar plates supplemented with 12.5 μ g/mL of chloramphenicol. The plates were incubated at 37 °C overnight to select for the Copy Control Fosmid clones and approximately 2000 colonies were obtained.

2.8.3 Screening the Fosmid Library for Clones containing *redG/redH* Orthologues

To check that the clones had different inserts, six clones were picked, used to inoculate LB liquid medium containing chloramphenicol and grown overnight at 37 °C and 180 rpm. The fosmid DNA was isolated, 5 μ L were digested with *Bam*HI enzyme and analysed by PFGE to confirm that the isolated clones have different digestion patterns.

To screen the library for clones containing *redG/redH* orthologues, 480 colonies were picked and grown separately in 96 well plates in LB liquid medium containing chloramphenicol (overnight at 37 °C). This number of clones was chosen to cover the *S.*

longispororuber genome (~8000 kb) 2.5 times (40 kb x 500 clones / 8000 kb = 2.5). This was the recommended number to identify a positive clone.

The clones were analysed by PCR using screening primers (complementary to the known fragments of the previously identified *redG* and *redH* orthologues). Initially, cultures from one row of the 96 well plate (12 wells) were mixed together and analysed in one PCR reaction along with a control reaction containing genomic DNA as the template. When a positive row was identified further PCR reactions were carried out on the 12 separate clones of that row to find the clone of interest, which was partially sequenced using the primers described in section 2.1.5 by GATC Biotech.

2.9 Growth and extraction of *Streptomyces* species for analyses of metabolite production

2.9.1 Prodiginines

R5 agar plates were overlaid with sterile semi-permeable membranes. 10 μ L of *S. coelicolor*, *S. longispororuber* or *S. venezuelae* spore suspension were spread on a one plate. After 5 to 7 days of incubation at 30 °C, mycelia were scraped off and collected in separate tubes to extract prodiginines with ~5 mL/plate of MeOH or a mixture of MeOH and MeCN (ratio 1:1, acidified to pH 3 with HCl). After vortexing and sonication (2 x 20s) the extract was centrifuged and the supernatant was analysed by LC-MS.

When feeding experiments were carried out, plates were inoculated with *Streptomyces* and after 2 or 3 days of incubation, 0.125-0.25 mg of synthetic 2-UP (2.5 mg/mL in 100% of MeOH) and/or MBC (2.5 mg/mL in DMSO) was dripped on the

plate (~20 drops). When the cultures were fed with undecylprodiginine, 0.05 mg in DMSO was dripped onto the plate (~20 drops). Incubation was carried out for a further 3 to 5 days, mycelia were scraped and extraction was carried out as described above.

When a liquid medium was used, 50 mL of SMM (Supplemented Minimal Medium) was inoculated with spores and the resulting cultures were grown (in flasks containing a spring as a baffle) shaking for 6 to 7 days at 30 °C and 180 rpm. After centrifugation (4000 rpm, 10 min at room temperature) the mycelial pellet was extracted as described above and was analysed by LC-MS.

Feeding strains with synthetic compounds could not be analysed quantitatively. Indeed feeding on solid medium (more preferable in this studied) was done by dripping compound solutions directly on the plate with growing strain, the entire plate was not covered with a known final concentration of the compound. Feeding cultures in liquid SMM medium would be more appropriate to quantify the yield of prodiginine produced however strains were not growing well in liquid medium. Therefore this method was not optimised.

For time-course analyses a small quantity of mycelia were scraped off the plate every 12 h and placed separate microcentrifuge tubes. The prodiginines were extracted by shaking for 2 h with 1 mL of MeOH acidified with 10 µL of 2N HCl. Samples were centrifuged and the absorbance of supernatant was measured at 533 nm. The mycelia were dried out overnight in the oven at 115 °C and the dry cell weight was measured.

2.9.2 Actinorhodins

To check actinorhodin production SMM liquid medium was used. The cultures were grown as described above for prodiginine production for 7 days. 2 mL of culture

(supernatant + mycelia) was mixed with 2 mL of MeOH. The samples were sonicated for 10 min and analysed by LC-MS to check the production of shunt metabolites. To measure the total blue pigment production, 1 mL of 5M KOH was added to 2 mL of culture supernatant. Samples were shaking for 1 h, centrifuged for 10 min at 14000 rpm and the absorption of the supernatant was measured at 640 nm. For dry cell weight measurements, 5 mL of culture supernatant containing mycelia was filtered through a filter paper of known weight. After drying overnight at 120 °C, the dry cell weight was measured.

2.9.3 Coelichelin

To check coelichelin production Iron Deficient Medium (IDM) was used. Spores were inoculated into 50 mL of IDM in plastic flasks and shaken for 6 to 7 days (30 °C, 180 rpm). 1 mL of culture supernatant was taken and 25 µL of 300 mM FeCl₃ was added. Samples were incubated for 30 min (at room temperature) and pelleted by centrifugation (3000 rpm, 5 min). The clarified supernatant was analysed by LC-MS.

2.9.4 Methylenomycin Production Bioassay

Strains were grown on AlaMM medium for 2 days at 30 °C to check methylenomycin production. After 2 days of incubation, agar plugs (about 1 cm by 1 cm) were cut out from each plate and placed in the middle of AlaMM plates with *S. coelicolor* M145 growing on them (as an indicator strain, sensitive to methylenomycin). After 3 days of incubation at 30 °C the zone of growth inhibition for M145 around each agar plug was recorded.

2.9.5 CDA Production Bioassay

To check production of CDA, patches of the *S. coelicolor* strains (about 1 cm x 1 cm) were grown on ONA agar plates in duplicate. After 2 days of incubation at 30 °C, the plates were overlaid with 3 mL of SNA containing 0.5 mL of a culture of the indicator strain *Bacillus mycoides* ($OD_{600nm} = 0.6$) +/- $Ca(NO_3)_2$. After overnight incubation at 37 °C, the zones of growth inhibition were recorded.

2.10 Chemistry Techniques

2.10.1 Conversion of desmethylundecylprodiginine to undecylprodiginine

HPLC purified desmethylundecylprodiginine (from 4 R5 agar plates) was resuspended in 1.5 mL of CH_2Cl_2 containing 48% aqueous fluoroboric acid (0.026 mL) at 0 °C under N_2 . Then, 3 x 0.05 mL portions of $TMSCHN_2$ (2.0M in diethyl ether) were added dropwise at intervals of 20 minutes to the reaction mixture. After the addition was complete, the solution was stirred at 0 °C for a further 30 minutes, followed by a further 30 min stirring at room temperature. The organic layer was separated and evaporated to dryness. The residue was resuspended in 1 mL of MeCN and analysed by LC-MS/MS.

2.10.2 Purification of prodiginines from *S. coelicolor* extract

Prodiginine antibiotics were extracted from eight agar plate cultures of *S. coelicolor* W31/pOSV556mcpG grown as described above. The solvent was evaporated; the residue was resuspended in $CHCl_3$ and washed 3 times with deionised water (adjusted to pH 3 with aqueous HCl). The organic layer was separated and evaporated to dryness. The prodiginines were purified from this crude extract by flash column chromatography on basic alumina eluting with 10% EtOAc/Hexane. Fractions containing prodiginines

were combined and concentrated *in vacuo*. The residue was partitioned between CHCl_3 and deionised water (pH 3) to convert the prodiginines to their HCl salts. The organic layer was separated and evaporated to dryness.

Partially purified metacycloprodigiosin was further purified using an Agilent 1200 Series preparative HPLC instrument equipped with a binary pump and a diode array detector. The prodiginine mixture obtained from the alumina column was resuspended in 6 mL of MeOH and passed through a 0.4 μm filter. 5.5 mL of the filtrate were purified on an Agilent Zorbax C18 column (150 x 21.2 mm, 5 μm) using the gradient elution profile in Table 2.10 and the compound with a retention time of 7 minutes was collected.

Table 2.10 HPLC conditions used for purification of metacycloprodigiosin on Agilent Zorbax C18 column (150 x 21.2 mm, 5 μm)

Time (min)	H ₂ O/HCl (pH 3) (%)	MeOH (%)	Flow Rate (mL/min)
0	30	70	20.0
5	35	75	20.0
7.5	20	80	20.0
10	10	90	20.0
11.25	10	90	20.0
11.50	30	70	20.0

The fraction was extracted with CHCl_3 and washed with deionised water (adjusted to pH 3 with aqueous HCl). The organic layer was separated and evaporated to dryness. The residue was further purified using the same HPLC instrument on an Agilent Zorbax Phenyl column (250 x 21.2 mm, 7 μm) using the conditions in Table 2.11 and the compound with a retention time of 6 minutes was collected and the fraction was extracted with CHCl_3 . The organic layer was separated and evaporated to dryness to

afford metacycloprodigiosin as a pink solid. The identity of this compound as metacycloprodigiosin was confirmed by CD and ^1H NMR (Bruker Avance spectrometer, 400 MHz, CDCl_3) spectroscopic comparisons with authentic samples of metacycloprodigiosin and streptorubin B isolated from *S. longispororuber* M-3 and *S. coelicolor* M511, respectively.

Table 2.11 HPLC conditions used to purify metacycloprodigiosin on an Agilent Zorbax Phenyl column (250 x 21.2 mm, 7 μm)

Time (min)	H ₂ O/HCl (pH 3) (%)	MeOH (%)	Flow Rate (mL/min)
0	24	76	20.0
10	18	82	20.0
11	10	90	20.0
13	10	90	20.0
16.50	24	76	20.0

2.10.2.1 Circular Dichroism (CD) spectroscopy

Metacycloprodigiosin purified from *S. longispororuber*/*S. coelicolor* W31/pOSV556*mcpG* and streptorubin B purified from *S. coelicolor* M511 were analysed by CD spectroscopy on a Jasco J-815 CD Spectrometer. Samples were dissolved in MeOH and the CD spectrum from 700 to 200 nm of each solution was measured in a 1 mm path length cuvette. Instrument settings were as follows: resolution 0.4 nm, band width 2.0 nm, sensitivity 200 mdeg, response 1 s, speed 200 nm/min.

2.10.3 Purification of Desmethylundecylprodiginine

An Agilent 1100 instrument equipped with a quaternary pump and variable wavelength detector set to monitor absorbance at 490 nm was used to purify desmethy-

lundecylprodiginine. 1 mL of filtered extract was injected onto an Agilent Zorbax C18 column (100 x 21.2 mm, 5 μ m) using the gradient elution profile shown in Table 2.12 and the compound with a retention time of 20 minutes was collected. The fraction was extracted with CHCl₃ and the organic layer was separated and washed with deionised water (adjusted with HCl to pH 3). The organic layer was separated and evaporated to dryness.

Table 2.12 HPLC conditions used in desmethylundecylprodiginine purification

Time (min)	H ₂ O/HCl (pH 3) (%)	Acetonitrile (%)	Flow Rate (mL/min)
0	20	80	5.0
10	20	80	5.0
20	0	100	5.0
30	0	100	5.0

2.10.4 LC-MS

Liquid chromatography – Mass Spectrometry (LC-MS) was used to analyse culture extracts/culture supernatants for prodiginines, actinorhodin-related metabolites and coelichelin. 50 μ L of each extract/supernatant was injected onto an Eclipse XDB-C18 column (150 x 4.6 mm, 5 μ m, column temperature 25 °C, Agilent) connected to an Agilent 1100 instrument equipped with a binary pump and a diode array detector. The HPLC outflow was connected via a splitter (10% flow to MS, 90% flow to waste) to a Bruker HCT+ mass spectrometer equipped with an electrospray source operated in positive ion mode with parameters as follows: nebulizer flow 40 psi, dry gas flow 10.0 L/min, dry temperature 300 °C, capillary – 4 kV, skimmer 40V, capillary exit 106 V, ion charge control target (ICC) 100,000, spectral averages 3. The gradient elution profile

used to analyse 2-UP, MBC, prodiginines and analogues is shown in Table 2.13 and that used to analyse actinorhodin and coelichelin is shown in Table 2.14.

Table 2.13 Gradient elution profile used in LC-MS analyses of prodiginine production

Time (mins)	Water (pH3 with HCl or 0.1% formic acid)	MeCN or MeOH	Flow Rate
0	50	50	1.0
1	50	50	1.0
4	25	75	1.3
21	20	80	1.4
23	50	50	1.0

Table 2.14 Gradient elution profile used in LC-MS analyses of actinorhodin and coelichelin production

Time (mins)	Water + 0.1% formic acid	MeOH + 0.1% formic acid	Flow Rate
0	50	50	1.0
1	50	50	1.0
4	25	75	1.0
21	20	80	1.0
23	50	50	1.0

2.10.5 High Resolution Mass Spectrometry

High Resolution Mass Spectrometry (HRMS) was done by University of Warwick Mass Spectrometry Service and was used to confirm the molecular formulae of the purified compounds. HRMS was carried out on an ESI-TOF-MS (Bruker MicroTOF) using direct infusion.

3. Mutagenesis of Genes in the *S. coelicolor* red Cluster

3.1 PCR-targeting Strategy

The strategy of PCR-targeting for mutagenesis in *Streptomyces coelicolor* was used to create rapid gene knockouts (Gust et al., 2002; Gust et al., 2003). The protocol allows replacement of a chromosomal DNA sequence (targeted gene) within a cosmid from the ordered genomic library (Redenbach et al., 1996) of *S. coelicolor* disruption with a cassette containing an apramycin resistance gene generated by PCR using primers with 39 nt 5' extensions, that are homologous to regions directly adjacent to the gene of interest. The inclusion of an origin of transfer (*oriT*) in the disruption cassette, allows conjugation to be used to transfer the PCR-targeted cosmid from *E. coli* to *S. coelicolor*. The presence of the FRT (FLP recombinase target) sites, flanking the disruption cassette allows the excision of the cassette when a FLP recombinase is expressed, generating "scar" cosmids in which the gene of interest is replaced by an 81 bp in-frame coding sequence.

The plasmid pIJ773 was used as a template for generating the disruption cassette (containing *apr* and *oriT*, flanked by FRT sites) (Figure 3.1). The plasmid pIJ773 was digested with *EcoRI* and *HindIII* restriction enzymes and the ~1.4 kb fragment purified from an agarose gel was used as a template for PCR amplification.

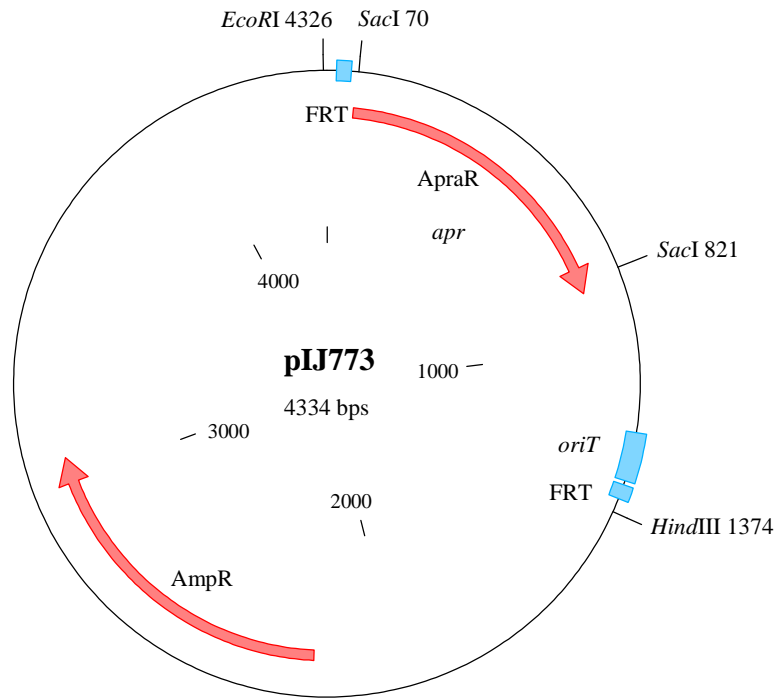


Figure 3.1 Feature map of pIJ773.

To amplify the *oriT-apr* cassette, long PCR primers of 59 nt (upstream primer) and 58 nt (downstream primer) were designed. Each had, at the 5' end 39 nt identical to the *S. coelicolor* sequence adjacent to the target gene, and at the 3' end 19 or 20 nt matching the right or left end of the disruption cassette. The primers were designed to be in-frame with the reading frame of the gene to be deleted (Figure 3.2).

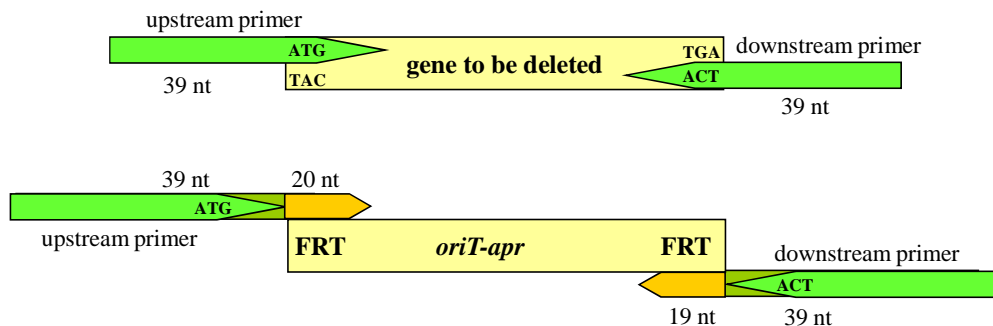


Figure 3.2 Design of PCR primers for making a gene replacement or in-frame deletion using PCR-targeting (Gust et al., 2002).

The cosmid containing the target gene was introduced into *E. coli* BW25113 carrying the recombination plasmid pIJ790. The next step consisted of introducing by electroporation the disruption cassette into the resulting transformant. The apramycin^R colonies, in which a double crossover between the cosmid and cassette should have occurred, were analysed by digestion with a restriction enzyme and by PCR. The primers used for PCR analyses (test primers) were 20 nt long and chosen to prime ~100 bp outside the region of the intended gene disruption. The size of the PCR product allowed discrimination between the presence in the cosmid of the wild type gene and disruption cassette. In addition, apramycin resistance was conferred to the mutated cosmids and apramycin was used for selection (Figure 3.3).

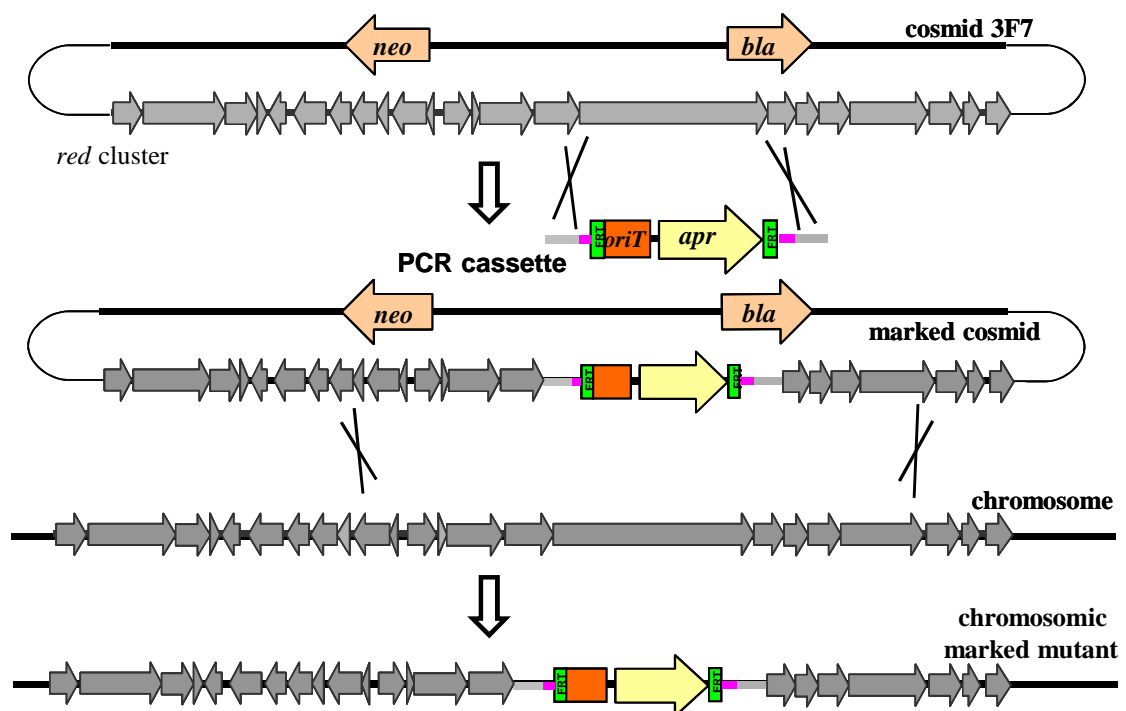


Figure 3.3 Homologous recombination of the disruption cassette with cosmid DNA to create a gene deletion in the cosmid, followed by conjugation from *E. coli* into *S. coelicolor* and double homologous recombination to give a mutant in which the gene of interest is replaced by the disruption cassette. Yellow gene – apramycin resistance, orange region – origin of transfer (*oriT*), green regions = FRT sites.

The cosmid containing a gene replacement was then used to transform *E. coli* ET12567/pUZ8002 by electroporation. This strain does not methylate DNA. Use of this strain was necessary due to *S. coelicolor* methylated DNA-sensing restriction system, which would degrade methylated cosmid DNA derived from normal *E. coli* strains.

From *E. coli* ET12567/pUZ8002, the disrupted cosmid could then be transferred into *S. coelicolor* by conjugation by mixing the *E. coli* strain carrying the mutant cosmid with *S. coelicolor* spores. After overnight incubation on SFM plates, *E. coli* cells were selectively killed using nalidixic acid and *Streptomyces* colonies that did not contain the introduced cosmid, were killed by addition of apramycin to the SFM plate.

As a result of this conjugal transfer double crossover was expected in some colonies between genomic DNA and the mutant cosmid, during which the target gene was replaced with the apramycin cassette. Double crossover colonies were identified on the basis of apramycin resistance (because the disruption cassette contains *apr*) and kanamycin sensitivity (because the cosmid backbone containing the kanamycin resistance gene has been lost). The integrity of putative double crossover mutants was confirmed by PCR (Figure 3.3).

To replace the disruption cassette by an 81 bp in-frame gene replacement, the marked cosmid was transferred into *E. coli* DH5 α /BT340, which produces a FLP-recombinase, used to remove the disruption cassette (Figure 3.4) and leave an 81 bp coding DNA sequence in its place.

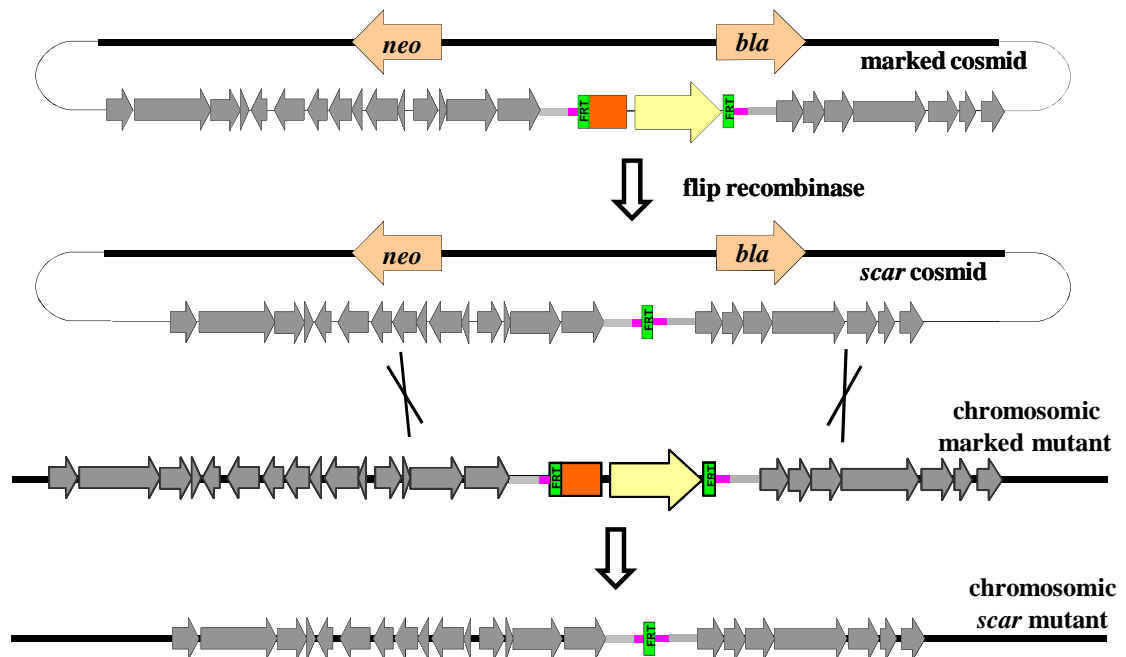


Figure 3.4 Flip recombinase-mediated step to give an 81 bp “scar” in place of the disruption cassette in the cosmid. Conjugal transfer of the cosmid to *S. coelicolor* can give a “scar” mutant. Yellow gene – apramycin resistance, orange region – origin of transfer (*oriT*), green regions = flip recombinase target (FRT) sites.

The ability to remove the *oriT-apr* cassette is important because its introduction into an operon could generate a polar effect meaning transcription of downstream genes could be affected. The generation of “scar” mutants also allows the same *apr* resistance gene to be used for making multiple knockouts sequentially in the same cosmid or strain.

In this study, polar effects on the expression of downstream genes did not appear to be a problem. Thus, in most cases, mutants containing *oriT-apr* cassette were created and analysed. “Scar” mutants were only made in the process of generating double knockout mutants, allowing the apramycin resistance gene to be used twice.

3.2 Gene Replacements Generated within the *red* Cluster

The DNA sequence of the *red* gene cluster was published in 2002 together with the entire sequence of *S. coelicolor* A3(2) (Bentley et al., 2002). Several genes in the cluster have previously been replaced (Table 3.1) and their function has been analysed. In this study several further genes within the *red* cluster, which had not been investigated previously, were deleted and their functions were investigated (Table 3.1). Some of the mutants made previously were also analysed as a part of this work.

Table 3.1 Mutants with genes from the *red* cluster deleted analysed in this study.

Disrupted Gene	Background	<i>oriT-apr</i> replacement	In-frame replacement
PREVIOUSLY CONSTRUCTED MUTANTS ANALYSED HERE			
<i>redG</i> (Odulete, 2005)	M511	X	✓
<i>redH</i> (Haynes et al., 2008)	M511	✓	X
<i>redL</i> (Mo et al., 2008)	M511	✓	X
<i>redN</i> (Cerdeño et al., 2001)	M511	X	✓
MUTANTS CONSTRUCTED AND ANALYSED IN THIS STUDY			
<i>redI</i>	M511	✓	X
<i>redJ</i>	M511	✓	✓
<i>redK</i>	M511	✓	X
<i>redL</i> A domain	M511	✓	X
<i>redL</i>	M595	✓	X
<i>redT</i>	M511	✓	X
<i>redV</i>	M511	✓	X

To replace the previously uninvestigated genes in the *red* cluster, specific primers were designed for each targeted gene and were used to amplify the *oriT-apr* cassette. For most of the gene replacements, the primers were designed as previously described (section 3.1) to encompass the start and stop codons of the targeted gene. Primers designed in this way were not successfully used for replacing *redT* and *redV* in *S. coelicolor* M511. Even that the right mutated cosmid was generated this construct with no obvious reasons did not allowed to generate right mutation within *S. coelicolor* genomic DNA and clones with double crossover were never found. To create *redT::oriT-apr* and *redV::oriT-apr* mutants, the priming sequences (39 nt) used were taken 20-50 bp after the start codon and before the stop codon of the targeted genes i.e. within the targeted genes. Approximately 1460 bp PCR products (cassette + primers) were amplified using pIJ773 as a template and purified by agarose gel electrophoresis and subsequent extraction. The purified disruption cassettes were introduced into *E. coli* BW2511/pIJ790, containing the cosmid Sc3F7 using electroporation. To check if the desired gene replacements had occurred correctly, cosmids were isolated and analysed by PCR using test primers designed to anneal ~100 bp upstream/downstream of the genes to be replaced (Figure 3.5), and by comparison of restriction enzymes digestion patterns of the mutated cosmids with the wild type cosmid (examples of digestion with *SacI*, which cuts twice within the *oriT-apr* cassette generating a specific 752 bp band indicative of the presence of the cassette, and *BamHI* enzymes are shown in Figure 3.6).

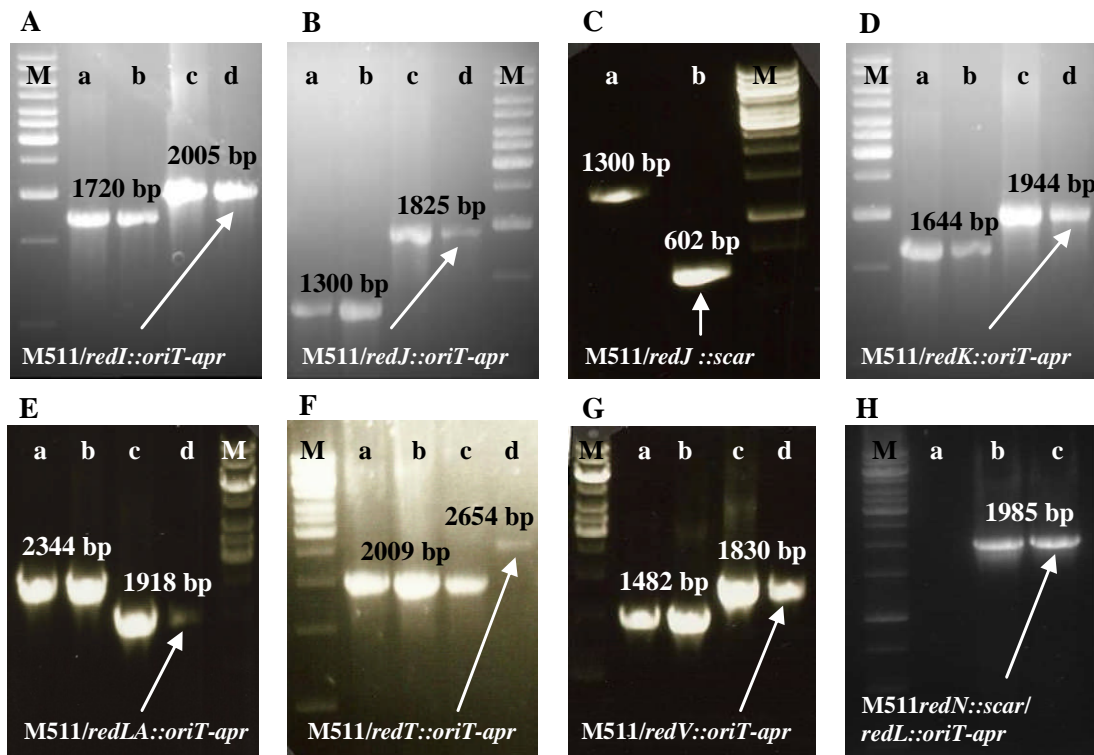


Figure 3.5 PCR analyses of mutagenised Sc3F7 cosmids and genomic DNA extracted from *S. coelicolor* M511 and M595 mutants, A: a – Sc3F7 cosmid, b – wild type, M511 DNA, c – Sc3F7/*redI::oriT-apr*, d – M511/*redI::oriT-apr*, with *redI* test primers; B: a – Sc3F7 cosmid, b – wild type, M511 DNA, c – Sc3F7/*redJ::oriT-apr*, d – M511/*redJ::oriT-apr*, with *redJ* test primers; C: a – wild type, M511 DNA, b – M511/*redJ::scar*, with *redJ* test primers; D: a – Sc3F7 cosmid, b – wild type, M511 DNA, c – Sc3F7/*redK::oriT-apr*, d – M511/*redK::oriT-apr*, with *redK* test primers; E: a – Sc3F7 cosmid, b – wild type, M511 DNA, c – Sc3F7/*redLA::oriT-apr*, d – M511/*redLA::oriT-apr*, with *redLA* test primers; F: a,b – Sc3F7 cosmid, c – wild type, M511 DNA, d – M511/*redT::oriT-apr*, with *redT* test primers; G: a – Sc3F7 cosmid, b – wild type, M511 DNA, c – Sc3F7/*redV::oriT-apr*, d – M511/*oriT-redV::apr*, with *redV* test primers; H: a – wild type, M511 DNA (expected size in wild type DNA 7502 bp), b – Sc3F7/*redL::oriT-apr*, d – M595/*redL::oriT-apr*, with *redL* test primers; M – 1 kb ladder.

Correctly modified cosmids were introduced into *S. coelicolor* M511 (or in one case M595) by intergenic conjugation from *E. coli* ET12567/pUZ8002. Apramycin-resistant, kanamycin-sensitive *Streptomyces* exconjugants were analysed by PCR (with test primers) to confirm double crossover gene replacement had taken place (Figure 3.5). The integrity of the mutants was further confirmed by Southern blot hybridisation using labelled Sc3F7 cosmid as a probe (Figure 3.7).

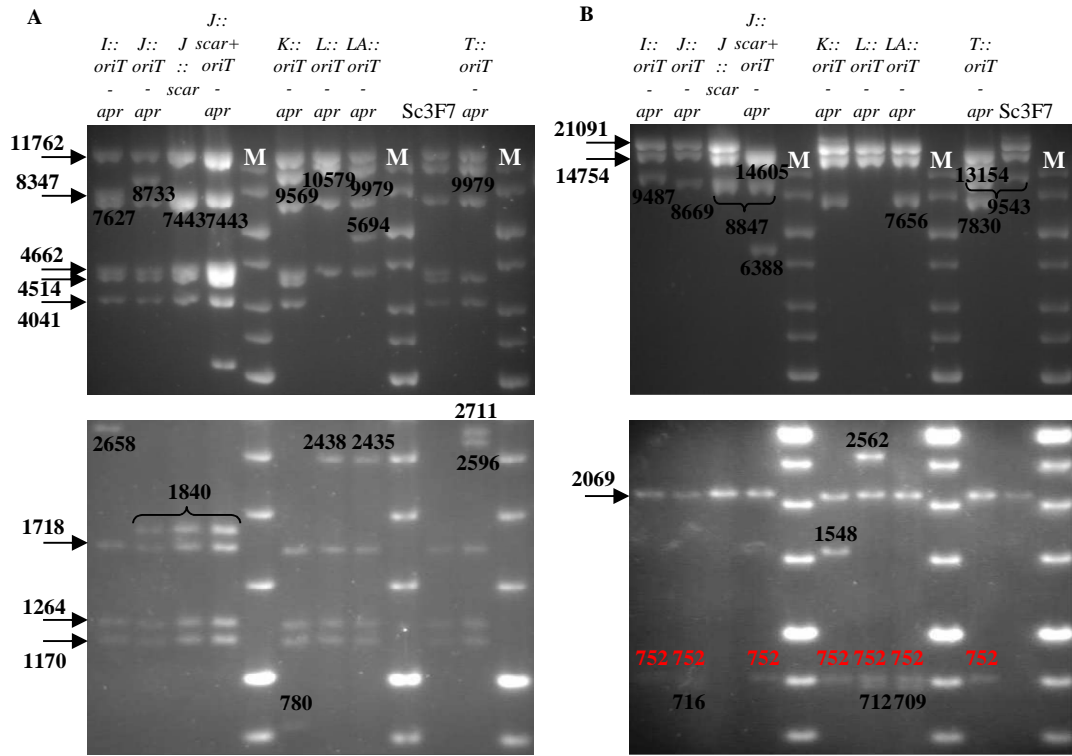


Figure 3.6 Agarose gel electrophoresis analysis of restriction enzymes digest of genetically-engineered cosmids used to disrupt the *S. coelicolor* genes within *red* cluster. A – *Bam*HI, B – digestion with *Sac*I. Top gels show high molecular weight bands, bottom gels show low molecular weight bands. Numbers indicated by arrows show the digestion pattern of Sc3F7 cosmid. Number written on the gel shows additional and/or changed bands characteristic for modified Sc3F7 cosmids. B – 752 bp band indicate the presence of the cassette.

The *redJ* gene was first replaced in 3F7 with the *oriT-apr* cassette and then the cassette was removed to have a “scar” sequence. Because *oriT* is lost from this mutagenised cosmid, conjugal DNA transfer from *E. coli* to *S. coelicolor* could not be carried out. Thus the *oriT-apr* cassette was reintroduced into the mutagenised cosmid in place of the *neo* gene (*Sc3F7/redJ::scar+neo::oriT-apr*). This construct was then transferred by conjugation from *E. coli* to *S. coelicolor* M511. An exconjugant with the mutagenised cosmid integrated into the chromosome by single crossover was picked on the basis of apramycin and kanamycin resistance. Several rounds of growth of the single cross-

over mutant on SFM agar plates with no antibiotics resulted in the colonies of M511/*redJ::scar*, where double crossover had taken place (backbone of the cosmid was lost). The resulting mutant was analysed by PCR and Southern blot hybridisation (Figure 3.6, Figure 3.5, Figure 3.7).

The M511/*redV::oriT-apr* mutant was analysed carefully by PCR, using test primers and a product of the expected size was amplified. Sequencing of the PCR product showed that the cassette is present in the correct genetic context. Southern blot hybridisation analysis was carried out to confirm the nature of the mutant. DIG-labelled Sc3F7 cosmid was used as a probe. Genomic DNA from the mutant and the M511 parent strain, as well as the probe were digested with *Bam*HI enzyme and after hybridisation, different patterns of bands were expected to be seen for the mutant and the M511 wild type. Careful inspection of the blot revealed a band from the wild type strain in the mutant. This band should have disappeared if the apramycin cassette had been correctly inserted into the chromosome of the mutant. Another unexpected and unidentified band ~6500 bp was observed in the blot of the mutant. Therefore it was concluded that the mutant does not have the desired genotype and that a copy of *redV* gene is still present. As a consequence, this mutant was not analysed further (Figure 3.5 G, Figure 3.7).

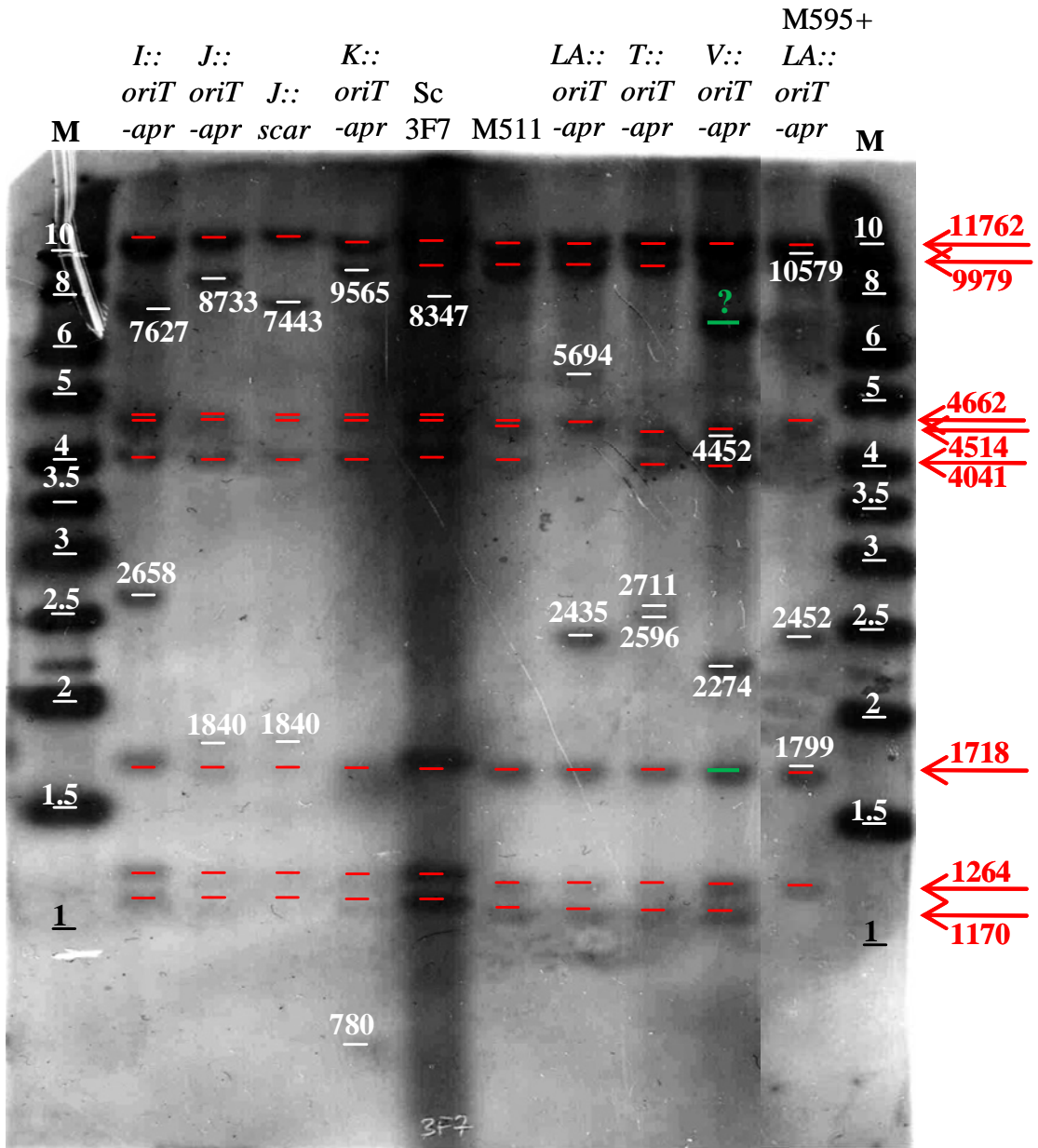


Figure 3.7 Southern blot hybridisation using labelled Sc3F7 cosmid as a probe confirming the nature of *S. coelicolor* mutants with genes deleted from the *red* cluster. Bands highlighted in red are all present in *S. coelicolor* M511. Bands highlighted in white are characteristic for each mutant. The 8347 bp bands in the Sc3F7 are derived from the SuperCos backbone. M511/*redV::oriT-apr* – green 1718bp and ~6500 bp bands should not be present in the mutant.

3.3 Genetic Complementation of the Mutants

Some of the mutants described above were complemented by *in trans* expression of the deleted genes from the integrative plasmid pOSV556 (Figure 3.8). Targeted genes were cloned into pOSV556 under the control of the constitutive *ermE** promoter. The plasmid contains two antibiotic resistance genes: one for ampicillin (for selection in *E. coli*) and the other for hygromycin (for selection in *Streptomyces*). It also contains *oriT*, which allows conjugal transfer of the plasmid from *E. coli* to *Streptomyces*. In addition, this vector can integrate into the *Streptomyces* chromosome through site-specific recombination between the *attP* site within the vector and the *attB* site within the chromosome. This integration is catalysed by an integrase that is encoded within pOSV556 (Raynal et al., 2002). In *S. coelicolor*, such DNA insertions are stable and no antibiotic selection is therefore needed to grow subsequent generations.

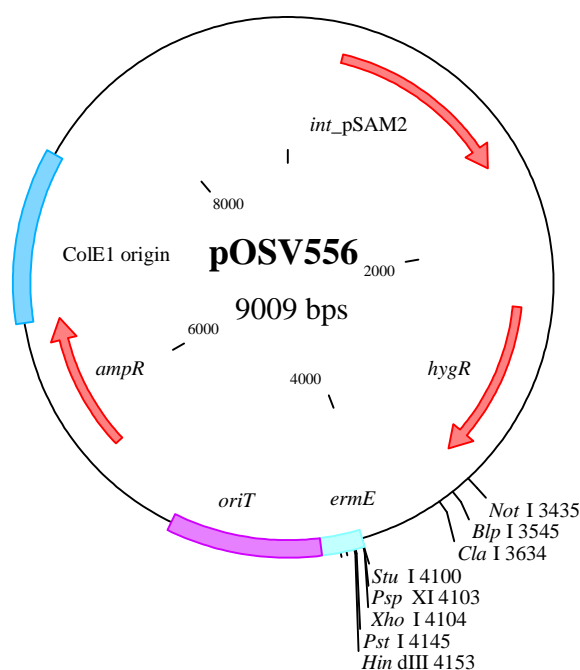


Figure 3.8 Feature and restriction site map of pOSV556.

pOSV556 constructs were not only used for genetic complementation of *S. coelicolor* mutants, but also to investigate the function of specific genes via heterologous expression in other *Streptomyces* strains.

PCR primers were designed to clone genes of interest into pOSV556. Initially cloning into the vector involved a forward primer that anneals starting 12 bp upstream of the start codon of the gene of interest and therefore includes the natural ribosome binding site (RBS). In later experiments, an artificial conserved RBS (5'-AGGAGG-3') (Strohl, 1992) was introduced into the primer followed by the 6 bp upstream of the start codon and the first 14 bp of the coding sequence. Reverse primers were designed to anneal around 100 bp downstream of the stop codon of the gene. The amplified product was designed to be cloned in the multiple cloning site of pOSV556. The forward primers in all cases contained *Hind*III restriction site and reverse primers contained *Xho*I, *Pst*I or *Not*I. Constructs in the pOSV556 plasmid were created by standard cloning procedures. Appropriately digested PCR products (with enzymes which restriction sites were introduced by primers) were ligated with similarly digested pOSV556. The ligation mixture was then used to transform *E. coli* DH5 α by electroporation and growing colonies were selected on LB agar with ampicillin. Correct insertion of the PCR product into the vector was confirmed by restriction digest and by PCR using the cloning primers. Plasmid clones were transferred by conjugation from *E. coli* ET12567/pUZ8002 to the appropriate *Streptomyces* strain and a single hygromycin resistant exconjugant was chosen for subsequent analyses.

Table 3.2 Created constructs in pOSV556 plasmid analysed in Chapters 4, 5 and 6.

Genes cloned to pOSV556 plasmid	Background strains/mutants
<i>redH</i>	<i>redH</i>
<i>redH</i>	<i>Streptomyces venezuelae</i>
<i>redG</i>	M511
<i>redG</i>	<i>redG</i>
<i>redG</i>	<i>Streptomyces venezuelae</i>
<i>redHG</i>	M511
<i>redHG</i>	<i>redG</i>
<i>redHG</i>	<i>Streptomyces venezuelae</i>
<i>mcpG</i>	<i>redG</i>
<i>mcpG</i>	<i>Streptomyces venezuelae</i>

3.4 Conclusions

The PCR-targeting method (Gust et al., 2002) was used to create rapid knockouts of genes within the *red* cluster and the mutants generated are going to be analysed in Chapter 4, 5 and 6. Marked mutants for *redI*, *redJ*, *redK*, *redL* A domain, *redT* and *redV* were generated, where each gene was replaced with an apramycin resistance cassette containing *oriT* (allows conjugal transfer of PCR-targeted cosmid from *E. coli* to *Streptomyces*). Correct construction of the mutants was confirmed by PCR analyses. Additional analysis by Southern blot showed that all mutants were constructed correctly except of *redV* mutant where wild type background of DNA was still present. M511/*redV::oriT-apr* was therefore not analysed further. In the case of *redJ* a scar mutant was also constructed; *redJ* gene was replaced by 81 bp in-frame coding sequence. Construction of M511/*redJ::scar* was necessary for planned further generation of double mutant together with *scoT*.

To further investigate the function of some of the genes within the *red* cluster genetic complementation of the mutants was carried out. Targeted genes were cloned to pOSV556 plasmid which can integrate with *Streptomyces* chromosome. Prepared constructs were then introduced to parent *S. coelicolor* strain as well as were heterogously expressed in *S. venezuelae*.

**4. Investigation of Genes Involved in Biosynthesis and
Condensation of 2-Undecylpyrrole and 4-Methoxy-2,2'-
bipyrrole-5-carboxaldehyde**

4.1 Analysis of Prodiginine Production

Analytical chemistry techniques (HPLC, LC-MS) were used to detect prodiginines and their intermediates in *Streptomyces coelicolor* M511 and in the analysed mutants. *S. coelicolor* accumulates two prodiginine antibiotics: undecylprodiginine (**2**) and streptorubin B (**3**). The tripyrrole structure of these compounds gives them an intense red colour, making them easy to detect visually and by UV-Vis spectroscopy. Both prodiginine antibiotics were known to have high extinction coefficient at 533 nm (Kieser et al., 2000). Not many other compounds absorb at this wavelength. Therefore absorbance at 533 nm is very characteristic for **2** and **3** and there is a low background from other compounds in HPLC chromatograms resulting from detection at 533 nm (Figure 4.1).

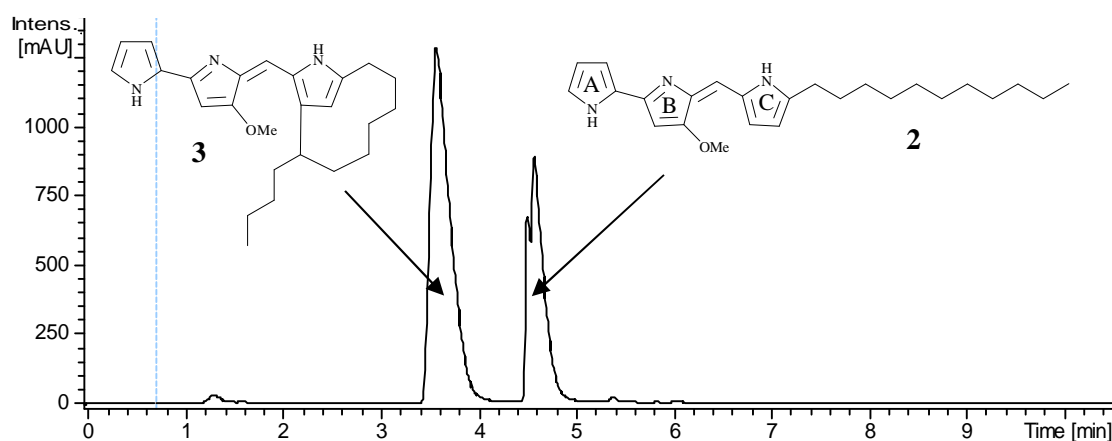


Figure 4.1 Typical HPLC chromatogram monitoring absorbance at 533 nm of acidified organic extracts of *S. coelicolor* M511, showing resolution of undecylprodiginine (**2**) and streptorubin B (**3**).

Liquid Chromatography – Mass Spectrometry (LC-MS) is also a convenient method for analysing prodiginines in extracts of *S. coelicolor* M511 (Figure 4.2).

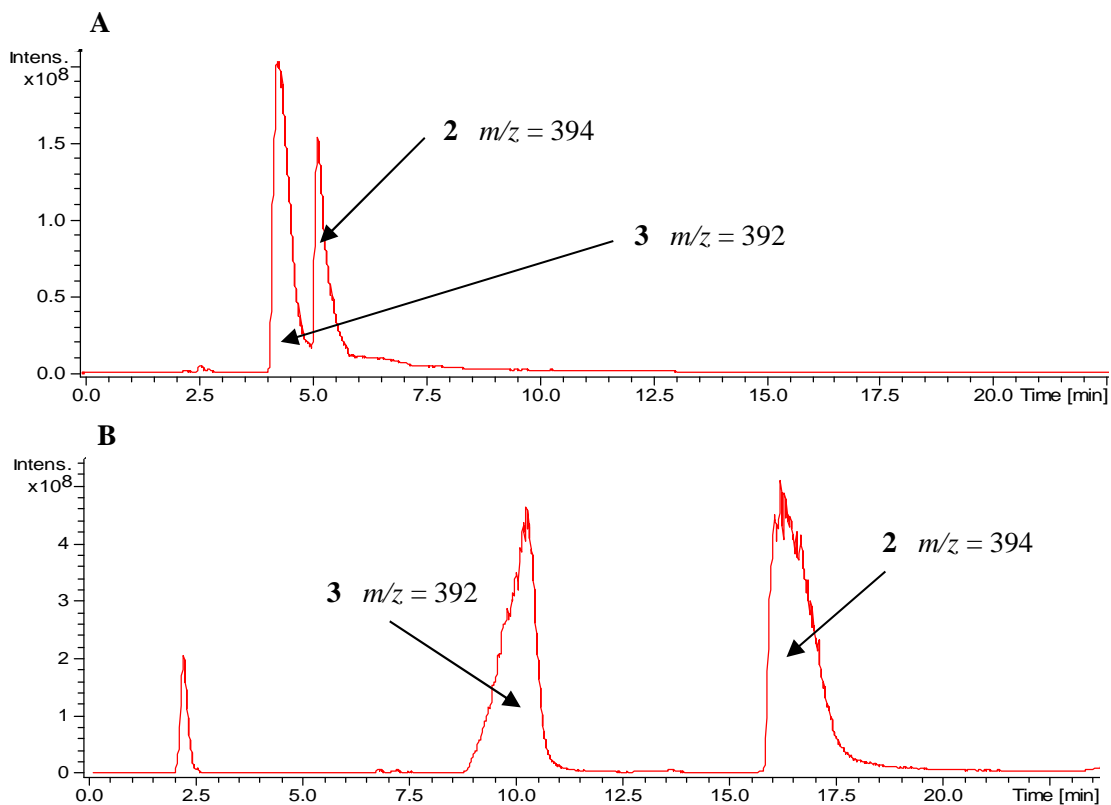


Figure 4.2 Extracted ion chromatograms (EICs) for $m/z = 392$ - 394 in positive ion mode from LC-MS analyses of acidified organic extracts of *S. coelicolor* M511. Both samples were eluted through a C-18 column with water and an organic solvent (A – MeCN or B – MeOH).

The first prodiginine eluted in LC-MS analyses is streptorubin B with $m/z = 392$ compound and the second one is undecylprodiginine with $m/z = 394$. Compound **2** sometimes gives two peaks in chromatograms, probably due to two interconverting configurational isomers of this molecule (resulting from rotation around the bonds between the B and C rings). These two configurations have been shown to be in rapid equilibrium on the column (Corre and Challis, unpublished results) (Figure 4.1). The difference in retention time between streptorubin B and undecylprodiginine in Figure 4.2 A and Figure 4.2 B results from the difference in the organic solvent used for elution. In early analyses, acetonitrile was used (giving a later retention time for **3** of

~4.5 min and for **2** of ~5.5 min, what could also cause broader peaks). Acetonitrile was later replaced by methanol (giving a retention time for **3** of ~10 min and for **2** of ~17 min). The solvent gradient used in these analyses is detailed in the Materials and Methods chapter.

LC-MS/MS analyses of **2** and **3** were also carried out. The results of this analyses and their interpretation are shown in Figure 4.3 (Chen et al., 2008).

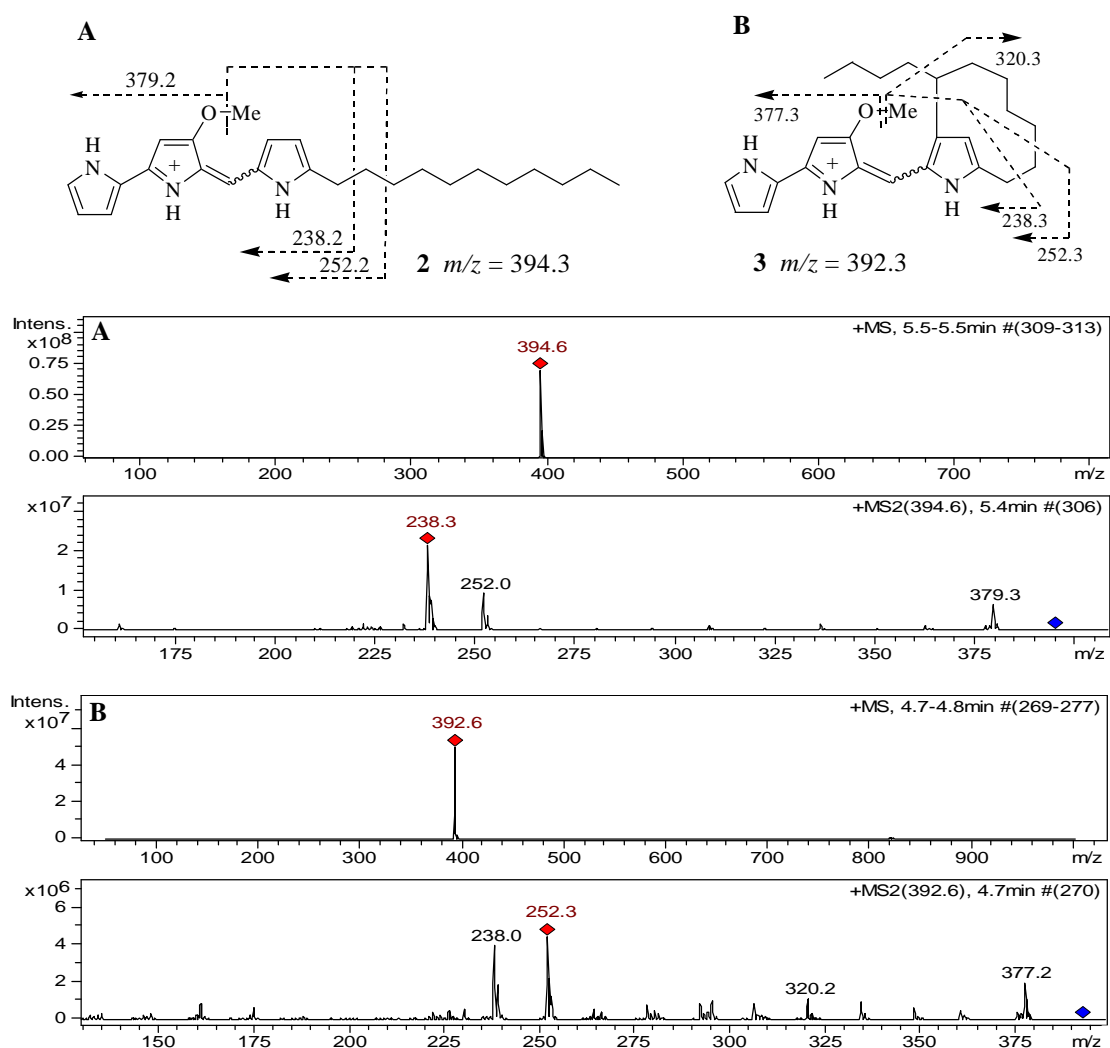


Figure 4.3 LC-MS/MS spectra for: A – undecylprodiginine (**2**) ($m/z = 394$) and B – streptorubin B (**3**) ($m/z = 392$) in positive ion mode. The proposed origins of the observed fragment ions are shown above the spectra.

Intermediates in the prodigine biosynthetic pathway, such as 2-undecylpyrrole (2-UP) (**21**) and 4-methoxy-2,2'-bipyrrole-5-carboxaldehyde (MBC) (**20**), which were detected in some mutants, were identified by comparisons with synthetic standards. LC-MS/MS data for synthetic **20** and **21** are shown in Figure 4.4 A and B.

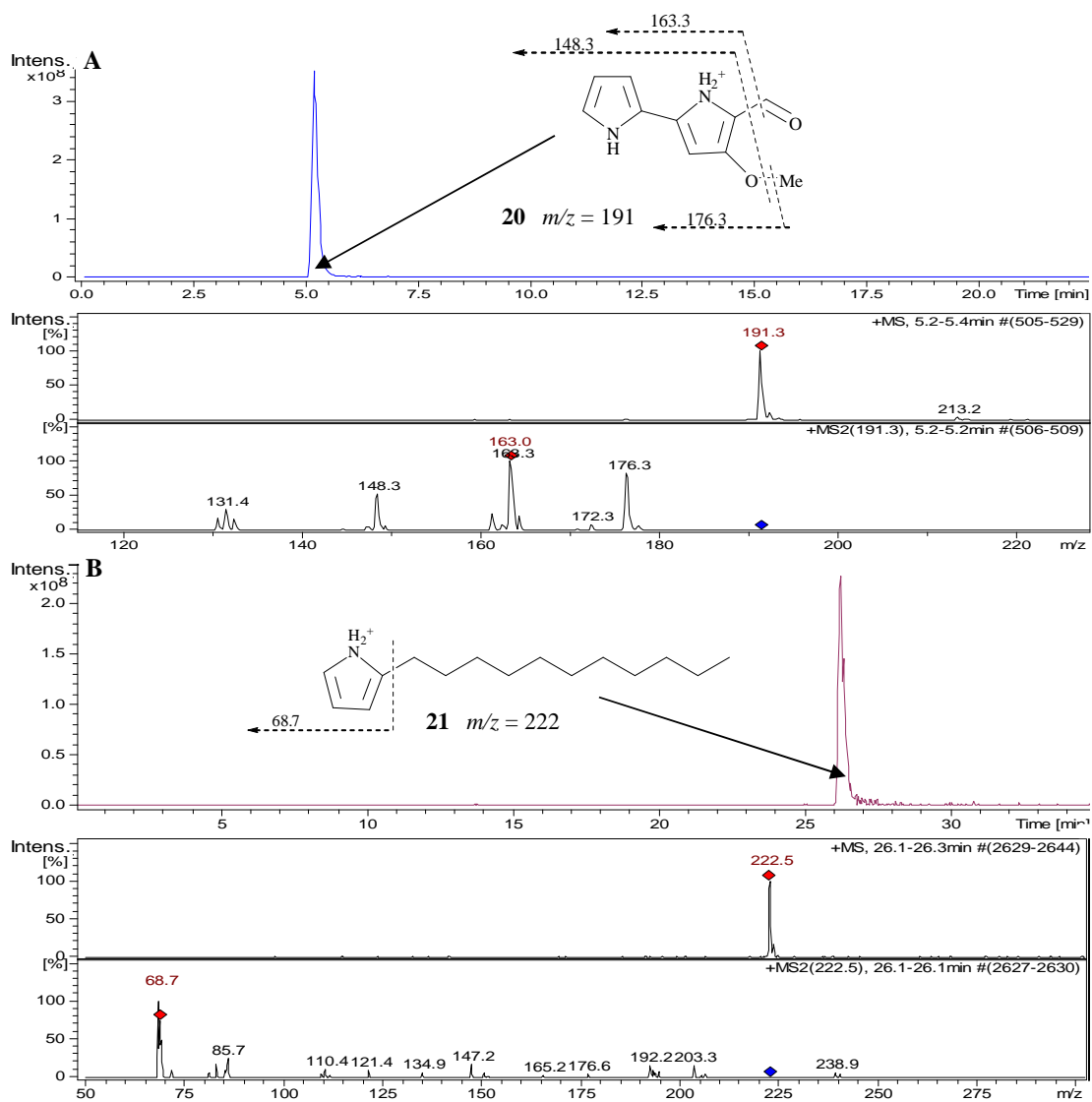


Figure 4.4 EICs and MS/MS spectra from LC-MS analyses of synthetic A – MBC (**20**) ($m/z = 191$); B – 2-UP (**21**) ($m/z = 222$).

4.2 Elucidation of the Biosynthetic Pathway to 2-Undecylpyrrole

Experimental evidence has been reported that supports the proposal by Cerdeño *et al.*, that RedP, RedQ and RedR are involved in early stages of 2-undecylpyrrole (2-UP) biosynthesis (Cerdeño *et al.*, 2001; Mo *et al.*, 2005; Mo *et al.*, 2008). The action of RedP and RedR together with reductase and dehydratase enzymes of fatty acids biosynthesis are proposed to generate an activated dodecanoyl thioester attached to the ACP RedQ (dodecanoyl-RedQ). The dodecanoyl group is then proposed to be transferred to the N-terminal ACP domain of the RedL multi-enzyme (Mo *et al.*, 2008). Two possible mechanisms for this transfer can be envisaged: (1) transfer of the dodecanoyl chain from RedQ to the ACP domain; (2) via transthioesterification hydrolysis of dodecanoyl-RedQ to give a free acid, which could be activated by the RedL A domain and subsequently loaded onto the ACP domain (Figure 4.5). In the second mechanism, a specific hydrolase would be required. RedJ is a candidate for this specific hydrolase. Once loaded onto the first ACP domain of RedL, the dodecanoyl chain could be transferred onto the active site Cys residue of the KS domain by transthioesterification where it could undergo condensation with a malonyl thioester loaded by the AT domain onto the second ACP domain to form β -ketomyristoyl-ACP (after decarboxylation). Subsequent condensation with glycine catalysed by the C-terminal OAS domain, followed by decarboxylation, cyclisation and dehydration would give 4-keto-2-undecylpyrroline (Mo *et al.*, 2008). RedK is proposed to catalyse reduction of the keto group in this intermediate to give the corresponding 4-hydroxy compound which undergoes elimination of water to afford 2-undecylpyrrole (Figure 4.5) (Williamson *et al.*, 2005).

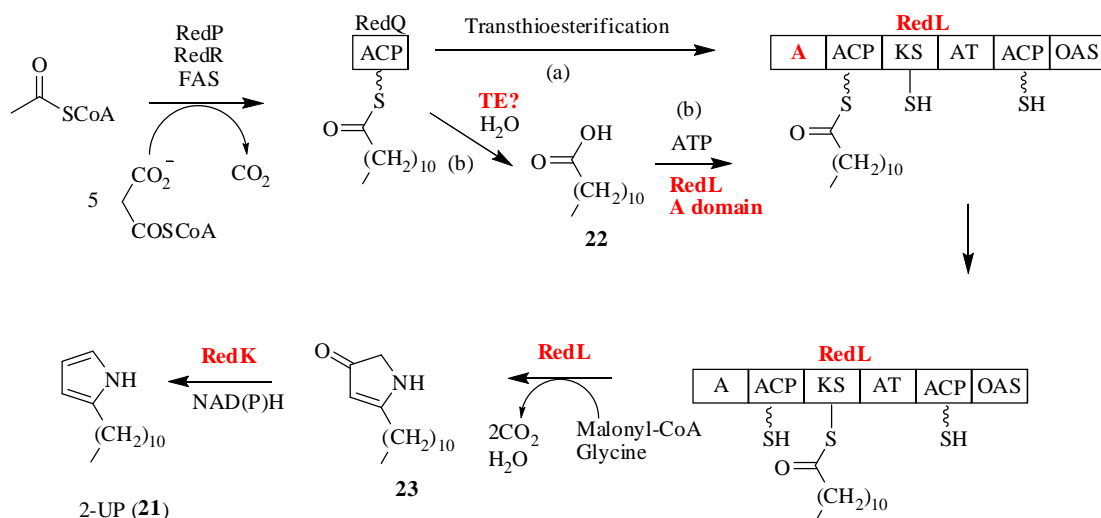


Figure 4.5 Entire proposed pathways to 2-UP including alternative mechanisms for transfer of the dodecanoyl chain from RedQ to the first ACP domain of RedL: (a) direct transacylation; (b) hydrolysis and reactivation by the RedLA domain.

The following sections describe analyses of the previously constructed *redL* mutant together with the *redL* A domain, *redK* and *redJ* mutants, constructed in this study, aimed at elucidating the roles of the RedL A domain, RedK and RedJ in 2-UP biosynthesis.

4.2.1 Investigation of *Streptomyces coelicolor* W37 Mutant (M511/*redLA::apr*)

An *S. coelicolor* M511/*redL::oriT-apr* mutant (W38) was constructed in the Challis group by Anna Stanley (a former PhD student) to investigate the role of RedL in prodiginine biosynthesis. The production of prodiginine antibiotics was abolished in the W38 mutant and could be restored by feeding synthetic 2-UP (Figure 4.6). Additionally, accumulation of MBC in cell extracts of the mutant was observed as expected and its presence can be also inferred by the fact that feeding synthetic 2-UP to the *redL* mutant restores prodiginine production (Stanley, 2007).

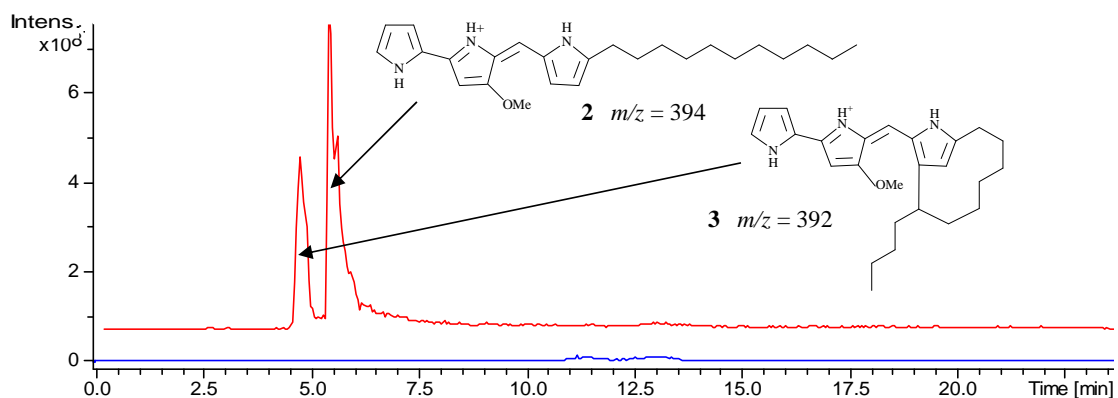


Figure 4.6 EIC ($m/z = 392-394$) from LC-MS analysis of acidified organic extracts of the *S. coelicolor* W38 (blue line) and W38 mutant fed with synthetic 2-UP (red line).

The *S. coelicolor* M511/*redLA::oriT-apr* (W37) mutant was generated to investigate the role of the RedL A domain in 2-UP biosynthesis. The amino acid sequence of RedL was aligned with the sequence of RedM (a standalone A domain involved in MBC biosynthesis) to identify the putative C-terminal the end of the A domain in RedL, to facilitate design of PCR primers for construction of the mutant. The amino acid sequence of RedM was found to be homologous to the first 600 aa of RedL and this fragment of the RedL A domain was thus targeted for deletion. Since it was planned to remove the native RedL start codon in this experiment, an additional in-frame ATG codon was introduced in to the reverse primer, to provide a start codon for the N-terminal truncated RedL protein. Without this, the 5-truncated *redL* gene would not be translated.

Growth of the W37 mutant on R5 agar plates led to mycelia that were white, indicating that prodiginines were not produced in this mutant. This observation was confirmed by LC-MS analysis (Figure 4.7). Dodecanoic acid (**22**) and synthetic 2-UP (**21**) were independently added to the growing W37 mutant to investigate if either is an

intermediate that can restore production of the antibiotics. Addition of **22** to the mutant did not restore prodiginine production. However, addition of **21** did restore undecylprodiginine production, albeit at a very low level. Undecylprodiginine could be detected both visually (extract was bright pink) and by LC-MS analysis (Figure 4.7).

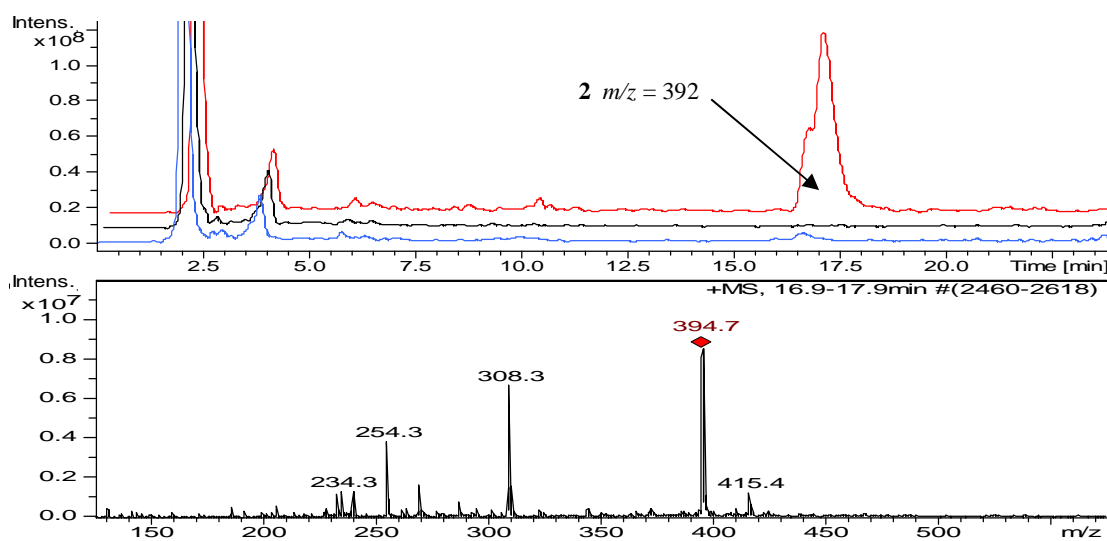


Figure 4.7 EIC ($m/z = 392-394$) from LC-MS analysis of acidified organic extracts of *S. coelicolor* W37 (blue line), W37 fed with dodecanoic acid (black line), and W37 fed with synthetic 2-UP (red line)

The accumulation of MBC (**20**) in the W37 mutant was also investigated. **20** was known from previous experiments done in the lab, not to be very stable in cell extracts and was very difficult to detect by LC-MS analysis. However **20** was detected in one sample of a W37 extract. Identical retention times, parent ion masses, and daughter ion masses were observed for MBC accumulated in the extract and synthetic MBC in LC-MS/MS analyses (Figure 4.4 A and Figure 4.8).

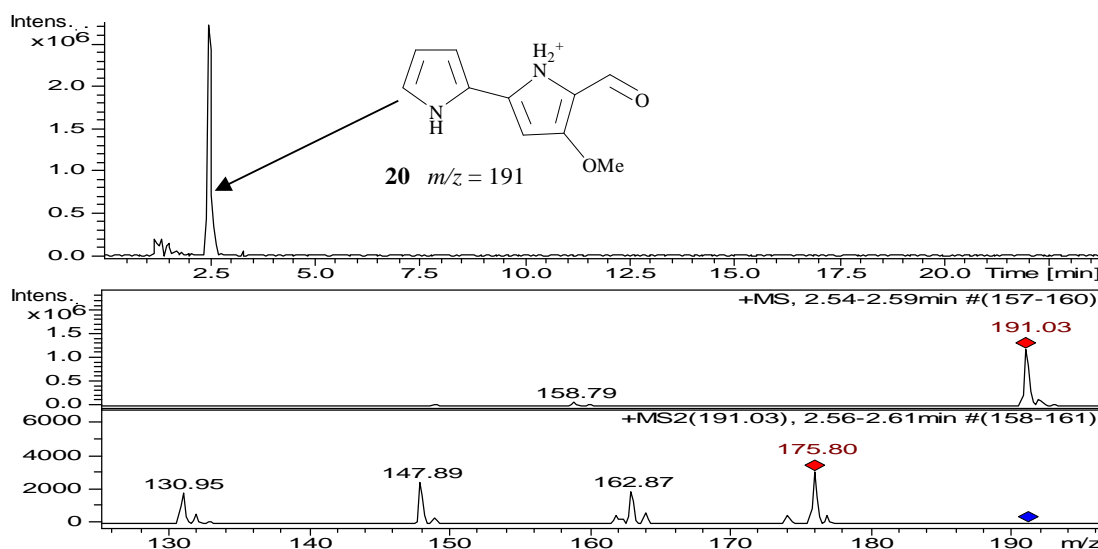


Figure 4.8 EIC ($m/z = 191$) and MS/MS spectra from LC-MS/MS analyses of acidified organic extracts of *S. coelicolor* W37.

The *redL* A domain encoding region was introduced into the W37 mutant, to genetically complement it and to determine if prodiginine production could be restored.

The fragment of *redL* A domain, corresponding to the one disrupted in the W37 mutant, was cloned into the pOSV556. The cloning primers were designed with restriction sites (*Hind*III and *Xho*I) at their 5' ends. A conserved RBS sequence was added to the forward primer upstream of the ATG start codon (as described previously) and a stop codon (TGA) was added to the reverse primer at the 3' end of the A domain-encoding sequence. The pOSV556*redLA* construct was created by standard cloning procedures and introduced by conjugation into the W37 mutant. The new strain M511*redLA::oriT-apr* + pOSV556*redLA* was grown on R5 agar plates to examine whether prodiginine production was restored. Growing cells were white and no prodiginine production was observed by LC-MS analysis (Figure 4.9).

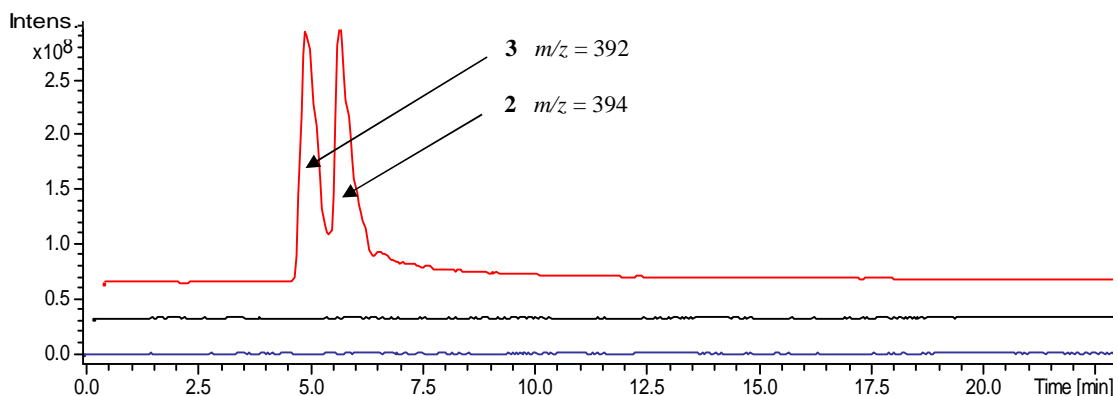


Figure 4.9 EIC ($m/z = 392-394$) from LC-MS analyses of acidified organic extracts of *S. coelicolor* W37 (blue line), W37 + pOSV556*redLA* (black line) and *S. coelicolor* M511 (red line)

Analyses of the W37 mutant did not result in a clear answer about the function of the RedL A domain. Indeed, prodiginine production was abolished in the mutant and feeding of dodecanoic acid (**22**), which was thought to be the substrate for the RedL A domain, did not restore prodiginine production. This suggested that the A domain could play a role in loading of **22** onto the first ACP domain of RedL. However, if the A domain is required for 2-UP biosynthesis, genetic complementation should restore the production of the antibiotics, but it did not. The only way to restore prodiginine production was to feed the mutant with 2-UP. The specific function of the A-domain could therefore not be deduced because prodiginine production was also restored upon feeding of 2-UP to the in M511/*redL::oriT-apr* mutant in which the whole *redL* gene was deleted.

Taken together, these data suggest that replacing the 5' end of the *redL* gene (corresponding to the N-terminal 600 aa of the 2297 aa RedL protein) with the apramycin cassette and introducing an extra start codon directly upstream of the remaining *redL* sequence, may have caused the other domains of RedL to become inactive. The trun-

cated RedL protein may not be folded properly and thus may not function correctly. Additionally in genetically complemented *redLA* mutant the separately expressed A domain and the N-terminal ACP domain in truncated RedL have to interact with each other *in trans*. Perhaps they can only recognise each other when they are part of the same polypeptide.

In future work, the function of the RedL A domain could be investigated by constructing a “scar” mutant, with an 81 bp in-frame “scar” sequence replacing the A domain. This would retain the natural *redL* start codon and would thus rule out a polar effect on expression of the truncated *redL* gene in the W37 mutant. If the “scar” mutant do not solve the problem of proper folding of RedL, creating a point mutations of essential active site residue in the A domain could be another strategy to make it non-functional but correctly folded.

4.2.2 Investigation of *Streptomyces coelicolor* W36 Mutant (M511/*redK::oriT-apr*)

To investigate the role of RedK in prodiginine biosynthesis, a *S. coelicolor* mutant (W36) with the *redK* gene deleted was constructed and characterised. After 3 to 4 days of growth on R5 solid medium, it was surprising to observe that the colour of the mycelia of this mutant was bright red. The mycelia were harvested, extracted and analysed by LC-MS. The extracted ion chromatogram for $m/z = 392-394$ from this analysis indicated that the production of **2** and **3** was abolished in the mutant (Figure 4.10).

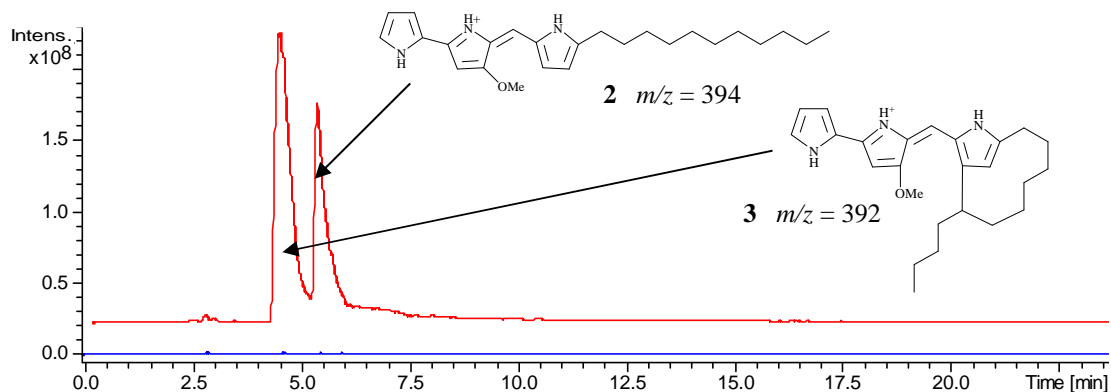


Figure 4.10 EIC ($m/z = 392-394$) from LC-MS analysis of acidified organic extracts of *S. coelicolor* M511 (red) and the W36 mutant (blue).

When the W36 mutant was grown in the presence of synthetic 2-UP (**21**), production of both **2** and **3** was restored, implying that only 2-UP production is abolished in the mutant (Figure 4.11).

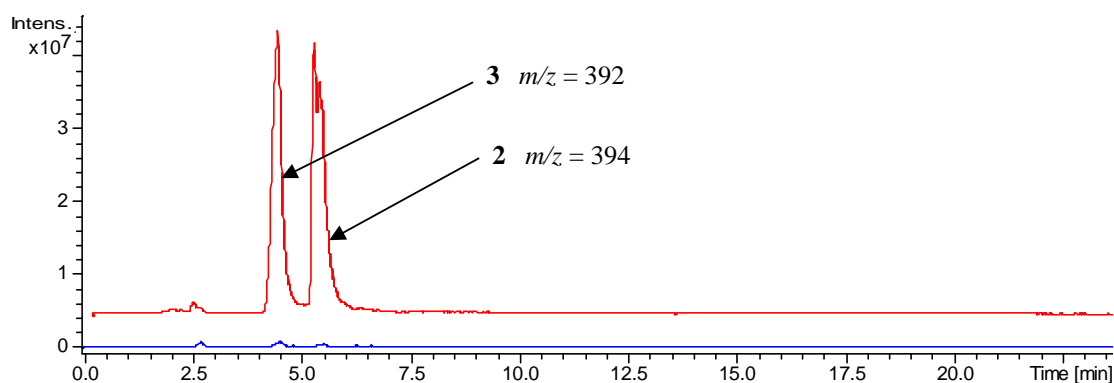


Figure 4.11 EIC ($m/z = 392-394$) from LC-MS analyses of acidified organic extracts of the W36 mutant (blue) and the W36 mutant fed with synthetic 2-UP (**3**) (red).

Examination of the UV chromatogram at 533 nm (a characteristic prodiginine absorbance) revealed that although **2** and **3** were not produced in the W36 mutant, a new putative prodiginine with $m/z = 410$ was accumulated (Figure 4.12 A, B). Small quanti-

ties of the same compound were detected in culture extracts of *S. coelicolor* M511 (Figure 4.12 A).

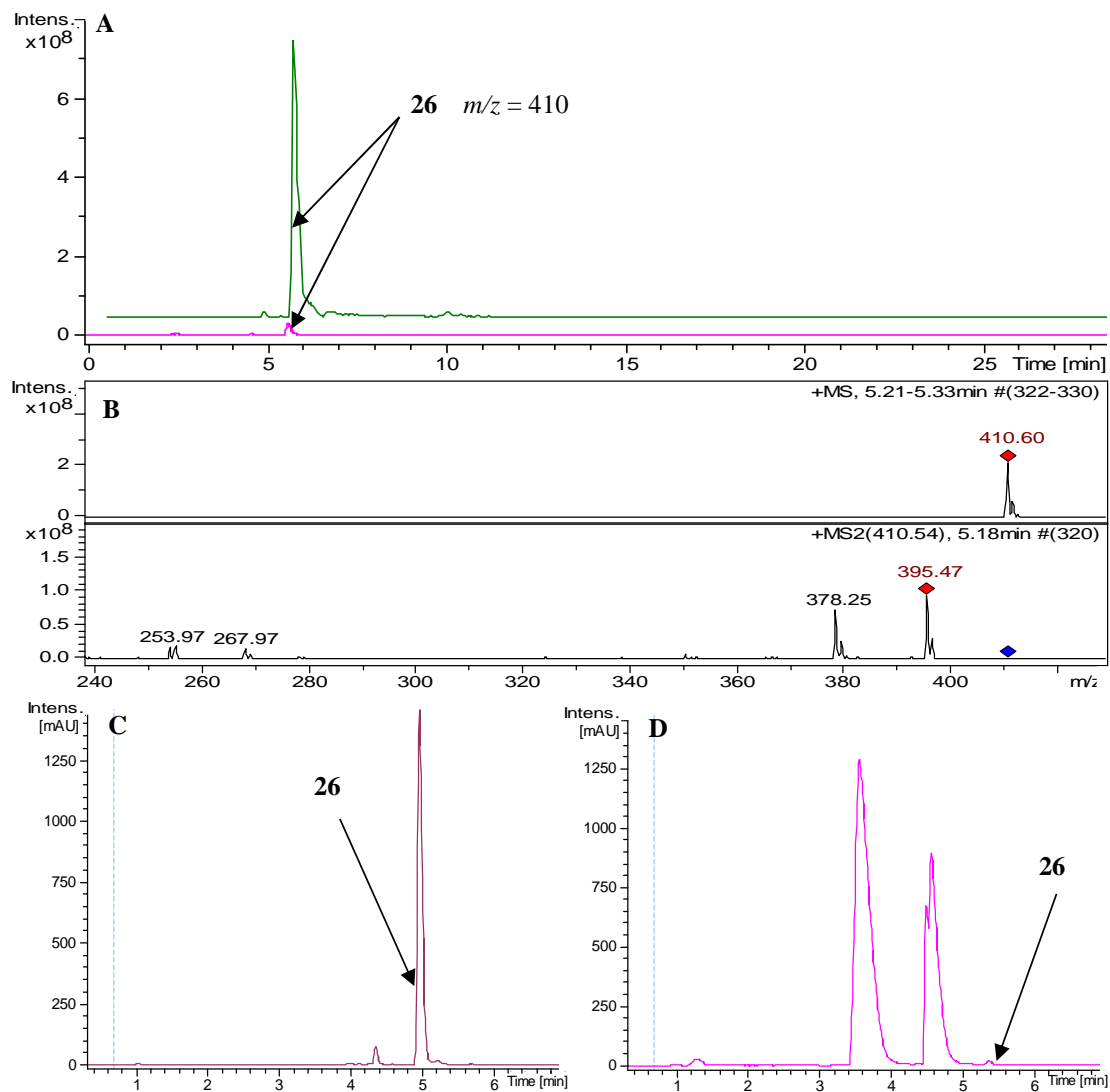


Figure 4.12 A – EIC ($m/z = 410$) from LC-MS analyses of acidified organic extracts from the W36 mutant (dark green) and *S. coelicolor* M511 (pink); B – MS/MS spectrum of compound with $m/z = 410$ accumulated in the W36 mutant. C, D – UV chromatogram monitoring absorbance at 533 nm from LC-MS analysis of acidified organic extract of the C – W36 mutant, D – M511.

An m/z value of 410 in positive ion mode would be expected for a hydroxylated analogue of undecylprodiginine (**26**). High resolution mass spectrometry analysis of this

compound confirmed its molecular formula as $C_{25}H_{35}N_3O_2$ (calculated for $C_{25}H_{36}N_3O_2^+$: 410.2802, found: 410.2806). MS/MS provided further support for the proposed hydroxylated undecylprodiginine structure of this compound presence and indicated that the hydroxyl group is not localised on the hydrocarbon chain but on the tripyrrole ring system. Feeding of synthetic 2-UP to the W36 mutant restored production of **2** and **3**, indicating that the hydroxyl group was located on the C ring. Thus, the structure shown in Figure 4.13 for the compound **26** accumulated in the W36 mutant was proposed.

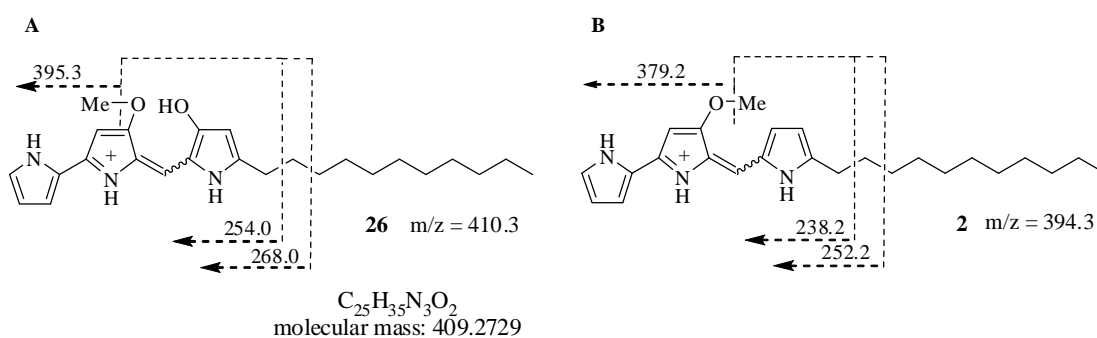


Figure 4.13 A – proposed structure and fragment ions observed in MS/MS analysis for the hydroxylated analogue of undecylprodiginine (**14**) with $m/z = 410$; B – structure and proposed fragment ions observed in MS/MS analysis of undecylprodiginine (**2**).

Further analyses showed that another compound with $m/z = 238$ was also accumulated in the W36 mutant. This was hypothesised to be the hydroxylated analogue of 2-UP, 4-hydroxy-2-undecylpyrrole (**23**), the proposed product of RedL (Figure 4.14).

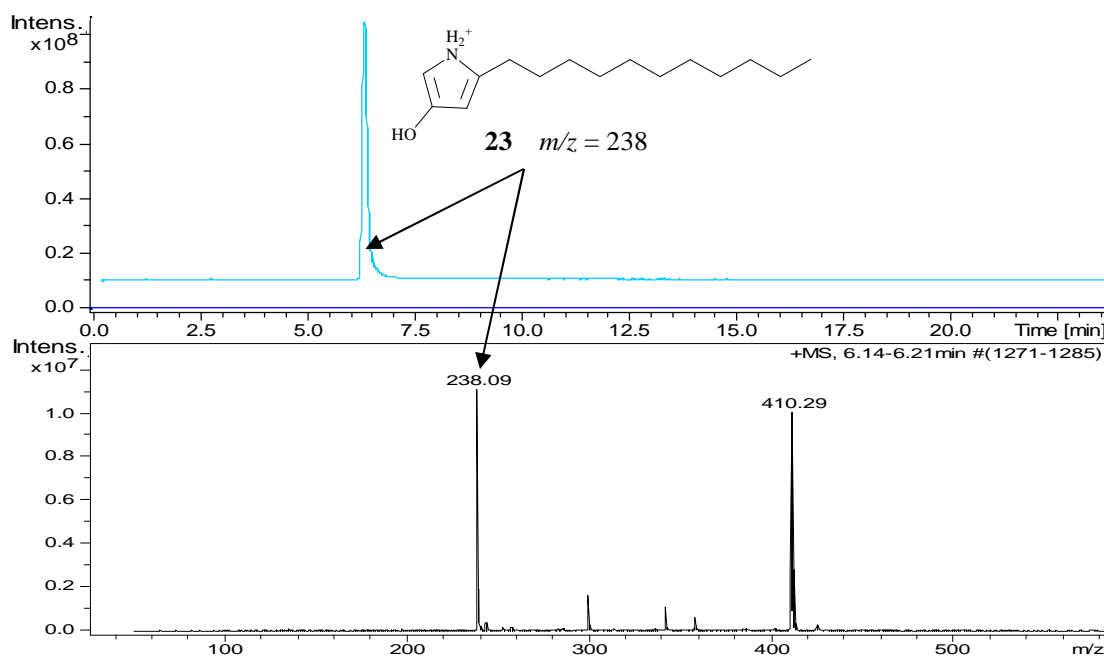


Figure 4.14 Top: EIC ($m/z = 238$) from LC-MS analyses of acidified organic extracts of the W36 mutant (light blue) and M511 (dark blue). Bottom: mass spectrum for the peak with retention time ~6 minutes in the chromatogram for the W36 mutant.

The accumulation of compounds **23** and **26** in the W36 mutant led us to propose a catalytic role for RedK in 2-undecylpyrrole (**9**) biosynthesis. RedK is similar to NAD(P)H-dependent oxidoreductases and is therefore proposed to catalyse reduction of the keto group in the tautomer of **23**. A water molecule is then eliminated from the product of this reaction to form **21** (Figure 4.15).

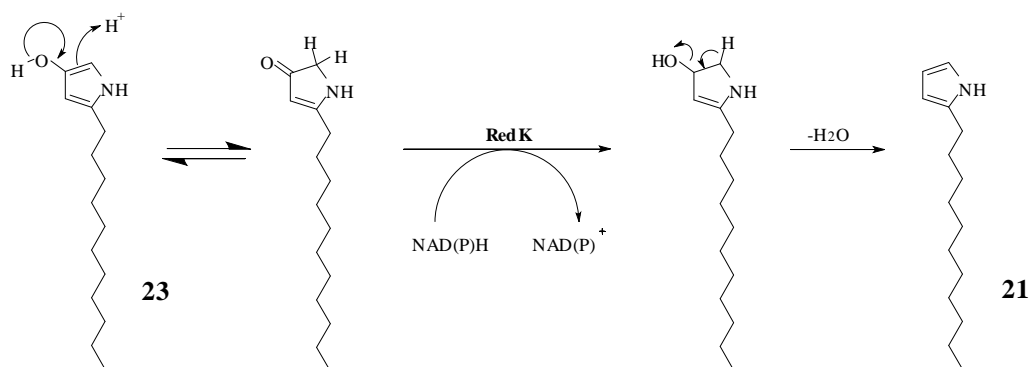


Figure 4.15 Reaction proposed to be catalysed by RedK.

To confirm the proposed structures of **23** and **26**, NMR experiments were envisaged. However, the chemical instability of both of these compounds made it difficult to purify enough material for characterisation by NMR spectroscopy.

To restore prodiginine production in both W36 (*redK* mutant) and W38 (*redL* mutant) mutants, the cosynthesis phenotype of these strains was investigated. Spores of the W36 and W38 mutants were mixed and the mixture was inoculated onto one R5 agar plate. LC-MS analysis of mycelia extracts after 5 days of growth showed the production of **2** and **3** by this co-culture (Figure 4.16). This experiment indicates that 4-hydroxy-2-undecylpyrrole made by the W38 mutant is converted by the W36 mutant to 2-undecylpyrrole and subsequently **2** and **3**. It also demonstrates that the *redK* gene in the W36 mutant is functional and that its expression is not abolished due to a polar effect resulting from replacement of the upstream *redL* gene with the *oriT-apr* cassette.

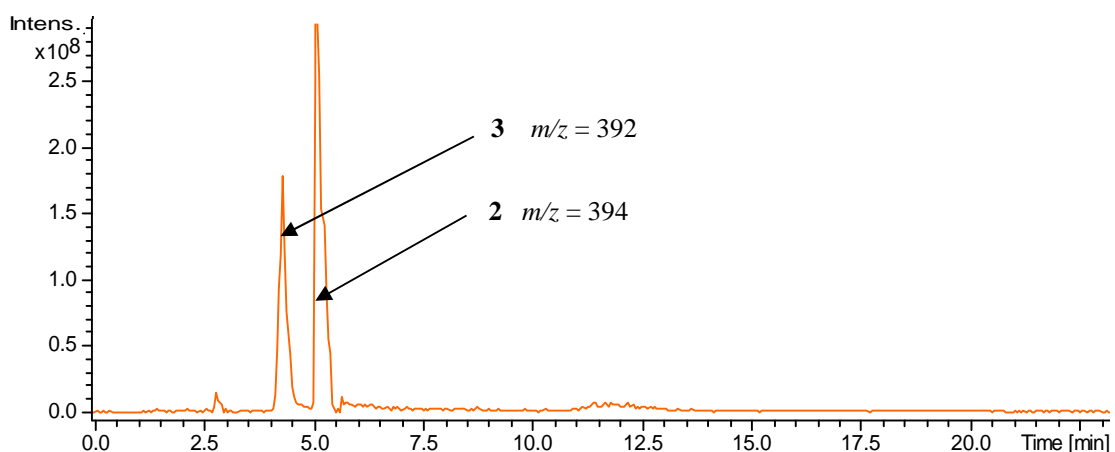


Figure 4.16 EIC ($m/z = 392-394$) from LC-MS analysis of acidified organic extracts of the W36 and W38 mutants grown in co-culture.

4.2.3 Investigation of *Streptomyces coelicolor* W35 Mutant (M511/*redJ::oriT-apr*)

In many non-ribosomal peptide synthetase (NRPS) and type I PKS gene clusters, additional standalone thioesterase (TE) enzymes are encoded. These are so-called type II thioesterases (Kotowska et al., 2002). Although in fatty acids biosynthesis they catalyse acyl thioester hydrolysis (Smith, 1994), their role in polyketides biosynthesis remains unclear. Disruption of TE II genes in various strains has resulted in highly reduced (up to 90% or more) levels of polyketide production, indicating their importance in polyketides biosynthesis (Xue et al., 1998; Butler et al., 1999). It has been suggested that they could also catalyse hydrolytic release of miscognate chains from the acyl carrier protein domains of PKSs and other multienzymes (Butler et al., 1999). While RedJ may perform an analogous role in prodiginine biosynthesis, it is also conceivable that it acts as a specific hydrolase to release a dodecanoyl chain from RedQ (Figure 4.17).

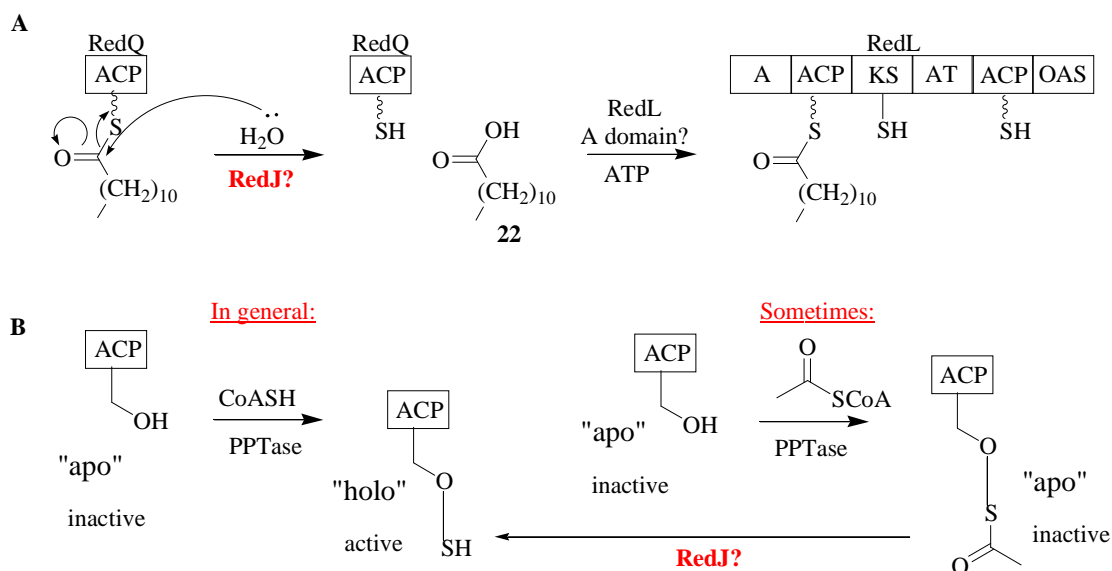


Figure 4.17 Proposed roles for RedJ in prodiginine biosynthesis: A – RedJ could catalyse hydrolytic release of dodecanic acid from RedQ; B – RedJ could produce active *holo* forms of carrier proteins and carrier protein domains involved in prodiginine biosynthesis that results from posttranslational modification with acetyl-CoA instead of coenzyme A.

A M511/*redJ::oriT-apr* (W35) mutant *S. coelicolor* (W35) was generated to investigate the role of RedJ in prodiginine biosynthesis. The *redJ* mutant was grown on a R5 agar plate. After a few days of growth, the plate started to turn red, in a similar way to the *S. coelicolor* M511 parent strain. LC-MS analysis of this mutant confirmed that prodiginine production was not abolished; undecylprodiginine (**2**) and streptorubin B (**3**) were still produced (Figure 4.18).

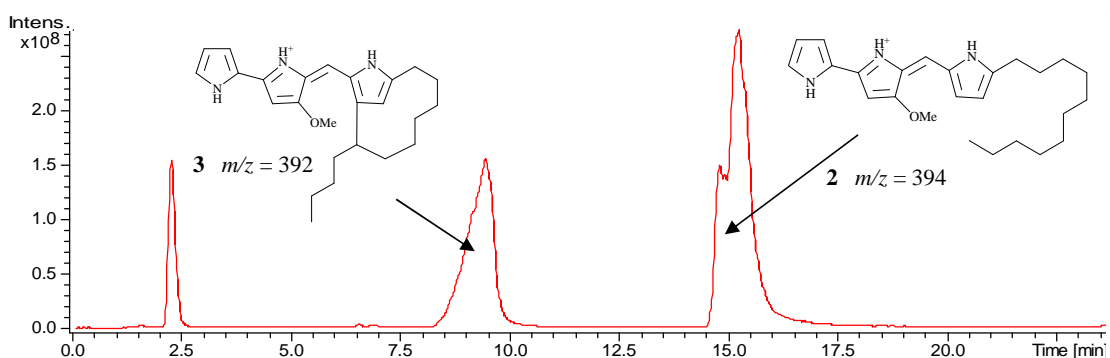


Figure 4.18 LC-MS analysis of undecylprodiginine (**2**) and streptorubin B (**3**) production by the W35 mutant.

Time-course experiments were next carried out with W35 mutant and the M511 wild type to compare the levels of antibiotic produced during cell grow. After 24 h of initial growth samples were collected, in triplicate, every 12 hours, for a total of 84 hours, after which time the stationary growth phase was finished. Prodiginine titres were determined by measuring the absorbance at 533 nm of the mycelial extracts. This absorbance value was converted into μg of prodiginine per mg of dry cell weight (DCW) using the known extinction coefficient of $100,500 \text{ M}^{-1}\text{cm}^{-1}$ for prodiginine absorption at 533 nm (Figure 4.19 A) (Kieser et al., 2000). Prodiginine levels in the extracts after 5 days of growth was also compared by HPLC, monitoring absorbance at

533 nm. The red pigments were extracted from the same amount of wet cell weight (WCW) and the same volume of extract was injected onto the column. The chromatograms for the extracts of W35 and M511 are compared in Figure 4.19 B.

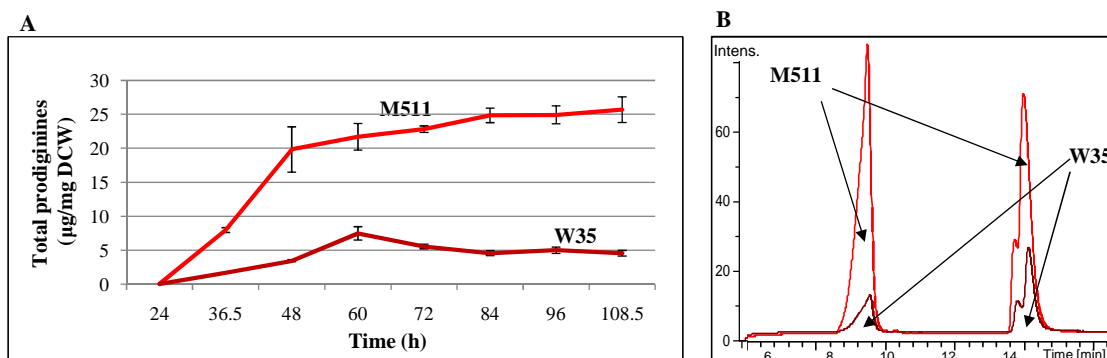


Figure 4.19 A – Time-course of antibiotic production by *S. coelicolor* M511 wild type (red line) and the W35 (M511/*redJ::oriT-apr*) mutant (brown line) grown on R5 medium B – HPLC analyses monitoring absorbance at 533 nm of acidified organic extracts of M511 (red line) and the W35 mutant (brown line) from the same amount of WCW after 4.5 days of growth. Errors bars indicate standard error calculated from three samples.

From these results it is clear that prodiginines are produced at lower levels in the *redJ* mutant than in the wild type M511 strain. The fact that prodiginine production is not abolished in the *redJ* mutant could be due to the presence of other type II thioesterases encoded elsewhere within the *S. coelicolor* genome that are able to partially complement the *redJ* mutation. Two such type II thioesterases were identified by BLAST searches of the *S. coelicolor* genome using the RedJ sequence as a probe: ScoT (encoded by SCO6287, with 36% identity to RedJ) and a putative thioesterase (encoded by SCO7687, with 32% identity to RedJ). ScoT has previously been shown to be able to complement the catalytic function of the TyIO type II TE of *S. fradiae* (40% identity). Expression of *scoT* in a *tylO* mutant restores desmycosin production to 48% of the level produced by the wild type strain (Kotowska et al., 2002). This data suggests that

prodiginine production in the W35 mutant (~20 +/- 3% of the level produced in the wild type during exponential phase (Figure 4.19 A)) could result from complementation of the *redJ* deletion by the two thioesterases encoded by SCO6287 and SCO7687.

Construction of a *redJ**scoT* double mutant was attempted to begin to investigate the cross-complementation hypothesis. First a M511/*redJ::scar* mutant was generated and the cosmid Sc1G7/*scoT::oriT-apr* was constructed. Conjugation between M511/*redJ::scar* and *E. coli* ET12567/pUZ8002 containing Sc1G7/*scoT::oriT-apr* was carried and replica plating was undertaken to attempt to find double crossover exconjugants. Although the conjugation was repeated several times and ~500 colonies were screened, no exconjugant with the *scoT* gene replaced with *oriT-apr* cassette, resulting from double crossover recombination could be found. This result suggests that either *redJ* or *scoT* is essential for *S. coelicolor* growth and survival.

4.3 Role of RedT in Prodiginine Biosynthesis

The *redT* gene appears to encode for protein for which no function has been proposed. BLAST searches did not identify any proteins of known function with sequence similarity to RedT (Cerdeño et al., 2001).

A M511/*redT::oriT-apr* (W28) mutant was constructed to investigate the role of RedT in prodiginine biosynthesis. Growth of this mutant on R5 agar medium indicated that much less red pigment was produced in comparison to the M511 wild type strain, but both **2** and **3** were still produced (Figure 4.20 D).

Prodiginine production over time was analysed in this mutant in a similar way to the time-course experiments done with the W35 mutant. This confirmed the observation that lower amounts of prodiginines were produced in the mutant than in the wild type.

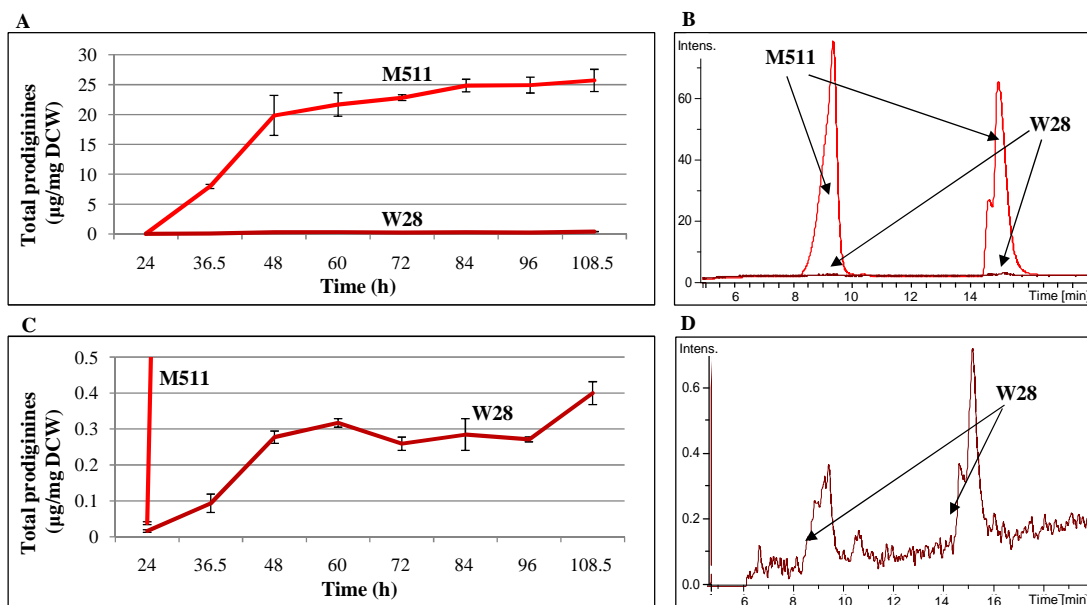


Figure 4.20 A, C – Time-course of prodiginine production by the M511 strain (red line) and W28 (M511/*redT::oriT-apr*) mutant (brown line) grown on R5 medium; B, D – HPLC analysis monitoring absorbance at 533 nm of acidified organic extract of M511 (red line) and W28 mutant (brown line), extracted after five days of growth from the same amount of WCW; D – zoomed UV chromatogram from extract of the W28 mutant. Errors bars indicate standard error calculated from three samples.

Feeding experiments with synthetic MBC (**20**) and 2-UP (**21**) were carried out to check if wild type levels of prodiginine production could be restored, LC-MS analyses indicated that higher prodiginine levels were produced in the M511/*redT::oriT-apr* fed with MBC (Figure 4.21), suggesting that **20** biosynthesis in the mutants is highly reduced but not abolished.

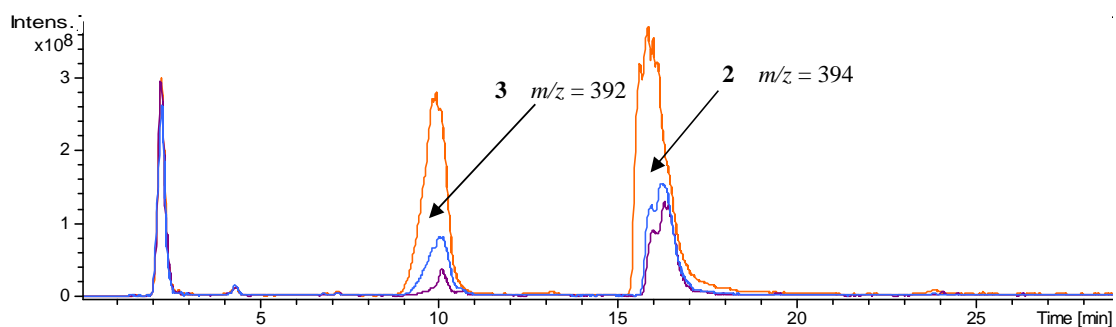


Figure 4.21 EIC ($m/z = 392-394$) from LC-MS analyses of acidified organic extracts of the *S. coelicolor* W28 mutant (violet line), the W28 mutant fed with 2-UP (**21**) (blue line) and the W28 mutant fed with synthetic MBC (**20**) (red line).

Additionally, **21** was also detected to be accumulated in *redT* mutant (Figure 4.22).

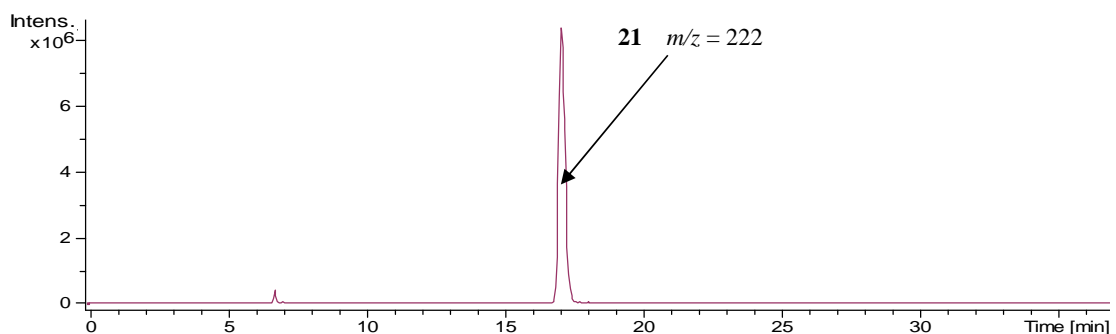


Figure 4.22 EIC ($m/z = 222$) from LC-MS analyses of acidified organic extracts of the *S. coelicolor* W28 mutant

The analysis of the *redT* mutant did not give an unambiguous indication of the role of RedT in prodiginine biosynthesis. This protein could be involved in (but not required for) MBC biosynthesis. However, its precise function could not be determined because low levels of antibiotics were still produced in the mutant (1%, in exponential phase, of level produced by M511 (Figure 4.20 A, C)) and no other potential intermediates were found to be accumulated.

4.4 Condensation of 2-Undecylpyrrole and MBC to Yield Undecylprodiginine

It was originally proposed that an enzyme may not be required for the condensation reaction between MBC and 2-UP to form undecylprodiginine (Cerdeño et al., 2001). However, subsequent experiments suggested that RedH may catalyse this reaction (Figure 4.23) (Stanley, 2007).

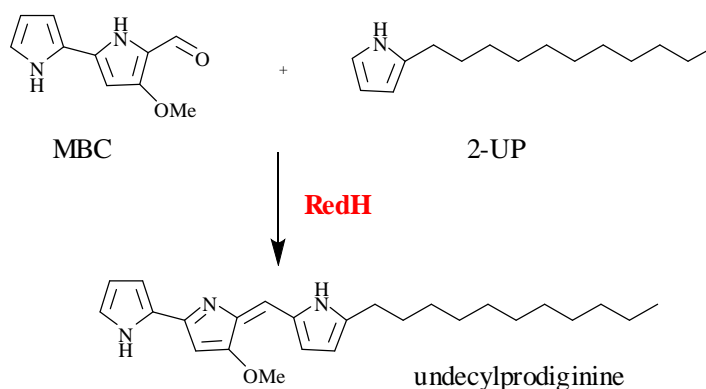


Figure 4.23 Proposed role of RedH in undecylprodiginine biosynthesis.

LC-MS analyses of a M511/*redH::oriT-apr* mutant created in the lab by former student Anna Stanley showed that this mutant does not produce prodiginines indicating that RedH is required for biosynthesis of these antibiotics (Stanley, 2007; Haynes et al., 2008). Small quantities of undecylprodiginine in mycelia extracts of the mutant were attributed to acid catalysed condensation of MBC (**20**) and 2-UP (**21**) during extraction (the solvent is acidified). In addition, feeding chemically-synthesised **20** or **21** to the mutant did not restore prodiginine production (Stanley, 2007; Haynes et al., 2008). Restoration of prodiginine production is commonly observed in such feeding experi-

ments with other mutants blocked in the biosynthesis of MBC and 2-UP (**20** or **21**) (Mo et al., 2005; Stanley et al., 2006).

4.4.1 Genetic Complementation of the *redH* Mutant

To further investigate the role of RedH in prodiginine biosynthesis genetic complementation of the *redH* mutant was undertaken. The *redH* gene with its natural ribosome binding site (RBS) (AGGAGA) 10 bp upstream of the start codon was amplified from the Sc3F7 cosmid.

Specific primers with restriction sites on the 5' ends were designed for this reaction. The forward primer (with a *Hind*III restriction site appended to its 5' end) contained the sequence upstream of the start codon and the reverse primer (with a *Xho*I restriction site appended to its 5' end) contained a 20 nt sequence identical to the sequence 100 bp downstream of the stop codon of the *redH* gene. The *Hind*III and *Xho*I digested PCR product was cloned with similarly digested pOSV556 to create pOSV556*redH*. This construct was transferred to the M511/*redH::oriT-apr* mutant by conjugation from *E.coli* ET12567pUZ8002. Hygromycin resistant exconjugants were picked and grown on R5 agar plates. Restoration of prodiginine production could be detected visually, because mycelia of M511/*redH::oriT-apr* + pOSV556*redH* became red (M511/*redH::oriT-apr* mycelia are yellow). These results were confirmed by LC-MS analyses, which revealed that in the M511/*redH::oriT-apr* + pOSV556*redH* strain both **2** and **3** were produced (restored to wild type level) (Figure 4.24).

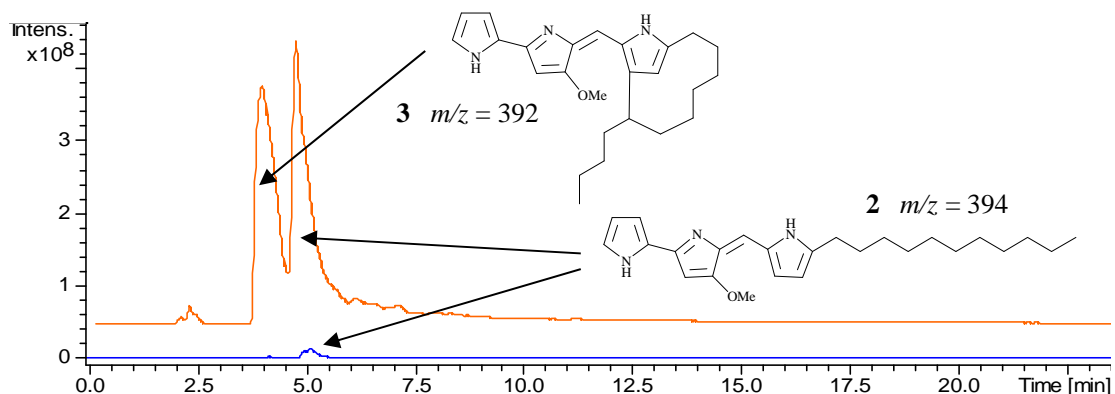


Figure 4.24 EIC ($m/z = 392-394$) from LC-MS analyses of organic extracts of the M511/*redH::oriT-apr* (blue line) and M511/*redH::oriT-apr* + pOSV556*redH* (red line) mutants.

The genetic complementation of the *redH* mutant was therefore successful even though the *redH* gene was expressed *in trans* from a constitutive promoter. Thus RedH is clearly required for production of undecylprodiginine.

4.4.2 Heterologous Expression of *redH* in *S. venezuelae* and Feeding of Synthetic MBC and 2-Undecylpyrrole

To further investigate the role of RedH in 2-undecylpyrrole biosynthesis, heterologous expression of *redH* in *Streptomyces venezuelae* ATCC10712 was performed. *S. venezuelae* was chosen as a host because it has been fully sequenced and its genome does not contain any gene cluster similar to the *red* cluster (Mervin Bibb, personal communication). Moreover it also contains no gene similar to *redH* and it does not produce prodiginines.

Conjugational transfer of pOSV556*redH* from *E. coli* between ET12567/pUZ8002 to *S. venezuelae* was carried out on a modified R2 medium (specific

medium for *S. venezuelae*), overlaid with hygromycin. After growth, a single exconjugant was selected to carry out feeding experiments on R5 agar medium.

Feeding of wild type *S. venezuelae* with synthetic 2-UP and MBC did not result in visible red-pigment production. However LC-MS analysis of acidified organic mycelial extracts showed that a small amount of undecylprodiginine was present. This was consistent with a similar observation made for the M511/*redH::oriT-apr* mutant. When *S. venezuelae*/pOSV556*redH* was fed with synthetic 2-UP and MBC, red-pigment production was visible and LC-MS/MS analysis of acidified organic extracts of the mycelia confirmed the presence of large quantities of undecylprodiginine (Figure 4.25) (Haynes et al., 2008).

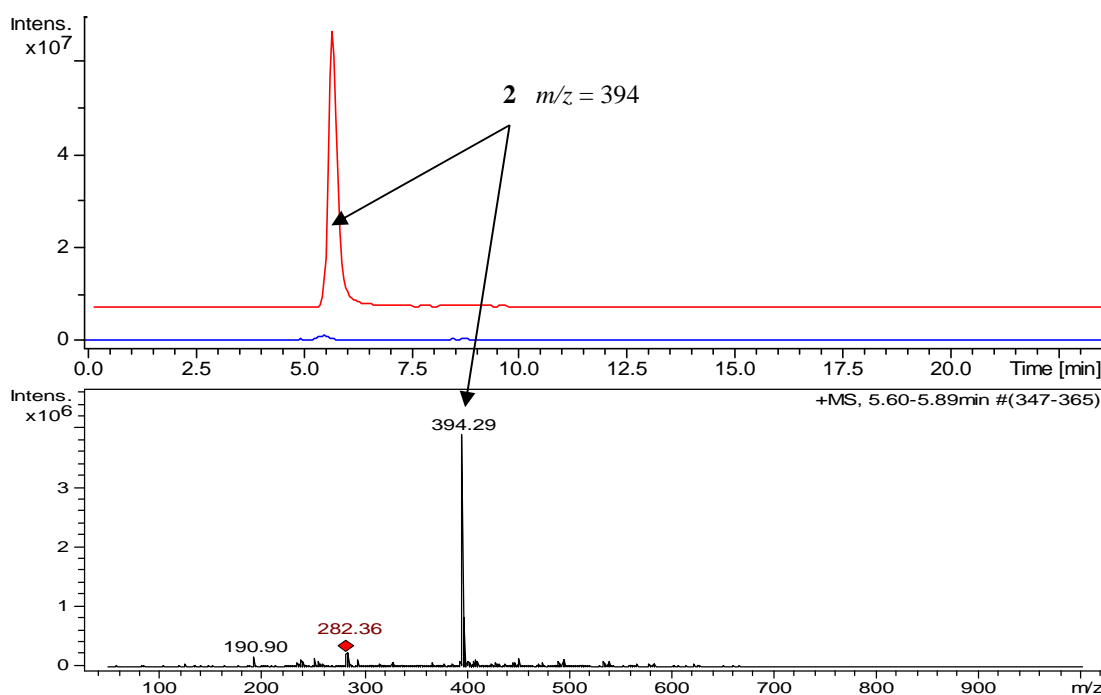


Figure 4.25 Top: EIC ($m/z = 394$) from LC-MS analyses of acidified organic extracts of *S. venezuelae* + 2-UP + MBC (bottom, blue trace) and *S. venezuelae* + pOSV556*redH* + 2-UP + MBC (top, red trace). Bottom: mass spectrum of peak with retention time of ~5.75 minutes of the upper (red) chromatogram.

Feeding of synthetic MBC and 2-UP to *S. venezuelae* expressing *redH* established the role of RedH as an enzyme responsible for the condensation of 2-UP and MBC to form undecylprodiginine in the *S. coelicolor* prodiginine biosynthetic pathway.

4.5 Conclusions

Among the genes within the *red* cluster that have not been previously characterised, several were replaced on the *S. coelicolor* chromosome with an apramycin resistance cassette using a PCR targeting strategy (Gust et al., 2002).

An M511/*redL*(A domain)::*oriT-apr* mutant was constructed and no prodiginine antibiotics were produced in the mutant. A feeding experiment with dodecanoic acid, the proposed A domain substrate, did not restore production of prodiginines, suggesting that the A domain of RedL is required for loading this intermediate onto the first ACP domain of RedL. Production of prodiginine antibiotics in the mutant was only restored when 2-UP was fed. Genetic complementation was carried out to examine whether the RedL A and ACP domains could interact *in trans*, but in the complemented mutant no prodiginines were produced. Perhaps deletion of the RedL A domain caused inactivation of entire protein. To circumvent this problem the region of *redL* encoding the A domain could be replaced with a in-frame “scar”. Point mutations of *redL* A domain active site could be an even better approach, making RedL A domain inactive and at the same time RedL correctly folded.

A *redK*::*oriT-apr* mutant of *S. coelicolor* M511 was constructed and it was observed that it did not produce **2** or **3**. A ring C hydroxylated analogue of undecyl-

prodiginine could be detected in the mutant as well as a hydroxylated analogue of 2-UP (probably 4-hydroxy-2-undecylpyrrole, the proposed product of RedL and the likely substrate of RedK). RedK is similar to putative NAD(P)H-dependent oxidoreductases and could catalyse reduction of the keto group in the ketone tautomer of 4-hydroxy-2-undecylpyrrole, followed by elimination of water to yield 2-UP.

The proposed role of RedJ as a specific hydrolase that cleaves the dodecanoyl chain from RedQ during 2-UP biosynthesis was investigated by constructing a *redJ* mutant. Prodiginine production was not abolished in the mutant, but only reduced (by about 80 +/- 3% to wild type level). The *redJ* gene encodes a type II thioesterase. Such genes are very often present in NRPS and type I PKS gene clusters. Although their role in secondary metabolite biosynthesis is not clear, deletions of them can be easily complemented with heterologous type II thioesterase genes. In *S. coelicolor*, another two type II thioesterases are encoded elsewhere in the genome and could perhaps complement the *redJ* deletion. To elucidate the exact function of RedJ it could be overproduced in *E. coli*, purified and biochemically investigated. Kevin Reynolds group is investigating this (Reynolds, personal communication).

No clear role for RedT in prodiginine biosynthesis has been proposed. Thus a M511/*redT::oriT-apr* mutant was constructed. **2** and **3** were still produced in the mutant but in very low amounts. Prodiginine production was increased by addition of MBC and accumulation of 2-UP was detected in the *redT* mutant, indicating that RedT is involved in, but not required for MBC biosynthesis. As BLAST searches did not identify any proteins of known function with similarity to RedT and no new intermediates were accumulated in the mutant, the function of this enzyme in MBC biosynthesis remains

unclear. To elucidate function of RedT it could be overproduced in *E. coli*, purified and crystallised. An X-ray structure could give insight into its function.

Once 2-UP and MBC are biosynthesised, condensation of these two intermediates, catalysed by RedH, was proposed to occur to yield undecylprodiginine (Stanley et al., 2006). To confirm the role of RedH, genetic complementation of the *redH* mutant was performed, resulting in restoration of prodiginine production. Heterologous expression of *redH* in *Streptomyces venezuelae* and feeding with synthetic 2-UP and MBC resulted in efficient undecylprodiginine production, unambiguously demonstrating the role of RedH in the biosynthetic pathway (Haynes et al., 2008).

5. Investigation of Oxidative Cyclisation Reactions in Prodiginine Biosynthesis

5.1 Oxidative Cyclisation Reaction of Undecylprodiginine to Give Streptorubin B in *Streptomyces coelicolor*

It was originally proposed by Cerdeño et al. (2001) that the Rieske oxygenase-like enzyme RedG catalyses oxidative cyclisation of undecylprodiginine (**2**) to give the carbocyclic derivative, streptorubin B (**3**).

Initial support for this hypothesis come from analysis of a *S. coelicolor* M511/*redG::scar* mutant, which produces **2** but not its cyclic derivative **3** (Odulete, 2005). However, this experiment does not tell us that RedG is the only enzyme required for oxidative cyclisation. Potentially other enzymes could also be involved. It as well did not shed light on the substrate of RedG. One possibility is that undecylprodiginine (**2**) undergoes oxidative cyclisation to give directly **3** (Figure 5.1, green path). The other possibility is that the substrate for RedG is 2-undecylpyrrole (**21**) and that RedH condenses the cyclic derivative of 2-UP (**27**) with MBC (**20**) to give **3** (Figure 5.1, blue path). In this case RedG would catalyse oxidative cyclisation of **21** and RedH would catalyse condensation of MBC **20** with either **21** or its cyclic derivative **27**.

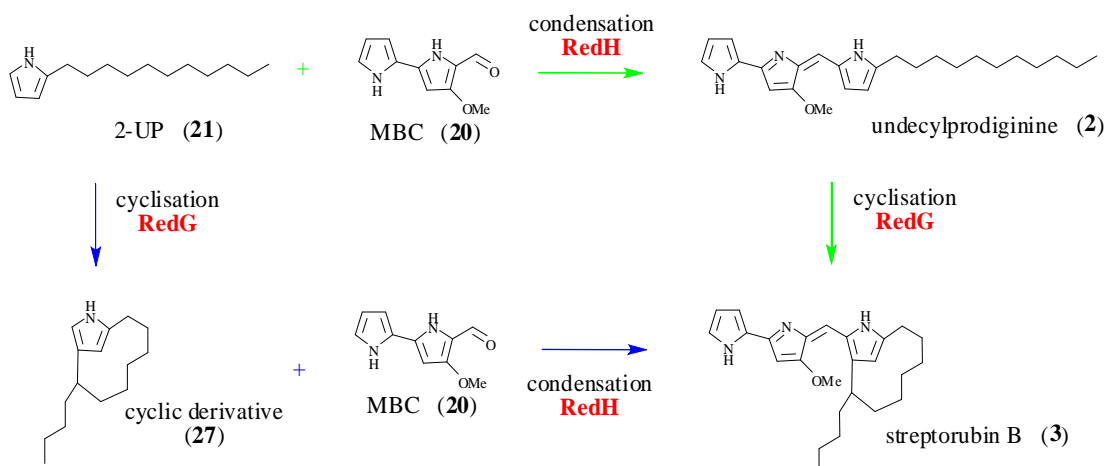


Figure 5.1 Possible pathways for the formation of streptorubin B (3) from 2-UP and MBC catalysed by RedG and RedH.

5.1.1 Analysis of a *Streptomyces coelicolor* M511/*redI::oriT-apr* (W34) Mutant Indicates the Likely Substrate of RedG

In the course of elucidating the functions of the other proteins encoded by the *red* cluster, a *S. coelicolor* M511/*redI::oriT-apr* mutant (W34) was created. The mutant was grown on R5 agar medium. After three to four days of growth, a difference in colour between the parent strain (M511) and the mutant was visible. The W34 mutant was yellow and LC-MS analyses of acidified organic extracts of the mycelia confirmed that neither undecylprodiginine (2) nor streptorubin B (3) being produced (Figure 5.2).

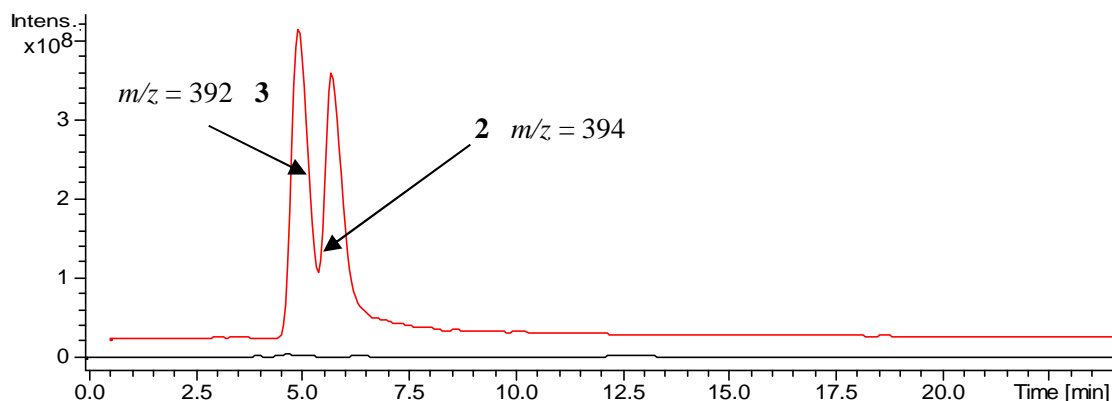


Figure 5.2 EICs ($m/z = 392-394$) from LC-MS analyses of acidified organic extracts of *S. coelicolor* M511 (red line) and a M511/*redI::oriT-apr* mutant (black line).

The protein encoded by *redI* is similar to *S*-adenosylmethionine (SAM)-dependent methyl transferases and has been proposed to catalyse *O*-methylation of the hydroxyl group on the B ring of HBC (**28**) during the MBC (**20**) biosynthesis (Figure 5.3 A).

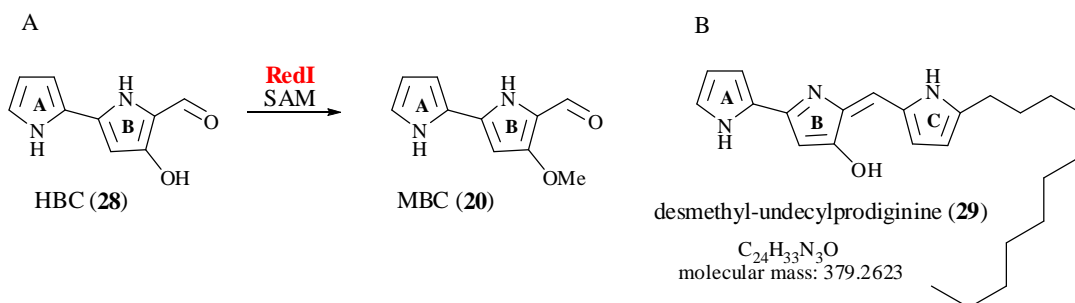


Figure 5.3 A – Proposed role for RedI in MBC biosynthesis; B – proposed structure of the undecylprodiginine derivative accumulated in the M511/*redI::oriT-apr* mutant.

Indeed, it was observed that the M511/*redI::oriT-apr* mutant accumulates a compound with $m/z = 380$ (Figure 5.4) which is consistent with the mass of desmethylundecylprodiginine (**29**), with an OH group in place of the OMe group (Figure 5.3 B). The same compound **29** is accumulated in small quantities relative to **2** (<1%) in the M511 wild type strain (confirmed by comparative MS/MS analysis) (Figure 5.4).

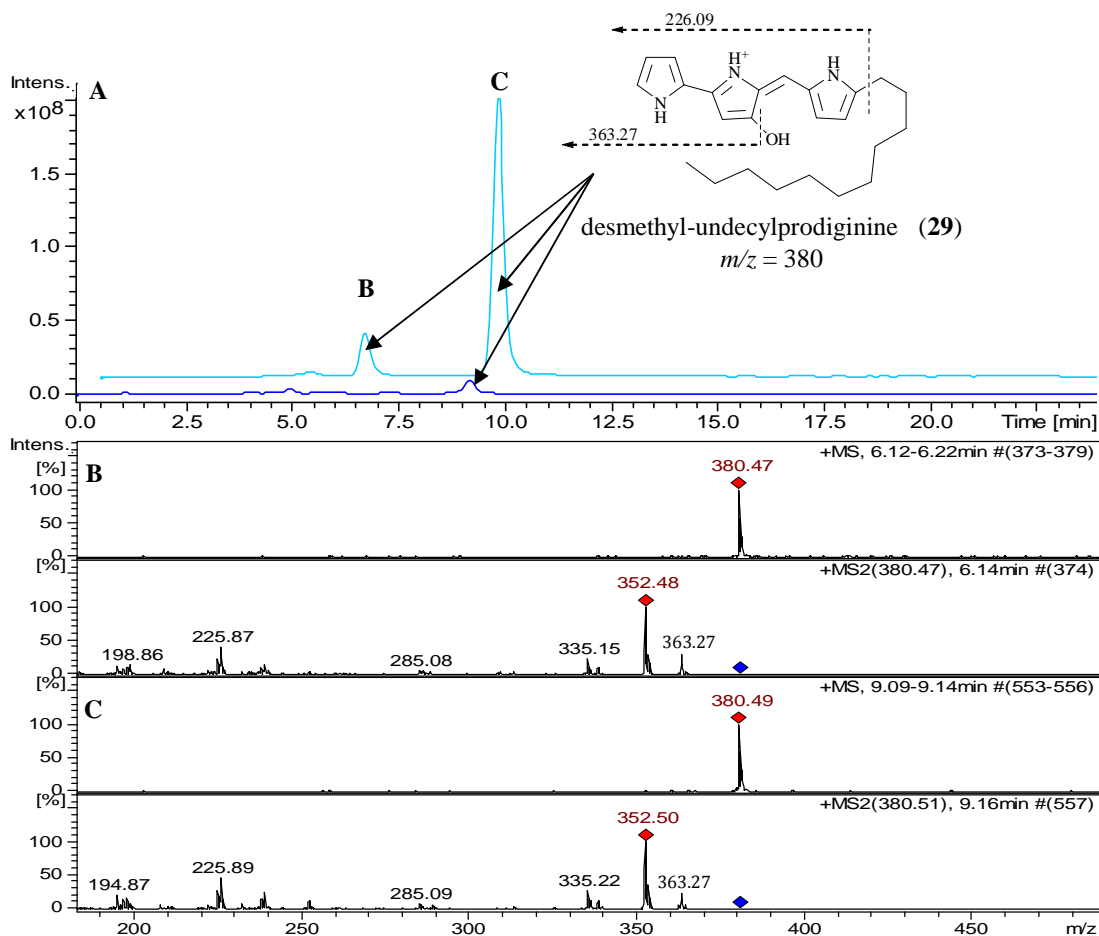


Figure 5.4 A – EICs ($m/z = 380$) from LC-MS analysis of organic extracts of the W34 mutant (top) and the M511 wild type (bottom). B,C – MS/MS spectra for $m/z = 380$ ions from organic extracts of the W34 mutant, B – peak with retention time ~6 min, C – peak with retention time ~9 min.

In the EIC for $m/z = 380$ from LC-MS analysis of organic extracts of the W34 mutant not one but two peaks for desmethylundecylprodiginine (**29**) were observed (Figure 5.4 B and C peaks). Each peak was collected separately and reanalysed by LC-MS. In both cases the original two peaks could be seen (data not shown). This indicated that peaks B and C correspond to rapidly inter-converting isomers of desmethylundecylprodiginine (**29**) (perhaps keto and enol tautomers).

Due to the structural change, the colour of desmethylundecylprodiginine was not red like other prodiginines. It was dark yellow, which corresponds to the observed change in λ_{max} from 533 nm to 490 nm. A wavelength of 490 nm was used for detection of **29** in further HPLC analyses and purification experiments.

Compound **29** was purified by semi-preparative HPLC from extracts of the W34 mutant and high resolution mass spectrometry analysis was carried out. The molecular formula of this compound was deduced to be $\text{C}_{24}\text{H}_{33}\text{N}_3\text{O}$ (calculated for $\text{C}_{24}\text{H}_{34}\text{N}_3\text{O}^+$: 380.2702, found: 380.2694), consistent with the hypothesis that it is desmethylundecylprodiginine.

Because of the instability of desmethylundecylprodiginine (**29**), insufficient quantities of pure material were obtained for NMR analysis. However to confirm the structure of **29**, chemical derivatisation by methylation of the $-\text{OH}$ group using trimethylsilyldiazomethane was carried out (Figure 5.5 A). The reaction mixture was analysed by LC-MS/MS which confirmed the compound had been converted to undecylprodiginine (Figure 5.5 B).

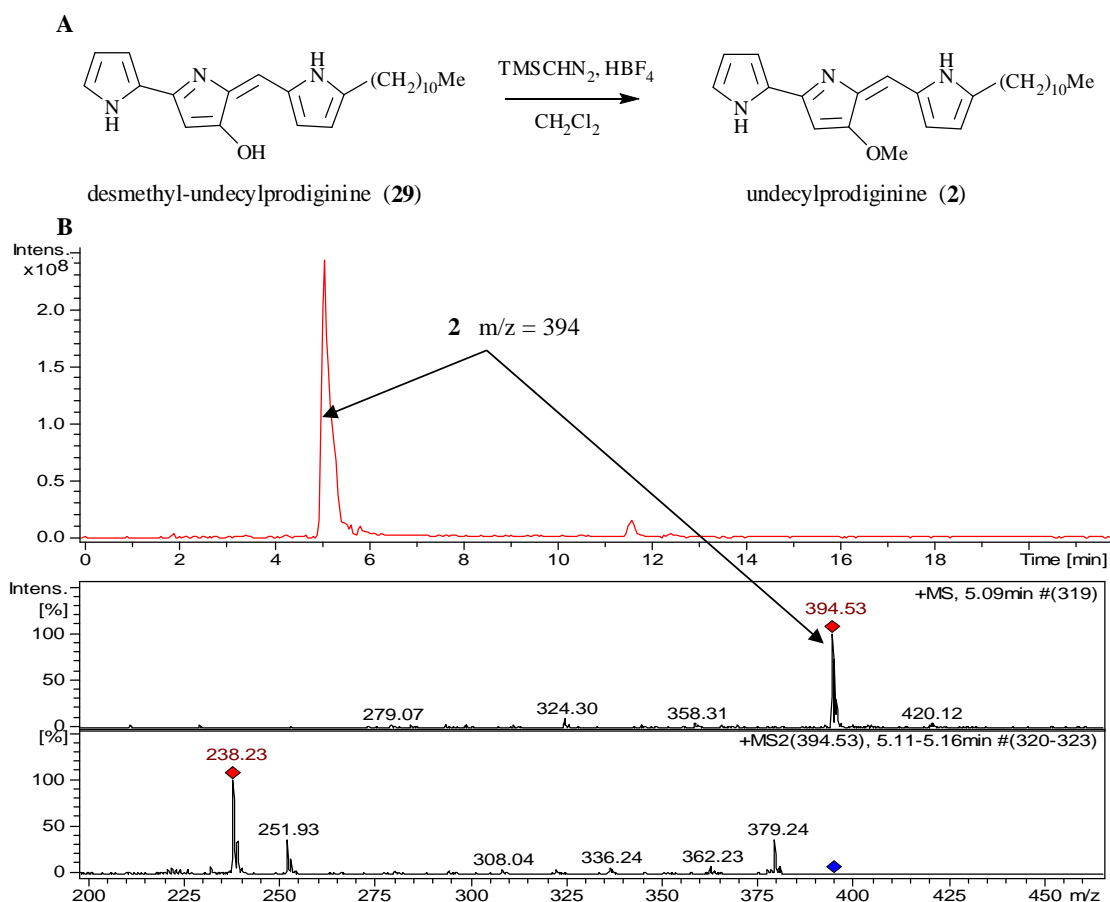


Figure 5.5 A – Reaction scheme for conversion of desmethylundecylprodiginine to undecylprodiginine. B – EIC ($m/z = 394$) from LC-MS/MS analysis of the methylation reaction. C – MS/MS spectra for peak with retention time of ~5 min.

Throughout the analyses of the W34 mutant, no accumulated compounds with $m/z = 378$ (corresponding to desmethylstreptorubin B) were observed. This indicates that oxidative cyclisation occurs after the condensation of 2-UP with MBC and that the methyl group in **2** is required for oxidative cyclisation reaction to form **3**.

5.1.2 Genetic Complementation of the *redG* Mutant

The *redG* gene was amplified by PCR from the Sc3F7 cosmid. Primers with restriction sites (forward primer – *HindIII*, reverse primer – *PstI*) appended to the 5'

ends were designed. The forward primer contained the natural RBS (5'-GGGAGA-3'), followed by the 7 nt upstream of the *redG* ATG start codon, followed by the start codon itself and the reverse primer contained a 20 nt homologous to the sequence ~70 bp downstream of the *redG* stop codon. The *Hind*III and *Pst*I digested PCR product was cloned into separately digested pOSV556. Correct insertion of the PCR product into the vector was confirmed by PCR with the cloning primers and restriction digest. The plasmid was introduced into *E. coli* ET12567/pUZ8002 and transferred by conjugation into *S. coelicolor* W31. One hygromycin resistant exconjugant was picked and grown on R5 agar medium. Production of prodiginines in the acidified organic extracts of the complemented mutant was analysed by LC-MS and it was observed that production of streptorubin B (**3**) was restored to the wild type level (Figure 5.6).

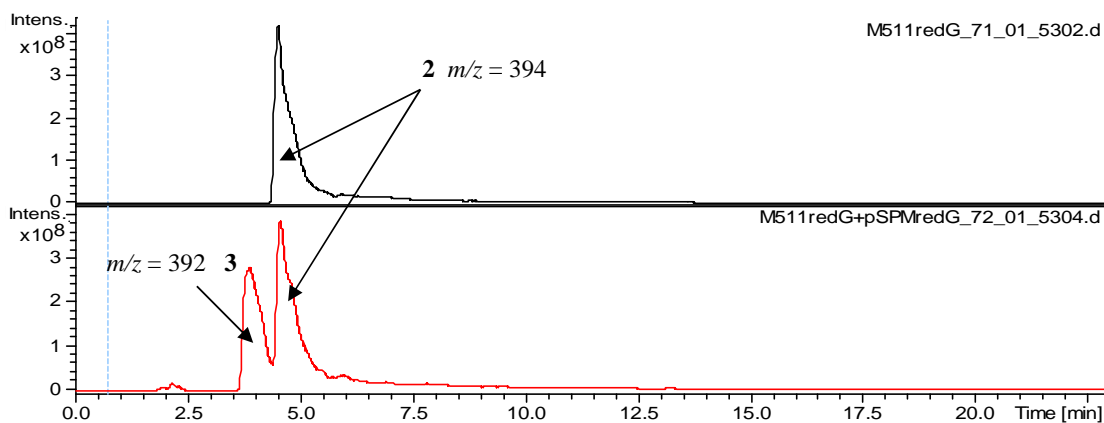


Figure 5.6 EIC ($m/z = 392-394$) from LC-MS analyses of acidified organic extracts of the W31 mutant (black line) and the W31/pOSV556*redG* strain (red line).

5.1.3 Expression of *redG* and *redHG* in *Streptomyces venezuelae* to Establish if RedG is the Only Enzyme from the *red* Cluster Required for Streptorubin B Biosynthesis

Based on the observation that feeding synthetic 2-UP and MBC to *S. venezuelae* expressing *redH* results in undecylprodiginine production, it was planned to investigate what would happen when MBC and 2-UP were fed to *S. venezuelae* in which both *redH* and *redG* are co-expressed. Because the genes are adjacent to each other in the same operon within the *red* cluster (separated by 77 nt of non-coding sequence), the *redHG*-encoding region was amplified from Sc3F7 in a single PCR reaction. The same forward primer employed for amplification *redH* (section 4.4.1), with a 5'-*Hind*III restriction site was used. The reverse primer had a 5'-*Not*I restriction site and was homologous to the sequence ~70 bp downstream of the *redG* stop codon. An ~4100 bp DNA fragment was amplified using these primers and cloned into pOSV556 under the control of the *ermE** promoter using standard techniques. Because the insert was quite big, the ligation was difficult to achieve. Eventually, after several repetitions, a correct clone was identified by restriction digest. The pOSV556*redHG* plasmid was transferred from *E. coli* ET12567/pUZ8002 to *S. venezuelae* by conjugation.

As described previously, when *S. venezuelae*/pOSV556*redH* was fed with synthetic MBC (**20**) and 2-UP (**21**), the undecylprodiginine (**2**) was produced (section 4.4.2). A similar experiment was carried out with *S. venezuelae* constitutively co-expressing *redH* and *redG*. After 3 days of growth on R5 agar medium, the plate was overlaid with solutions of synthetic **20** and **21**. After an additional 3 days of growth, the culture became dark red and LC-MS analyses of acidified mycelial extracts showed that

streptorubin B (**3**) is produced as well as undecylprodiginine (**2**) by this strain (Figure 5.7). Wild type *S. venezuelae*, fed with **20** and **21** did not produce any prodiginine antibiotics (Figure 5.7).

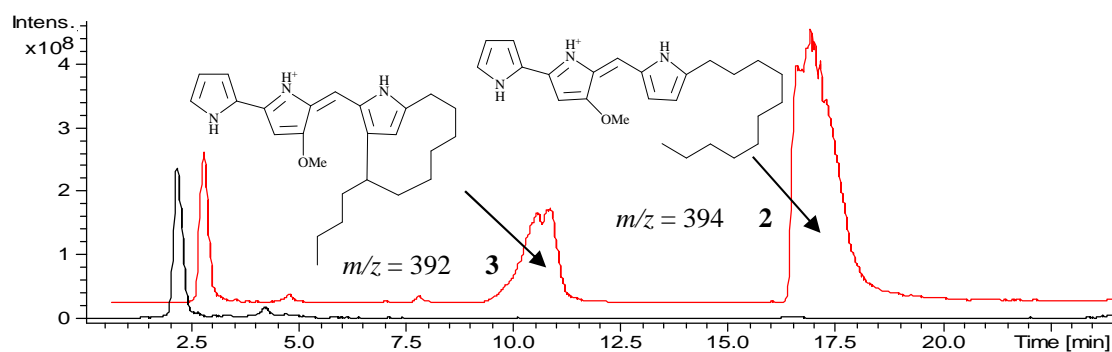


Figure 5.7 EIC ($m/z = 392-394$) from LC-MS analyses of acidified organic extracts from *S. venezuelae*/pOSV556redHG + 2-UP + MBC (red line) and from *S. venezuelae* + 2-UP + MBC (black line).

This observation indicates that RedG is responsible for the oxidative cyclisation reaction in *S. coelicolor* prodiginine biosynthesis and is required in addition to RedH for the assembly of streptorubin B from 2-UP and MBC.

To directly investigate whether undecylprodiginine (**2**) is the substrate of RedG just *redG* was constitutively expressed in *S. venezuelae*. The resulting strain was fed with extracts from the *S. coelicolor* W31 mutant (M511/*redG::scar* mutant accumulating undecylprodiginine, but not streptorubin B) as well as with synthetic **2** (kindly provided by Stuart Haynes). In both cases, LC-MS/MS analyses of the acidified organic extracts showed that streptorubin B is produced (Figure 5.8 B and Figure 5.9 B).

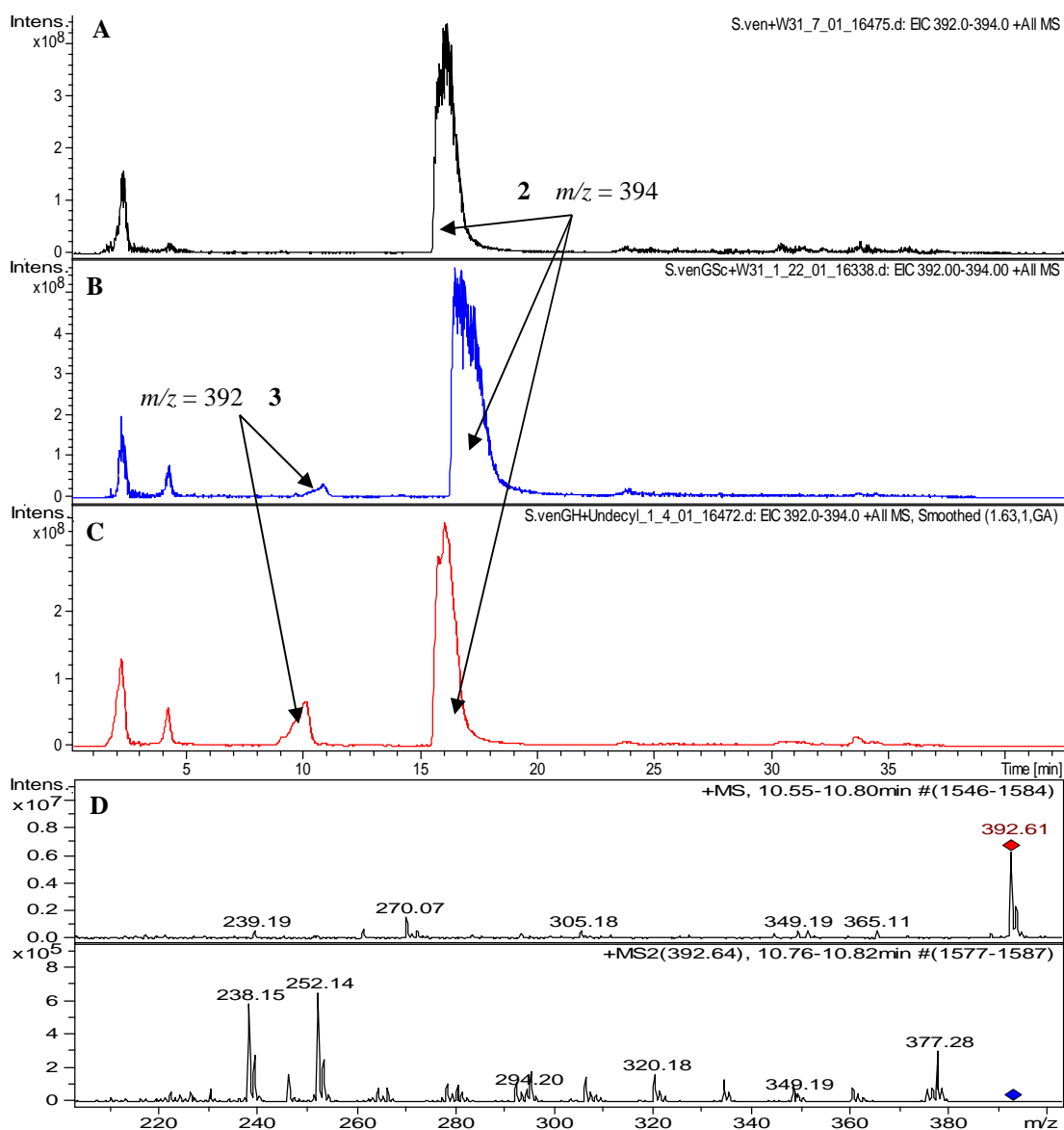


Figure 5.8 EIC ($m/z = 392-394$) from LC-MS/MS analyses of acidified organic extracts of A – *S. venezuelae* + W31 extract (black line), B – *S. venezuelae*/pOSV556redG + W31 extract (blue line), C – *S. venezuelae*/pOSV556redHG + W31 extracts (red line); D – MS/MS spectra for the peak with a retention time of ~10.5 min in the extract of *S. venezuelae*/pOSV556redG fed with W31 extract.

The same feeding experiments were repeated for *S. venezuelae* expressing *redH* and *redG*. When *S. venezuelae*/pOSV556redHG was fed with W31 extract and with synthetic **2**, more streptorubin B (**3**) was produced than when the W31 extract was fed to

S. venezuelae expressing just *redG* comparing (Figure 5.8 C, Figure 5.9 C). This indicates that RedG activity is higher in the presence of RedH. Perhaps RedH and RedG form a complex *in vivo* but this hypothesis was not further investigated.

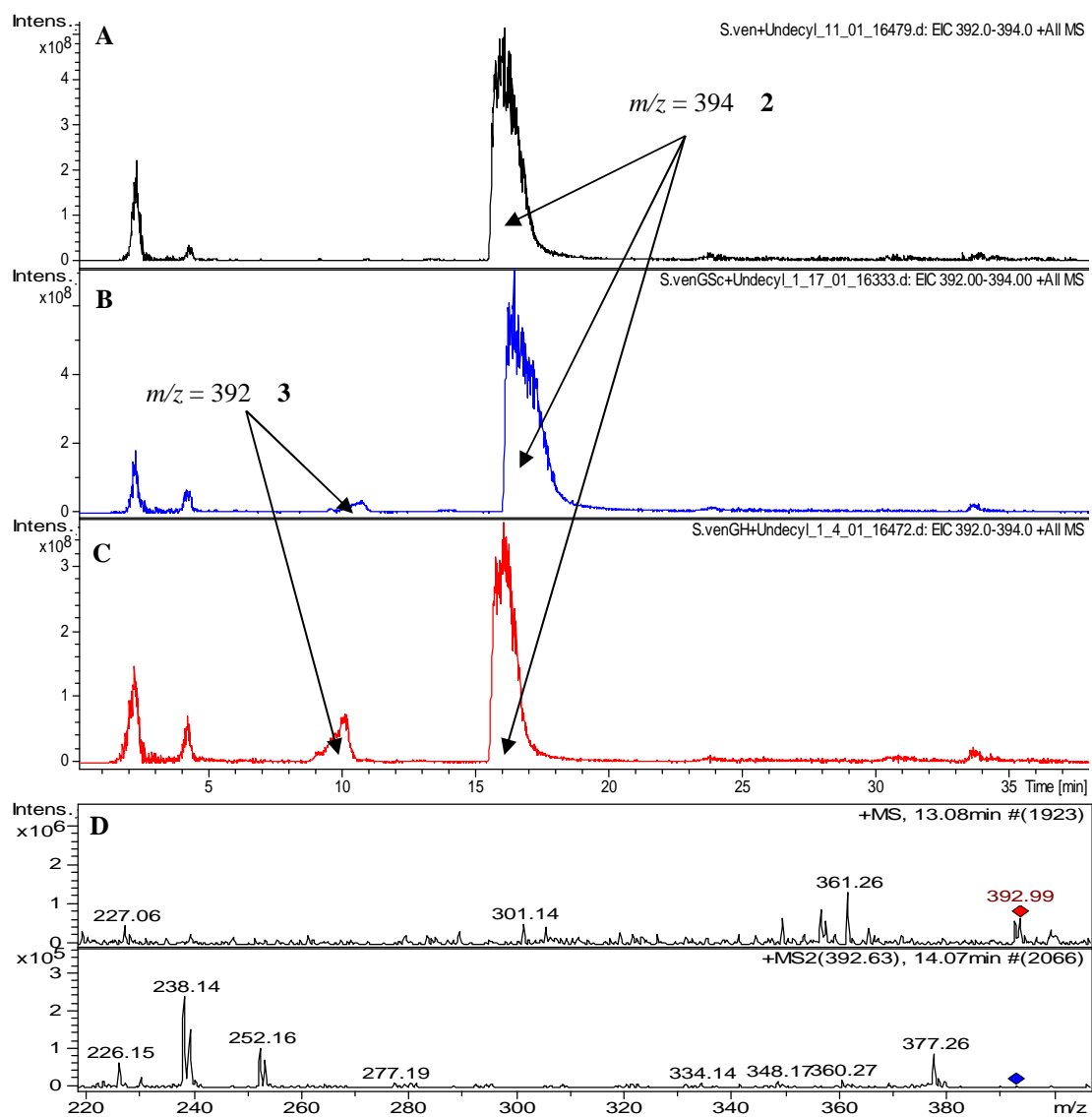


Figure 5.9 EIC ($m/z = 392-394$) from LC-MS analyses of acidified organic extracts of A – *S. venezuelae* + synthetic undecylprodiginine (2) (black line), B – *S. venezuelae/pOSV556redG* + synthetic 2 (blue line), C – *S. venezuelae/pOSV556redHG* + synthetic 2 (red line); D – MS/MS spectra for the peak with retention time of ~10 minutes in the extract from *S. venezuelae/pOSV556redG* fed with synthetic 2.

5.1.4 Introduction of Additional Copies of *redG* and *redH* into *S. coelicolor* M511

To examine the effect of introducing multiple copies of *redH* and *redH* + *redG* on the ratio of **2** to **3** produced by *S. coelicolor*, the pOSV556*redHG* construct was transferred by conjugation into *S. coelicolor* W31 (M511/*redG*::*scar*) and M511 strains. The pOSV556*redG* construct was introduced into *S. coelicolor* M511 for comparison with the previously constructed *S. coelicolor* W31/pOSV556*redG* strain. The W31/pOSV556*redG*, W31/pOSV556*redHG*, M511, M511/pOSV556*redG* and M511/pOSV556*redHG* strains were grown on R5 agar plates and acidified mycelial extracts were analysed by LC-MS. More streptorubin B (**3**) relative to undecylprodiginine (**2**) was consistently produced when an extra copy of *redG* was introduced into *S. coelicolor* and the amount of **3** relative to **2** further increased when the extra copy of *redG* was expressed downstream of an extra copy of *redH* (Figure 5.10). These observations could also indicate that RedG and RedH act as a complex *in vivo*, resulting in increased production of streptorubin B.

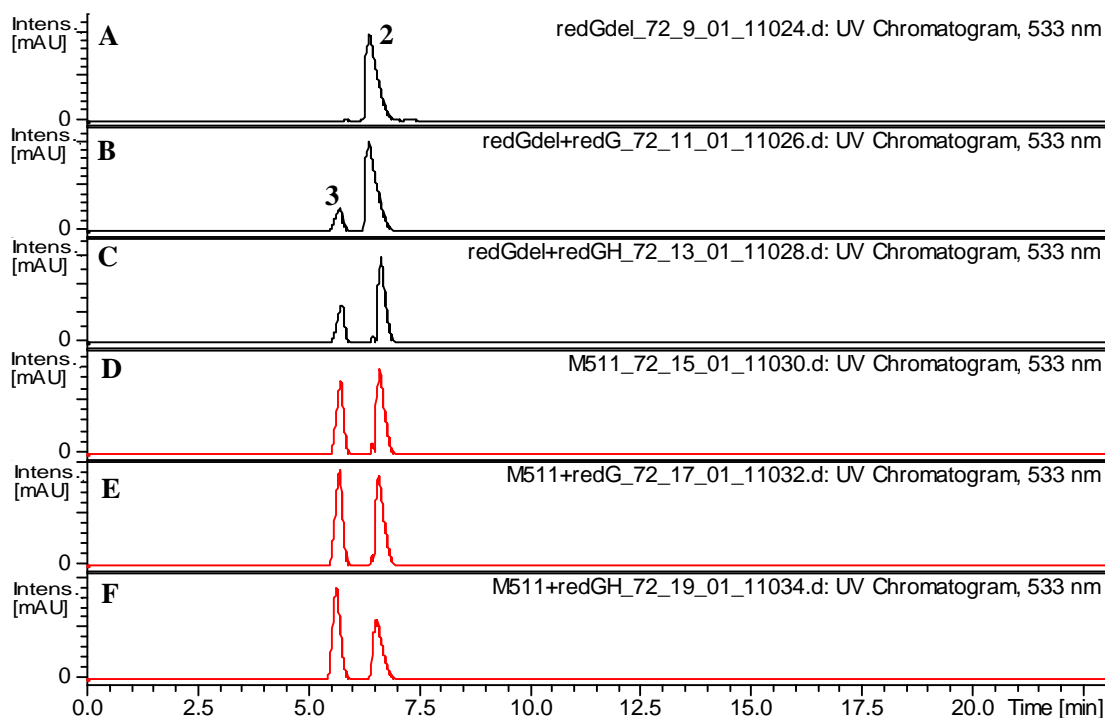


Figure 5.10 HPLC analysis monitoring absorbance at 533 nm of acidified organic extracts of *S. coelicolor* A – W31, B – W31/pOSV556*redG*, C – W31/pOSV556*redHG*, D – M511, E – M511/pOSV556*redG*, F – M511/pOSV556*redHG*; 2 = undecylprodiginine, 3 = streptorubin B.

In Chapter 3 (section 4.2.1) it was shown that prodiginine production in the M511/*redL::oriT-apr* (W38) can be restored by feeding 2-UP. However streptorubin B was produced at low levels relative to undecylprodiginine. Thus, pOSV556/*redHG* was introduced into *S. coelicolor* W38 by conjugation. Feeding this strain with 2-UP resulted in higher quantities of streptorubin B relative to undecylprodiginine than when 2-UP was fed to the W38 strain (Figure 5.11).

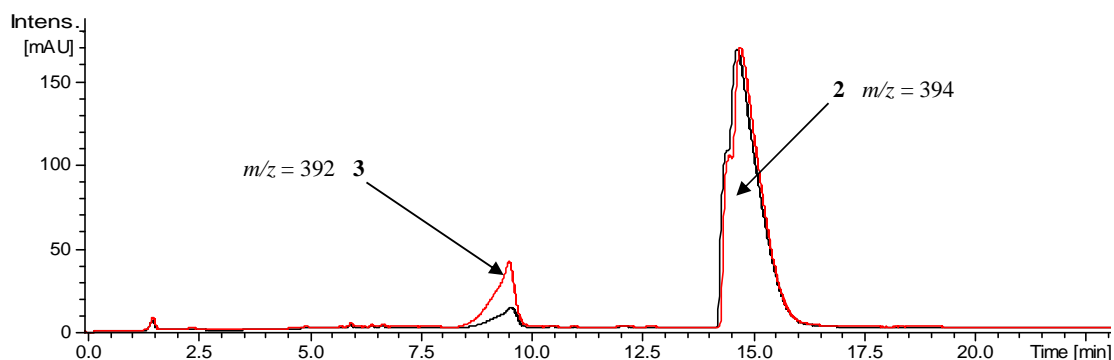


Figure 5.11 HPLC analyses monitoring absorbance at 533 nm of acidified organic extracts of *S. coelicolor* W38 (black line) and W38/pOSV556redHG (red line) fed with synthetic 2-UP.

The observations that more streptorubin B was produced in the W38/pOSV556redHG strain than in W38 itself, was exploited in the mutasynthesis of streptorubin B analogues (Haynes, 2010). Feeding the W38/pOSV556redHG strain with synthesised 2-undecylpyrrole analogues resulted in higher yields of the corresponding analogues of streptorubin B.

The above data clearly show that introducing an extra copy of *redHG* under the control of the *ermE** promoter into the chromosomes of *S. coelicolor* W31 and M511 increases the production of streptorubin B. To check if introduction of multiple copies of *redG* and *redHG* into the *S. coelicolor* strains would further increase the production of streptorubin B, a multicopy plasmid (pIJ86) was used (kindly provided by Mervyn Bibb, John Innes Centre) (Bibb et al., 1994). pIJ86 contains an apramycin resistance gene, *oriT* (for conjugal transfer) and origins of replication for *Streptomyces* species and *E. coli*. Similarly to pOSV556, cloned genes can be expressed under the control of the constitutive *ermE** promoter (Figure 5.12).

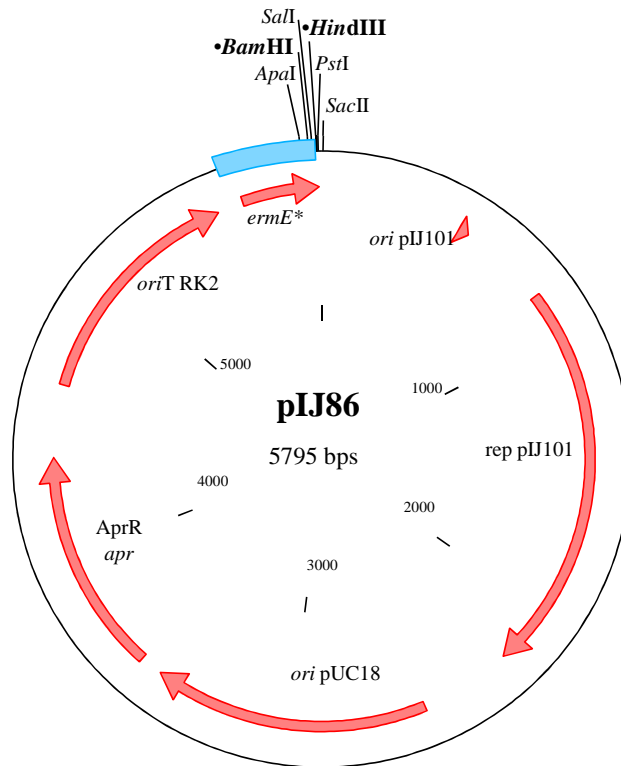


Figure 5.12 Feature map of pIJ86.

To clone *redG* and *redHG* into pIJ86, similar PCR primers to those used to clone these genes to pOSV556 were used. Two forward primers containing 5'-*Bam*HI restriction sites and the natural RBSs followed by 10 nt upstream of *redG* or *redH* (including the start codon) were designed. The reverse primer was the same for both PCRs with a 5'-*Hind*III restriction site, followed by 18 nt homologous to the sequence ~70 bp downstream of the *redG* stop codon. Both DNA fragments were amplified by PCR using Sc3F7 as a template. A 1307 bp band was obtained for *redG* and a 4204 bp band was obtained for *redHG*. The *Bam*HI/*Hind*III-digested PCR products were cloned into similarly-digested pIJ86 using standard procedures. The integrity of clones was confirmed by restriction enzyme digests and one correct clone of each construct was separately transferred from *E. coli* ET12567/pUZ8002 to W31 mutant by conjugation.

One apramycin resistant exconjugant each of W31/pIJ86*redG* and W31/pIJ86*redHG* was picked and grown separately on R5 agar medium. After 5 days of growth an acidified organic mycelial extract of each strain was prepared and analysed by LC-MS (Figure 5.13). The production of streptorubin B in both strains could be detected.

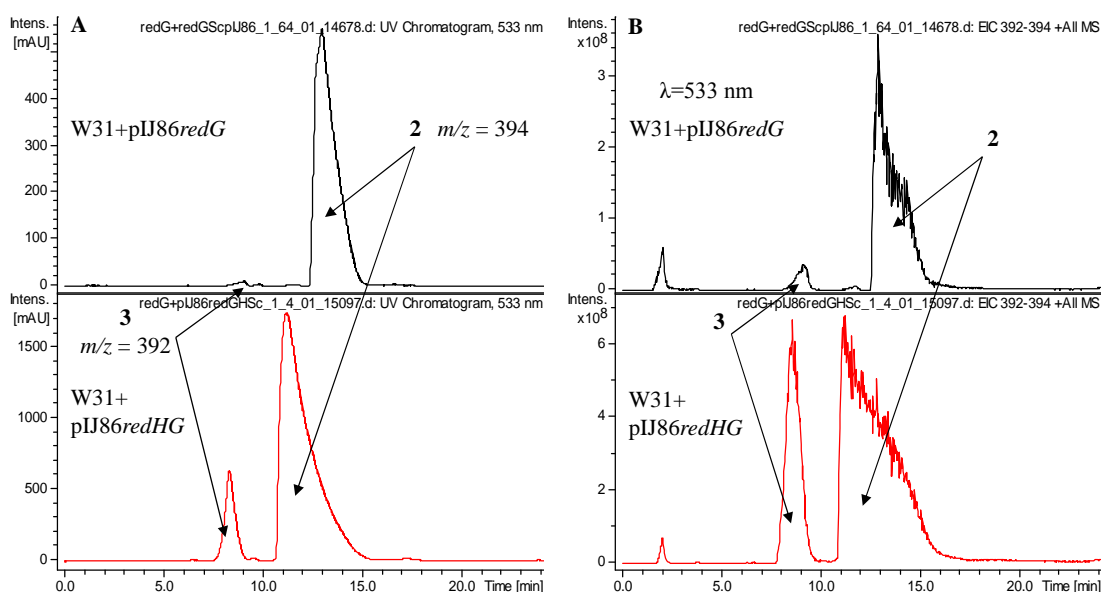


Figure 5.13 Analyses of acidified organic extracts from W31/pIJ86*redG* (black line) and W31/pIJ86*redHG* (red line); A – HPLC analyses monitoring absorbance at 533 nm, B – EICs ($m/z = 392-394$) from LC-MS analyses.

Although more streptorubin B relative to undecylprodiginine is produced when *redHG* is expressed from pIJ86 in *S. coelicolor* M511 compared with W31 (Figure 5.13), it does not look as if the ratio of streptorubin B to undecylprodiginine is higher than when the genes are expressed from pOSV556. Additionally, pIJ86 contains the apramycin resistance gene (not hygromycin resistance gene that is present in pOSV556),

so it could not be used in most of the apramycin resistant mutants created in the lab. Thus, the expression of *redHG* from pIJ86 in *S. coelicolor* was not pursued further.

5.2 Cloning, Sequencing and Functional Analysis of *Streptomyces longispororuber redG* Orthologue: *mcpG*

Streptomyces coelicolor produces two prodiginine antibiotics: undecylprodiginine (**2**) and its 10-membered carbocyclic derivative streptorubin B (**3**). *Streptomyces longispororuber* also produces undecylprodiginine (**2**) along with a different 12-membered carbocyclic derivative called metacycloprodigiosin (streptorubin A) (**16**) (Figure 5.14).

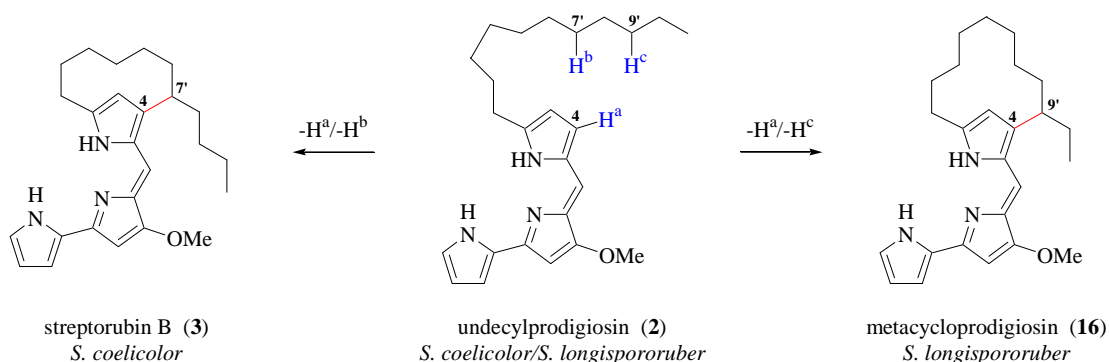


Figure 5.14 Prodiginines produced by *S. coelicolor* and *S. longispororuber*.

In the Challis group, a RedG homologue in *S. longispororuber* was proposed to catalyse the formation of the C-C bond between C-4 of ring C and C-9' in undecylprodiginine (**2**) to form metacycloprodigiosin (streptorubin A) (**16**) (Figure 5.14). Highly conserved regions of *S. coelicolor redG* and the upstream gene *redH* were used to design two degenerate oligonucleotides. A PCR reaction using these two oligonucleotides and genomic DNA of *S. longispororuber* as a template resulted in an amplicon of

637 bp that was cloned and sequenced (Barry, 2007). Analysis of the sequence revealed two partial coding sequences (CDSs). The first partial CDS contained a stop codon and encoded a polypeptide (44 aa) that was 90% similar to the C-terminus of *S. coelicolor* RedH. The second partial CDS contained an ATG start codon and encoded a polypeptide (162 aa) showing high similarity (78%) to the N-terminal domain of *S. coelicolor* RedG (Barry, 2007). On this basis, these two CDSs were proposed to encode for enzymes required for the biosynthesis of **2** and **16** in *S. longispororuber*, suggesting that the RedG orthologue may be involved in a regiospecific oxidative cyclisation between C-4 on ring C and C-9' in **2** to give **16**.

My work was aimed at obtaining the entire sequence of the *S. longispororuber* *redG* orthologue and at investigating its role in the regiospecific oxidative cyclisation of undecylprodiginine to give metacycloprodiginin.

5.2.1 Construction of a *Streptomyces longispororuber* Fosmid Library

A fosmid library was constructed using the commercially available CopyControl™ Fosmid Library Production Kit supplied by Epicentre Biotechnologies (EpicentreBiotechnologies, 2007) to obtain the entire sequence of the *redG* orthologue from *S. longispororuber*.

The pCC1 FOS fosmid vector (Figure 5.15) contains a chloramphenicol resistance

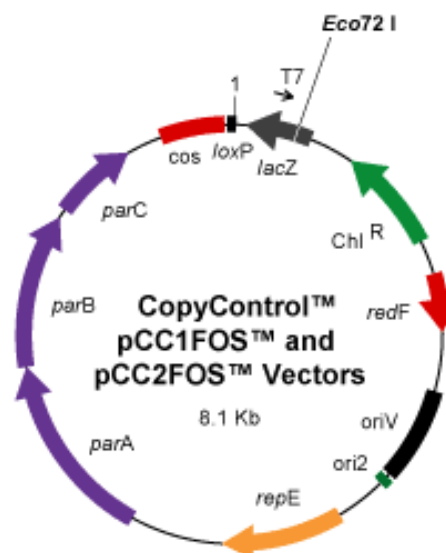


Figure 5.15 Map of the pCC1 FOS vector.

gene for selection, the *cos* site for lambda phage packaging and two origins of replica-

tion: a single copy number *ori2* origin and the high copy number *oriV* origin. A single copy origin of replication ensures insert stability and allows cloning of genes which code for potentially toxic proteins. A high copy origin of replication can be induced to produce up to 50 copies of the fosmid per cell to improve DNA yields for applications, such as sequencing (EpicentreBiotechnologies, 2007).

The total genomic DNA of *S. longispororuber* was isolated and sheared to give fragments of approximately 40 kb leading to the highly random generation of DNA fragments. After shearing the DNA was repaired with an End-Repair Enzyme to generate blunt-ended, 5'-phosphorylated DNA. After the reaction, the DNA was separated on a low melting point (LMP) agarose gel by electrophoresis and a band of ~40 kb was cut from the gel (Figure 5.16).

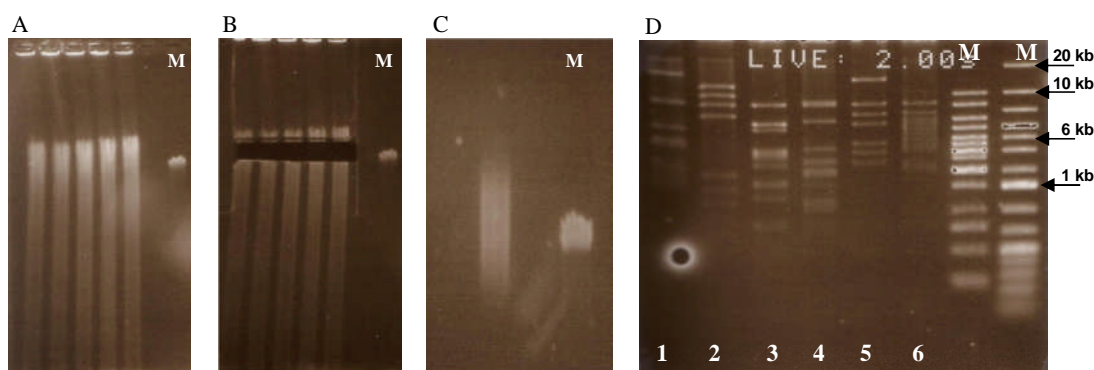


Figure 5.16 A – *S. longispororuber* genomic DNA after shearing, B – *S. longispororuber* genomic DNA after ~40 kb band DNA was excused, C – *S. longispororuber* ~40 kb genomic DNA fraction; D – agarose gel electrophoresis analysis of 6 fosmid clones digested with *Bam*HI. For A-C, M = 40 kb molecular size marker; for D – M = 10 – 0.25 kb and 20 – 0.1 kb molecular size markers.

After gel extraction, the 40 kb genomic DNA fragments were ligated with pCC1FOS and packaged with the MaxPlax Lambda Packaging Extract. *E. coli* EPI300-T1^R host cells were then infected by the Lambda Phages containing the clones. After

incubation the cells were plated on LB agar growing ~2000 colonies. The steps involved in the construction of the fosmid library are shown in Figure 5.17.

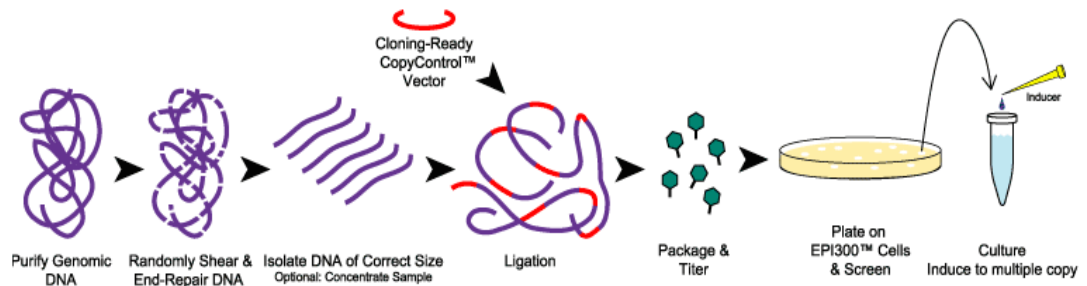


Figure 5.17 Steps involved in creating a genomic fosmid library(EpicentreBiotechnologies, 2007).

Fosmid DNA was isolated from a few colonies of the library and digested with *Bam*HI. The isolated clones exhibited different digestion patterns, which confirmed the presence of different inserts in each clone (Figure 5.16 D).

~500 clones from the library were picked and grown separately in 96 well plates and the clones were screened by PCR using primers that are homologous to regions of the DNA sequence of the previously identified *S. longispororuber* fragment of the *redG* orthologue. PCR reactions were analysed by agarose gel electrophoresis and two clones were found to give products of the expected size (Figure 5.18).

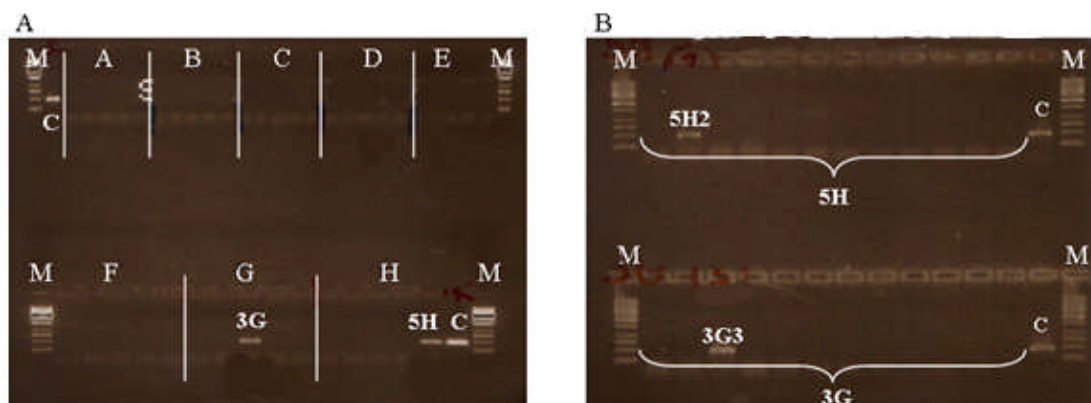


Figure 5.18 Screening of *S. longispororuber* fosmid library for clones containing the *redG* orthologue. 500 colonies grown in 96 well plates were screened in two stages: A – first, screening with twelve clones in each PCR reaction, B – second screening of twelve clones from two positive PCR reactions checked separately; M – DNA marker; C – control PCR reaction with genomic DNA as a template.

The amplified DNA fragments of expected size from the two clones were sequenced. The results showed that the amplifier from the 3G3 fosmid encodes a polypeptide that is similar to the N-terminal region of RedG (identities = 84/123 (68%), positives = 103/123 (83%)) and is also identical to the previously sequenced fragment of the *redG* orthologue amplified from *S. longispororuber* genomic DNA. The sequencing results for the amplifier from the 5H2 fosmid did not show any similarity to genes in the *S. coelicolor red* cluster. Therefore, the 5H2 clone was not analysed further.

5.2.2 Fosmid 3G3 Analysis – Sequence Determination of *redG* and *redH* Orthologues (*mcpG* and *mcpH*) of *Streptomyces longispororuber*

The 3G3 fosmid was sent for further sequencing (GATC Biotech, Germany) using primers homologous to the vector backbone each side of the insert (Figure 5.19, primer a and b). This resulted in the determination of the sequences of the ends of the insert. Afterwards a set of oligonucleotides that prime inside the insert was designed

(Figure 5.19, primers c, d and others) and the fosmid insert was partially sequenced in order to determine the whole sequence of the *redG* and *redH* orthologue. Based on the obtained DNA sequence, the genetic organisations of the *red* cluster from *S. coelicolor* and the *mcp* cluster from *S. longispororuber* were compared as shown in Figure 5.19.

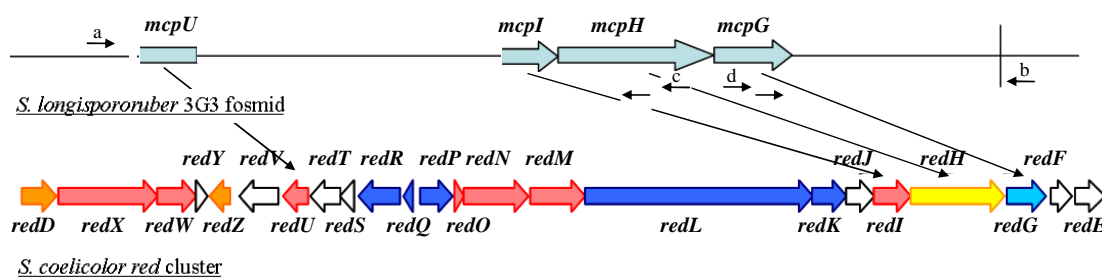


Figure 5.19 Comparison of genetic organisation of the *S. coelicolor* *red* cluster with the fragment of the *S. longispororuber* *mcp* cluster cloned in the 3G3 fosmid.

The complete CDSs for the *redH* and *redG* orthologue were named *mcpH* and *mcpG*, respectively, and the putative prodiginine biosynthetic gene cluster in *S. longispororuber* was named the *mcp* cluster. The amino acid sequences of the McpH and McpG proteins showed very high similarity to RedH and RedG of *S. coelicolor* (Figure 5.20) (Table 5.1).



Figure 5.20 A – sequence alignment of the McpH and RedH; B – sequence alignment of the McpG and RedG; conserved residues within RedG and McpG that ligate the [2Fe-2S] cluster and Fe(II) atom in NDO are highlighted in blue, an Asp residue of NDO (mutated to Glu in RedG and McpG) proposed to mediate electron transfer between the [2Fe-2S] cluster and the Fe(II) atom is highlighted in red. Black letters, no background – non-similar amino acids, black letters, green background – block of similar amino acids, red letter, yellow background – identical amino acids.

In McpG, conserved sequence motifs characteristic of Rieske oxygenase-like enzymes (including RedG) were identified (Figure 5.20 B). One partial CDS encoding a protein highly similar to the C-terminus of RedI and another partial CDS encoding a protein similar to the N-terminus of RedU were also identified (Table 5.1 and Figure

5.19). These four coding sequences in the *mcp* cluster showed a similar relative organisation to the corresponding genes in the *red* cluster of *S. coelicolor*. Thus we speculate that the genetic organisation of the *mcp* cluster is very similar to that of the *red* cluster in *S. coelicolor* (Figure 5.19).

Table 5.1 Comparison of the proteins encoded by the four CDSs identified in the *mcp* cluster of *S. longispororuber* with their orthologues encoded by the *S. coelicolor red* cluster.

<i>S. longispororuber</i>	<i>S. coelicolor</i>	identity	similarity
McpG – 340 aa	RedG – 363 aa	58% (199/340)	75% (256/340)
McpH – 926 aa	RedH – 834 aa	69% (641/926)	78% (723/926)
McpI – 129 aa fragment	RedI – 362 aa	68% (70/102)	79% (81/102)
McpU – 160 aa fragment	RedU – 261 aa	56% (90/160)	69% (111/160)

5.2.3 Heterologous Expression of *Streptomyces longispororuber mcpG* in the *Streptomyces coelicolor/redG::scar* Mutant

The *S. coelicolor* W31 mutant (M511/*redG::scar*) does not produce streptorubin B (it only produces undecylprodiginine) (section 5.1.2). We decided to investigate the effect of introducing *mcpG* into the mutant. If this resulted in production of metacycloprodigiosin (streptorubin A), it would show that McpG catalyses the regiodivergent oxidative cyclisation of undecylprodiginine to form metacycloprodigiosin.

The *S. longispororuber mcpG* gene was cloned into pOSV556 plasmid. PCR primers for amplification of *mcpG* were designed as described in section 5.1.2 with a *HindIII* restriction site at the 5' end of the forward and a *PstI* site at the 5' end in the

reverse primer. After amplification the product was digested with *HindIII/PstI* and ligated into similarly digested pOSV556 using standard procedures. One verified as a correct clone was introduced into *E. coli* ET12567/pUZ8002 and conjugation was carried out with *S. coelicolor* W31 (M511/*redG::scar*). One hygromycin resistant exconjugant was picked and grown on R5 agar medium. LC-MS analysis of the acidified organic cell extract showed two peaks in the EIC for $m/z = 392-394$ with masses corresponding to undecylprodiginine (**2**) ($m/z = 394$) and a cyclic derivative ($m/z = 392$) metabolites (Figure 5.21 A, B, C, F).

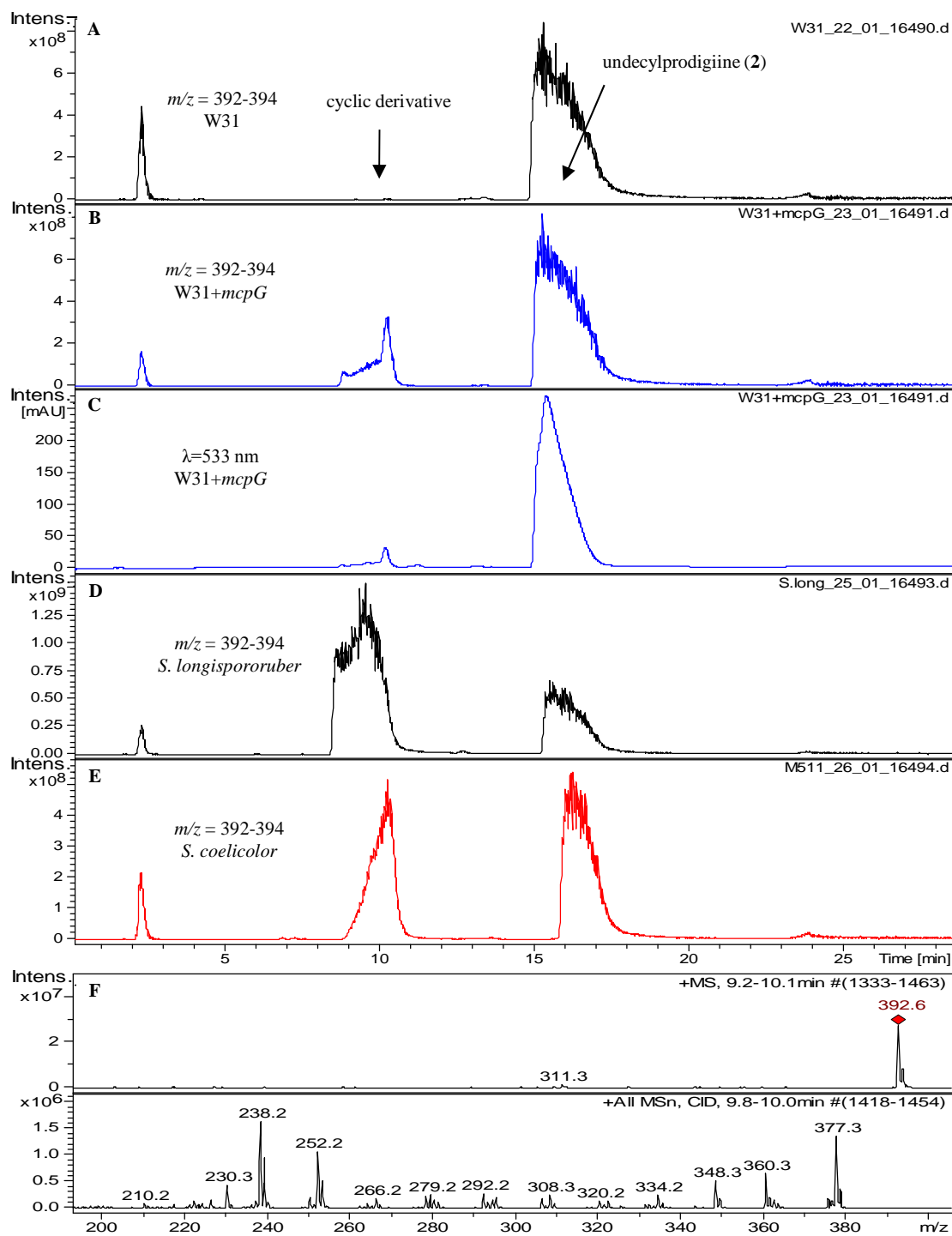


Figure 5.21 A, B, D, E: EICs ($m/z = 392-394$) from LC-MS analyses of acidified organic extracts of: A – *S. coelicolor* W31 (top black line), B – W31/pOSV556mcpG (blue line), D – *S. longispororuber* (black line), E – *S. coelicolor* M511 (red line); C – HPLC analysis monitoring absorbance at 533 nm of acidified organic extracts of W31/pOSV556mcpG, F – MS/MS spectra of the cyclic undecylprodiginine derivative produced by W31/pOSV556mcpG.

Streptorubin A and B, have the same retention time (Figure 5.21 D, E), m/z in positive ion mode and fragmentation pattern (Figure 5.21 F and Figure 5.22) However, they can be distinguished by ^1H NMR spectroscopy.

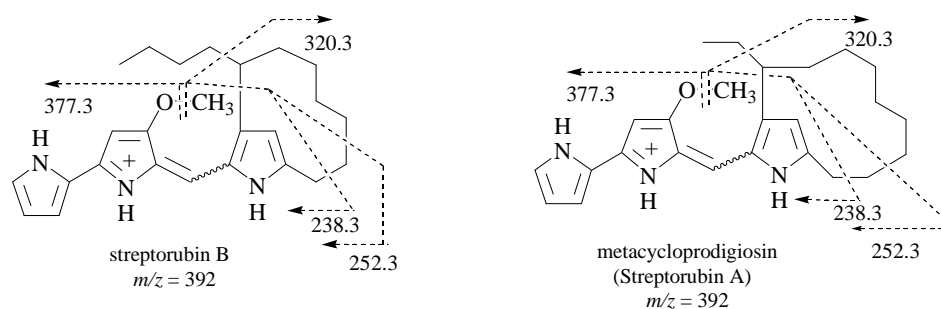


Figure 5.22 Proposed fragment ions of streptorubin A (metacycloprodigiosin) and streptorubin B observed in positive ion ESI-MS/MS spectra.

The most significant difference between the ^1H NMR spectra of streptorubin A and B is that a characteristic signal at -1.53 ppm of streptorubin B is missing in the spectrum of streptorubin A (Laatsch et al., 1991). This signal is coming from one of the C'4 hydrogen atom which is shielded by electrons from the pyrrole ring causing such high chemical shift. Instead of signal at -1.53 ppm a signal at 0.2 ppm appears in the spectrum of streptorubin A (Figure 5.23). Additionally methine protons and hydrocarbon protons α to the pyrrole ring have characteristically different chemical shift.

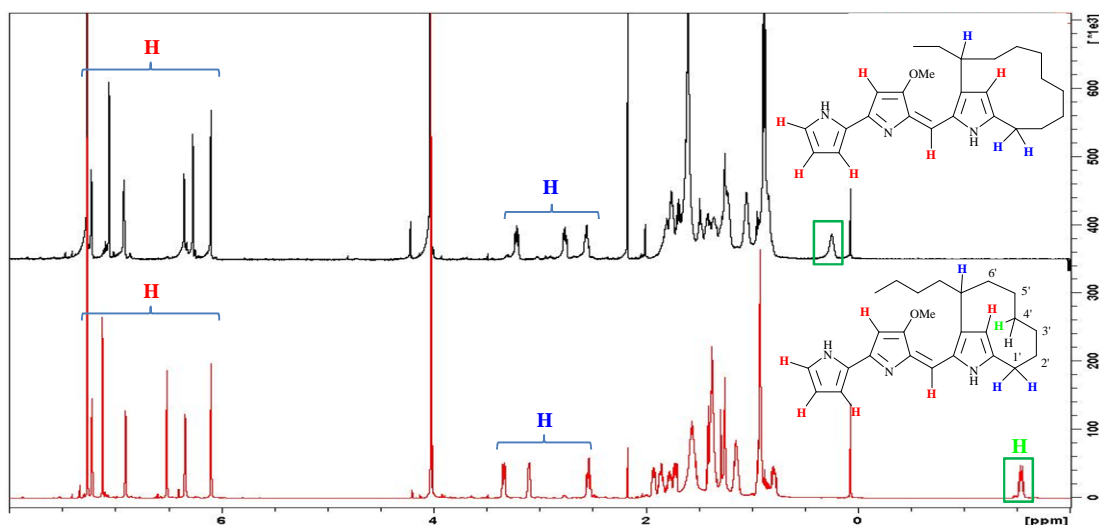


Figure 5.23 ^1H NMR spectra (CDCl_3 , 700 MHz) of streptorubin A (top) and streptorubin B (bottom). The characteristic signals at 0.2 ppm and -1.53 ppm for streptorubin A and B, respectively are highlighted by a box.

The compound with $m/z = 392$ was purified from large scale cultures of *S. coelicolor* W31/pOSV556mcpG. First, alumina flash chromatography was carried out to isolate the prodiginine mixture, followed by semi-preparative reverse-phase HPLC to separate undecylprodiginine from its cyclic derivative.

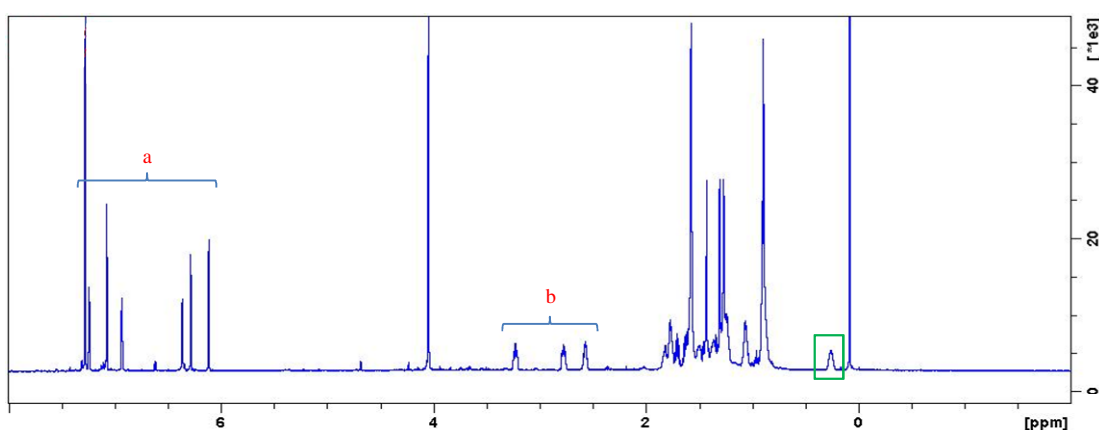


Figure 5.24 ^1H NMR spectrum of the cyclic undecylprodiginine derivative produced by *S. coelicolor* W31/pOSV556mcpG. The characteristic signal at 0.2 ppm is highlighted by a box; a – methylene protons, b – hydrocarbon protons α to the pyrrole ring.

The ^1H NMR spectrum of the purified compound contained the characteristic signal at 0.2 ppm for streptorubin A and lacked the signal at -1.53 ppm characteristic of streptorubin B (Figure 5.24). Other protons (methine protons and hydrocarbon protons α to the pyrrole ring) had the same chemical shifts like streptorubin A (Figure 5.24 a and b). Furthermore, the CD spectrum of the compound was measured. Streptorubin A and B have different CD spectra with equal and opposite signals (Figure 5.25 A). The CD spectrum of the purified compound (Figure 5.25 B) was identical to the spectrum of streptorubin A, confirming the identity of the compound purified from the *S. coelicolor* W31/pOSV556mcpG mutant as streptorubin A.

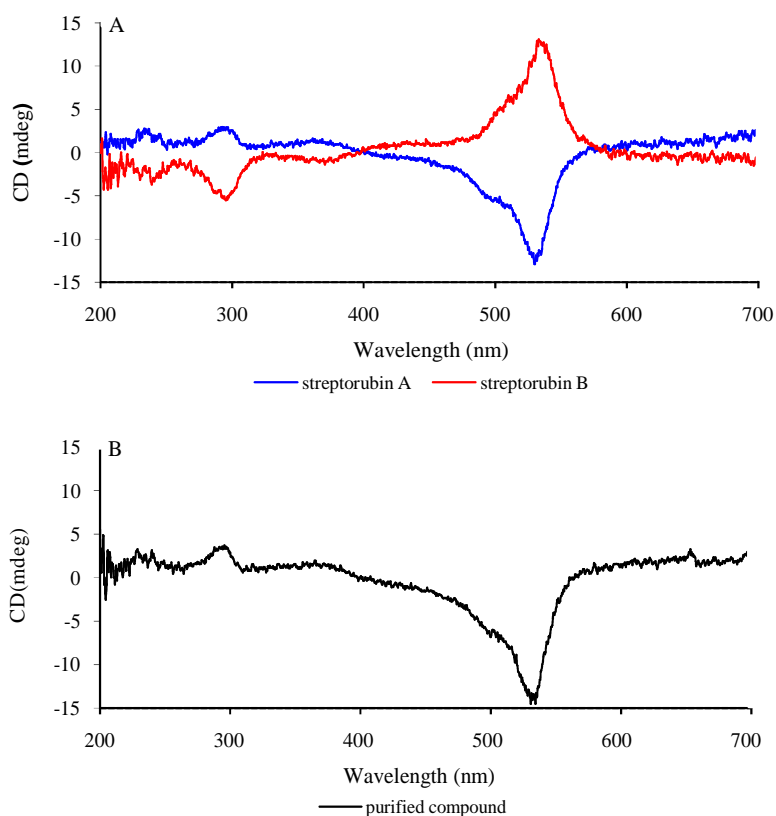


Figure 5.25 A – CD spectra of streptorubin A (blue line) and streptorubin B (red line); B – CD spectrum of compound with $m/z = 392$ produced by *S. coelicolor* W31/pOSV556mcpG.

In conclusion sequences of RedG from *S. coelicolor* and McpG from *S. longispororuber* were shown to be highly similar by creating a *S. longispororuber* genomic library and determining the complete sequence of *mcpG*. Both of these proteins belong to a new family of Rieske non-heme iron-dependent oxygenase-like enzymes. Cloning and expression of *mcpG* in *S. coelicolor* W31 resulted in production of streptorubin A, providing strong evidence that RedG and McpG are responsible for the regiodivergent oxidative cyclisation of the undecylprodiginine to form streptorubin B and metacycloprodigosin (streptorubin A), respectively.

5.3 The Role of *redG* Orthologues in Other Microorganisms

Streptorubin B and streptorubin A belong to a large family of prodiginines, which also include other red tripyrrole and furano-dipyrrole containing cyclic compounds like prodigosin R1 (**18**), dechlororoseophilin (**30**) or roseophilin (**19**), all produced by *Streptomyces griseoviridis* (Kayakawa et al., 1992; Kawasaki et al., 2008; Hayakawa et al., 2009). Recently, the *rph* gene cluster responsible for prodiginine biosynthesis in *S. griseoviridis* was identified, cloned and sequenced (Kawasaki et al., 2009). The cluster contains 21 genes homologous to genes in the *red* cluster of *S. coelicolor*, including 4 *redG* orthologue (*rphG1*, *rphG2*, *rphG3*, *rphG4*). **19** is thought to be biosynthesised by the same pathway as **18**, but the pathway diverge at the late stage. The different RedG orthologues could generate the different carbon-carbon bridges in **18** and **19** (Figure 5.26). One of these enzymes could also catalyse the oxida-

tive conversion of the central pyrrole ring in a tripyrrole precursor of **19** to the sponding furan (Figure 5.26).

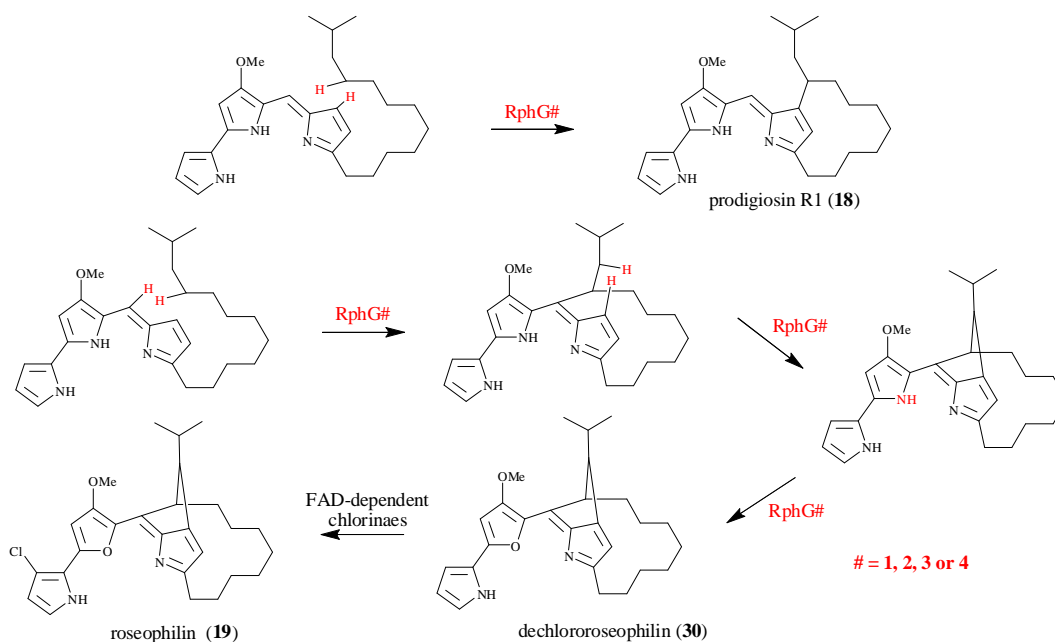


Figure 5.26 Proposed roles for RphG1, RphG2, RphG3 and RphG4 in 18 and 19 biosynthesis.

Alignment of the RedG sequence with RphG sequences highlights their high similarity. In addition, all the conserved sequence motifs characteristic of Rieske oxygenase like enzymes are present in three of the RphG enzymes. However, RphG3 appears to be missing the N-terminal Rieske domain (Figure 5.27).

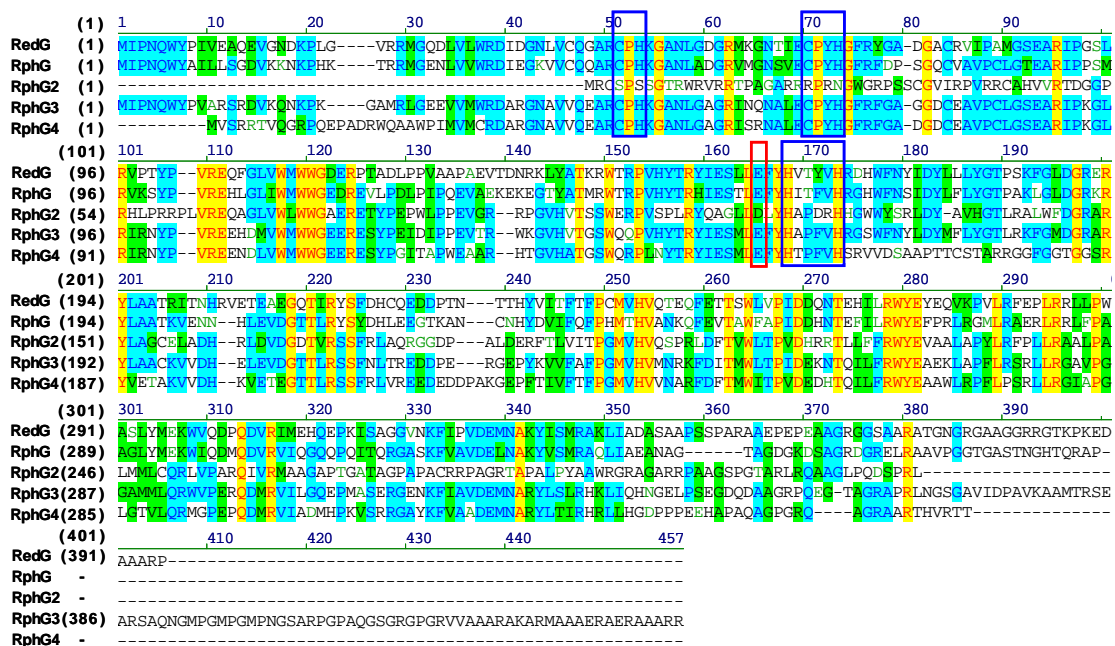


Figure 5.27 Sequence alignment of the RedG, RphG, RphG2, RphG3 and RphG4. Conserved residues within RedG, RphG, RphG2, RphG3 and RphG4 that ligate the [2Fe-2S] cluster (missing in the RphG3) and Fe(II) atom in NDO are highlighted in blue, an Asp residue of NDO (mutated to Glu in RedG, RphG, RphG2 and RphG4) proposed to mediate electron transfer between the [2Fe-2S] cluster and the Fe(II) atom is highlighted in red. Black letters, no background – non-similar amino acids; black letters, green background – block of similar amino acids; red letters, yellow background – identical amino acids; dark blue letters, torques background – conservative amino acids; dark green letters, no background – weakly similar amino acids.

5.3.1 Expression of Four *redG* Orthologues from *Streptomyces griseoviridis* in *Streptomyces coelicolor* W31

The objective was to express each *S. griseoviridis rphG* gene separately in *S. coelicolor* W31 to investigate the function of the four *redG* orthologues. Genomic DNA of *S. griseoviridis* was not available, but a partial sequence of the *rph* gene cluster was deposited in the GenBank database (accession nr AB469822), including the sequences of the four *rphG* genes. Thus the genes were commercially synthesised (Epoch Biolabs, USA). Genes were received in four separate constructs, each containing one of the gene in pBSK, a basic ampicillin resistance plasmid.

Each of the *rphG* genes was amplified and cloned into pOSV556. The forward PCR primers used contained a 5'-*Hind*III restriction site, followed by an artificial RBS, six random nucleotides and the ATG start codon of the gene along with 13 downstream nucleotides. Reverse primers all contained a 5'-*Xho*I restriction site and the last 16 nucleotides of each gene, including the stop codon. When a correct clone for each construct was identified and confirmed, it was introduced via conjugation from *E. coli* ET12567/pUZ8002 into *S. coelicolor* W31. A hygromycin resistant exconjugant in each case was picked and grown on R5 agar medium. After 5 days of growth, acidified organic extracts of the mycelia were analysed by HPLC to determine if any cyclic derivative(s) of undecylprodiginine (**2**) were generated (Figure 5.28).

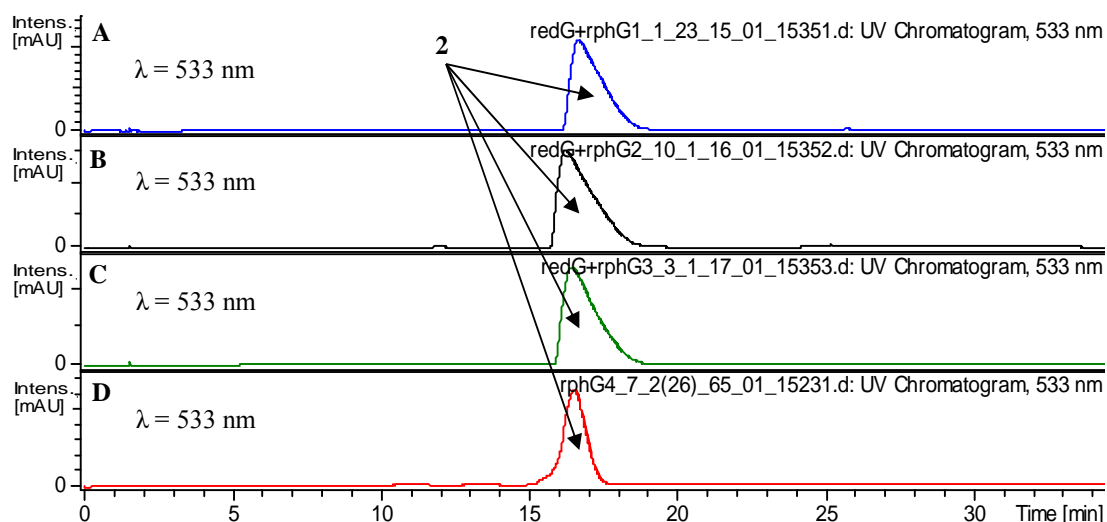


Figure 5.28 HPLC analyses monitoring absorbance at 533 nm of acidified organic extracts of A – W31/pOSV556*rphG1* (blue line), B – W31/pOSV556*rphG2* (black line), C – W31/pOSV556*rphG3* (green line), D – W31/pOSV556*rphG4* (red line).

In each case, only a peak with a retention time of ~16.5 minutes corresponding to **2** was detected. Absorbance at 533 nm (Figure 5.28) and EICs (data not shown) for masses for potential cyclic compounds corresponding to prodigiosin R1 or roseophilin

derivatives were also checked but no new peak was observed. There are several possible explanations for these negative results. Perhaps one or more of the RphG enzymes requires its RedH homologue RphH to function correctly or the RphGs cannot interact with the *S. coelicolor* ferredoxins and thus cannot be reduced to be functional. Perhaps the RphG enzymes have high substrate specificity and cannot recognise the undecyl chain in undecylprodiginine (the corresponding alkyl chain in the putative roseophilin (prodigiosin R) precursor is dodecyl with a methyl substituent at C-11').

5.4 Conclusions

The *S. coelicolor* M511/*redG::scar* mutant, W31, created by Olanipekun Odulate showed that production of **3** but not **2** was abrogated in the mutant (Odulate, 2005). When the $\Delta redG$ mutation was complemented *in trans* production of **3** was restored to the wild type level. These data demonstrate that RedG plays a crucial role in the formation of the C-C bond between C-4 on ring C and C-7' of **2** in *S. coelicolor*.

Heterologous expression of *redHG* in *S. venezuelae* and feeding with synthetic 2-UP and MBC showed that streptorubin B was produced in addition to undecylprodiginine by this strain. This observation shows that RedG is the only enzyme required, in addition to RedH, for the assembly of streptorubin B from MBC and 2-UP.

S. venezuelae/pOSV556redG and *S. venezuelae/pOSV556redHG* fed with undecylprodiginine (**2**) produces streptorubin B. A higher level of **3** was accumulated when *redG* and *redH* were co-expressed together. These results suggest that the RedG substrate is **2** and that RedG and RedH might form a catalytically important complex.

LC-MS analysis of M511/*redI::oriT-apr* gave further evidence for the nature of the RedG substrate. The *redI* gene encodes for a methyl transferase and a mutant lacking this gene only produces desmethylundecylprodiginine ($m/z = 380$). No desmethylstreptorubin B could be detected in the mutant suggesting that oxidative cyclisation takes place after condensation of MBC and 2-UP.

Based on these results, we propose that RedG catalyses an oxidative cyclisation reaction of undecylprodiginine to form the 10-membered carbocycle of streptorubin B. To investigate if the RedG orthologue McpG from *S. longispororuber* catalyses an analogous reaction to form the 12-membered carbocycle of metacycloprodigosin, an *S. longispororuber* genomic library was created and gene encoding McpG was identified. The *mcpG* expression in the *S. coelicolor redG* mutant resulted in production of metacycloprodigosin (**16**) instead of streptorubin B (**3**). All of these results suggest that RedG and McpG encode members of a family of Rieske non-heme iron-dependent oxygenase-like enzymes involved in regiodivergent oxidative cyclisation reactions that form new C-C bonds between C-4 of ring C and C-7' or C-9' of the hydrocarbon chain in **2** to yield the cyclic prodiginines **3** and **16**, respectively.

The *rphG1*, *rphG2*, *rphG3*, *rphG4* (all *redG* orthologues) genes from the *S. griseoviridis rph* gene cluster are believed to direct roseophilin and prodigosin R1 biosynthesis. Their separate expression in the *S. coelicolor* W31 mutant did not reveal production of any cyclic undecylprodiginine derivatives. Given that several *redG* orthologues are encoded in *S. griseoviridis*, maybe two or more of these genes have to be co-expressed in the W31 mutant or maybe the genes have to be expressed with *rphH* (*redH* orthologue) to result in production of cyclic undecylprodiginine derivatives.

Another possibility is that RphGs cannot recognise the undecylchain in **2** having high substrate specificity to roseophilin/prodigiosin R precursor.

Members of this new family of Rieske-oxygenase-like enzymes have been used in the chemoenzymatic synthesis of analogues of streptorubin B (by Stuart Haynes in the Challis group). They could also be used to produce analogues of metacycloprodiginosin and other carbocyclic prodiginines. These carbocyclic prodiginines are very difficult to access by conventional synthetic methods. In future, other genetic manipulations could also be carried out to generate more analogues of cyclic prodiginines.

6. Genetic Engineering of *Streptomyces coelicolor* to Create Prodiginine Analogues

6.1 Undecylprodiginine and Streptorubin B Halogenated Analogues

Streptomyces griseoflavus produces hormaomycin (**31**), which contains a 5-chloropyrrole-2-carboxamide moiety (Figure 6.1). The *hrmQ* gene of *S. griseoflavus* which encodes a protein with sequence similarity to FADH₂-dependent halogenases was proposed to catalyse the chlorination of the pyrrole in hormaomycin biosynthesis (Heide et al., 2008).

Streptomyces roseochromogenes produces clorobiocin (**32**), which contains a 5-methylpyrrole-2-carboxyl moiety, that is linked by an ester bond to the deoxysugar (Westrich et al., 2003). Heterologous expression of *hrmQ* in a *S. roseochromogenes* *clon6* mutant (which accumulates a clorobiocin derivative, that is not methylated at position 5 of the pyrrole-2-carboxyl moiety), led to the formation of new chlorinated clorobiocin analogues – novclorobiocin 124 (**33**) and 125 (**34**), in which the pyrrole-2-carboxyl moiety was chlorinated to give a 5-chloropyrrole-2-carboxyl moiety (Heide et al., 2008).

The pyrrole-2-carboxylic acid moiety of **32** is biosynthesised from L-proline and the 5-methyl group is subsequently added (Figure 6.1) (Westrich et al., 2003). The pyrrole A ring of MBC is also derived from L-proline via a pyrrole-2-carboxyl-PCP intermediate (section 1.3.4). It was therefore interesting to investigate if any halogenated analogues of undecylprodiginine and streptorubin B could be produced by *S. coelicolor* M511 strains in which *hrmQ* is expressed. We hypothesised that HrmQ could halogenate the pyrrolyl-2-carboxyl-PCP intermediate in MBC biosynthesis.

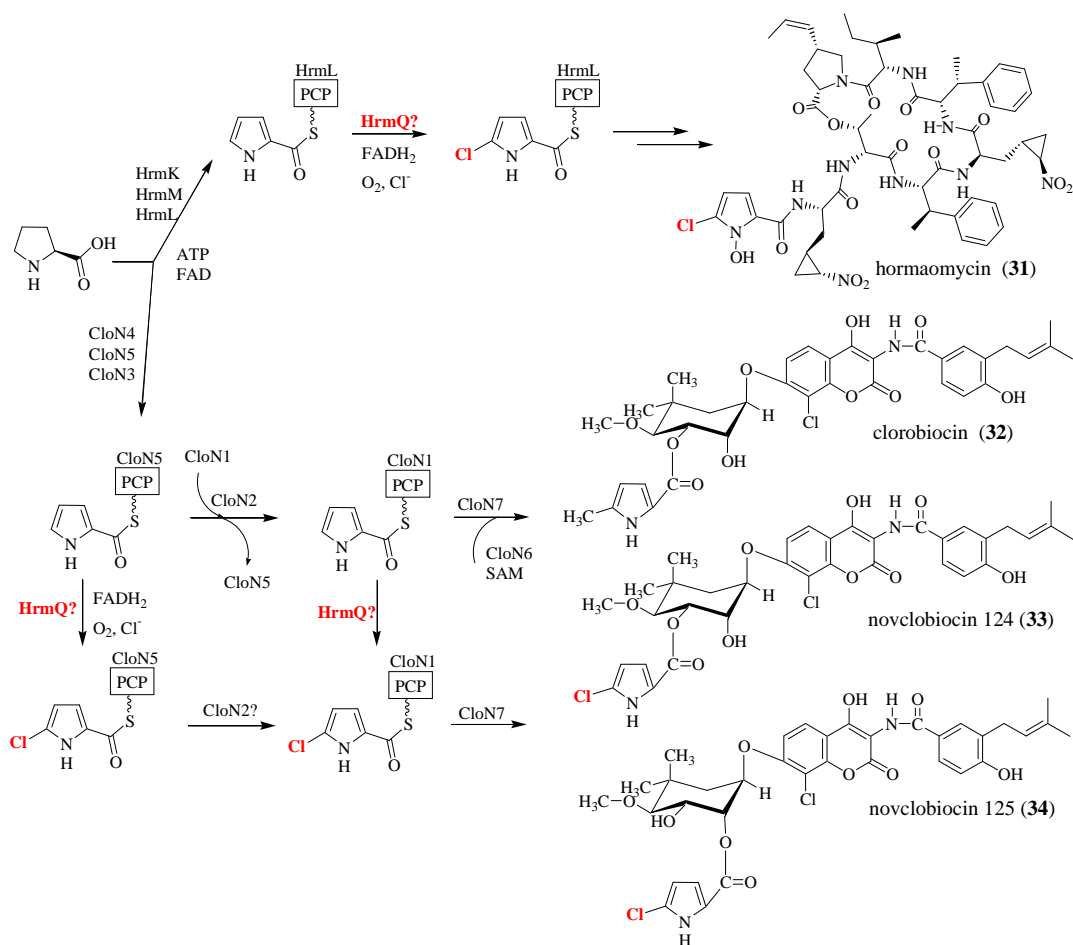


Figure 6.1 Hypothetical pyrrole-2-carboxyl thioester-5-halogenation reactions in the biosynthesis of hormaomycin (31) (*S. griseoflavus*) and in the formation of the new clorobiocin (32) derivatives novclorobiocin 124 (33) and novclorobiocin 125 (34) (*S. roseochromogenes*). HrmK, CloN4 – prolyl-AMP ligases; HrmL, CloN5, CloN1 – acyl carrier proteins; HrmM, CloN3 – flavin-dependent dehydrogenases; CloN2, CloN7 – acyltransferases; HrmQ – halogenase.

Plasmid pLW42 containing *hrmQ* (Heide et al., 2008) was kindly provided by Prof. Dr Lutz Heide, University of Tübingen. The *hrmQ* gene was amplified by PCR and cloned into pOSV556, using primers designed as in section 5.3.1. A verified clone was introduced by conjugation into *S. coelicolor* M511. After selection of transformants using hygromycin, the engineered strain was plated on R5 agar medium and after 5 days of growth, an acidified organic extract of the mycelia was prepared and analysed. LC-

MS analyses showed that, in the positive mode, two chlorinated prodiginine analogues with $m/z = 428$ (probably chlorinated undecylprodiginine) (**35**) and $m/z = 426$ (probably chlorinated streptorubin B) (**36**) were produced at low levels (<2% of unchlorinated prodiginines) (Figure 6.2 A and B).

Both new compounds showed a characteristic isotope ratio for chlorinated molecules that result from the relatively high natural abundance (24.23%) of the heavy ^{37}Cl isotope together with the dominant (76.67%) ^{35}Cl isotope (Figure 6.2 D). High resolution mass spectrometry confirmed that the molecular formula for these compounds were: $\text{C}_{25}\text{H}_{34}\text{ClN}_3\text{O}$ (calculated for $\text{C}_{25}\text{H}_{35}\text{ClN}_3\text{O}^+$: 428.2463, found: 428.2471) for chlorinated undecylprodiginine and $\text{C}_{25}\text{H}_{32}\text{ClN}_3\text{O}$ (calculated for $\text{C}_{25}\text{H}_{33}\text{ClN}_3\text{O}^+$: 426.2307, found: 426.2314) for chlorinated streptorubin B. LC-ESI-MS/MS analyses carried out by Lijiang Song (Mass Spectrometry Service, University of Warwick) indicated that the chlorine atom was incorporated into the A pyrrole ring of these new prodiginines (Figure 6.3). However the very low level of chlorinated prodiginine analogues produced did not make possible the purification of enough compounds by HPLC for NMR analyses.

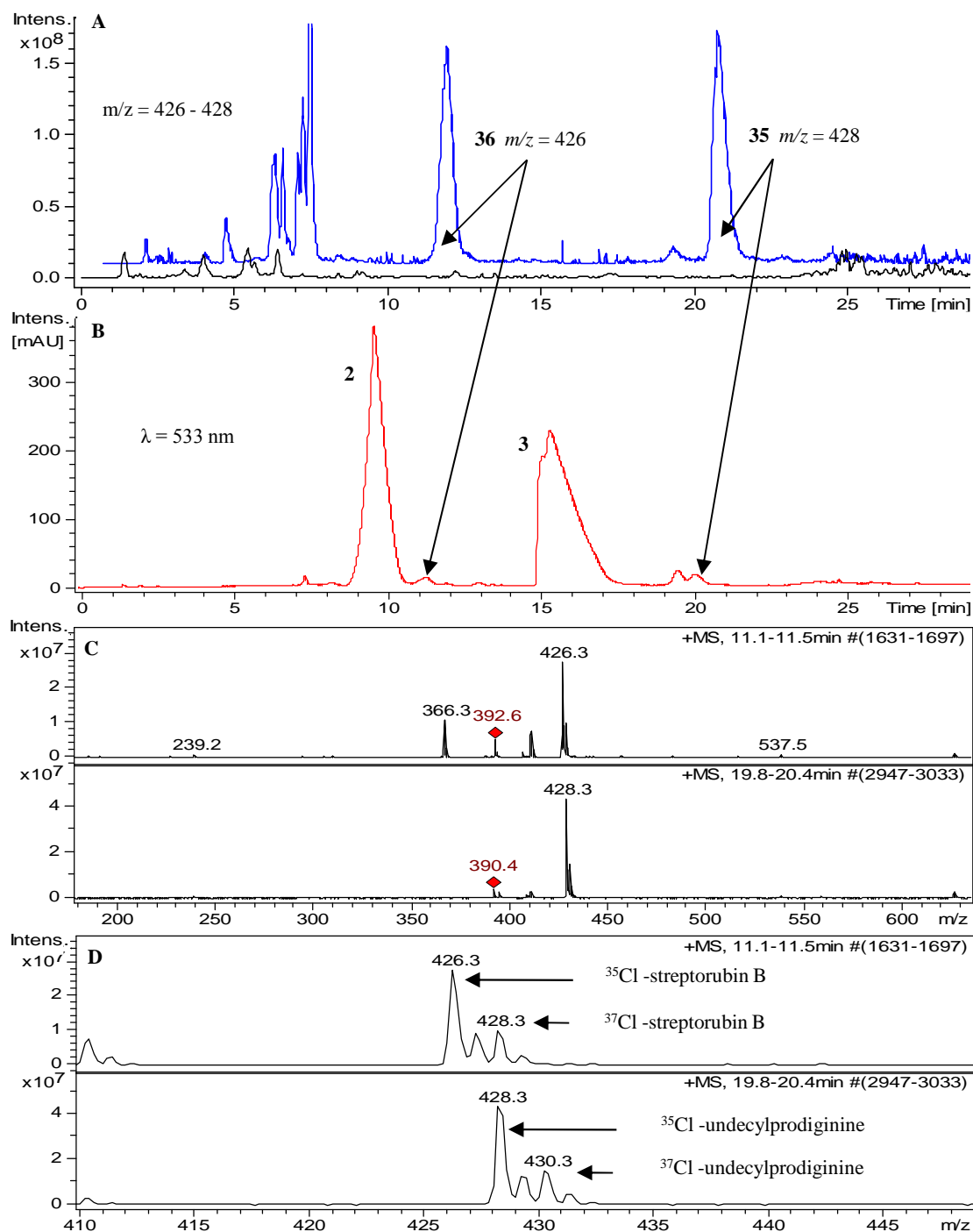


Figure 6.2 A – EICs ($m/z = 426-428$) from LC-MS analyses of acidified organic extracts of M511 (black line) and M511/pOSV556hrmQ (blue line), B – LC-MS analysis monitoring absorbance at 533 nm of acidified organic extracts of M511/pOSV556hrmQ, C – MS spectrum of the $m/z = 426$ and $m/z = 428$ ions, D – zoom of MS spectra of $m/z = 426$ and $m/z = 428$ ions showing a characteristic isotopic ratio for chlorinated compounds.

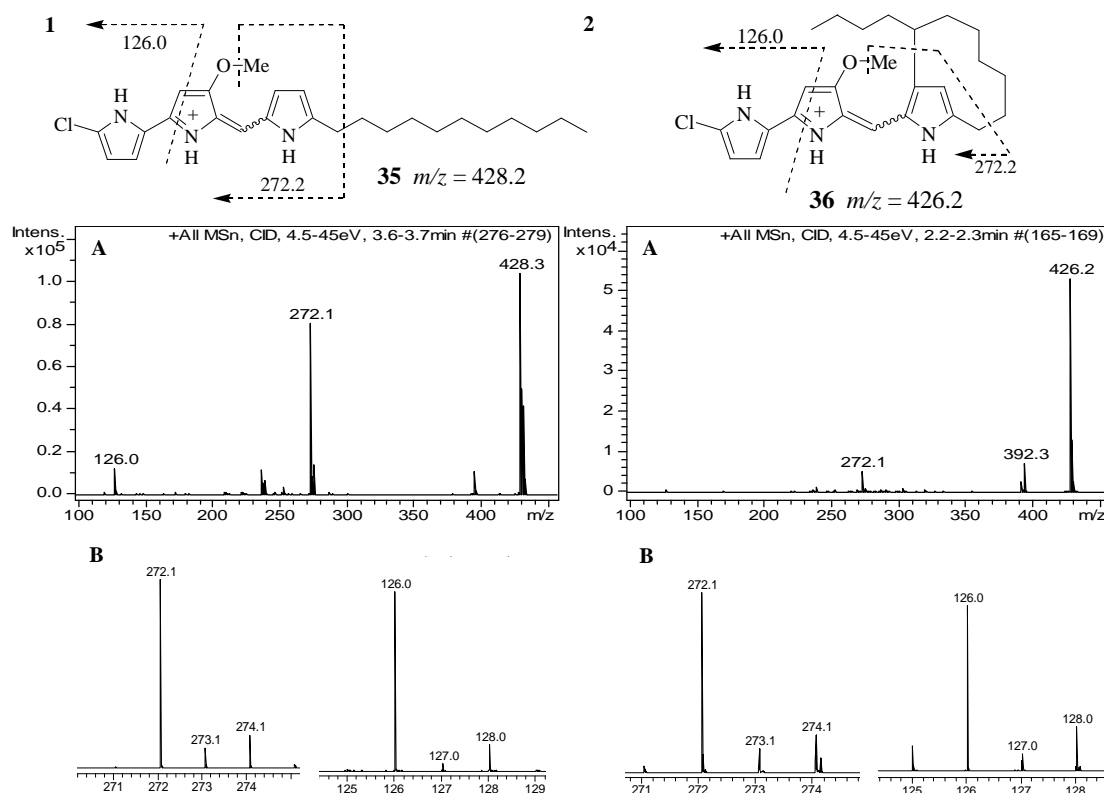


Figure 6.3 LC-MS/MS spectra for 1 A – chlorinated undecylprodiginine (**35**) ($m/z = 428$) and 2 A – chlorinated streptorubin B (**36**) in positive ion mode. The proposed origins of the observed fragment ions are shown above the spectra. 1 B, 2 B – zoomed fragment ions with characteristic isotope ratio for chlorinated molecules indicating that the chlorine atom was incorporated into the A pyrrole ring.

No experimental data has determined at which stage halogenation of the pyrrole moiety catalysed by HrmQ takes place in the hormaomycin biosynthesis pathway. However, it was proposed that HrmQ could use pyrrole-2-carboxyl-HrmL thioester as a substrate based on investigations of the halogenation reactions during pyoluteorin biosynthesis in *Pseudomonas fluorescens* (Figure 6.1) (Dorrestein et al., 2005). We therefore proposed that in the *S. coelicolor* strain where *hrmQ* is expressed, pyrrole-2-carboxyl-RedO could be the substrate for chlorination. However, it is possible that any of the subsequent intermediates in the biosynthesis of undecylprodiginine and strepto-

rubin B (e.g. MBC) could be the substrate for HrmQ (Figure 6.4). No experimental data is currently available that allows discrimination between the different possibilities.

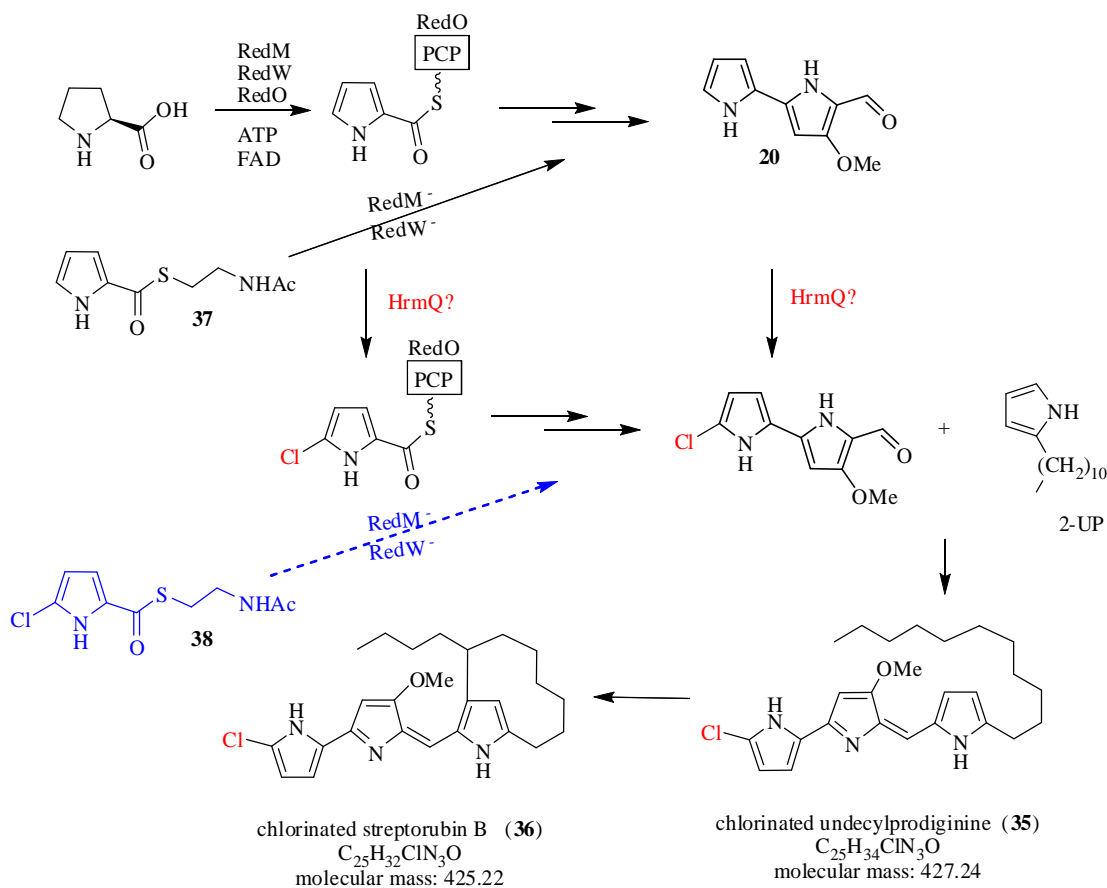


Figure 6.4 Hypothetical pyrrole halogenation reactions in the biosynthesis of *S. coelicolor* prodiginines (black scheme); future experiment to investigate when chlorination is taking place is shown in blue. RedM – prolyl-PCP synthase, RedO – peptidyl carrier protein (PCP), RedW – prolyl-PCP-oxidase/ desaturase.

The *redM* and *redW* genes were shown to be involved in MBC (**20**) biosynthesis. The M511/*redM::oriT-apr* and M511/*redW::oriT-apr* both accumulated 2-UP (**21**) and no **20** could be detected. Feeding of synthetic **20** to the mutants restored prodiginine production. To further elucidate MBC pathway, NAC thioester (**37**), analogue of pyrrole-2-carboxyl-RedO was synthesised. Feeding of **37** to the M511/*redM::oriT-apr* or to

the M511/*redW::oriT-apr* restored prodiginine production suggesting that **37** can effectively mimic pyrrole-2-carboxyl-RedO *in vivo* .

Future work to investigate chlorinated prodiginine analogues could involve feeding of synthetic chlorinated NAC thioester (**38**) to *S. coelicolor* M511/*redM::oriT-apr* or M511/*redW::oriT-apr* (neither of which produces any prodiginines) to examine whether it can be incorporated into chlorinated prodiginines (Figure 6.4, blue scheme). This experiment will show that **38** can be incorporated as an analogue of the pyrrole-2-carboxyl-PCP intermediate. This can also suggest at which stage HrmQ catalyses chlorination of the pyrrole moiety. Only chlorinated prodiginines should be produced in this experiment. This would be useful because it would make purification of the chlorinated prodiginine analogues by HPLC much easier and would facilitate full characterisation of them by NMR spectroscopy.

6.2 Construction of a *Streptomyces coelicolor* Mutant Abolished in Production of Both 2-undecylpyrrole and MBC

A double mutant, with abolished production of MBC (**20**) and 2-UP (**21**) could be useful for investigating production of new prodiginine analogues by mutasynthesis. Feeding the mutant with analogues of **20** and **21** could yield undecylprodiginine and streptorubin B analogues.

A double mutant *S. coelicolor* M511/*redN::scar+redL::oriT-apr* (W119), which should not produce 2-UP or MBC was therefore constructed. RedL is a Type I PKS involved in the biosynthesis of **20** (Mo et al., 2008) and RedN is an α -oxoamine synthase with 2 N-terminal ACP domains required for the biosynthesis of **21** (Stanley et al.,

2006). In the independent mutants: *S. coelicolor* M511/*redL::oriT-apr* and *S. coelicolor* M511/*redN::scar*, prodiginine production was abolished but could be restored by feeding the strains with **20** and **21**, respectively (Stanley et al., 2006; Mo et al., 2008).

The *S. coelicolor* M511/*redN::scar* strain (M595) (kindly provided by Prof. Mervyn Bibb, John Innes Centre) was used to generate the W119 double mutant by replacing *redL* in it with the apramycin resistance cassette. After conjugal transfer of the *Sc3F7/redL::oriT-apr* (prepared by A. Stanley) from *E. coli* ET12567/pUZ8002 to *S. coelicolor* M595, one double crossover mutant was identified and characterised. This mutant was then grown on R5 agar medium and analysed by LC-MS described as previously.

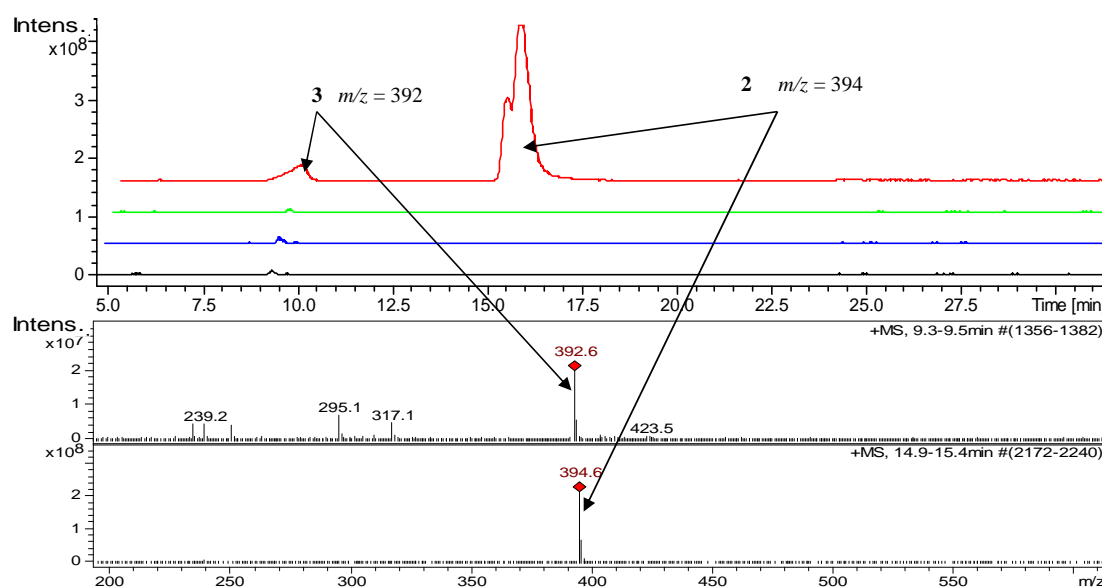


Figure 6.5 EICs ($m/z = 392-394$) from LC-MS analyses of acidified organic extracts from *S. coelicolor* 119 (M511/*redN::scar+redL::oriT-apr*) (black line), W119 fed with synthetic 2-UP (blue line), W119 fed with synthetic MBC (green line) and W119 fed with synthetic 2-UP + MBC (red line).

Neither 2-UP with $m/z = 222$ or MBC with $m/z = 191$ were produced in the W119 mutant (data not shown), as expected. The mutant was fed with synthetic **20** and

21 separately, and with **20** and **21** together, to determine whether prodiginine production could be restored. Only when both **20** and **21** were added to W119 was visible prodiginine production restored. LC-MS/MS analyses confirmed these results (Figure 6.5).

Although the level of streptorubin B produced in W119 fed with 2-UP and MBC is not very high (~10 +/- 2% of undecylprodiginine), this mutant could be useful for the generation of streptorubin B analogues. After optimisation, e.g. by co-expression *redHG*, W119 could be fed with analogues of **20** and **21** (at the same time) to generate novel streptorubin B analogues.

6.3 Conclusions

Introducing the *hrmQ* gene encoding a putative FADH₂-dependent halogenase into the *S. coelicolor* M511 strain led to the production of chlorinated analogues of undecylprodiginine and streptorubin B in addition to natural products. The M511/*redN::scar+redL::oriT-apr* double mutant, with abolished production of MBC and 2-UP, but with still functional RedH and RedG enzymes (responsible for the condensation and carbocyclisation reactions) could also be used to generate new compounds by feeding the strain with both 2-UP and MBC analogues.

**7. Investigation of the Roles of Phosphopantetheinyl
Transferases in *Streptomyces coelicolor* Metabolite
Biosynthesis**

7.1 Phosphopantetheinyl Transferases

Phosphopantetheinyl transferases (PPTases) are required to catalyse the post-translational modification of carrier proteins involved in the biosynthesis of primary and secondary metabolites, such as fatty acids, polyketides and nonribosomal peptides. The inactive *apo* form of these carrier proteins is activated by the post-translational transfer of the 4'-phosphopantetheinyl moiety of coenzyme A to a conserved serine residue. The function of the active *holo* form is to covalently tether molecules in the growing fatty acid polyketide or polypeptide chain and pass them between the various enzyme active sites (Lambalot et al., 1996).

S. coelicolor produces numerous metabolites including prodiginine antibiotics, actinorhodins, methylenomycins, calcium-dependent antibiotics (CDAs), a grey spore pigment, the siderophore coelichelin and a broad range of fatty acids, all of which rely on carrier proteins for their biosynthesis. Three genes encoding putative PPTases were identified. In *Streptomyces coelicolor* A3(2) genome: SCO4747 (AcpS), SCO5883 (RedU) and SCO6673. The small number of PPTases in *S. coelicolor* compared to the number of carrier proteins can indicate that the PPTases are multifunctional and capable of activating a variety of carrier proteins. SCO4747 encodes an AcpS-type PPTase and several different biochemical experiments showed that this PPTase can catalyse phosphopantetheinylation of several different of *S. coelicolor* ACPs e.g. the fatty acid synthase ACP and the actinorhodin ACP (Cox et al., 2002). The *redU* gene is located within the *red* cluster and production of prodiginines was found to be abolished in a *redU* mutant (Stanley et al., 2006). However, actinorhodin and CDA are still produced by this mutant (Lu et al., 2008). SCO6673 encodes a protein with significant similarity

to the Svp PPTase from *Streptomyces verticillus* (58% identities aa, 68% similarities aa) (Sanchez et al., 2001) and to SePptII from *Saccharopolyspora erythraea* (56% identities aa, 67% similarities aa) (Weissman et al., 2004). It was reported that actinorhodin and prodiginines are still produced in a *sco6673* mutant of *S. coelicolor* but production of CDA is abolished (Lu et al., 2008).

In this study the production of all known secondary metabolites that require carrier proteins for their biosynthesis was investigated in a set of *S. coelicolor* mutants lacking one or more PPTases (M145/*redU::oriT-apr*, M145/*sco6673::oriT-apr*, M145/*redU::oriT-apr+sco6673::scar*). The inactivation of *sco4747* was also investigated. Although similar mutants were described by Lu et al. (2008) in a recent investigation of the role of *S. coelicolor* PPTase genes in antibiotic production, the study was limited to the investigation of actinorhodin, prodiginine and CDA production using absorbance measurements of organic cell extracts and bioassays. In the present study, the production of methylenomycins and coelichelin was investigated in the PPTase mutants, in addition to actinorhodins, prodiginines and CDA. The role of the different PPTases in prodiginine biosynthesis was also dissected and more sophisticated analytical methods for analysing the production of actinorhodin and related metabolites and prodiginines were employed. Moreover my mutants were all constructed and the analysis of them was underway, prior to the report of Lu *et al.* (Lu et al., 2008)

The publication of the results published by Lu et al. (2008) affected the order of priority of my objectives. As their mutant analysis was not very comprehensive, only three secondary metabolites (actinorhodin, prodiginine and CDA) were analysed, I have

focused on characterising the same mutants more accurately and more extensively. Production of actinorhodin and prodiginine was therefore analysed by LC-MS (they simply measured absorbance of organic extracts). Additionally I have investigated the production of methylenomycin and coelichelin in these mutants.

7.2 Construction of PPTase Mutants

A *redU::oriT-apr* mutant was created by Anna Stanley, a former PhD student in the Challis group, in two *S. coelicolor* strains: M145 (SCP1⁻, SCP2⁻) and M511 (an *actII-orfIV* mutant of the M145 strain) (Stanley et al., 2006). The M145/*redU::oriT-apr* mutant was further analysed in the present study.

Construction of *S. coelicolor* M145/*acpS::oriT-apr* and M511/*acpS::oriT-apr* mutants was attempted but not achieved by Anna Stanley. Only colonies with single crossover integration of the gene replacement construct into the chromosome (*apr*^R, *kan*^R) were obtained, indicating that the *acpS* gene cannot be replaced by a double crossover recombination event. This was explained by the hypothesis that AcpS is required for fatty acid biosynthesis and is thus essential for *S. coelicolor* growth (Stanley, 2007).

My study began by cloning the *acpS* gene into pOSV556 to examine whether an *S. coelicolor/acpS::oriT-apr* mutant could be obtained when an extra copy of *acpS* is expressed *in trans*. A forward primer containing a 5'-*Hind*III restriction site followed by the natural RBS and start codon of the *acpS* gene and a reverse primer with a 5'-*Xho*I restriction site and nucleotides identical to the nucleotides ~50 nucleotides downstream of *acpS* stop codon, were designed. The pOSV556/*acpS* construct was assembled by

standard PCR, restriction digestion and cloning procedures and was introduced by conjugation from *E. coli* ET12567/pUZ8002 into *S. coelicolor* M511 and M145 strains into which the cosmid Sc1G7/*acpS::oriT-apr* had been previously introduced by single crossover recombination. A single *apr*^R, *kan*^R and *hyg*^R exconjugant of each strain was selected and grown on SFM agar without antibiotic selection through several generations. Then spores were spread onto SFM agar to get single colonies and replica plating was carried out to identify *apr*^R, *hyg*^R, *kan*^S clones. Selected *apr*^R, *hyg*^R, *kan*^S colonies were checked by PCR to confirm that double crossover recombination had occurred to replace the *acpS* gene with the *oriT-apr* cassette. Such mutants were found (Figure 7.2 A), indicating that the wild type *acpS* gene can only be deleted if a second copy of the gene is present *in trans*. This suggests that AcpS is essential for *S. coelicolor* growth, as hypothesised.

The M145/*sco6673::oriT-apr* was then created using the PCR-targeting strategy (section 3.1)(Gust et al., 2002). After replacing *sco6673* with the *oriT-apr* cassette, a “scar” mutant needed to be constructed to facilitate the construction of the double *sco6673 redU* mutant (M145/*sco6673::scar+redU::oriT-apr*). First, the 5A7/*sco6673::scar* cosmid was constructed according to the PCR-targeting protocol (Gust et al., 2002). The *oriT* was then reintroduced together with a tetracycline resistance gene into the non-coding region of the cosmid backbone. The 5A7/*sco6673::scar+oriT-tet* cosmid was introduced into *S. coelicolor* M145/*sco6673::oriT-apr* by conjugation from *E. coli* ET12567/pUZ8002 and exconjugants were screened for the expected combination of antibiotic resistances and sensitivities to identify mutants that had undergone gene replacement by double ho-

mologous recombination. The *sco6673* deletion in potential mutants was confirmed by PCR.

The *S. coelicolor* M145/*sco6673::scar+redU::oriT-apr* mutant was constructed as described previously using PCR-targeting (Gust et al., 2002). Thus the *redU* gene was replaced with the *oriT-apr* cassette and introduced into the M145/*sco6673::scar* mutant. A *sco6673 redU* mutant was identified and analysed by PCR and Southern blot hybridisation (Figure 7.2 B).

Genetic complementation of M145/*sco6673::oriT-apr* and M145/*redU::oriT-apr* mutants by expression of the deleted genes *in trans* from pOSV556 was carried out. A 5'-*HindIII* restriction site was incorporated into the forward primers for *sco6673* and *redU* amplification. The natural RBS of *sco6673* and a synthetic RBS for *redU* were also incorporated into the forward primers, together with the start codons of the genes and several downstream nucleotides. The reverse primers contained 5'-*XhoI* restriction sites, and several nucleotides of sequence downstream of the stop codon of each gene. The expression constructs were assembled by standard cloning procedures and introduced into the mutants by intergenic conjugation. The resulting M145/*sco6673::oriT-apr*+pOSV556*sco6673* and M145/*redU::oriT-apr*+pOSV556*redU* strains were analysed by PCR to confirm they had the desired genotype (Figure 7.2 B).

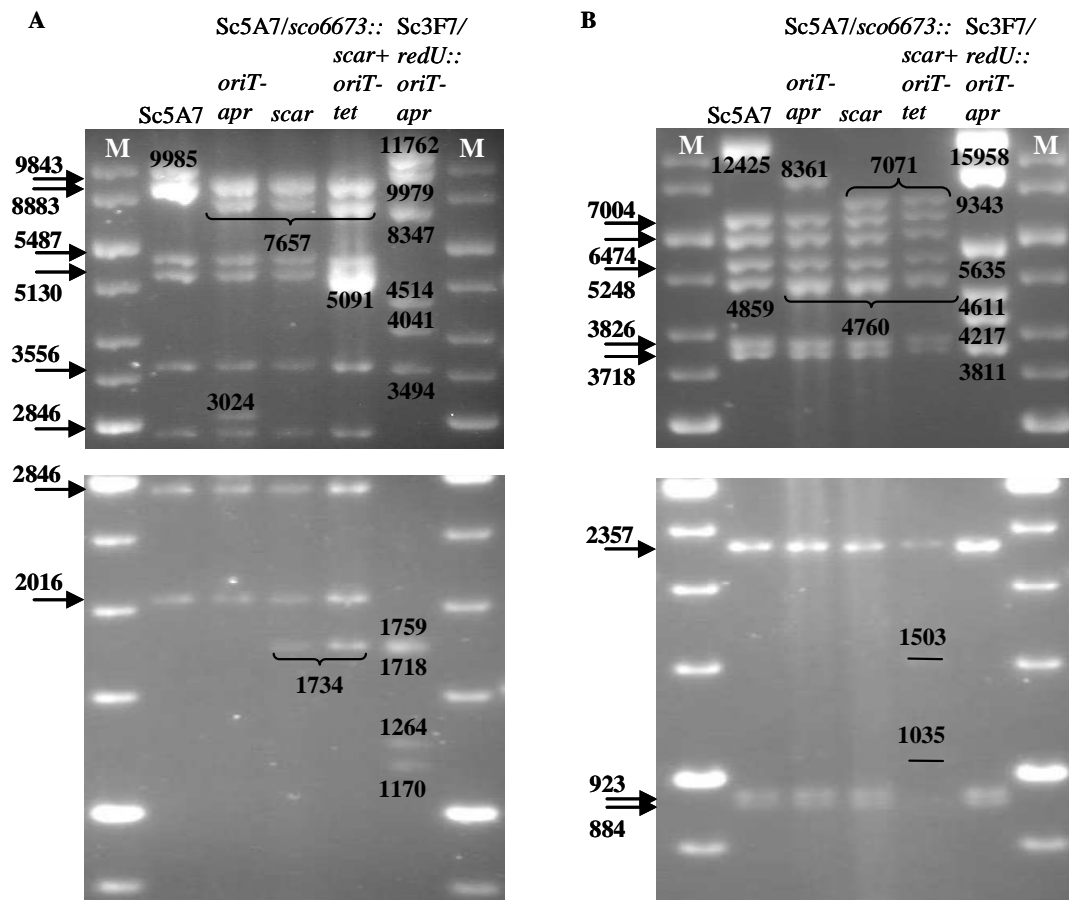


Figure 7.1 Agarose gel electrophoresis analysis of restriction enzyme digests of genetically-engineered cosmid used to disrupt the *S. coelicolor* PPTase genes. A – digestion with *Bam*HI; B – digestion with *Pst*I. Top gels show high molecular weight bands, bottom gels show low molecular weight bands. Numbers indicated by arrows show the digestion pattern of Sc5A7 cosmid. Numbers written on the gel shows additional bands characteristic for genetically-engineered Sc5A7 cosmid. Digestion pattern of Sc3F7/*redU::oriT-apr* is written on the gels.

All of the cosmid generated during the construction of these mutants were digested with *Bam*HI and *Pst*I restriction enzymes and the digest were analysed by agarose gel electrophoresis (Figure 7.1 A, B). The genomic DNA of the *S. coelicolor* mutants was analysed by PCR to confirm the mutations were as expected (Figure 7.2 B). Additionally, the genotype of the M145/*sco6673::scar+redU::oriT-apr* double mutant

was confirmed by Southern blot hybridisation to ensure that no unexpected rearrangements of the genome at the *red* locus had occurred (Figure 7.2 C).

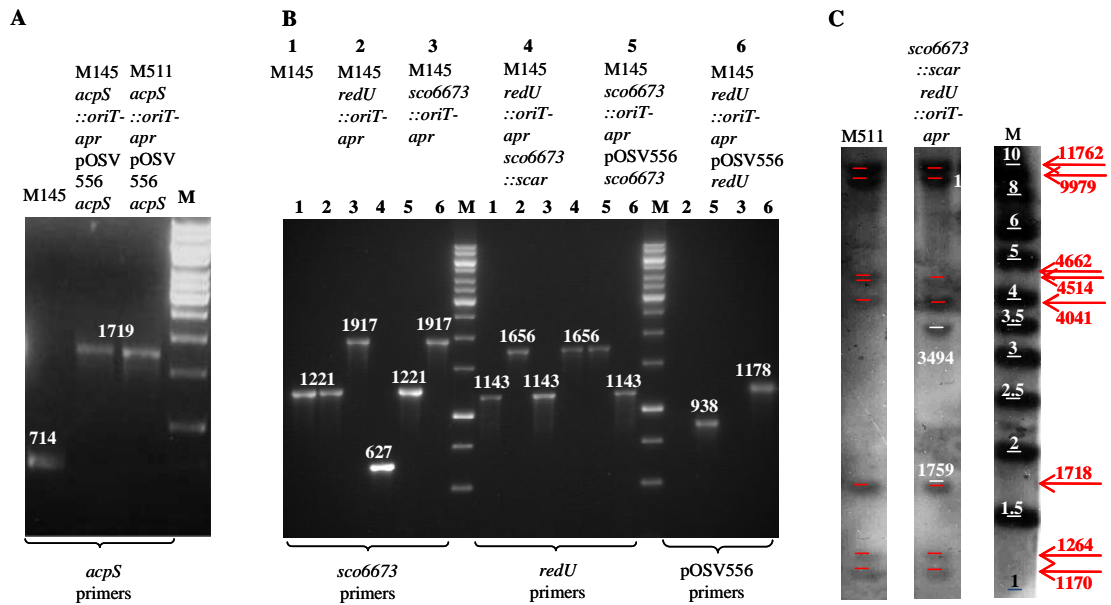


Figure 7.2 A – PCR analyses of genomic DNA extracted from M145, M145/*acpS*::*oriT-apr*+pOSV556*acpS* and M511/*acpS*::*oriT-apr*+pOSV556*acpS*, B – PCR analyses of genomic DNA extracted from *S. coelicolor* M145 and *S. coelicolor* PPTase mutants. A, B – PCR reactions were carried out with test primers priming ~100 bp outside the disrupted regions. Size differences between PCR products are caused by size differences between wild type DNA and *oriT-apr* or “scar” sequence introduced in its place. C – Southern blot analysis of *redU*::*oriT-apr* mutant in the M145/*sco6673*::*scar* background. Bands in red are the same as in M511 (for *redU* mutant band 4662 bp is missing), white bands are characteristic for the *redU* mutant (3494 bp and 1759 bp). M – molecular size markers.

7.3 Investigation of the Role of PPTases in Secondary Metabolite

Biosynthesis in *Streptomyces coelicolor* A3(2)

7.3.1 Prodiginine Production

In the prodiginine biosynthetic pathway, there are six ACP and PCP domains involved in the biosynthesis of MBC (one PCP within RedO and two ACPs within RedN) and 2-UP (one ACP within RedQ and two ACPs within RedL) (Figure 7.3). The *red* cluster contains one PPTase-encoding gene *redU* (Cerdeño et al., 2001).

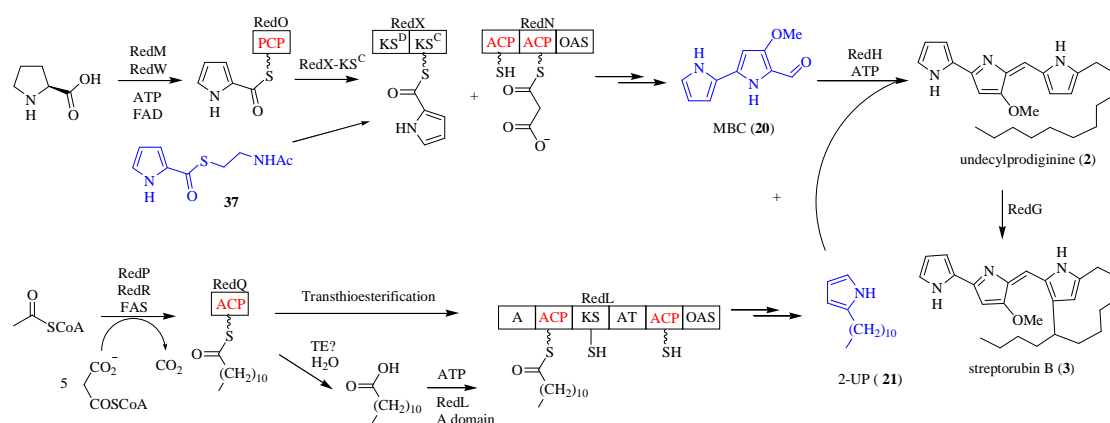


Figure 7.3 Prodiginine biosynthetic pathway with ACP and PCP domains (highlighted in red). Intermediates or analogues of intermediates fed to double mutant are in blue.

LC-MS analysis of an acidified organic extract of the *redU* mutant showed that it is deficient in MBC (**20**) production but not 2-UP (**21**) production. Feeding **20** to the *redU* mutant restored prodiginine production giving evidence that RedU is required for MBC biosynthesis. However, RedU is therefore not required for phosphopantetheinylation of all carrier proteins encoded by the *red* cluster, contrary to expectations. Feeding of the synthetic pyrrole-2-carboxyl-NAC thioester (**37**) also restored prodiginine pro-

duction and showed that RedU is only essential for phosphopantetheinylation of the PCP RedO (Stanley et al., 2006).

In the genetically complemented *redU* mutant (M145/*redU::oriT-apr+pOSV556redU*), where *redU* was introduced into the ØC31 *att* site under the control of the constitutive *ermE** promoter, prodiginine production was restored to wild type level (Figure 7.4 A, B, C). These results confirmed that the *redU* mutant has the intended genotype and that the extra copy of *redU* introduced was fully functional.

LC-MS analysis of acidified organic extract of the *sco6673* mutant indicated that prodiginines were still produced; although at a lower level (~40 +/- 5% of wild type) (Figure 7.4 D). LC-MS analysis of the genetically complemented mutant (M145/*sco6673::oriT-apr+pOSV556sco6673*) indicated that prodiginine production was not restored to wild type levels (Figure 7.4 E).

LC-MS analysis of the *sco6673 redU* double mutant showed that it is not producing any prodiginines (Figure 7.5 C). This is consistent with the previous observation that RedU is required for prodiginine biosynthesis.

Although the genotype of the *sco6673* mutant appeared to be as intended, the level of prodiginine production appear to be lower than in the similar PPTase mutant constructed by Lu et al. (2008). They found, that the *sco6673* mutant overproduced prodiginines (producing four times more than M145) on rich solid medium (R2YE) and the levels of prodiginines produced in the genetically complemented mutant were similar to the parent strain. However, in liquid minimal medium, prodiginine production in their mutant was reduced to ~40% comparing with wild type strain and no data was shown for the complemented mutant (Lu et al., 2008). In our study, prodiginine produc-

tion by the *sco6673* mutant and the genetically complemented *sco6673* mutant on rich R5 medium was similar to their observation on minimal medium (being reduced to ~40% +/- 5% comparing with wild type strain). We also never observed that our mutants could produce more prodiginines than the M145 parent strain despite using various media including R2YE (data not shown). The origins of these differences remain unclear, but they could suggest that growth conditions have a big influence on antibiotic production in *S. coelicolor*.

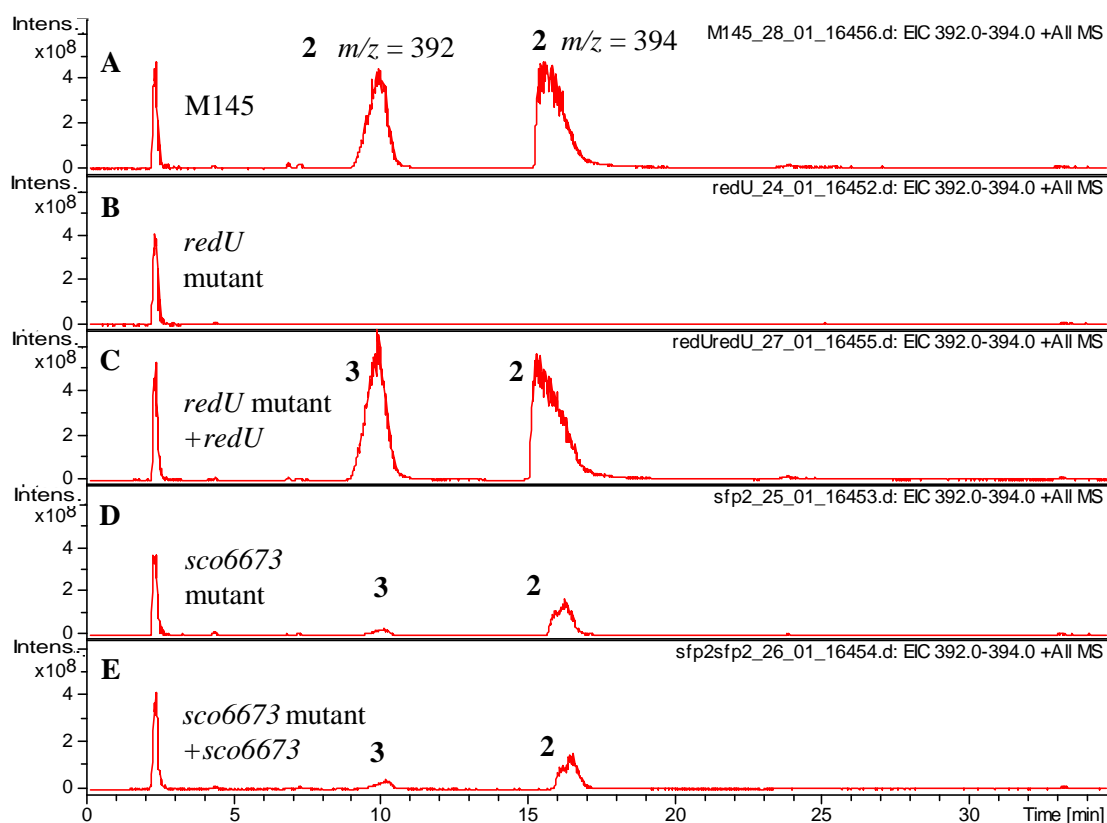


Figure 7.4 EICs ($m/z = 392-394$) from LC-MS analyses of acidified organic extracts of: A – *S. coelicolor* M145 (wild type), B – *redU* mutant, C – *redU* mutant complemented with *redU*, D – *sco6673* mutant, E – *sco6673* mutant complemented with *sco6673*.

RedU was shown to be essential for phosphopantetheinylation of the RedO PCP and it was shown that prodiginine production could be restored in the *redU* mutant by feeding synthetic pyrrole-2-carboxyl-NAC thioester (**37**), which mimics pyrrole-2-carboxyl-RedO (Figure 7.5 A, B) (Stanley et al., 2006). Based on these results, the next question was: is SCO6673 required for phosphopantetheinylation of the other carrier proteins of the *red* cluster?

The *sco6673 redU* mutant was fed with different intermediates, and prodiginine production was analysed by LC-MS, to address this question. The double mutant was first fed with both synthetic 2-UP (**21**) and MBC (**20**). This restored prodiginine production, proving that further feeding experiments were likely to be successful and that RedH and RedG are functional in the mutant (Figure 7.5, F). When the mutant was fed with pyrrole-2-carboxyl NAC thioester (**37**) no prodiginines were produced (Figure 7.5 D), suggesting that SCO6673 is required for phosphopantetheinylation of at least some of the five remaining carrier proteins. Feeding the double mutant with **37** and 2-UP (**21**) restored production of the prodiginines (Figure 7.5 E) indicating that SCO6673 is required to activate at least one of the ACP domains within RedQ or RedL, and that the two ACP domains of RedN can be activated by AcpS (Figure 7.3).

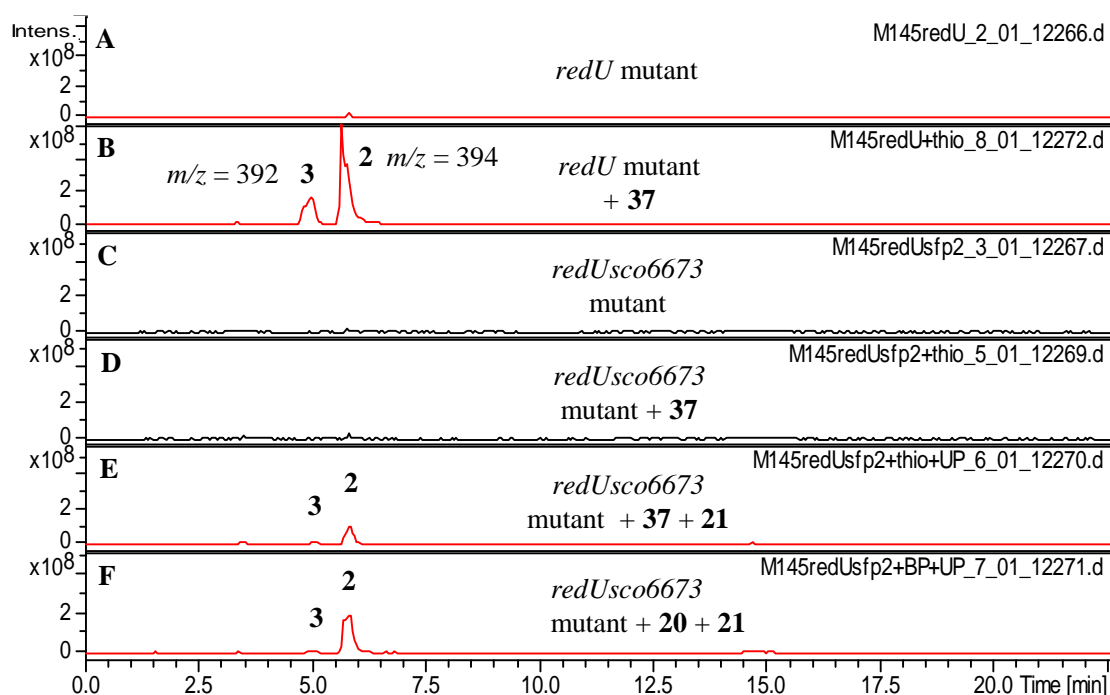


Figure 7.5 EICs (m/z 392-394) from LC-MS analyses of acidified organic extracts of *S. coelicolor*: A – *redU* mutant, B – *redU* mutant fed with pyrrole-2-carboxyl NAC thioester (37), C – *sco6673 redU* mutant, D – *sco6673 redU* mutant fed with 37, E – *sco6673 redU* mutant fed with 37 and 2-UP (21), F – *sco6673 redU* mutant fed with MBC (21) and 2-UP (20).

The above investigation of roles of *S. coelicolor* PPTases in prodiginine biosynthesis indicates how multifunctional they can be. Even if one PPTase (RedU) is encoded by the *red* cluster, it is only required for phosphopantetheinylation of one carrier protein (RedO) (although it may be capable of activating all six carrier proteins). The other five carrier proteins can be activated by SCO6673 (required for activation of at least one ACP involved in 2-UP biosynthesis, in the absence of RedU) and/or AcpS. Similarly in the *sco6673* mutant prodiginines are still produced, showing that when SCO6673 is absent, RedU and AcpS can activate all six carrier proteins encoded by the *red* cluster.

7.3.2 Actinorhodin Production

Actinorhodins are blue-pigmented antibiotics produced by *S. coelicolor* A3(2) (Figure 7.6) (Wright and Hopwood, 1976). The *act* gene cluster that directs actinorhodin biosynthesis contains twenty two genes, including three that encode a type II minimal PKS involving an ACP. This PKS is responsible for producing a linear octaketide, which is modified by a series of tailoring enzymes to generate actinorhodins (Fernandez-Moreno et al., 1992).

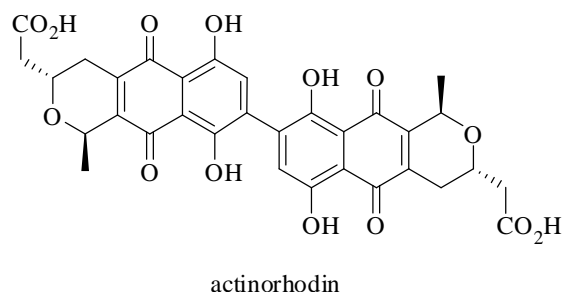


Figure 7.6 Structure of actinorhodin, one of the blue pigmented antibiotics produced by *S. coelicolor* A3(2).

Genetic manipulation of the *act* cluster has resulted in several novel “unnatural” polyketide natural products (probably mostly shunt metabolites derived from intermediates in actinorhodin biosynthesis) (McDaniel et al., 1994; Okamoto et al., 2009). Recently the same shunt metabolites and some new metabolites were identified as a product of the *act* cluster in wild type *S. coelicolor* (Song and Challis, unpublished results) (Figure 7.8).

All PPTase mutants were analysed for production of extractable blue-pigment (actinorhodin and congeners) and actinorhodin-related shunt metabolites. SMM liquid medium, inoculated with 10^9 spores, was grown for 7 days. Production of blue-pigmented actinorhodin and congeners was determined by adjusting pH of the super-

natant to pH 12 and measuring the absorbance at 640 nm. This value was converted into μg of ACT per mg of dry cell weight (DCW) using the known extinction coefficient of $25,320 \text{ M}^{-1}\text{cm}^{-1}$ for actinorhodin absorption at 640 nm (Bystrykh et al., 1996). Production of actinorhodins was not abolished in any of the PPTases mutants although it was highly reduced in the *sco6673* mutant and in the double *sco6673 redU* mutant. In the genetically complemented *sco6673* mutant with *sco6673* expressed *in trans*, slightly higher actinorhodin seem to be produced but this level was still ~3-fold lower than in the M145 wild type. The *redU* mutant and the genetically complemented *redU* mutant produced similar amounts of the blue-pigmented actinorhodins to M145 (Figure 7.7).

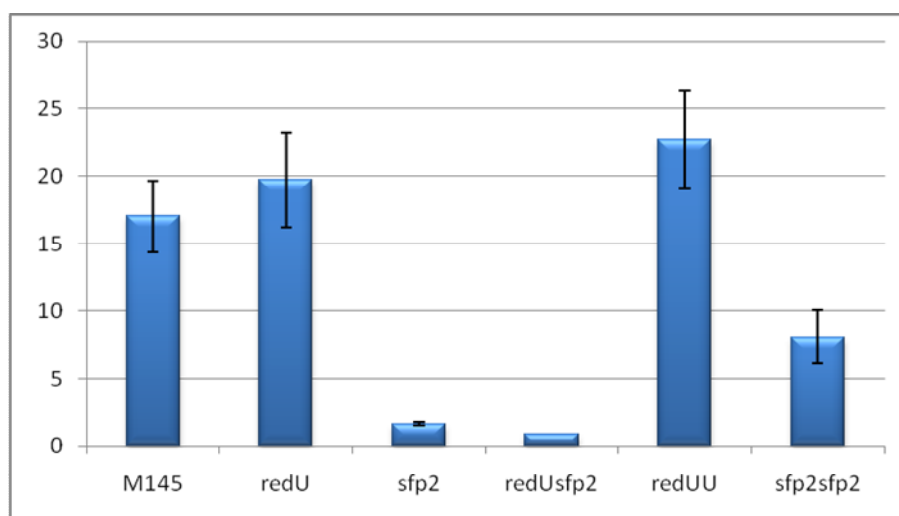


Figure 7.7 Production of actinorhodins by PPTase mutants grown in SMM medium determined in μg of pigment extracted per mg of DCW (dry cell weight) by UV-Vis spectroscopy.

Supernatants from the same SMM cultures were analysed by LC-MS to determine the production of actinorhodin-related shunt metabolites (data not shown). Production of the previously reported compounds SEK4a, SEK4b, SEK34, SEK34b and EM18 (Figure 7.8) (McDaniel et al., 1994) was examined, as well as the production of

previously unreported shunt metabolites, including LJS1 (Figure 7.8) and two other metabolites with $m/z = 372$ and 388 , for which the structure is currently not known (Song and Challis, unpublished results). As a negative control, the M511 strain was grown and analysed in the same way. M511 contains the *act* minimal PKS but lacks the *actIII-orfIV* pathway specific transcriptional activator for the *act* clusters and therefore actinorhodin and related compounds are not produced. All LC-MS analyses (data not shown) revealed a similar pattern for shunt metabolite production and blue-pigment production in the PPTase mutants. All of the metabolites were produced in similar level in M145, the *redU* mutant and the complemented *redU* mutant. Production of all of these metabolites was reduced but still detectable in the *sco6673* mutant and the complemented *sco6673* mutant (reduced ~4-fold lower, 25 +/- 5% comparing to WT). In the *sco6673 redU* double mutant, only traces of shunt metabolites could be detected.

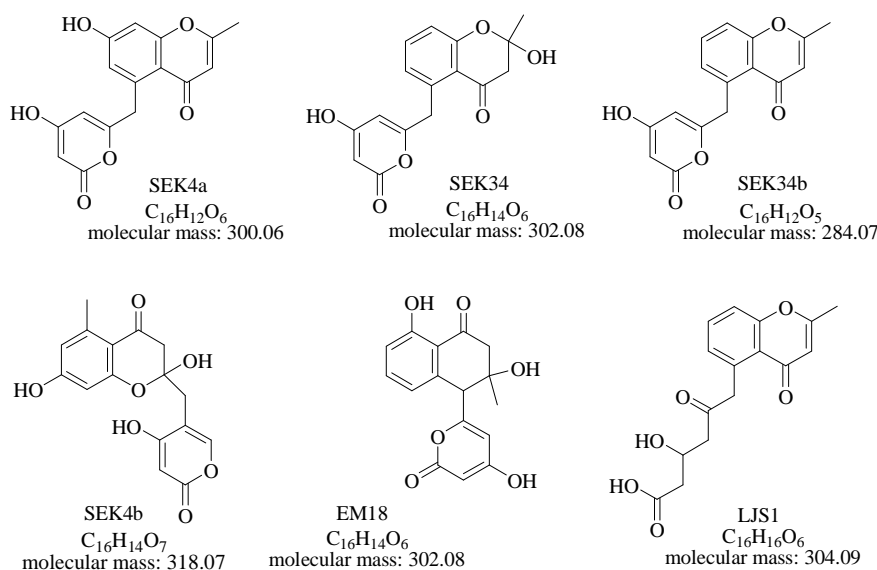


Figure 7.8 Structures of some shunt metabolites from the actinorhodin pathway produced by the M145 parent strain and the PPTase mutants. Structures of SEK4a, SEK4b, SEK34, SEK34b, EM18 were previously known (McDaniel et al., 1994). The structure of LJS1 is novel (Song and Challis, unpublished results).

The three PPTase mutants together with the M145 parent strain were plated on R5 agar medium to visually compare the effect of the mutation(s) on production of the blue and red pigments. The observed phenotypes were consistent with the above molecular analyses. The *redU* mutant did not produce visible prodiginines and produced blue pigments at wild type levels. In the *sco6673* mutant, prodiginines were still visible (at lower levels than in M145) and production of blue pigments was also reduced. In the *sco6673 redU* double mutant no red pigment was produced and production of blue pigments was highly reduced (Figure 7.9).

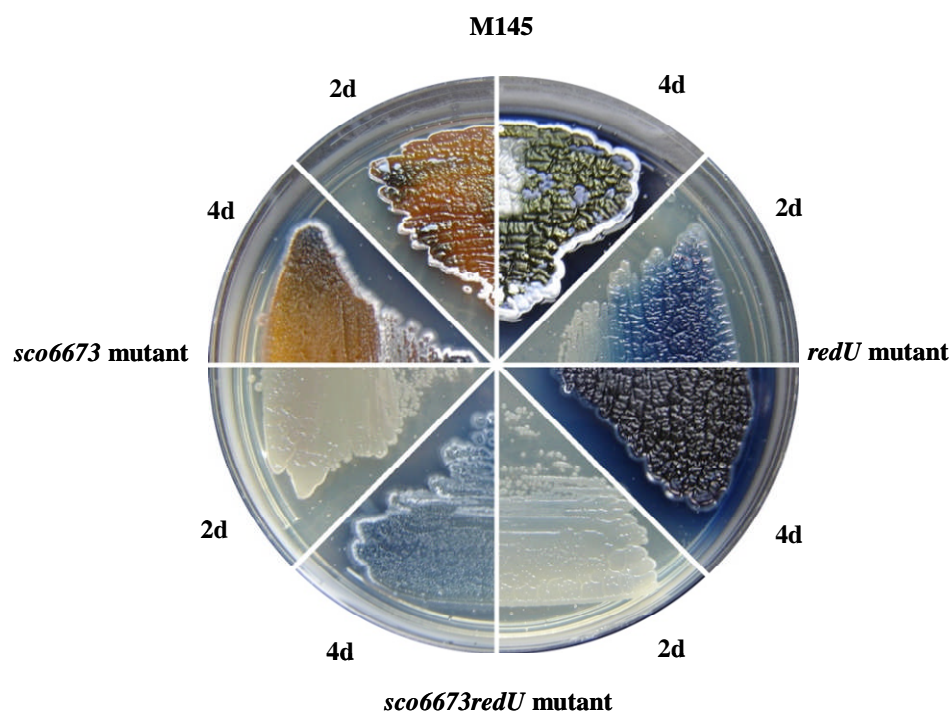


Figure 7.9 PPTase mutants plated onto R5 agar medium (top view of the plate). Pictures were taken two (2d) and four (4d) days after incubation.

The production of blue-pigmented actinorhodins by the *redU*, *sco6673* and *sco6673 redU* mutants was also analysed by Lu *et.al*. In liquid minimal medium, they observed that actinorhodin production was slightly reduced in the *redU* and *sco6673*

mutants (to ~80% of wild type levels), and reduced significantly in the *sco6673 redU* double mutant (to ~20% of wild type) compared to the M145 parent strain. On rich solid medium (R2YE), they observed that slightly lower quantities of actinorhodins were produced in the *sco6673* mutant (~80% of wild type), *redU* mutant (~65% of wild type), whereas slightly higher quantities of actinorhodin were produced by the *sco6673 redU* double mutant (~120% of wild type) than in M145 (Lu et al., 2008). These observations were again different from ours. We observed that the *sco6673* mutant and *sco6673 redU* double mutant produced much lower quantities of actinorhodin than the M145 strain (~25 +/- 5% of WT production) and that the *redU* mutant produced similar amounts of actinorhodin to the wild type strain (Figure 7.7). As with the prodiginines, it appears that growth conditions can significantly affect actinorhodin production levels.

7.3.3 Methylenomycin Production

Two methylenomycins are produced by *S. coelicolor* A3(2): methylenomycin A and its desepoxy-4,5-dehydro derivative, methylenomycin C (Figure 7.10) Methylenomycin A displays antibiotic activity against Gram-positive bacteria (Wright and Hopwood, 1976; Hornemann and D.A., 1978). Within the methylenomycin biosynthetic gene cluster (the *mmy* cluster, located on the giant linear plasmid SCP1), there is one ACP encoded by *mmyA*, which needs to undergo phosphopantetheinylation to be active.



Figure 7.10 Structures of methylenomycins produced by *S. coelicolor* A3(2).

S. coelicolor M145, used as a parent strain for constructing the double mutant, does not produce methylenomycins, because it lacks the SCP1 plasmid. The whole C73_787/*mmyR::oriT-apr* cosmid (provided by Dr. C. Corre, Challis group), which contains the entire *mmy* cluster, was introduced into *sco6673 redU* double mutant. The C73_787/*mmyR::oriT-apr* cosmid, with a disrupted transcriptional repressor for the *mmy* cluster regulatory gene (*mmyR*) causes overproduction of methylenomycins when introduced into a *Streptomyces* host such as *S. coelicolor* M145 (O'Rourke et al., 2009). When the C73_787/*mmyR::oriT-apr* was introduced to M145/*redU::oriT-apr+sco6673::scar*, kanamycin was used to select correct exconjugant (kanamycin resistance cassette is presented in the cosmid backbone).

Methylenomycin production in the PPTase mutants containing the cosmid was examined using a methylenomycin A bioassay. A plug of Ala MM agar inoculated with the strain to be tested was placed on an Ala MM agar plate with a growing confluent lawn of *S. coelicolor* M145 (sensitive to methylenomycin A and thus used as an indicator strain). Methylenomycin production resulted in a zone of clearing on the plate (Figure 7.11). The M145 strain (not producing methylenomycins) was used as a negative control and the M145/C73_787/*mmyR::oriT-apr* (overproducing methylenomycin) was used as a positive control. Using this assay the *sco6673 redU* double mutant containing the C73_787/*mmyR::oriT-apr* cosmid was found to produce methylenomycin A (zone of clearing similar in size to the positive control). This suggests that methylenomycin biosynthesis does not require posttranslational modification of the MmyA ACP by the RedU or SCO6673 PPTases. Either MmyA is activated by AcpS or an intermedi-

ate in fatty acid biosynthesis (e.g. acetoacetyl-FabC) can substitute for acetoacetyl-MmyA in methylenomycin biosynthesis.

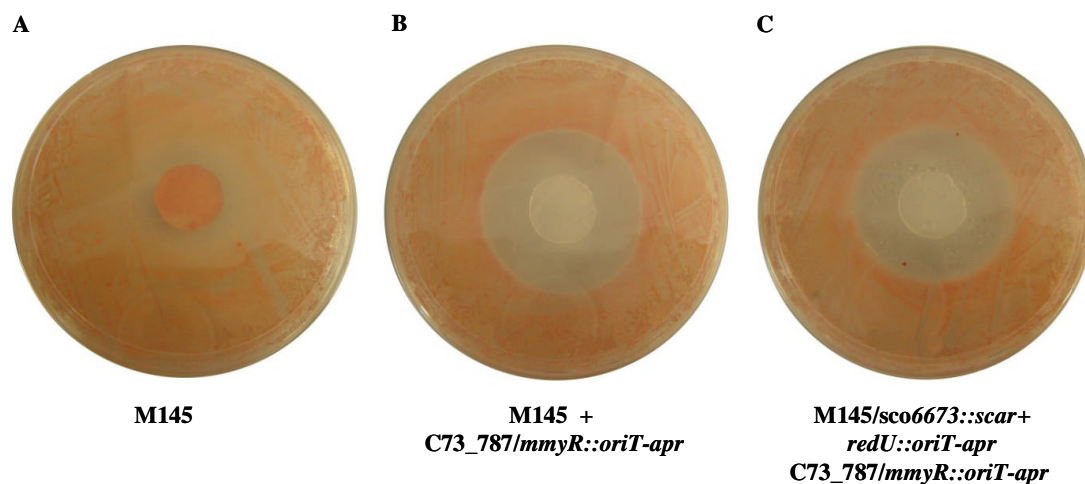


Figure 7.11 Analysis of methylenomycin production by bioassay in A – *S. coelicolor* M145, B – M145/C73_787/mmyR::oriT-apr, C – M145/sco6673::scar+redU::oriT-apr+C73_787/mmyR::oriT-apr. M145 was used as a methylenomycin sensitive indicator strain.

7.3.4 Calcium-Dependent Antibiotic (CDA) Production

S. coelicolor produces a variety of CDAs with different functional groups, but all contain the same peptide sequence (Figure 7.12). These antibiotics are effective against a wide range of Gram-positive bacteria but only in the presence of calcium ions (Lakey et al., 1983). The *cda* gene cluster contains three large NRPS genes, encoding multienzymes containing a total of eleven PCP or thiolation domains and one separate gene coding for an ACP (Hojati et al., 2002), all of which have to be phosphopantetheinylated.

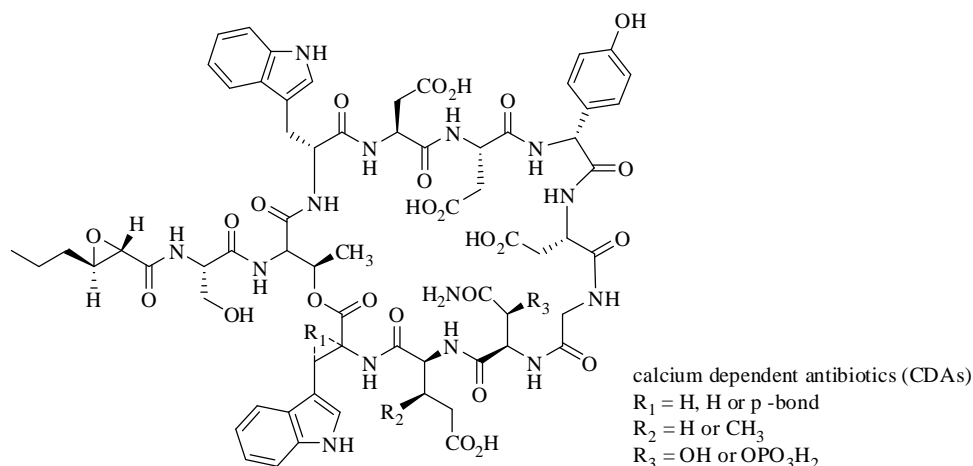


Figure 7.12 Structures of CDAs produced by in *S. coelicolor*.

The PPTase mutants were analysed for CDA production using a specific, previously described bioassay (Kieser et al., 2000; Lautru et al., 2007). Strains were spotted onto Oxoid nutrient agar plates and incubated at 30 °C. After two days, plates were overlaid with soft nutrient agar containing indicator strain *Bacillus mycoides* and calcium nitrate. When CDA was produced, growth of *B. mycoides* was inhibited, ensuing in a zone with no bacteria around the spot where *Streptomyces* grew. The *S. coelicolor* M145 strain, which produces CDA, was used as a positive control (Figure 7.13).

As a result of the CDA bioassays the *redU* mutant was found to still produce the CDAs but CDA production was abolished in the *sco6673* mutant and in the *sco6673 redU* double mutant. Genetic complementation of the *sco6673* mutant with pOSV556*sco6673* restored CDA production to the wild type level (Figure 7.13), suggesting that SCO6673 is required for CDA biosynthesis. These results confirmed the observation made by Lu et al. (2008).

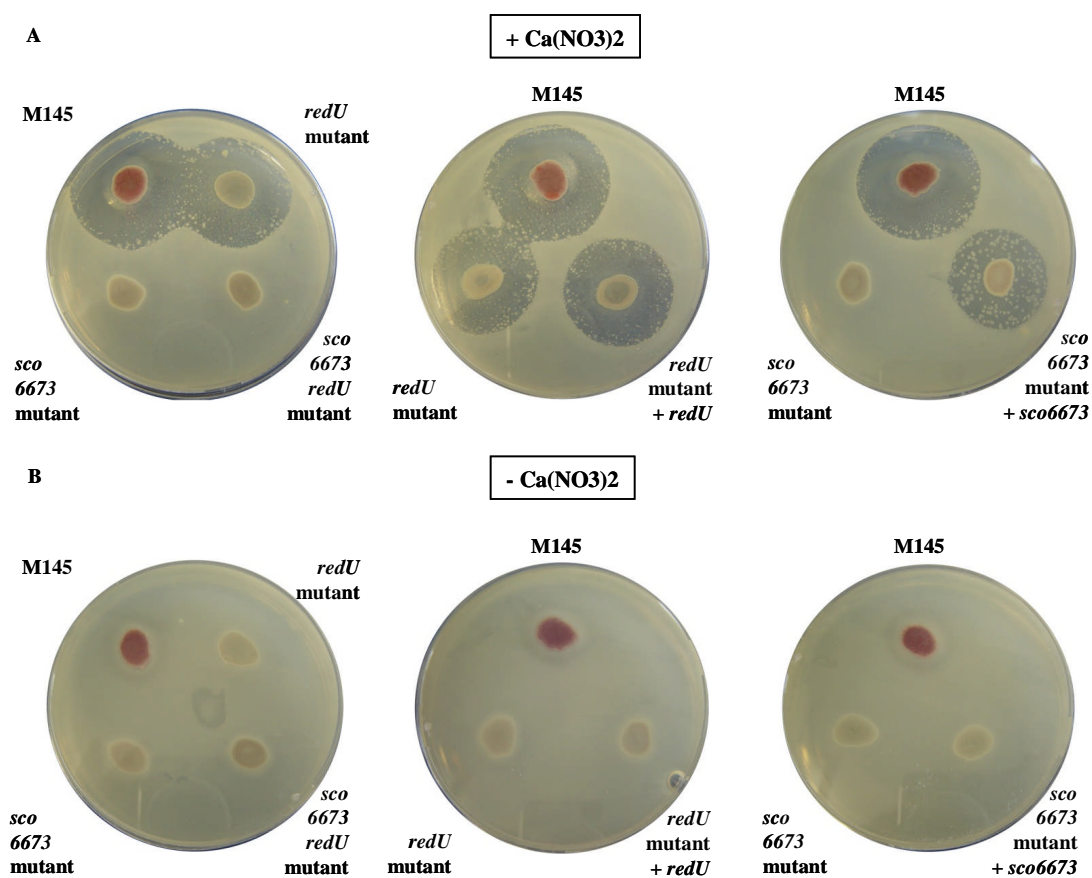


Figure 7.13 Analysis of PPTase mutants for CDA production using a bioassay. *Bacillus mycoides* was used as an indicator strain. A – + Ca(NO₃)₂ (top plates), B – - Ca(NO₃)₂ (bottom plates).

7.3.5 Coelichelin Production

Coelichelin is a recently discovered siderophore, which was first predicted to be produced by analysis of the *S. coelicolor* genome sequence (Challis and Ravel, 2000). Coelichelin has recently been isolated and structurally characterised (Lautru et al., 2005) and its production was shown to be directed by the *cch* gene cluster (Lautru et al., 2005). The *cchH* gene encodes a trimodular NRPS with three PCP domains, which have to be activated by PPTases.

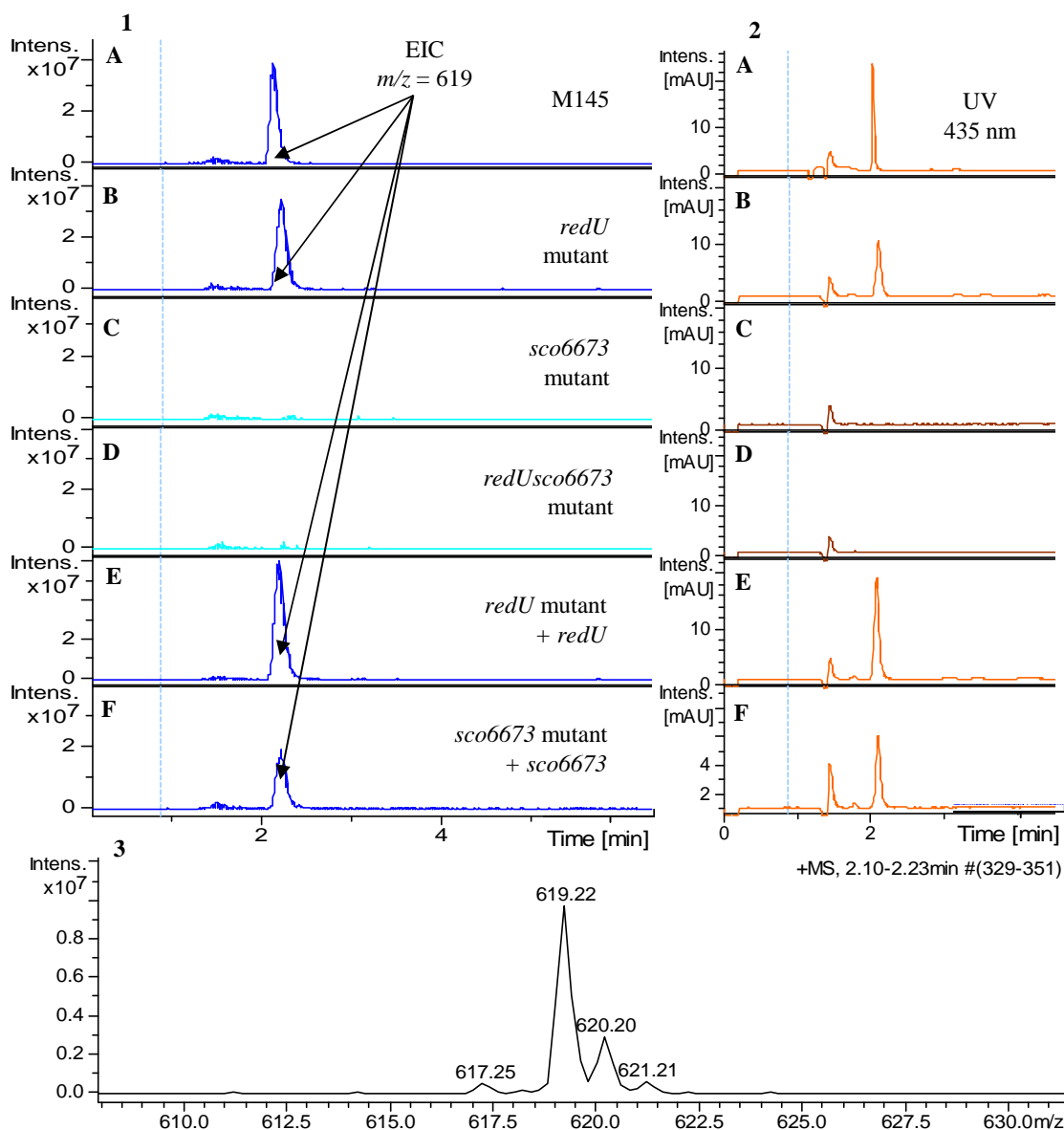


Figure 7.15 LC-MS analyses of culture supernatants of *S. coelicolor* M145 and PPTase mutants; 1: EIC at $m/z = 619$. 2: UV chromatogram at 435 nm; A – M145 wild type, B – *redU* mutant, C – *sco6673* mutant, D – *sco6673 redU* mutant, E – *redU* mutant + *redU*, F - *sco6673* mutant + *sco6673*. 3: mass spectrum for the peak with retention time ~2.2 minutes.

LC-MS analyses of the *redU* mutant showed that coelicelin production was not abolished and that it is produced in a similar amount to the wild type M145 strain (Figure 7.15, 1B, 2B). A similar observation was made for the complemented *redU*

mutant (Figure 7.15, 1E, 2E). LC-MS analyses of the *sco6673* mutant showed that coelichelin production was abolished (Figure 7.15, 1C, 2C), indicating that SCO6673 is required for phosphopantetheinylation of at least one PCP within the CchH NRPS enzyme. In the genetically complemented *sco6673* mutant production of coelichelin was restored to the wild type level (Figure 7.15, 1F, 2F), confirming that the mutant was correctly constructed and i.e. the *sco6673* gene expresses *in trans*. LC-MS analyses of the *sco6673 redU* double mutant showed that coelichelin was not produced (Figure 7.15 1D, 2D), because expected as coelichelin production was abolished in the *sco6673* mutant.

7.3.6 Grey Spore Pigment Production and Colony Morphology

The colour of *S. coelicolor* spores results from the synthesis of grey spore pigments (Davis and Chater, 1990). The polyketide nature of these pigments was deduced from the analysis of mutants of the *whiE* cluster. However, the spore pigments have never been purified and structurally analysed (Kelemen et al., 1998). The *whiE* gene cluster contains eight genes including three encoding a minimal a PKS with one ACP (Davis and Chater, 1990). The genes are transcribed just before the onset of sporulation in the aerial mycelium (Yu and Hopwood, 1995).

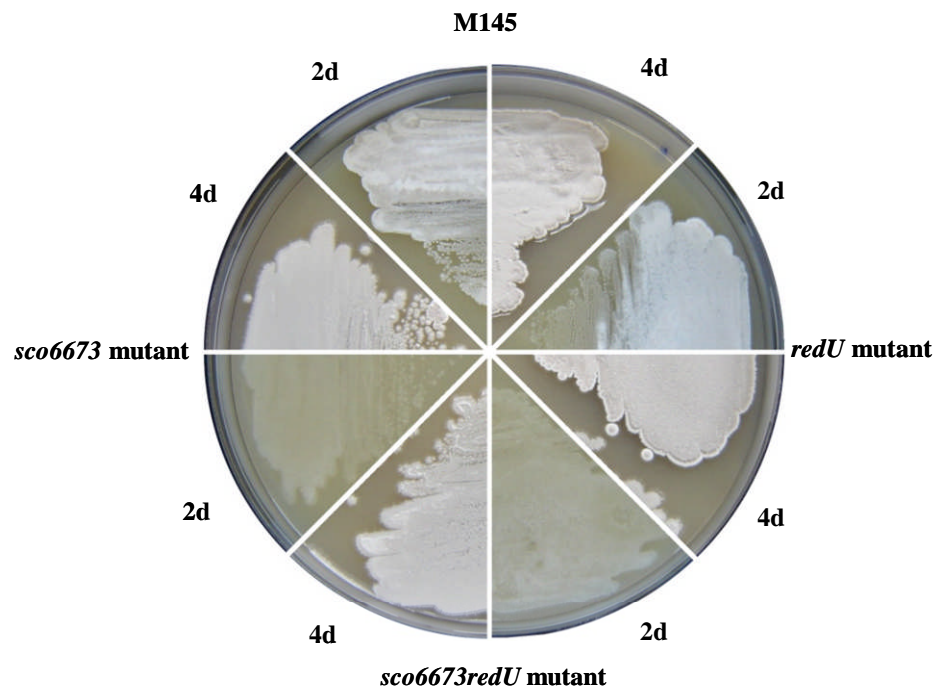


Figure 7.16 Phenotypes of PPTase mutants plated onto SFM medium, after 2 days (2d) and 4 days (4d) of growth.

All PPTase mutants were grown on a single SFM agar plate (SFM is a good medium for sporulation of the wild type *S. coelicolor* M145) to compare the colour of the spores. After 2 and 4 days incubation, there is no difference in the spore colour between all PPTase mutants and M145 parent strain. However the production of aerial mycelia and sporulation in the *sco6673* and *sco6673 redU* mutants was delayed (Figure 7.16). Similar results were obtained when the PPTase mutants were grown as single colonies. The *redU* mutant and the *redU* mutant + *redU* were growing similarly to the parent strain and large, well sporulating colonies were observed. The *sco6673*, *sco6673* + *sco6673* and *sco6673 redU* mutants were growing slower; colonies were smaller and were not sporulating very well (Figure 7.17).

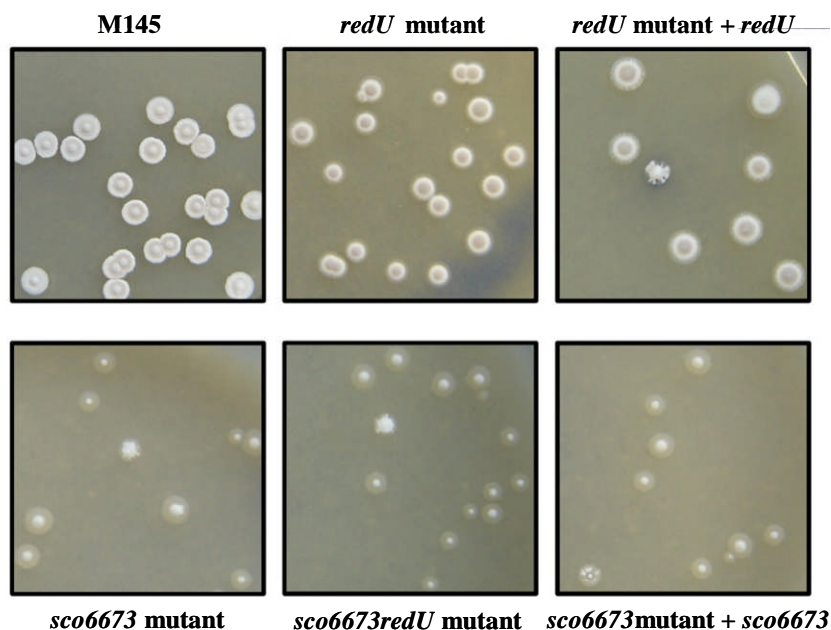


Figure 7.17 Growth of single colonies of PPTase mutants on SFM agar medium.

It is interesting to note that the same strains with delayed sporulation (the *sco6673*, *sco6673* + *sco6673* and *sco6673 redU* mutants) also produced smaller quantities of actinorhodin from the wild type. The two type II PKS systems encoded by the *act* and *whiE* gene clusters are similar and maybe both ACP proteins (one encoded by the *act* cluster and one by the *whiE* cluster) are most efficiently activated by SCO6673-dependent phosphopantetheinylation. When this PPTase enzyme is absent, sporulation and actinorhodin production are both influenced.

The role of PPTases on sporulation was also checked by Lu *et al.* who grew the mutants on R2YE agar plates and observed that only the *sco6673* mutant had delayed aerial mycelium formation and delayed sporulation. The other mutants and the parental M145 sporulated very well on R2YE medium (Lu et al., 2008). In our study, delayed sporulation was observed for three strains (the *sco6673*, *sco6673* + *sco6673* and *sco6673*

redU mutants). However, good sporulation of even the wild type strain was never observed either on R5 medium (Figure 7.9) or on R2YE medium (data not shown).

7.4 Conclusions

In the *S. coelicolor* genome, three putative PPTases are encoded by *acpS*, *redU* and *sco6673* genes. These enzymes are very likely to be multifunctional and capable of activating a wide range of carrier proteins involved in the biosynthesis of various primary and secondary metabolites.

Mutants lacking these three genes were investigated. Construction of an M145/*acpS*::*oriT-apr* was only possible when an extra copy of the *acpS* gene was incorporated into the genome, indicating that this gene is essential for *S. coelicolor* growth, probably because it plays a key role in fatty acid biosynthesis. The other mutants: M145/*redU*::*oriT-apr* (created by Anna Stanley), M145/*sco6673*::*oriT-apr* and the M145/*sco6673*::*scar+redU*::*oriT-apr* double mutant, along with the genetically complemented mutants were analysed for production of prodiginines, actinorhodins and related metabolites, methylenomycin A, CDAs, coelichelin and grey spore pigments. The results are summarised in Table 7.1.

Table 7.1 Secondary metabolite production by PPTase mutants. Number of pluses indicates the level of production compared to the M145 parent strain. Grey spore pigment was estimated by looking at growth of single colonies.

	M145	M145/ <i>redU</i> ::<i>oriT</i>- <i>apr</i>	M145/ <i>sco6673</i> ::<i>oriT</i>- <i>apr</i>	M145/ <i>sco6673</i> ::<i>scar</i>+ <i>redU</i> ::<i>oriT</i>- <i>apr</i>	M145/ <i>redU</i>:: <i>oriT</i>- <i>apr</i>+ <i>pOSV</i> <i>556 redU</i>	M145/ <i>sco6673</i> ::<i>oriT</i>- <i>apr</i>+ <i>pOSV</i> <i>556</i> <i>sco6673</i>
RED	+++	-	++	-	+++	++
ACT	+++	+++	+	+	+++	+
methylenomycin*	+++			+++		
CDA	+++	+++	-	-	+++	+++
coelichelin	+++	+++	-	-	+++	+++
grey spore pig- ment /sporulation	+++/ normal	+++/ normal	+++/ slow	+++/ slow	+++/ normal	+++/ slow

* strain + cosmid *C73_78mmyR::oriT-apr*

Above results show that *SCO6673* plays an important role in the phosphopantetheinylation of PCP and ACP proteins, which are involved in secondary metabolite production in *S. coelicolor*. *SCO6673* was not very efficiently complemented by any of the other two PPTases. In contrast, RedU could be complemented by either *SCO6673* or *AcpS*. In *redU* mutant just prodiginine production is abolished but feeding experiment showed that RedU is only required for phosphopantetheinylation of RedO. In double mutant just methylenomycin and low level of actinorhodin are produced showing multifunctional role of only active PPTase – *AcpS*.

Although the genotypes of the *sco6673*, *redU* mutants and the *sco6673 redU* double mutant appeared to be as intended and genetic complementation of the *sco6673*

and *redU* mutants restored production of affected metabolites, sporulation and levels of prodiginine and actinorhodin production were different from similar mutants constructed by Lu et al. (2008). These authors suggested that PPTases could influence secondary metabolite biosynthesis but are not essential, for this process under certain growth conditions. Consistent with this idea, Streptomyces regulate antibiotic production in highly controlled manner and probably many environmental and physiological cues, as well as morphological differentiation, influence this process (Bibb, 2005).

8. Summary, Conclusions and Future Work

8.1 Investigation of the Prodiginine Biosynthetic Pathway in

Streptomyces coelicolor M511

Putative functions for most of the twenty-three genes within the *red* cluster have been proposed (Cerdeño et al., 2001) and biosynthetic pathways to the prodiginines have been suggested on the basis of bioinformatics and experimental studies (Figure 8.1) (Cerdeño et al., 2001; Thomas et al., 2002; Stanley et al., 2006; Haynes et al., 2008; Mo et al., 2008). However, the biosynthetic roles of some genes within this cluster were still not clear. Replacement of the region of *redL* encoding an A domain, *redI*, *redK*, *redJ*, *redT* and *redV* with an Apramycin resistance cassette was carried out during the course of this research. The nature of each mutant was confirmed by PCR and Southern blot analysis (except for the *redV* mutant). Then each mutant strain was analysed by LC-MS and other techniques to investigate the role of the gene deleted in prodiginine biosynthesis.

Construction and analysis of M511/*redK::oriT-apr* and M511/*redI::oriT-apr* indicated that the *redK* and *redJ* genes encode enzymes involved in 2-UP and MBC biosynthesis, respectively. Analogues of undecylprodiginine were accumulated in both mutants (desmethylundecylprodiginine in the *redI* mutant and a hydroxylated analogue of undecylprodiginine in the *redK* mutant). This provides insight into the role played by each enzyme in the biosynthetic pathway (Figure 8.1).

Analyses of the M511/*redJ::apr* and M511/*redLA::oriT-apr* mutants (RedJ and the RedL A domain) are both proposed to play a role in 2-UP biosynthesis (Figure 8.1) were not conclusive. In the *redJ* mutant, prodiginines were still produced (up to 20% of wild type level). Thus the role of RedJ could not be deduced. Thioesterases are known

to be multifunctional (Kotowska et al., 2002) and the lack of RedJ in the mutant might thus be complemented by one of two other standalone thioesterases encoded within *S. coelicolor* genome. Construction of mutants lacking one or both of these additional standalone thioesterase encoding gene in addition to *redJ* could shed further light in this question. Other experiments that could be carried out on the *redJ* mutant include genetic complementation which would rule out polar effects on the question of downstream genes if production of prodiginines is restored to wild type levels. Feeding analogues of dodecanoic acid to the *redJ* mutant to examine whether prodiginine analogues are produced could indicate that RedJ plays a role in initiating 2-UP biosynthesis (Figure 8.1) as was originally proposed (Cerdeño et al., 2001).

Prodiginine production was abolished in the mutant lacking the region of *redL* encoding the A domain and genetic complementation of the mutant failed to restore prodiginine production. RedL is a big (~230 kDa) NRPS-PKS enzyme (Figure 8.1) and removing its first enzymatic domain may have influenced its proper folding and function. A point mutation of an essential active site residue within the A domain would be a better approach for the future, because it should cause minimal disruption to the protein's 2^y and 3^y structure.

Interesting and unexpected results were obtained from the M511/*redT::oriT-apr* mutant. Although no function for *redT* could be proposed (RedT does not show significant sequence similarity to any other proteins in the databases) LC-MS analyses of the mutant suggested that RedT plays a role in MBC biosynthesis. These results were unexpected because no step was missing in the proposed biosynthesis of MBC (Figure 8.1). However RedT might form a complex with other enzymes from this biosynthetic

pathway. A crystal structure of RedT could help elucidate its role. Genetic complementation of this mutant could also confirm the absence of any polar effect on the expression of downstream genes.

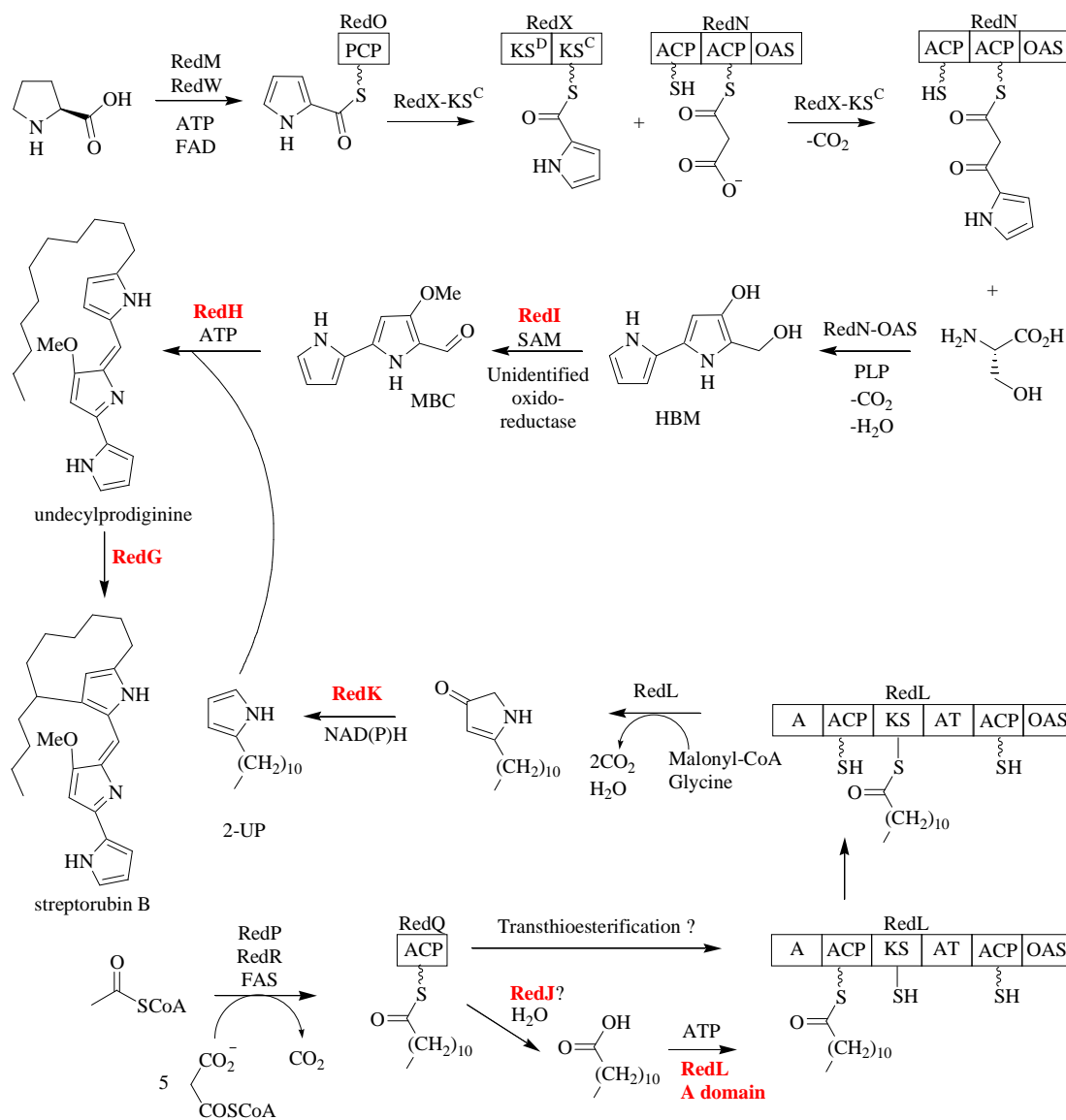


Figure 8.1 Proposed biosynthetic pathway to undecylprodiginine and streptorubin B. The functions of genes highlighted in red were investigated in this work.

Analyses of the preexisting M511/*redH::oriT-apr* mutant (Haynes et al., 2008), genetic complementation of the mutant and heterologous expression of *redH* coupled with feeding of synthetic MBC and 2-UP proved strong evidence for a role for RedH in the condensation of 2-UP and MBC to generate undecylprodiginine (Figure 8.1).

8.2 Investigation of an Oxidative Carbocyclisation Reaction in Streptorubin B Biosynthesis

The last step in streptorubin B biosynthesis was proposed to be the oxidative carbocyclisation of undecylprodiginine. RedG, which is a Rieske oxygenase-like enzyme, was proposed to catalyse this reaction. The M511/*redG::scar* (W31) mutant previously constructed in the lab was confirmed to produce undecylprodiginine but not streptorubin B (Odulete, 2005), consistent with this hypothesis. Further investigation of the role of RedG was carried out during this research.

Expression of *redG* and *redHG* in *S. coelicolor* and *S. venezuelae* coupled, in some cases, with feeding of synthetic MBC, 2-UP or undecylprodiginine allowed several conclusions to be drawn: (1) RedG plays a role in the oxidative carbocyclisation of undecylprodiginine to form streptorubin B (*redG* mutant was successfully genetically complemented); (2) RedG is the only enzyme required for generating streptorubin B from undecylprodiginine (feeding of synthetic undecylprodiginine to a strain of *S. venezuelae* expressing *redG* produced streptorubin B); (3) Oxidative cyclisation of undecylprodiginine to yield streptorubin B is the last step in prodiginine biosynthesis (a *redI* mutant accumulates desmethylundecylprodiginine, but not desmethylundecylstrep-

torubin B); (4) RedG and RedH appear to make a complex (when *redG* and *redH* are expressed together more streptorubin B is produced).

The hypothesis that RedG and RedH form a complex was not further investigated in this study. Future cocrystallisation experiments with both purified proteins could give more information about their interaction. Using the yeast two hybrid system, or expression of RedH and RedG in fusion with fluorescent proteins *in vivo* could provide further information about complex formation.

8.3 Cloning, sequencing and analysis of *redG* and *redH* orthologues from *Streptomyces longispororuber*

Streptomyces longispororuber produces two prodiginine antibiotics: undecylprodiginine (as produced by *S. coelicolor*) and the carbocyclic derivative metacycloprodigiosin (streptorubin A) with a 12-membered carbocycle instead of the 10-membered carbocycle in streptorubin B (Figure 8.2). A RedG orthologue in *S. longispororuber* was thought to catalyse an analogous oxidative carbocyclisation reaction to the one catalysed by RedG in *S. coelicolor*. Two partial CDSs, highly similar to *redH* and *redG* from *S. coelicolor*, were identified in *S. longispororuber* consistent with this hypothesis (Barry, 2007).

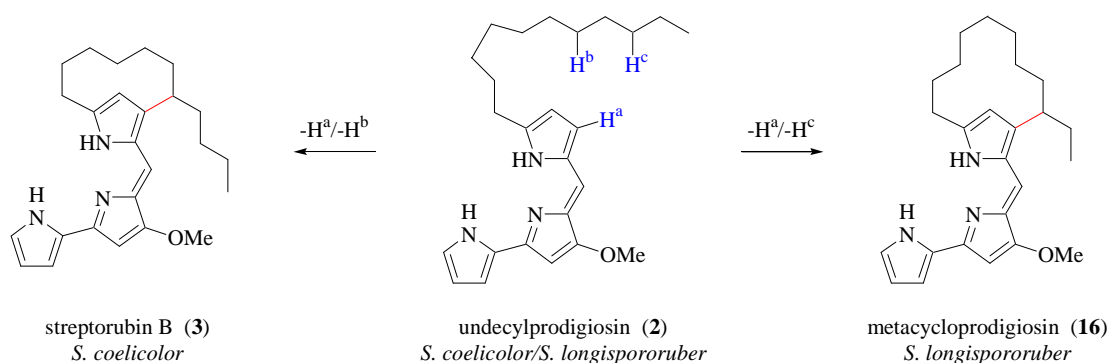


Figure 8.2 Prodiginines produced by *S. coelicolor* and *S. longispororuber*.

A *S. longispororuber* genomic library was constructed in this study. From one isolated fosmid clone, the whole sequence of the *S. longispororuber* *redH* and *redG* orthologues was obtained (complete CDSs were named *mcpH* and *mcpG*). Two partial CDSs also identified by further sequencing of the clone encode proteins with similarity to RedI and RedU. These analyses indicated that the general organisation of the *S. longispororuber* *mcp* gene cluster is likely to be similar to that of the *red* cluster in *S. coelicolor*. The identified *mcpG* gene was then expressed in the *S. coelicolor* *redG* mutant (W31), which resulted in production of metacycloprodigiosin.

All these results showed that RedG and the newly identified McpG can be classified as two members of a new family of Rieske oxygenase-like enzymes, which catalyse regiodivergent oxidative carbocyclisation reactions in the biosynthesis of streptorubin B and metacycloprodigiosin (streptorubin A), respectively. Although oxidative cyclisation reactions are known to be important steps in the biosynthesis of many natural products (Konomi et al., 1979; Elson et al., 1987; Hammerschmidt, 1991; Seto et al., 1991; Zerbe et al., 2004) no example that generates a C-C bond is known.

Oxidative carbocyclisation for Rieske non-haem iron-dependent oxygenase-like enzymes represents a new type of catalytic activity especially from the mechanistic view point which could be further investigated. It would be interesting to investigate the use of these enzymes in chemoenzymatic synthesis of analogues of streptorubin B and metacycloprodigiosin, which are not easily accessible by synthetic methods.

After successful expression of *mcpG* in W31, other RedG orthologues were investigated. Four different *rphG* genes, which are believed to encode RedG/McpG homologues that catalyse oxidative carbocyclisation and pyrrole to furan conversion reactions in roseophilin and prodigiosin R1 biosynthesis, were expressed separately in the *S. coelicolor* W31 mutant. Unfortunately no new compounds were detected. This result suggests that more than one *rphG* gene has to be coexpressed in the W31 mutant or that the *rphG* genes have to be coexpressed with *rphH* (*redH* orthologue) for carbocycle formation. Positive results from coexpression of the *rphGs* and *rphH* would provide further support for the formation of complexes by these proteins *in vivo*.

8.4 Novel Approaches for Generating Prodiginine Analogues

Genetic manipulation to generate novel prodiginine analogues was explored in particular because streptorubin B represents a challenging target in synthetic chemistry.

Chlorinated analogues of undecylprodiginine and streptorubin B were detected when the *hrmQ* gene (involved in hormaomycin biosynthesis) (Heide et al., 2008) was introduced into *S. coelicolor* M511, although they were produced at low levels. When a double M511/*redN::scar + redL::oriT-apr* (W119) mutant (with abolished production of both 2-UP and MBC) was fed with synthetic substrates prodiginine production was

restored. In the future, feeding this strain with synthetic analogues of 2-UP and MBC could result in the production of novel prodiginine analogues with improved biological activity.

8.5 Investigation of the Roles of Enzymes Catalysing Post-translational Phosphopantetheinylation of ACP and PCP

Proteins/Domains

Three putative PPTases are encoded within the *S. coelicolor* genome: AcpS, RedU and SCO6673. The substrate specificity of these multifunctional enzymes, presumed to be responsible for the posttranslational phosphopantetheinylation of several ACP and PCP proteins/domains, were investigated using a genetic approach.

The fact that the *S. coelicolor* M145/*acpS::oriT-apr* and M511/*acpS::oriT-apr* mutants could only be generated in the presence of an extra copy of the *acpS* gene indicated that AcpS is essential for growth and survival and probably plays an essential role in fatty acid biosynthesis.

S. coelicolor M145/*redU::oriT-apr* (constructed by Anna Stanley), M145/*sco6673::oriT-apr*, M145/*sco6673::scar+redU::oriT-apr*, M145/*redU::oriT-apr*+pOSV556*redU* and M145/*sco6673::oriT-apr*+pOSV556*sco6673* mutants were constructed and analysed for production of prodiginines, actinorhodins, CDAs, methylenomycins, coelichelin, and the grey spore pigment, all of which require ACPs and PCPs for their biosynthesis.

RedU was found to be required only for prodiginine biosynthesis (in the *redU* mutant the other secondary metabolites were produced at similar levels to wild type).

SCO6673 was required for CDA and coelichelin biosynthesis. In the *sco6673::oriT-apr* mutant, actinorhodin production was reduced, sporulation was slower and colonies were smaller. In the *sco6673::scar+redU::oriT-apr* mutant (where only AcpS was expressed), methylenomycins and low levels of actinorhodin were produced, but production of prodiginines, CDAs and coelichelin was abolished. Sporulation was affected in a similar way to the *sco6673::oriT-apr* mutant. Genetic complementation of the *redU::oriT-apr* and *sco6673::oriT-apr* mutants restored the production of abolished secondary metabolites, indicating that the mutants were correctly constructed.

Sporulation and prodiginine/actinorhodin production in the *sco6673::oriT-apr*, *redU::oriT-apr*, *sco6673::scar+redU::oriT-apr*, M145/*redU::oriT-apr*+pOSV556*redU* and M145/*sco6673::oriT-apr*+pOSV556*sco6673* mutants were not consistent with results reported for similar mutants constructed by Lu et al. (2008). This could be due to different growth conditions between the two laboratories. Indeed secondary metabolite production in streptomycetes is known to be tightly regulated and many environmental and physiological factors can influence it (Bibb, 2005).

The role of PPTases in primary and secondary metabolism makes them an interesting target for antibiotic development (Yasgar et al., 2010). If they are required for toxins biosynthesis or biosynthesis of compounds required for growth of pathogenic bacteria (e.g. fatty acids or siderophores) they could be an attractive target for drug discovery. Additionally PPTases can be explored for the possibility to optimize industrial strains for high level production of desired secondary metabolites. A better understanding of their role in the model organism *S. coelicolor* could facilitate inhibitor development and industrial strain improvement.

References

- Ansari, M. Z.; Yadav, G.; Gokhale, R. S.; Mohanty, D. *Nucleic Acids Res* **2004**, *32* (Web Server issue), W405-13.
- Axcell, B. C.; Geary, P. J. *Biochem. J.* **1975**, *146*, 173-183.
- Azuma, T.; Watanabe, N.; Yagisawa, H.; Hirata, H.; Iwamura, M.; Kobayashi, Y. *Immunopharmacology* **2000**, *46* (1), 29-37.
- Barona-Gomez, F.; Lautru, S.; Francou, F. X.; Leblond, P.; Pernodet, J. L.; Challis, G. L. *Microbiology* **2006**, *152* (Pt 11), 3355-66.
- Barry, S. M. Non-Heme Iron Oxidase Enzymes & Enzyme Mimics in Synthesis & Biosynthesis. PhD Thesis, University College Dublin, Dublin, 2007.
- Bennett, J. W.; Bentley, R. *Adv Appl Microbiol* **2000**, *47*, 1-32.
- Bentley, S. D.; Chater, K. F.; Cerdeno-Tarraga, A. M.; Challis, G. L.; Thomson, N. R.; James, K. D.; Harris, D. E.; Quail, M. A.; Kieser, H.; Harper, D.; Bateman, A.; Brown, S.; Chandra, G.; Chen, C. W.; Collins, M.; Cronin, A.; Fraser, A.; Goble, A.; Hidalgo, J.; Hornsby, T.; Howarth, S.; Huang, C. H.; Kieser, T.; Larke, L.; Murphy, L.; Oliver, K.; O'Neil, S.; Rabbinowitsch, E.; Rajandream, M. A.; Rutherford, K.; Rutter, S.; Seeger, K.; Saunders, D.; Sharp, S.; Squares, R.; Squares, S.; Taylor, K.; Warren, T.; Wietzorrek, A.; Woodward, J.; Barrell, B. G.; Parkhill, J.; Hopwood, D. A. *Nature* **2002**, *417* (6885), 141-7.
- Bentley, S. D.; Brown, S.; Murphy, L. D.; Harris, D. E.; Quail, M. A.; Parkhill, J.; Barrell, B. G.; McCormick, J. R.; Santamaria, R. I.; Losick, R.; Yamasaki, M.; Kinashi, H.; Chen, C. W.; Chandra, G.; Jakimowicz, D.; Kieser, H. M.; Kieser, T.; Chater, K. F. *Mol Microbiol* **2004**, *51* (6), 1615-28.

- Bibb, M. J.; White, J.; Ward, J. M.; Janssen, G. R. *Mol Microbiol* **1994**, *14* (3), 533-45.
- Bibb, M. J. *Curr Opin Microbiol* **2005**, *8* (2), 208-15.
- Brockmann, H.; Pini, H.; Plotho, O. *Chem Ber* **1950**, *83*, 161.
- Bugg, T. D. *Tetrahedron* **2003**, *59*, 7075-7101.
- Butler, A. R.; Bate, N.; Cundliffe, E. *Chem Biol* **1999**, *6* (5), 287-92.
- Bystrykh, L. V.; Fernandez-Moreno, M. A.; Herrema, J. K.; Malpartida, F.; Hopwood, D. A.; Dijkhuizen, L. *J Bacteriol* **1996**, *178* (8), 2238-44.
- Cerdeño, A. M.; Bibb, M. J.; Challis, G. L. *ChemBio* **2001**, *8* (8), 817-29.
- Challis, G. L.; Ravel, J. *FEMS Microbiol Lett* **2000**, *187* (2), 111-4.
- Challis, G. L.; Ravel, J.; Townsend, C. A. *Chem Biol* **2000**, *7* (3), 211-24.
- Chen, K.; Rannulu, N. S.; Cai, Y.; Lane, P.; Liebl, A. L.; Rees, B. B.; Corre, C.; Challis, G. L.; Cole, R. B. *J Am Soc Mass Spectrom* **2008**, *19* (12), 1856-66.
- Cherepanov, P. P.; Wackernagel, W. *Gene* **1995**, *158* (1), 9-14.
- Corre, C.; Challis, G. L. *ChemBioChem* **2005**, *6* (12), 2166-70.
- Corre, C.; Song, L.; O'Rourke, S.; Chater, K. F.; Challis, G. L. *Proc Natl Acad Sci U S A* **2008**, *105* (45), 17510-5.
- Corre, C.; Challis, G. L. unpublished results.
- Cortes, J.; Wiesmann, K. E.; Roberts, G. A.; Brown, M. J.; Staunton, J.; Leadlay, P. F. *Science* **1995**, *268* (5216), 1487-9.
- Cox, R. J.; Crosby, J.; Daltrop, O.; Glod, F.; Jarzabek, M. E.; Nicholson, T. P.; Reed, M.; Simpson, T. J.; Smith, L. H.; Soulas, F.; Szafranska, A. E.; Westcott, J. *J Chem Soc Perkin Trans 1* **2002**, 1644-1649.
- Danial, N. N.; Korsmeyer, S. J. *Cell* **2004**, *116* (2), 205-19.

- Datsenko, K. A.; Wanner, B. L. *Proc Natl Acad Sci U S A* **2000**, *97* (12), 6640-5.
- Davis, N. K.; Chater, K. F. *Mol Microbiol* **1990**, *4* (10), 1679-91.
- Debono, M.; Abbott, B. J.; Molloy, R. M.; Fukuda, D. S.; Hunt, A. H.; Daupert, V. M.; Counter, F. T.; Ott, J. L.; Carrell, C. B.; Howard, L. C.; et al. *J Antibiot (Tokyo)* **1988**, *41* (8), 1093-105.
- Donadio, S.; Monciardini, P.; Sosio, M. *Nat Prod Rep* **2007**, *24* (5), 1073-109.
- Dorrestein, P. C.; Yeh, E.; Garneau-Tsodikova, S.; Kelleher, N. L.; Walsh, C. T. *Proc Natl Acad Sci U S A* **2005**, *102* (39), 13843-8.
- Doumith, M.; Weingarten, P.; Wehmeier, U. F.; Salah-Bey, K.; Benhamou, B.; Capdevila, C.; Michel, J. M.; Piepersberg, W.; Raynal, M. C. *Mol Gen Genet* **2000**, *264* (4), 477-85.
- Eaton, R. W.; Chapman, P. J. J. *J Bacteriol* **1992**, *174*, 7542-7554.
- Eliot, A. C.; Kirsch, J. F. *Annu Rev Biochem* **2004**, *73*, 383-415.
- Elson, S. W.; Baggaley, K. H.; Gillett, J.; Holland, S.; Nicholson, N. H.; Sime, J. T.; Wroniecki, S. R. *J. Chem. Soc. Chem. Commun.* **1987**, (1736).
- Ensley, B. D.; Gibson, D. T. *J Bacteriol* **1983**, *155*, 505-511.
- EpicentreBiotechnologies *CopyControl™ HTP Fosmid Library Production Kit*. 2007.
- Fernandez-Moreno, M. A.; Martinez, E.; Boto, L.; Hopwood, D. A.; Malpartida, F. *J Biol Chem* **1992**, *267* (27), 19278-90.
- Finking, R.; Marahiel, M. A. *Annu Rev Microbiol* **2004**, *58*, 453-88.
- Floriano, B.; Bibb, M. *Mol Microbiol* **1996**, *21* (2), 385-96.
- Foerstner, K. U.; Doerks, T.; Creevey, C. J.; Doerks, A.; Bork, P. *PLoS One* **2008**, *3* (10), e3515.

- Furstner, A. *Angew Chem Int Ed Engl* **2003**, *42* (31), 3582-603.
- Gaughran, E. R. L. *Trans. N. Y. Acad. Sci.* **1969**, *31*, 3-24.
- Gerber, N.; McInnes, A.; Smith, D.; Walter, J.; Wright, J.; Vining, L. *Can J Chem* **1978**, *56*, 1155-1163.
- Gerber, N. N. *CRC Crit Rev Microbiol* **1975**, *3* (4), 469-85.
- Gerber, N. N. *J Antibiot (Tokyo)* **1975**, *28* (3), 194-9.
- Gibson, D. T.; Koch, J. R.; Kallio, R. E. *Biochemistry* **1968**, *7*, 2653-2662.
- Gust, B.; Kieser, T.; Chater, K. F. REDIRECT(c) Technology: PCR-targeting system in *Streptomyces coelicolor*. 2002.
- Gust, B.; Challis, G. L.; Fowler, K.; Kieser, T.; Chater, K. F. *Proc Natl Acad Sci U S A* **2003**, *100* (4), 1541-6.
- Guthrie, E. P.; Flaxman, C. S.; White, J.; Hodgson, D. A.; Bibb, M. J.; Chater, K. F. *Microbiology* **1998**, *144* (Pt 3), 727-38.
- Hammerschmidt, F. *J. Chem. Soc. Perkin Trans.* **1991**, *1* (1993).
- Haneishi, T.; Terahara, A.; Arai, M.; Hata, T.; Tamura, C. *J Antibiot (Tokyo)* **1974**, *27* (6), 393-9.
- Harris, A. K.; Williamson, N. R.; Slater, H.; Cox, A.; Abbasi, S.; Foulds, I.; Simonsen, H. T.; Leeper, F. J.; Salmond, G. P. *Microbiology* **2004**, *150* (Pt 11), 3547-60.
- Haug, I.; Weissenborn, A.; Brolle, D.; Bentley, S.; Kieser, T.; Altenbuchner, J. *Microbiology* **2003**, *149* (Pt 2), 505-13.
- Hayakawa, Y.; Nagatsuka, S. Y.; Kawasaki, T. *J Antibiot (Tokyo)* **2009**, *62* (9), 531-2.
- Haynes, S. W.; Sydor, P. K.; Stanley, A. E.; Song, L.; Challis, G. L. *Chem Commun* **2008**, (16), 1865-7.

- Haynes, S. W. Mutasythesis approaches to the preparation of streptorubin B analogues. PhD Thesis, University of Warwick, Coventry, 2010.
- Heide, L.; Westrich, L.; Anderle, C.; Gust, B.; Kammerer, B.; Piel, J. *ChemBioChem* **2008**, *9* (12), 1992-9.
- Herzberg, O.; Chen, C. C.; Kapadia, G.; McGuire, M.; Carroll, L. J.; Noh, S. J.; Dunaway-Mariano, D. *Proc Natl Acad Sci U S A* **1996**, *93* (7), 2652-7.
- Higgins, L. J.; Yan, F.; Liu, P.; Liu, H. W.; Drennan, C. L. *Nature* **2005**, *437* (7060), 838-44.
- Hojati, Z.; Milne, C.; Harvey, B.; Gordon, L.; Borg, M.; Flett, F.; Wilkinson, B.; Sidebottom, P. J.; Rudd, B. A.; Hayes, M. A.; Smith, C. P.; Micklefield, J. *Chem Biol* **2002**, *9* (11), 1175-87.
- Hopwood, D. A. *Chem Rev* **1997**, *97* (7), 2465-2498.
- Hornemann, U.; D.A., H. *Tetrahedron Lett.* **1978**, *33*, 2977-2978.
- Imbert, M.; Bechet, M.; Blondeau, R. *Curr. Microbiol.* **1995**, *31*, 129-133.
- Isaka, M.; Jaturapat, A.; Kramyu, J.; Tanticharoen, M.; Thebtaranonth, Y. *Antimicrob Agents Chemother* **2002**, *46* (4), 1112-3.
- Jiang, H.; Parales, R. E.; Lynch, N. A.; Gibson, D. T. *J Bacteriol* **1996**, *178*, 3133-3139.
- Jiang, J.; He, X.; Cane, D. E. *J Am Chem Soc* **2006**, *128* (25), 8128-9.
- Jiang, J.; He, X.; Cane, D. E. *Nat Chem Biol* **2007**, *3* (11), 711-5.
- Jung, D.; Rozek, A.; Okon, M.; Hancock, R. E. *Chem Biol* **2004**, *11* (7), 949-57.
- Kauppi, B.; Lee, E.; Carredano, E.; Parales, R. E.; Gibson, D. T.; Eklund, H.; Ramaswamy, S. *structure* **1998**, *6*, 571-586.
- Kawasaki, T.; Sakurai, F.; Hayakawa, Y. *J Nat Prod* **2008**, *71* (7), 1265-7.

- Kawasaki, T.; Sakurai, F.; Nagatsuka, S. Y.; Hayakawa, Y. *J Antibiot (Tokyo)* **2009**, *62* (5), 271-6.
- Kayakawa, Y.; Kawakami, K.; Seto, H.; Furihata, K. *Tetrahedron Lett.* **1992**, *33* (19), 2701-2704.
- Kelemen, G. H.; Brian, P.; Flardh, K.; Chamberlin, L.; Chater, K. F.; Buttner, M. J. *J Bacteriol* **1998**, *180* (9), 2515-21.
- Kempter, C.; Kaiser, D.; Haag, S.; Nicholson, G.; Gnau, V.; Walk, T.; Gierling, K. H.; Decker, H.; Zahner, H.; Jung, G.; Metzger, J. W. *Angew Chem Int Ed Engl* **1997**, *36*, 498-501.
- Kieser, T.; Bibb, M. J.; Buttner, M. J.; Chater, K. F.; Hopwood, D. A. *Practical Streptomyces Genetics*. 2 ed.; The John Innes Centre Foundation: Norwich, 2000.
- Kirby, R.; Hopwood, D. A. *J Gen Microbiol* **1977**, *98* (1), 239-52.
- Konomi, T.; Herchen, S.; Baldwin, J. E.; Yoshida, M.; Hunt, N. H.; Demain, A. L. *Biochem J.* **1979**, *184* (427).
- Kotowska, M.; Pawlik, K.; Butler, A. R.; Cundliffe, E.; Takano, E.; Kuczek, K. *Microbiology* **2002**, *148* (Pt 6), 1777-83.
- Laatsch, H.; Kellner, M.; Weyland, H. *J Antibiot (Tokyo)* **1991**, *44* (2), 187-91.
- Lakey, J. H.; Lea, E. J.; Rudd, B. A.; Wright, H. M.; Hopwood, D. A. *J Gen Microbiol* **1983**, *129* (12), 3565-73.
- Lambalot, R. H.; Gehring, A. M.; Flugel, R. S.; Zuber, P.; LaCelle, M.; Marahiel, M. A.; Reid, R.; Khosla, C.; Walsh, C. T. *Chem Biol* **1996**, *3* (11), 923-36.
- Lautru, S.; Deeth, R. J.; Bailey, L. M.; Challis, G. L. *Nat Chem Biol* **2005**, *1* (5), 265-9.

- Lautru, S.; Oves-Costales, D.; Pernodet, J. L.; Challis, G. L. *Microbiology* **2007**, *153* (Pt 5), 1405-12.
- Lee, M. H.; Kataoka, T.; Honjo, N.; Magae, J.; Nagai, K. *Immunology* **2000**, *99* (2), 243-8.
- Lei, L.; Waterman, M. R.; Fulco, A. J.; Kelly, S. L.; Lamb, D. C. *Proc Natl Acad Sci U S A* **2004**, *101*, 494-499.
- Liu, P.; Murakami, K.; Seki, T.; He, X.; Yeung, S. M.; Kuzuyama, T.; Seto, H.; Liu, H. *J Am Chem Soc* **2001**, *123* (19), 4619-20.
- Lu, Y. W.; San Roman, A. K.; Gehring, A. M. *J Bacteriol* **2008**, *190* (20), 6903-8.
- Madigan, M.; Martinko, J. *Brock Biology of Microorganisms*. 11 ed.; Prentice Hall: New Jersey, 2005.
- Magae, J.; Miller, M. W.; Nagai, K.; Shearer, G. M. *J Antibiot (Tokyo)* **1996**, *49* (1), 86-90.
- Malpartida, F.; Niemi, J.; Navarrete, R.; Hopwood, D. A. *Gene* **1990**, *93* (1), 91-9.
- McDaniel, R.; Ebert-Khosla, S.; Fu, H.; Hopwood, D. A.; Khosla, C. *Proc Natl Acad Sci U S A* **1994**, *91* (24), 11542-6.
- McGuire, J. M.; Binch, R. L.; Anderson, R. C.; Boaz, H. E.; Flynn, E. H.; Powell, M.; Smith, J. W. *Antibiot. Chemother.* **1952**, *2* (281).
- McMurry, J.; Begley, T. *The Organic Chemistry of Biological Pathways*. Roberts and Company Publisher: Englewood, CO, 2005.
- Mo, S.; Kim, B. S.; Reynolds, K. A. *Chem Biol* **2005**, *12* (2), 191-200.
- Mo, S.; Sydor, P. K.; Corre, C.; Alhamadsheh, M. M.; Stanley, A. E.; Haynes, S. W.; Song, L.; Reynolds, K. A.; Challis, G. L. *Chem Biol* **2008**, *15* (2), 137-48.

- Mofid, M. R.; Marahiel, M. A.; Ficner, R.; Reuter, K. *Acta Crystallogr D Biol Crystallogr* **1999**, *55* (Pt 5), 1098-100.
- Mofid, M. R.; Finking, R.; Marahiel, M. A. *J Biol Chem* **2002**, *277* (19), 17023-31.
- Mortellaro, A.; Songia, S.; Gnocchi, P.; Ferrari, M.; Fornasiero, C.; D'Alessio, R.; Isetta, A.; Colotta, F.; Golay, J. *J Immunol* **1999**, *162* (12), 7102-9.
- Narva, K. E.; Feitelson, J. S. *J Bacteriol* **1990**, *172* (1), 326-33.
- Nguyen, M.; Marcellus, R. C.; Roulston, A.; Watson, M.; Serfass, L.; Murthy Madiraju, S. R.; Goulet, D.; Viallet, J.; Belec, L.; Billot, X.; Acoca, S.; Purisima, E.; Wiegmans, A.; Cluse, L.; Johnstone, R. W.; Beauparlant, P.; Shore, G. C. *Proc Natl Acad Sci U S A* **2007**, *104* (49), 19512-7.
- O'Rourke, S.; Wietzorrek, A.; Fowler, K.; Corre, C.; Challis, G. L.; Chater, K. F. *Mol Microbiol* **2009**, *71* (3), 763-78.
- Odule, O. M. Investigation of prodiginine biosynthesis in *Streptomyces coelicolor* M511. PhD Thesis, University of Warwick, Coventry, 2005.
- Okamoto, S.; Taguchi, T.; Ochi, K.; Ichinose, K. *Chem Biol* **2009**, *16* (2), 226-36.
- Percudani, R.; Peracchi, A. *EMBO Rep* **2003**, *4* (9), 850-4.
- Raynal, A.; Friedmann, A.; Tophile, K.; Guerineau, M.; Pernodet, J. L. *Microbiology* **2002**, *148* (Pt 1), 61-7.
- Redenbach, M.; Kieser, H. M.; Denapaite, D.; Eichner, A.; Cullum, J.; Kinashi, H.; Hopwood, D. A. *Mol Microbiol* **1996**, *21* (1), 77-96.
- Reuter, K.; Mofid, M. R.; Marahiel, M. A.; Ficner, R. *EMBO J* **1999**, *18* (23), 6823-31.
- Reynolds, K. personal communication.

- Roach, P. L.; Clifton, I. J.; Fulop, V.; Harlos, K.; Barton, G. J.; Hajdu, J.; Andersson, I.; Schofield, C. J.; Baldwin, J. E. *Nature* **1995**, 375 (6533), 700-4.
- Rock, C. O.; Cronan, J. E. *Biochim Biophys Acta* **1996**, 1302 (1), 1-16.
- Rudd, B. A.; Hopwood, D. A. *J Gen Microbiol* **1980**, 119 (2), 333-40.
- Sambrook, J.; Russell, D. W. *Molecular Cloning - A Laboratory Manual*. 3 ed.; Cold Spring Harbor Laboratory Press: New York, 2001.
- Sanchez, C.; Du, L.; Edwards, D. J.; Toney, M. D.; Shen, B. *Chem Biol* **2001**, 8 (7), 725-38.
- Saxena, P.; Yadav, G.; Mohanty, D.; Gokhale, R. S. *J Biol Chem* **2003**, 278 (45), 44780-90.
- Seto, H.; Hidaka, T.; Kuzuyama, T.; Shibahara, S.; Usui, T.; Sakanaka, O.; Imai, S. *J. Antibiot.* **1991**, 44 (1286).
- Smith, S. *FASEB J* **1994**, 8 (15), 1248-59.
- Song, L.; Barona-Gomez, F.; Corre, C.; Xiang, L.; Udvary, D. W.; Austin, M. B.; Noel, J. P.; Moore, B. S.; Challis, G. L. *J Am Chem Soc* **2006**, 128 (46), 14754-5.
- Song, L.; Challis, G. L. unpublished results.
- Stanley, A. E.; Walton, L. J.; Kourdi Zerikly, M.; Corre, C.; Challis, G. L. *Chem Commun* **2006**, (38), 3981-3.
- Stanley, A. E. Investigation of Prodiginine Biosynthesis in *Streptomyces coelicolor* A3(2). PhD Thesis, University of Warwick, Coventry, 2007.
- Staunton, J.; Wilkinson, B. *Chem Rev* **1997**, 97 (7), 2611-2630.
- Strohl, W. R. *Nucleic Acids Res* **1992**, 20 (5), 961-974.

- Sydor, P. K.; Barry, S. M.; Odulate, O. M.; Barona-Gómez, F.; Haynes, S. W.; Corre, C.; Song, L.; Challis, G. L. in preparation. 2010.
- Takano, E.; Nihira, T.; Hara, Y.; Jones, J. J.; Gershater, C. J.; Yamada, Y.; Bibb, M. *J Biol Chem* **2000**, 275 (15), 11010-6.
- Takano, E.; Kinoshita, H.; Mersinias, V.; Bucca, G.; Hotchkiss, G.; Nihira, T.; Smith, C. P.; Bibb, M.; Wohlleben, W.; Chater, K. *Mol Microbiol* **2005**, 56 (2), 465-79.
- Takano, E. *Curr Opin Microbiol* **2006**, 9 (3), 287-94.
- Thomas, M. G.; Burkart, M. D.; Walsh, C. T. *Chem Biol* **2002**, 9 (2), 171-84.
- Trudel, S.; Li, Z. H.; Rauw, J.; Tiedemann, R. E.; Wen, X. Y.; Stewart, A. K. *Blood* **2007**, 109 (12), 5430-8.
- Urlacher, V. B.; Schmid, R. D. *Curr Opin Chem Biol* **2006**, 10 (2), 156-61.
- Vertesy, L.; Ehlers, E.; Kogler, H.; Kurz, M.; Meiwes, J.; Seibert, G.; Vogel, M.; Hammann, P. *J Antibiot (Tokyo)* **2000**, 53 (8), 816-27.
- Walsh, C. T.; Gehring, A. M.; Weinreb, P. H.; Quadri, L. E.; Flugel, R. S. *Curr Opin Chem Biol* **1997**, 1 (3), 309-15.
- Wandersman, C.; Delepelaire, P. *Annu Rev Microbiol* **2004**, 58, 611-47.
- Wang, C. M.; Cane, D. E. *J Am Chem Soc* **2008**, 130 (28), 8908-9.
- Wasserman, H. H.; Keith, D. D.; Nadelson, J. *J Am Chem Soc* **1969**, 91 (5), 1264-5.
- Wasserman, H. H.; Rodgers, G. C.; Keith, D. D. *J Am Chem Soc* **1969**, 91 (5), 1263-4.
- Wasserman, H. H.; Skles, R. J.; Peverada, P.; Shaw, C. K.; Cushley, R. J.; Lipsky, C. R. *J Am Chem Soc* **1973**, 95 (20), 6874-5.
- Wasserman, H. H.; Shaw, C. K.; Sykes, R. J. *tetrahedron Lett* **1974**, 15, 2787-2790.

- Weber, J. M.; Leung, J. O.; Maine, G. T.; Potenz, R. H.; Paulus, T. J.; DeWitt, J. P. *J Bacteriol* **1990**, *172* (5), 2372-83.
- Weissman, K. J.; Hong, H.; Oliynyk, M.; Siskos, A. P.; Leadlay, P. F. *ChemBioChem* **2004**, *5* (1), 116-25.
- Westrich, L.; Heide, L.; Li, S. M. *ChemBioChem* **2003**, *4* (8), 768-73.
- White, J.; Bibb, M. *J Bacteriol* **1997**, *179* (3), 627-33.
- Williamson, N. R.; Simonsen, H. T.; Ahmed, R. A.; Goldet, G.; Slater, H.; Woodley, L.; Leeper, F. J.; Salmond, G. P. *Mol Microbiol* **2005**, *56* (4), 971-89.
- Williamson, N. R.; Fineran, P. C.; Gristwood, T.; Chawrai, S. R.; Leeper, F. J.; Salmond, G. P. *Future Microbiol* **2007**, *2*, 605-18.
- Woodcock, D. M.; Crowther, P. J.; Doherty, J.; Jefferson, S.; DeCruz, E.; Noyer-Weidner, M.; Smith, S. S.; Michael, M. Z.; Graham, M. W. *Nucleic Acids Res* **1989**, *17* (9), 3469-78.
- Wright, L. F.; Hopwood, D. A. *J Gen Microbiol* **1976**, *96* (2), 289-97.
- Xue, Y.; Zhao, L.; Liu, H. W.; Sherman, D. H. *Proc Natl Acad Sci U S A* **1998**, *95* (21), 12111-6.
- Yasgar, A.; Foley, T. L.; Jadhav, A.; Inglese, J.; Burkart, M. D.; Simeonov, A. *Mol Biosyst* **2010**, *6*, 365-375.
- Yu, T. W.; Hopwood, D. A. *Microbiology* **1995**, *141*, 2779-91.
- Zerbe, K.; Woithe, K.; Li, D. B.; Vitali, F.; Bigler, L.; Robinson, J. A. *Angew Chem Int Ed Engl* **2004**, *43* (48), 6709-13.
- Zhang, J.; Shen, Y.; Liu, J.; Wei, D. *Biochem Pharmacol* **2005**, *69* (3), 407-14.

Zhang, Z.; Ren, J.; Stammers, D. K.; Baldwin, J. E.; Harlos, K.; Schofield, C. J. *Nat Struct Biol* **2000**, 7 (2), 127-33.

Zhao, B.; Lin, X.; Lei, L.; Lamb, D. C.; Kelly, S. L.; Waterman, M. R.; Cane, D. E. *J Biol Chem* **2008**, 283 (13), 8183-9.